

Universität  
Rostock



Traditio et Innovatio



# Molybdenum Pincer Complexes: Synthesis and Application in Catalytic Hydrogenations

## Cumulative Dissertation

to acquire the academic degree  
*doctor rerum naturalium* (Dr. rer. nat.)  
of the Faculty of Mathematics and Natural Sciences  
at the University of Rostock

Submitted by Thomas Leischner, born on 16<sup>th</sup> October 1989 in Kassel  
Rostock, 29.07.2020

[https://doi.org/10.18453/rosdok\\_id00002871](https://doi.org/10.18453/rosdok_id00002871)

The present work was accomplished at the Leibniz-Institute for Catalysis e. V., at the chair for Applied Catalysis in the group of Professor Dr. Matthias Beller during the period October 2016 to June 2020.

Reviewer #1: Prof. Dr. Matthias Beller

Leibniz-Institut für Katalyse e.V.

Abteilung: Angewandte Homogenkatalyse

Albert-Einstein-Straße 29a

18059 Rostock

Reviewer #2: Prof. Dr. Rhett Kempe

University of Bayreuth

**Date of submission** : 29.07.2020

**Date of defense** : 17.11.2020

## **Statement of Authorship**

I hereby affirm that I have written the present work by myself without outside assistance. No other resources were utilized than stated. All references as well as verbatim extracts were quoted, and all sources of information were specifically acknowledged.

Ich versichere hiermit an Eides statt, dass ich die vorliegende Arbeit selbstständig angefertigt und ohne fremde Hilfe verfasst habe. Dazu habe ich keine außer den von mir angegebenen Hilfsmitteln und Quellen verwendet und die den benutzten Werken inhaltlich und wörtlich entnommenen Stellen habe ich als solche kenntlich gemacht.

Rostock, 20.07.2020

.....

**Thomas Leischner**

## Acknowledgements – Danksagung

Zuallererst möchte ich mich bei Herrn **Prof. Dr. Matthias Beller** für die Aufnahme in seinen Arbeitskreis und die Vergabe des hochinteressanten Themas bedanken. Deine Bereitschaft zu wissenschaftlichen Diskussionen und die schier endlosen neuen Anreize und Ideen bezüglich meiner Forschung haben mich persönlich weitergebracht und maßgeblich zum Gelingen dieser Arbeit beigetragen. Des Weiteren möchte ich mich für die Möglichkeit bedanken, an einem Forschungsprojekt für die Bayer AG zu arbeiten.

**Dr. Kathrin Junge** danke ich für die überaus herzliche Aufnahme in Ihre Themengruppe und die Begleitung meiner Arbeit von Beginn an. Vielen Dank dafür, dass du mich nie hast hängen lassen und mir mehr als einmal extra Zeit in deiner Arbeitsgruppe ermöglicht hast.

Frau **Dr. Anke Spannenberg** danke ich für die gemessenen X-Ray Strukturen und deren Auswertung. Trotz teils schwieriger kristallographischer Probleme konntest du mir immer eine Kristallstruktur liefern und hast so erheblichen Anteil an nahezu allen meinen veröffentlichten Arbeiten. Frau **Dr. Christiane Fischer**, Frau **Susanne Schareina**, Frau **Susann Buchholz**, Frau **Astrid Lehmann** und Frau **Katrin Fiedler** danke ich ausdrücklich für die zahllosen Messungen verschiedenster Art.

Ebenso danke ich allen Mitgliedern der **Redox-Gruppe** die ich über die Jahre kennen lernen durfte. Besonders möchte ich Dr. Veronica Papa und Dr. Pavel Ryabchuk hervorheben. Veronica, you have been simply an awesome lab mate and I want to let you know that I genuinely more than enjoyed our common time at LIKAT. I yet can not imagine how much I am going to miss these times, but I will always remember them as one of the best I have ever had. You have always been an exhilarating personality and helped me more than once to go through some hard times. I thank you so much for always having an open ear for me, on a personal as well a professional level. I wish you all the best for your future career, however, I have no doubt that it is going to be more than successful. One more thing: I am simply amazed that you survived the time in the office with Pavel, David and me. Probably most people would have gone crazy. Similarly Pavel: Thank you so much for all the advices you gave me and the time we had at LIKAT. You helped me a lot to grow as a person and a chemist. I clearly remember our first meetings after we both joined the team. It was fall and we discussed chemistry on our way home. Soon after I met you and your daughter in front of the Kröperliner Tor and we had a long chat while you waited for Anastasia to finish the gym. In you, I found a brother in mind who shared the same sense of humor. I just want to say: It was a hilarious, amazing, and unforgettable time. I will simply miss it. Our whatsapp group has to survive!!!! I also wish you and your family a great start in Belgium at Galapagos. I hope you found yourself



a nice to place to live and thrive. But, to be honest, I have no doubt, that you have amazing times ahead of you and that you and your family will do great.

Weiterhin gilt mein Dank der **Mittagsgruppe**, welche neben der Chemie auch andere Themen zur Diskussion stellten. Hierbei sind vor allem Herr Dr. Jacob Schneekönig, Frau Dr. Reni Grauke und David Kevin Leonard zu erwähnen. Zusammen haben wir dem Mittagessen interessante, oft tagesaktuelle, hin und wieder wiederkehrende und oft abstrakte Diskussionsthemen zur Verfügung gestellt. Möglicherweise manchmal auch zum Leidwesen einiger Anwesender: Hallo Frau Dr. Möller :).

Erwähnen möchte ich auch die „LIKAT Betriebssport Laufgruppe“. Training mit euch war immer ein erheiternder Start in die Woche und eine angenehme Abwechslung zum Arbeitsalltag.

Meiner Freundin Vivian danke ich für die unglaubliche Zeit, die wir bis hierher hatten und weiter haben werden. Danke, dass du und auf jeglicher Ebene für mich da bist. Ich freue mich auf unsere nächsten, gemeinsamen Lebensabschnitte.

Zu guter Letzt danke ich meiner **Familie** für die Unterstützung während meiner gesamten Ausbildung und der Möglichkeit, dass ich diesen Weg bestreiten konnte. Ohne euch wäre das alles nicht möglich gewesen!

**Vielen Dank.**

## Summary

The thesis in hand describes the synthesis of novel molybdenum pincer complexes and their application as catalysts for the homogeneous hydrogenation of unsaturated organic molecules. PNP-type pincer ligands with aliphatic backbones were a focal point in this respect, as related molybdenum complexes and their catalytic properties were previously only scarcely explored. A synthetic methodology for the preparation of such organometallic compounds was developed, giving access to diverse Mo(0), Mo(I) and Mo(II) compounds. In a first catalytic protocol, the reduction of acetophenones and styrenes to the corresponding alcohols and alkanes, catalyzed by a Mo(I) complex, is described. Subsequently, employing the same catalyst, we developed a highly selective hydrogenolysis of *N*-methylated formamides to amines and alcohols *via* C–N bond cleavage. Finally, we reported a selective hydrogenation of aromatic and aliphatic nitriles to the respective primary amines, catalyzed by a Mo(0) complex. In addition, a chiral Ir-catalyst for the enantioselective hydrogenation of an agrochemical building block was developed in cooperation with an industrial partner. Moreover, an *in situ*-cobalt/triphos catalyst for the hydrogenation of structurally diverse epoxides to the respective *anti*-Markovnikov alcohols is disclosed.

## Zusammenfassung

Die vorliegende Arbeit beschreibt die Synthese neuartiger Molybdän-Pincer Komplexe sowie deren Anwendung als Katalysatoren für die homogenkatalytische Hydrierung ungesättigter organischer Verbindungen. Der Einsatz von PNP Pincerliganden mit aliphatischem Ligandenrückgrat stand hierbei im Vordergrund, da entsprechende Molybdänverbindungen sowie deren katalytische Eigenschaften bisher nur wenig untersucht wurden. Zunächst wurde eine Synthesestrategie zur Herstellungen solcher Komplexverbindungen entwickelt und so Zugang zu verschiedenen Mo(0)-, Mo(I)- und Mo(II)-Komplexen erhalten. In einer ersten Publikation wurde die Hydrierung verschiedener Acetophenone und Styrole zu den korrespondierenden Alkoholen und Ethylbenzolen mittels eines Mo(I)-Katalysators beschrieben. Nachfolgend, unter Verwendung des gleichen Mo-Komplexes, wurde eine hochselektive Hydrogenolyse *N*-methylierter Formanilide *via* C–N Bindungsspaltung entwickelt. Abschließend konnten wir die Eignung eines auf Molybdän(0) basierenden Katalysatorsystems für die selektive Hydrierung aromatischer und aliphatischer Nitrile zu den entsprechenden primären Aminen demonstrieren. Zusätzlich wurde im Rahmen dieser Promotion ein chiraler Ir-Katalysator für die enantioselective Hydrierung einer Zwischenstufe zur Herstellung einer Agrochemikalie, sowie ein auf Cobalt/Triphos basierendes *in situ* Katalysatorsystem zur Hydrierung von terminalen und internen Epoxiden zu *anti*-Markovnikov Alkoholen entwickelt.

# Inhalt

List of Abbreviations .....	IX
Units of Measurement.....	X
List of Figures.....	XI
List of Tables.....	XII
List of Schemes.....	XIII
1 Introduction.....	1
1.1 Molybdenum – General Information .....	1
1.2 Molybdenum – Biological Role.....	3
1.3 Catalytic Homogeneous Hydrogenation .....	5
1.3.1 Pincer Complexes in Catalytic Homogeneous Hydrogenation.....	6
1.3.1.1 Hydrogenation of Ketones Catalyzed by Base Metal Pincer Complexes.....	8
1.3.1.2 Hydrogenation of Amides Catalyzed by Base Metal Pincer Complexes.....	10
1.3.1.3 Hydrogenation of Nitriles Catalyzed by Base Metal Pincer Complexes.....	12
1.4 Molybdenum (PNP) Pincer Complexes and their Application in Homogeneous Hydrogenations.....	13
2 Objectives of this work.....	17
3 Results and Discussion.....	18
3.1 Synthesis and Characterization of Molybdenum Pincer Complexes .....	18
3.2 Catalytic Hydrogenations using Molybdenum Pincer Complexes .....	23
3.2.1 Catalytic Hydrogenations of Ketones and Styrenes .....	23
3.2.2 Catalytic Hydrogenations of Formanilides.....	26
3.2.3 Catalytic Hydrogenations of Nitriles.....	32
3.2.4 Ir-Catalyzed Enantioselective Hydrogenation of an Agrochemical Building Block.....	37
3.2.5 Catalytic Hydrogenations of Epoxides to <i>anti</i> -Markovnikov-Alcohols by a Cobalt/Triphos Catalyst .....	41
4 Summary and Outlook .....	45
5 References.....	47
6 Selected Publications.....	54

6.1 Molecular Defined Molybdenum Pincer Complexes and Their Application in Catalytic Hydrogenations.....	54
6.2 Highly Selective Hydrogenation of Amides Catalyzed by a Molybdenum Pincer Complex: Scope and Mechanism.....	62
6.3 Synthesis of Molybdenum Pincer Complexes and Their Application in the Catalytic Hydrogenation of Nitriles.....	74
6.4 Application of Crabtree/Pfaltz-Type Iridium Complexes for the Catalyzed Asymmetric Hydrogenation of an Agrochemical Building Block.....	82
6.5 A General Regioselective Synthesis of Alcohols by Cobalt Catalyzed Hydrogenation of Epoxides.....	88
7. Appendix.....	93
7.1 Curriculum Vitae.....	93
7.2 List of Publications.....	94
7.3 Conference Participations.....	95

## List of Abbreviations

<b>BAr<sub>F</sub></b>	tetrakis[3,5- <i>bis</i> (trifluormethyl)phenyl]borate	<b>KHMDS</b>	potassium 1,1,1-trimethyl- <i>N</i> - (trimethylsilyl)silaneamide
<b>Bn</b>	benzyl	<b>KO<sup>t</sup>Bu</b>	potassium <i>tert</i> -butoxide
<b>Bu</b>	<i>n</i> -butyl	<b>L-DOPA</b>	levodopa L-3,4-dihydroxyphenylalanine
<b>cat.</b>	catalyst	<b>LiOTf</b>	lithium trifluoromethanesulfonate
<b>COD</b>	cyclooctadiene	<b><i>m</i></b>	<i>meta</i>
<b>Cy</b>	cyclohexyl	<b>Me</b>	methyl
<b>δ</b>	chemical shift (NMR)	<b>Mes</b>	2,4,6-trimethylphenyl
<b>DBU</b>	2,3,4,6,7,8,9,10-octahydropyrimido[1,2- a]azepine	<b>MHz</b>	megahertz
<b>DCE</b>	1,2-dichloroethane	<b>NaHMDS</b>	sodium 1,1,1-trimethyl- <i>N</i> - (trimethylsilyl)silaneamide
<b>DCM</b>	dichloromethane	<b><sup>n</sup>BuLi</b>	<i>n</i> -butyllithium
<b>DFT</b>	density functional theory	<b>NHC</b>	<i>N</i> -heterocyclic carbene
<b>DMSO</b>	dimethylsulfoxide	<b>NMR</b>	<i>Nuclear Magnetic Resonance</i> (Kernspinresonanzspektroskopie)
<b>ee</b>	enantiomeric excess	<b><i>o</i></b>	<i>ortho</i>
<b>EPR</b>	Electron Paramagnetic Resonance	<b><i>p</i></b>	<i>para</i>
<b>Et</b>	ethyl	<b>Ph</b>	phenyl
<b>equiv.</b>	equivalents	<b>ppb</b>	<i>parts per billion</i>
<b>HFIP</b>	1,1,1,3,3,3-hexafluoroisopropanol	<b>ppm</b>	<i>parts per million</i>
<b>HR-ESI</b>	high-resolution electrospray ionization mass spectrometry	<b>rac</b>	racemic
<b>HSAB</b>	hard and soft acids and bases	<b>r.t.</b>	room temperature
<b><sup>i</sup>Bu</b>	<i>iso</i> -butyl	<b>TBAF</b>	tetrabutylammoniumfluoride
<b><sup>i</sup>Pr</b>	<i>iso</i> -propyl	<b>TBS</b>	<i>tert</i> -butyldimethylsilyl
<b>IR</b>	infrared	<b><sup>t</sup>Bu</b>	<i>tert</i> -butyl
<b><i>J</i></b>	coupling constant	<b>THF</b>	tetrahydrofuran

## Units of Measurement

The International System of Units (SI) is utilized throughout this work to measure experimental or theoretical quantities. All derived units and their expression in terms of the SI base units are given below.

Quantity	Unit	Name	Conversion to SI base units
Frequency	MHz	megahertz	$1 \text{ MHz} = 10^6 \text{ s}^{-1}$
	Hz	hertz	$1 \text{ Hz} = 1 \text{ s}^{-1}$
Length	Å	Ångström	$1 \text{ Å} = 10^{-10} \text{ m}$
Temperature	°C	degree Celcius	$T/\text{K} = T/\text{C}^\circ - 273.15$
Volume	mL	millilitre	$1 \text{ mL} = 1 \text{ cm}^3 = 10^{-6} \text{ m}^3$
Energy	kJ	kilojoule	$1 \text{ kJ} = 10^3 \text{ m}^2 \cdot \text{kg} \cdot \text{s}^{-2}$
	cal	calorie	$1 \text{ cal} = 4.2 \text{ Joules}$
Time	h	hour	$1 \text{ h} = 3600 \text{ s}$
	min	minute	$1 \text{ min} = 60 \text{ s}$

## List of Figures

Figure 1. Molecular structure of several molybdopterin co-factors.....	4
Figure 2. Selected examples of industrially relevant homogeneous hydrogenations. ....	6
Figure 3. General structure of pincer complexes.....	7
Figure 4. Selected examples of base metal pincer complexes, active in the hydrogenation of ketones.....	8
Figure 5. Selected examples of non-noble metal pincer complexes for the catalytic hydrogenation of nitriles to primary amines.....	13
Figure 6. Selected examples of molybdenum PNP pincer complexes.....	14
Figure 7. Aliphatic PNP pincer ligands <b>L1–L4</b> used for the synthesis of Mo-PNP complexes. .....	18
Figure 8. Overview of synthesized molybdenum complexes.....	45

## List of Tables

Table 1. Selected examples of molybdoenzymes. <sup>[4]</sup> .....	3
Table 2. Catalytic hydrogenation of acetophenone in the presence and absence of <b>Mo-10</b> and selected additives. ....	23
Table 3. Hydrogenation of <i>N</i> -methylformanilide <b>19a</b> to <i>N</i> -methylaniline <b>20a</b> and methanol <b>21</b> using different [Mo]-catalysts.....	26
Table 4. Initial screening of [Mo]-catalysts and reaction parameters.....	32
Table 5. Screening of different substrate concentrations.....	33
Table 6. Selected hydrogenation results of <b>34</b> .....	39
Table 7. Optimization of cobalt-catalyzed hydrogenation of epoxide <b>36a</b> .....	41
Table 8. Control experiments regarding the role of Zn(OTf) <sub>2</sub> . ....	44



## List of Schemes

Scheme 1. Selected applications of molybdenum in industrial catalysis.....	2
Scheme 2. Metal-ligand cooperation as well as outer- <sup>[57]</sup> and inner-sphere <sup>[58]</sup> mechanism.....	7
Scheme 3. Catalytic pathways for the hydrogenation of amides via C–O and C–N bond cleavage.....	10
Scheme 4. Selected examples of non-noble metal pincer complexes for the catalytic hydrogenation of amides.....	11
Scheme 5. Catalytic pathways for the hydrogenation of nitriles.....	12
Scheme 6. a) Synthesis of <b>Mo-2</b> . b) Selected examples of the hydrogenation of secondary imines catalyzed by <b>Mo-2</b> .....	14
Scheme 7. Selected examples of the hydrogenation of nitriles catalyzed by <b>Mo-2</b> .....	15
Scheme 8. a) Synthesis of molybdenum PNP complexes <b>Mo-8</b> , <b>Mo-9</b> , <b>Mo-10</b> , and <b>Mo-11</b> . a) 1.) Toluene, reflux, 16 h, 1.05 equiv. <b>L1</b> ; b) 1.) CH <sub>3</sub> CN/benzene, 1.10 equiv. C <sub>3</sub> H <sub>5</sub> Br, reflux, 16h; 2.) 3.00 equiv. PPh <sub>3</sub> , CH <sub>3</sub> CN, reflux, 1 h; 3.) 1.05 equiv. <b>L1</b> , toluene, 23 °C, 16 h; c) 1.) CH <sub>3</sub> CN/benzene, 1.10 equiv. C <sub>3</sub> H <sub>5</sub> Br, reflux, 16 h; 2.) 3.00 equiv. PPh <sub>3</sub> , CH <sub>3</sub> CN, reflux, 1 h; 3.) 1.05 equiv. <b>L1</b> , DCM, 23 °C, 16 h; d) 1.) CH <sub>3</sub> CN/benzene, 1.10 equiv. C <sub>3</sub> H <sub>5</sub> Br, reflux, 16 h; 2.) 1.05 equiv. <b>L1</b> , toluene, 23 °C, 24 h. b) Molecular structures of <b>Mo-8</b> , <b>Mo-9</b> , <b>Mo-10</b> , and <b>Mo-11</b> in the solid state. For <b>Mo-8</b> , only one molecule of the asymmetric unit is depicted. Thermal ellipsoids are drawn at 30% probability. Hydrogen atoms, except the <i>N</i> -bound, are omitted for clarity.....	19
Scheme 9. a) Synthesis of Mo-PNP complexes <b>Mo-12a</b> , <b>Mo-12b</b> , <b>Mo-13a</b> , <b>Mo-14</b> and <b>Mo-15</b> . b) Molecular structures of <b>Mo-12a</b> , <b>Mo-12b</b> , <b>Mo-13a</b> , and <b>Mo-15</b> in the solid state. For <b>Mo-15</b> only one molecule of the asymmetric unit is depicted. Thermal ellipsoids are drawn at 30% probability. Hydrogen atoms, except the <i>N</i> -bound are omitted for clarity.....	21
Scheme 10. a) Synthesis of molybdenum NNN complex <b>Mo-16</b> . Molecular structure of <b>Mo-16</b> in the solid state. b) Thermal ellipsoids are drawn at 30% probability. Hydrogen atoms, except the <i>N</i> -bound are omitted for clarity.....	22
Scheme 11. Catalytic hydrogenation of acetophenones in the presence of <b>Mo-10</b> /NaBHET <sub>3</sub> . Reaction conditions: 0.5 mmol Substrate, 5 mol% <b>Mo-10</b> , 5 mol% NaBHET <sub>3</sub> (0.5M in THF), 2 mL toluene, 50 bar H <sub>2</sub> , 80 °C, 16 h. Conversions were determined by GC using hexadecane as internal standard. Isolated yields in parenthesis. <sup>[1]</sup> Reaction carried out for 24 h. 1,3-diphenyl-1-propanol was obtained as the reaction product.....	24

- Scheme 12. Catalytic hydrogenation of styrenes in the presence of **Mo-10**/NaBHET<sub>3</sub>. Reaction conditions: 0.5 mmol substrate, 5 mol% **Mo-10**, 5 mol% NaBHET<sub>3</sub> (0.5M in THF), 2 mL toluene, 50 bar H<sub>2</sub>, 80 °C, 24 h. <sup>[1]</sup>Yield determined by GC using hexadecane as internal standard. <sup>[2]</sup>Yield determined by <sup>19</sup>F NMR of the reaction mixture using hexafluorobenzene as internal standard. <sup>[3]</sup>Yield determined by <sup>1</sup>H NMR of the reaction mixture using 1,3,5-trimethoxybenzene as internal standard. .... 25
- Scheme 13. Substrate scope of amide hydrogenation catalyzed by **Mo-10**. Reaction conditions: 0.5 mmol substrate, 5 mol% **Mo-10**, 5 mol% NaBHET<sub>3</sub> (0.5M in THF), 2 mL toluene, 50 bar H<sub>2</sub>, 80 °C, 24 h. Conversions of amides were determined by GC using hexadecane as internal standard. Isolated yields of anilines given in parenthesis. Yields of methanol were not determined. <sup>[1]</sup>Reaction at 130 °C. <sup>[2]</sup>Yield determined by GC using hexadecane as internal standard. .... 27
- Scheme 14. a) Hydrogenation of different amides to the corresponding amines and alcohols catalyzed by **Mo-10**.<sup>[1][2]</sup> b) Selective hydrogenation of a formamide moiety in the presence of another amide catalyzed by **Mo-10**.<sup>[1][3]</sup> Reaction conditions: 0.5 mmol substrate, 5 mol% **Mo-10**, 5 mol% NaBHET<sub>3</sub> (0.5M in THF), 2 mL toluene, 50 bar H<sub>2</sub>, 80 °C, 24 h. <sup>[1]</sup>Conversions were determined by GC using hexadecane as internal standard. <sup>[2]</sup>Yields were determined by GC using hexadecane as internal standard and refer to anilines. Yields of alcohols were not determined. <sup>[3]</sup>Isolated yield of **27** given, yield of **21** was not determined..... 28
- Scheme 15. a) Synthesis of catalytic intermediate **Mo-17** from **Mo-10**. Reaction conditions: 1.) 100 μmol **Mo-10**, 105 μmol NaBHET<sub>3</sub> (1M in THF), 10 mL THF, 21 °C, 1 h. 2.) 105 μmol *N*-formylaniline, 21 °C, 1 h. b) Molecular structure of **Mo-17** in the crystal. Only one molecule of the asymmetric unit is depicted. Displacement ellipsoids correspond to 30% probability. Hydrogen atoms except the *N*-bound are omitted for clarity. c) Control experiments to get insight on the active catalyst species (dashed arrows) with the experimentally observed products (H<sub>2</sub> and the crystal structure of **Mo-17**) and the intermediates proposed (**Mo-18** and **Mo-19**). Gibbs energies calculated for the dehydrogenation of **Mo-19** at different pressure. .... 29
- Scheme 16. General mechanism for the amide hydrogenation in the absence (green) and presence (black) of methanol. Squares indicate the catalyst resting state in the presence of MeOH and substrate (orange)..... 31
- Scheme 17. Substrate scope for nitrile reduction catalyzed by **Mo-9**. Reaction conditions: 0.5 mmol substrate, 5 mol% **Mo-9**, 5 mol% NaBHET<sub>3</sub> (0.5M in THF), 5 mL toluene, 50 bar H<sub>2</sub>, 80 °C, 24 h. Isolated yields given..... 34

Scheme 18. Selected examples of unsuccessful nitriles. Reaction conditions: 0.5 mmol substrate, 5 mol% <b>Mo-9</b> , 5 mol% NaBHET <sub>3</sub> (0.5M in THF), 5 mL toluene, 50 bar H <sub>2</sub> , 80 °C, 24 h. Conversions and yields (in parenthesis) were determined by GC using hexadecane as internal standard. <sup>[1]</sup> Secondary imine was detected as the main product.....	35
Scheme 19. a) Synthesis of <b>Mo-9a</b> . b) Solid state structure of <b>Mo-9a</b> . Thermal ellipsoids are drawn at 30% probability level. Hydrogen atoms, except the <i>N</i> -bound are omitted for clarity. Disordered parts of the molecule are only shown in one orientation. ....	36
Scheme 20. a) Desired transformation. b) Lead structure <b>Ir-1</b> and potential parameters for structural optimization. c) General synthesis of pyridyl alcohols <b>37a–r</b> , used for the ligand synthesis.....	37
Scheme 21. Synthesis of [Ir]-catalysts.....	38
Scheme 22. Labeling experiments using D <sub>2</sub> . Reaction conditions: 3 mmol Substrate, 0.025 mol% <b>Ir-18</b> , 4 mL HFIP, 40 bar D <sub>2</sub> , 85 °C, 16h. ....	40
Scheme 23. Cobalt-catalyzed hydrogenation of internal epoxides. Reaction conditions: 0.5 mmol substrate, 3 mol% Co(NTf <sub>2</sub> ) <sub>2</sub> , 6 mol% triphos, 7 mol% Zn(OTf) <sub>2</sub> , 4 mL THF, 40 bar H <sub>2</sub> , 80 °C, 16 h. <sup>[1]</sup> The diastereoisomeric ratio is 1:1.1. <sup>[2]</sup> 3 mol% Co(BF <sub>4</sub> ) <sub>2</sub> ·6 H <sub>2</sub> O, 4 mL 1,4-dioxane, 60 °C, 20 h. <sup>[3]</sup> The diastereoisomeric ratio (2.8:1) and yield were determined by GC.....	42
Scheme 24. Cobalt-catalyzed hydrogenation of terminal epoxides. Reaction conditions: 0.5 mmol substrate, 3 mol% Co(BF <sub>4</sub> ) <sub>2</sub> ·6 H <sub>2</sub> O, 6 mol% triphos, 6 mL 1,4-dioxane, 40 bar H <sub>2</sub> , 80 °C, 16 h. <sup>[1]</sup> 4 mL THF as solvent. <sup>[2]</sup> Yield was determined by GC using hexadecane as internal standard. <sup>[3]</sup> 3 mol% Co(NTf <sub>2</sub> ) <sub>2</sub> , 7 mol% Zn(OTf) <sub>2</sub> . <sup>[4]</sup> The major isomers are shown.....	43
Scheme 25. Selected mechanistic studies. a) 0.5 mmol Substrate, 3 mol% Co(NTf <sub>2</sub> ) <sub>2</sub> , 6 mol% triphos, 7 mol% Zn(OTf) <sub>2</sub> , 4 mL THF, 80 °C. ....	43

# 1 Introduction

## 1.1 Molybdenum – General Information

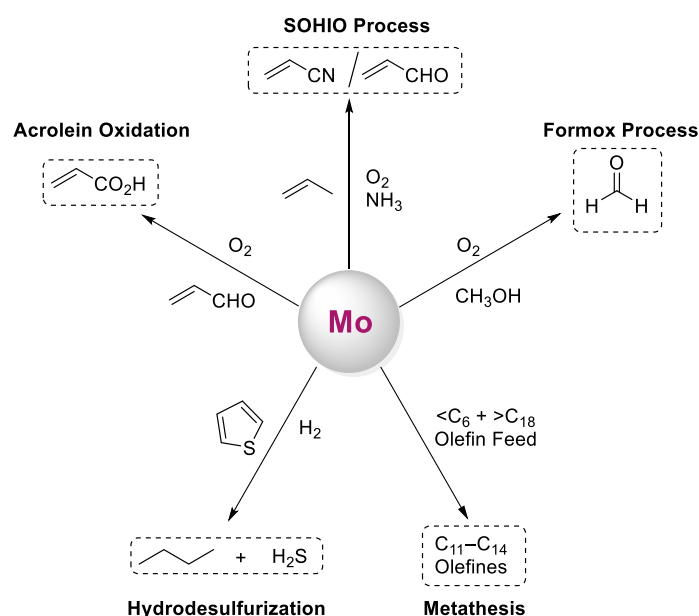
Molybdenum represents the 54<sup>th</sup> most abundant element in the Earth's crust and the 25<sup>th</sup> most abundant element in the oceans with average concentrations of 1.5 ppm and 10 ppb, respectively.<sup>[1]</sup> It was discovered in 1778 by Carl Wilhelm Scheele, who was able to isolate MoO<sub>3</sub> from a sample of the ore molybdenite.<sup>[2]</sup> Scheele named the new element molybdenum, referring to the ancient Greek term for lead, *molybdos*, as molybdenite was previously often confused with the common lead ore galena.<sup>[1]</sup> In 1781, Peter Jacob Hjelm eventually prepared elemental molybdenum by reduction of MoO<sub>3</sub> with carbon in linseed oil.<sup>[3]</sup> Naturally, molybdenum always occurs as a constituent of ores such as wulfenite (PbMoO<sub>4</sub>), powellite (CaMoO<sub>4</sub>) and molybdenite (MoS<sub>2</sub>), deposits of the pure element are not known. On an industrial scale, it is mainly mined in the form of MoS<sub>2</sub> or recovered as a by-product of copper and tungsten mining.<sup>[4]</sup> In 2018, worldwide production of molybdenum was nearly 300.000 metric tons with the most important suppliers being the United States and China as well as Chile, Peru, and Mexico.<sup>[5]</sup>

Molybdenum has the sixth highest melting point of all naturally occurring elements (2.623 °C), yet its density (10.22 g/cm<sup>3</sup>) exceeds the one of iron by only 25%. It has the lowest coefficient for thermal expansion of all engineering materials, while the thermal conductivity is among the highest of all elements.<sup>[6]</sup> Molybdenum metal does not react with dioxygen or water at room temperature, indeed weak oxidation only starts at 300 °C. Moreover, it is stable towards non-oxidizing acids, including hydrogen fluoride.<sup>[7]</sup> Molybdenum displays an extensive redox chemistry, and oxidation states ranging from -II to +VI are known. In general, it adopts coordination numbers between four and eight, and various complex geometries have been reported, predominantly in the oxidation states 0, +II, +IV and +VI. Particularly in its lower oxidation states, molybdenum has a rich organometallic chemistry, as best illustrated by the familiar hexacarbonyl Mo(CO)<sub>6</sub>.<sup>[8]</sup>

The distinct physical and chemical properties of molybdenum have been transformed into numerous applications, particularly since the beginning of the 20<sup>th</sup> century.<sup>[8]</sup> On a bulk level, it is mainly used for the manufacturing of special alloys.<sup>[9]</sup> Molybdenum-alloyed materials display unique features, including low thermal expansion, high strength at elevated temperatures, high thermal and electrical conductivity as well as high corrosion resistance, durability, and weldability.<sup>[10]</sup> In power plants, molybdenum is utilized in NO/NO<sub>2</sub>/NO<sub>x</sub> sensors for pollution control. At 350 °C, it facilitates the selective degradation of NO<sub>2</sub> and NO<sub>x</sub> to NO, enabling a consistent monitoring by IR spectroscopy.<sup>[11]</sup> Molybdenum (IV) sulfide is an important solid

lubricant and high-pressure high-temperature (HPHT) anti-wear agent in industrial settings.<sup>[12]</sup> The radioisotope <sup>99</sup>Mo is used as parent nuclide for the generation of <sup>99m</sup>Tc, which is employed for medical purposes.<sup>[13]</sup> Ammonium heptamolybdate is of relevance as fertilizer for molybdenum-depleted soils and is additionally applied in biological staining procedures. Similarly, phosphomolybdic acid is a popular staining agent for thin layer chromatography in synthetic chemistry.<sup>[4]</sup>

More important in the context of this work, molybdenum has several large-scale applications in industrial catalysis (Scheme 1). The synthesis of acrolein and acrylonitrile, respectively, from propene *via* the SOHIO process are carried out in the presence of Bi/Mo oxides as catalysts.<sup>[14]</sup> Mo/V oxides are used to promote the selective oxidation of propenal to acrylic acid on a bulk scale.<sup>[15]</sup> The Formox process uses Fe/Mo oxides for the selective oxidation of methanol to formaldehyde.<sup>[16]</sup> Moreover, in the Shell Higher Olefin Process, alumina supported Mo oxides are utilized for the synthesis of linear internal C<sub>11</sub>–C<sub>14</sub> alkenes *via* cross metathesis of olefinic mixtures.<sup>[17]</sup> The hydrodesulfurization (HDS) of natural gas and refined petroleum streams is routinely carried out in the presence of MoS<sub>2</sub>-based catalysts. This process is of crucial nature for oil refining, as the Re and Pt-catalysts used for catalytic reforming are rapidly poisoned by sulfur, even in extremely low concentrations.<sup>[18]</sup> Moreover, the removal of sulfur is of extreme importance from an environmental point of view, as ultra-low-sulfur fuels emit considerably lower amounts of SO<sub>2</sub>, a known cause of acidic rain.<sup>[19]</sup>



**Scheme 1.** Selected applications of molybdenum in industrial catalysis.

Every petrol refining site around the world nowadays operates at least one HDS reactor and hence makes use of molybdenum's catalytic properties on a daily basis.<sup>[20]</sup> Therefore, molybdenum certainly adopts a special role in industrial catalysis and for society in general.

## 1.2 Molybdenum – Biological Role

Molybdenum occurs in all kinds of life, ranging from ancient archaea to man. It is an essential dietary mineral for most species, including humans, where it typically serves as the active site of certain enzymes.<sup>[21]</sup> Notably, it represents the only second-row transition metal that is required by living organisms.<sup>[22]</sup> The omnipresence of molybdenum in biological systems is ascribed to its abundant nature in the oceans, the birthplace of life, where it is the most common of the redox active transition metals. Naturally, the bioavailable form of molybdenum is the water soluble molybdate anion  $[\text{MoO}_4]^{2-}$ , which closely resembles the sulfate anion,  $\text{SO}_4^-$ , structurally and electronically. Organisms have developed various strategies to take up sufficient quantities of molybdenum from their respective environments. As a result of the *vide supra* described structural relationship, molybdenum transport systems often closely resemble their sulfate analogous.<sup>[21]</sup>

Enzymes dependent on molybdenum are pervasive in the biosphere and to date more than fifty different examples have been discovered.<sup>[22]</sup> The overwhelming majority occurs in bacteria.<sup>[21]</sup> However, several mammalian molybdenum-containing examples have been disclosed, including sulfite oxidase, xanthine oxyreductase, the mitochondrial amidoxime reductase and aldehyde oxidase (Table 1).<sup>[24]</sup> These molybdenum enzymes exert vital tasks, mainly in the metabolism, where they facilitate the oxidation, and in some cases even the reduction, of small molecules as part of sulfur, nitrogen, and carbon regulating mechanisms.<sup>[25]</sup>

**Table 1.** Selected examples of molybdoenzymes.<sup>[4]</sup>

Enzyme	Catalyzed Reaction
Nitrogenase	$\text{N}_2 + 6 \text{H}^+ \rightarrow 2 \text{NH}_3$
Nitrate reductase	$\text{NO}_3^- + 2 \text{H}^+ + 2 \text{e}^- \rightarrow \text{NO}_2^- + \text{H}_2\text{O}$
Xanthine oxidase	$\text{Xanthine} + \text{H}_2\text{O} \rightarrow \text{Uric acid} + 2 \text{H}^+ + 2 \text{e}^-$
Xanthine dehydrogenase	$\text{RCHO} + \text{H}_2\text{O} \rightarrow \text{RCO}_2\text{H} + 2 \text{H}^+ + 2 \text{e}^-$
Aldehyde oxidase	$\text{SO}_3^{2-} + \text{H}_2\text{O} \rightarrow \text{SO}_4^{2-} + 2 \text{H}^+ + 2 \text{e}^-$
Sulfite oxidase	

This can be exemplified by the task of the xanthine oxidase, which catalyzes the oxidation of xanthine to uric acid within the purine catabolism. Interestingly, the activity of xanthine oxidase was found to directly correlate with the amounts of molybdenum present in the body. However, above certain concentrations, an inhibitory effect was observed.<sup>[26]</sup>

In general, molybdenum-containing enzymes can be distinguished into two main families, depending on the structural nature of their active site. The first category relies on a distinct molybdenum cofactor, called molybdopterin, to carry out their biological tasks (Figure 1a). On

a molecular level, this cofactor consists of a fragment featuring a mononuclear Mo atom in the +VI oxidation state, coordinated by a unique pterindithiolene ligand.<sup>[21]</sup> Depending on the molecular structure of the complexed  $[\text{Mo}]^{\text{VI}}$  fragment, all molybdopterin derived enzymes can be further distinguished into xanthine oxidases (Figure 1b), sulfite oxidases (Figure 1c) and DMSO reductases (Figure 1d).<sup>[22]</sup> In terms of function, the molybdenum center typically catalyzes one-electron redox reactions, commonly switching between the +IV, +V and +VI oxidation states.<sup>[4]</sup> Interestingly, all known mammalian examples of Mo-dependent enzymes belong to the molybdopterin cofactor derived class.<sup>[27]</sup>

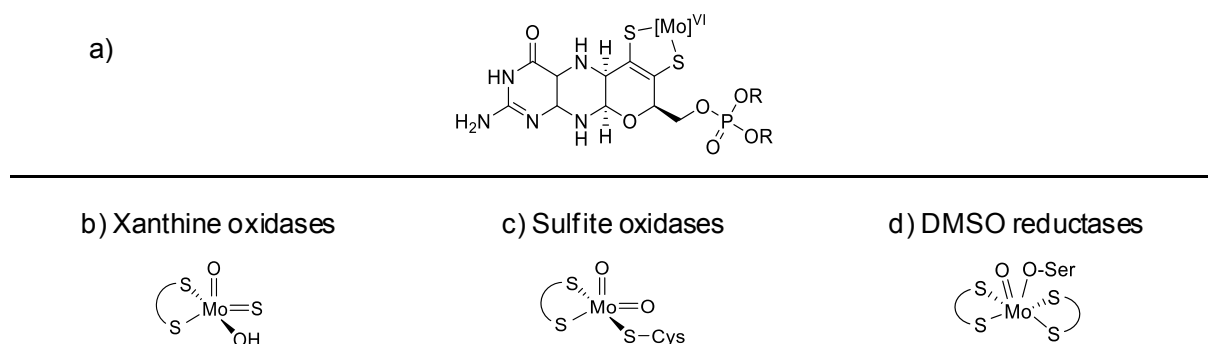


**Figure 1.** Molecular structure of several molybdopterin co-factors.

The second group of molybdenum-containing enzymes hosts the famous nitrogenases. Among molybdoenzymes, nitrogenases adopt a unique position, as they do not feature the molybdopterin co-factor. Instead they utilize an unusual  $[\text{MoFe}_7\text{S}_9]$  iron-molybdenum-sulfur cluster, called FeMo-co, as the active site.<sup>[21]</sup> These enzymes exclusively occur in certain bacteria and are of utmost importance for the earth's nitrogen cycle and concomitantly for life. They are capable of fixing and reducing atmospheric dinitrogen into bioavailable ammonia under ambient conditions.<sup>[28]</sup> *Per annum*, an estimated 200–300 million metric tons of  $\text{N}_2$  are converted into  $\text{NH}_3$  *via* this way.<sup>[29]</sup>

In terrestrial environments, it has been observed, that excess molybdenum in soils can cause severe copper deficiencies in ruminant animals. This so-called copper-molybdenum antagonism is based on the reduction of sulfate to sulfide in the rumen of sheep and cattle. The produced sulfide reacts with present molybdenum to tetrathiomolybdate  $[\text{MoS}_4]^{2-}$ , which readily coordinates and precipitates copper.<sup>[21]</sup> This effect was initially exploited in the form of  $\text{NH}_4[\text{MoS}_4]$  to treat copper toxicosis in animals.<sup>[30]</sup> More recently, it showed promising results for potential treatment of Wilson's disease, a hereditary metabolism disorder in humans resulting in high levels of copper in certain body parts. Presumably, tetrathiomolybdate competes with copper for absorption in the bowel resulting in lower copper uptakes and additionally promotes biliary excretion by *in vivo* formation of  $\text{Cu}[\text{MoS}_4]$ .<sup>[31]</sup>

### 1.3 Catalytic Homogeneous Hydrogenation

Catalytic hydrogenation generally describes a chemical reaction upon which dihydrogen is added to an (unsaturated) organic substrate by the aid of a catalyst. More specifically, the term homogeneous hydrogenation is applied, when the catalyst and reactants are in the same, typically the liquid, phase.<sup>[32]</sup> The most common examples applied to this methodology are the reduction of alkynes, olefins and aromatic rings to the corresponding hydrocarbons; aldehydes and ketones to primary and secondary alcohols; respectively, esters and carboxylic acids to aldehydes and alcohols; nitriles to imines and amines as well as amides and nitro compounds to amines. Catalytic hydrogenation as a synthetic strategy originates at the end of the 20<sup>th</sup> century. Pioneering work by French chemist Paul Sabatier disclosed the ability of heterogeneous nickel catalysts to hydrogenate olefins to alkanes.<sup>[33]</sup> In 1912, Sabatier was awarded with the Nobel Prize in Chemistry for his achievements and is nowadays commonly regarded as the father of catalytic hydrogenation.<sup>[34]</sup>

Historically, the first example of a homogeneously catalyzed hydrogenation was reported by Calvin in 1938. Applying simple copper acetate as catalyst and a hydrogen pressure as low as one atmosphere, he was able to reduce 1,4-benzoquinone to 1,4-dihydroxybenzene in quinoline at 100 °C.<sup>[35]</sup> Interestingly, homogeneously catalyzed hydrogenations remained a laboratory curiosity for many years and no significant progress was made.<sup>[36]</sup> However, in 1965, Wilkinson published his seminal report on  $[\text{RhCl}(\text{PPh}_3)_3]$  and its catalytic activity in the hydrogenation of olefins and alkynes.<sup>[37]</sup> This landmark finding is today often reviewed as the origin of modern homogeneous catalysis.<sup>[38]</sup> Subsequently, Schrock and Osborn made profound contributions introducing cationic Ir- and Rh-phosphine complexes, thus paving the way for the development of asymmetric protocols.<sup>[39]</sup> Later, Knowles and co-workers described catalysts featuring chiral bisphosphines for the stereoselective reduction of functionalized olefins.<sup>[40]</sup> Eventually, Noyori developed  $[\text{RuCl}_2(\text{diphosphine})(1,2\text{-diamine})]$  catalysts for asymmetric reductions of prochiral substrates, especially ketones and aldehydes. By exploiting the nowadays famous “metal-ligand bifunctional concept”, the described Ru-complexes offer high turnover numbers, high turnover frequencies and high enantioselectivities.<sup>[41]</sup> In 2001, Knowles and Noyori were awarded with the Nobel Prize in Chemistry for their contributions on asymmetric catalyzed hydrogenation reactions.<sup>[42]</sup>

Nowadays, catalytic homogeneous hydrogenation represents a powerful synthetic methodology. It is widely applied in academia and has multiple applications in industry, mainly for the (enantioselective) synthesis of agrochemicals and pharmaceuticals (Figure 2). The most prominent examples in this respect represent the stereoselective reductions of prochiral



precursors for the preparation of L-Dopa **1** (used for the treatment of Morbus Parkinson) and the herbicide (*S*)-metolachlor **2**, respectively.<sup>[43]</sup>

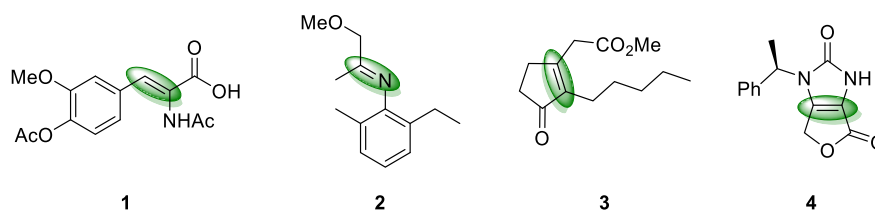


**Figure 2.** Selected examples of industrially relevant homogeneous hydrogenations.

Catalytic homogeneous hydrogenation generally offers various unique advantages over the application of stoichiometric reducing agents, e. g. metal hydrides like LiAlH<sub>4</sub>. It operates under atom-economic and waste-free conditions and moreover utilizes an abundant, environmentally benign, and cheap reductant. Furthermore, the employment of stoichiometric reducing agents is typically attributed with poor chemoselectivities.<sup>[44]</sup> On the contrary, the coordination of an organic ligand to a transition metal fragment results in profound changes of the steric and electronic properties of the central atom. Consequently, this unique principle allows for the design and synthesis of tailor-made catalysts with fine-tuned features e. g. functional group tolerance.

Traditionally, homogenous hydrogenations in academic and industrial setting overwhelmingly rely on platinum group metal phosphine catalysts.<sup>[45]</sup> However, the volatile prices, limited availability, and toxic nature of these elements resulted in extensive efforts by the scientific community for their replacement with more abundant and environmentally alternatives. In the past two decades significant progress in this direction, including stereoselective protocols, has been achieved, particularly with respect to iron<sup>[46]</sup>, cobalt<sup>[47]</sup>, and manganese<sup>[48]</sup> (PNP) pincer complexes. In addition to this, also several examples employing nickel<sup>[49]</sup>, copper<sup>[50]</sup> and zinc<sup>[51]</sup> complexes were reported, highlighting the general aptitude of non-precious metals to serve as catalysts for homogeneous hydrogenation reactions.

### 1.3.1 Pincer Complexes in Catalytic Homogeneous Hydrogenation

The development of novel ligand systems, with which the properties of a metal center can be easily tuned in a predictable fashion, continues to attract significant attention from synthetic chemists. Among the numerous ligand motifs that have been reported in literature, pincer ligands and their respective complexes have been a focal point, due to their remarkable stability, unique activity, and flexibility.<sup>[52]</sup> The first examples of pincer ligands and their respective organometallic coordination compounds were reported in the late 1970s by Shaw and van Koten.<sup>[53]</sup> However, the term “pincer” was coined by van Koten as late as 1989, due

to the distinct coordination mode to metal centers.<sup>[54]</sup> Structurally, pincer complexes feature a metal center whose adjacent coordination sites are occupied by a tridentate ligand, typically in a meridional fashion. Related ligands and organometallic compounds can commonly be prepared within a few steps. Consequently, they can be easily altered and fine-tuned with respect to their steric and electronic properties e.g. by varying the nature of the donor atoms **L** and/or **X**, or the substituents **R** at the donor atoms (Figure 3).<sup>[55]</sup>

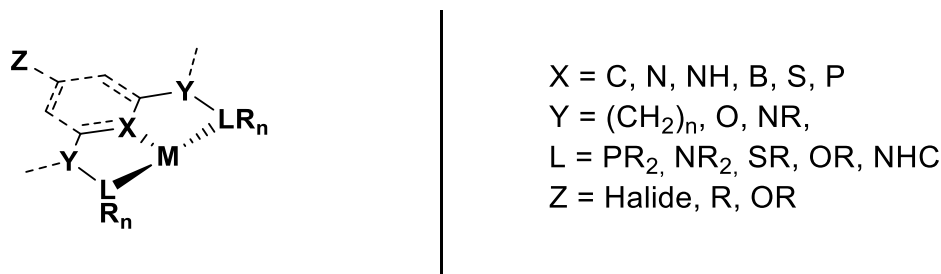
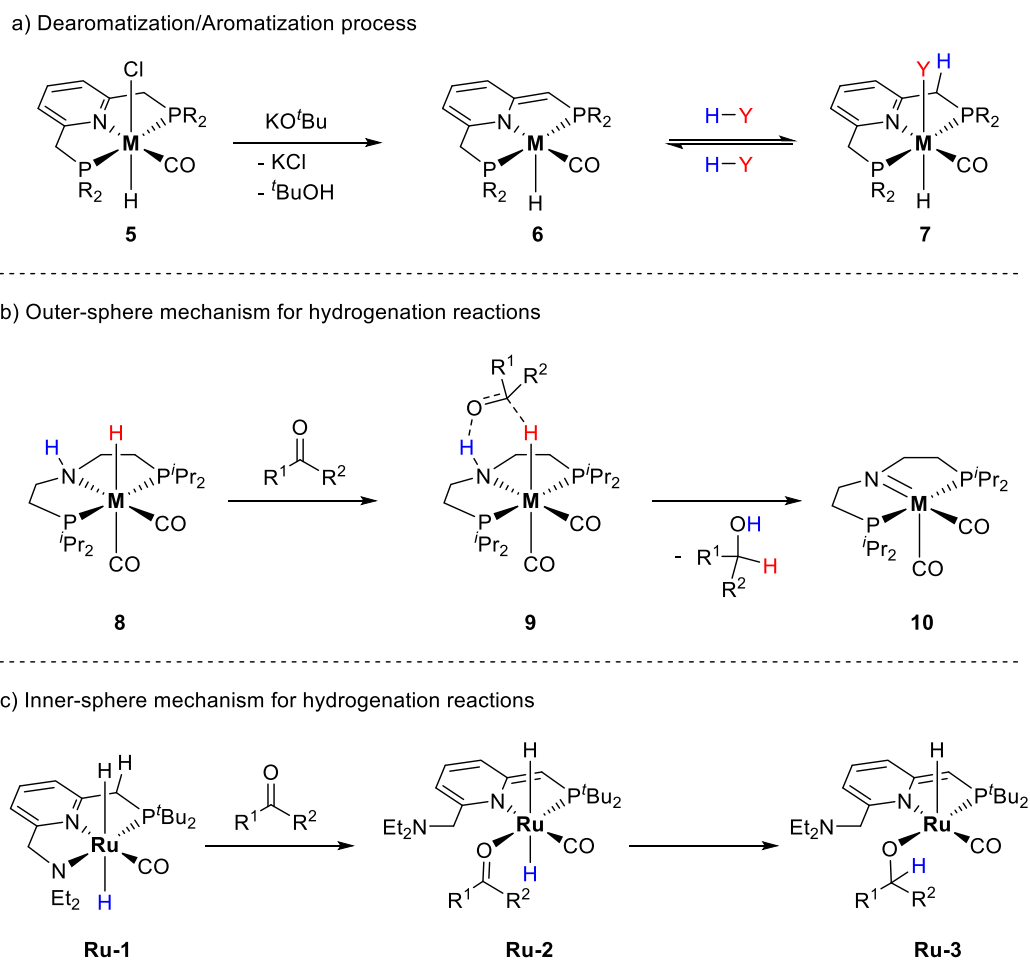


**Figure 3.** General structure of pincer complexes.

A distinct feature of pincer complexes is the ability of the ligand to actively participate in catalytic transformations, without changing the metals oxidation state.<sup>[56]</sup>



**Scheme 2.** Metal-ligand cooperation as well as outer-<sup>[57]</sup> and inner-sphere<sup>[58]</sup> mechanism.

Consequently, pincer ligands are referred to as non-innocent, and the joint reactivity with the metal center is described as metal–ligand cooperation (MLC).<sup>[56]</sup> Pincer complexes featuring a (central) pyridine donor moiety, typically operate through an aromatization/dearomatization mode. The ligand backbone is initially dearomatized upon deprotonation with a base (**6**), and rearomatizes subsequently by the activation of H<sub>2</sub> or dehydrogenation of substrates like alcohols or amines or by C–H bond activation (**7**) (Scheme 2a).<sup>[56b,59]</sup> On the contrary, aliphatic pincer ligands typically proceed *via* amine/amide pathway (Scheme 2b).<sup>[60]</sup> More specifically, bond activation can occur by means of an inner- or outer-sphere mechanism. During an outer-sphere mechanism, no direct metal–substrate interaction is observed (Scheme 2b).<sup>[57]</sup> However, in cases where a direct interaction between the metal center and the substrate takes place the reaction works *via* an inner sphere mechanism (Scheme 2c).<sup>[58]</sup>

### 1.3.1.1 Hydrogenation of Ketones Catalyzed by Base Metal Pincer Complexes

The catalytic hydrogenation of aldehydes and ketones to the corresponding primary and secondary alcohols represents an important synthetic methodology in organic synthesis.<sup>[61]</sup> While noble-metal complexes have long been known to facilitate this transformation<sup>[52a,52b,59a,62]</sup>, the activity of base-metal catalysts featuring pincer ligands represent a rather new discovery in this field. In 2011, Milstein and co-workers reported Fe-PNP catalysts **Fe-1a** and **Fe-1b** (Figure 4) for the hydrogenation of various aliphatic and (hetero)aromatic ketones. Both complexes operate under remarkably mild conditions (0.05 mol% **Fe-1a/Fe-1b**, 0.1 mol% KO<sup>t</sup>Bu, 4.1 atm H<sub>2</sub>, rt, EtOH) and furnish the desired products in high yields. Notably, complex **Fe-1b** represents a dihydride species, which does not require the application of KO<sup>t</sup>Bu as base.<sup>[63]</sup>

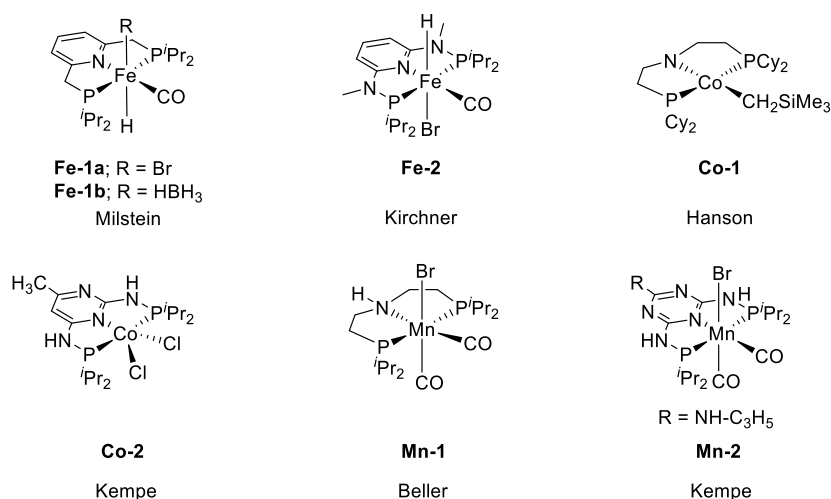
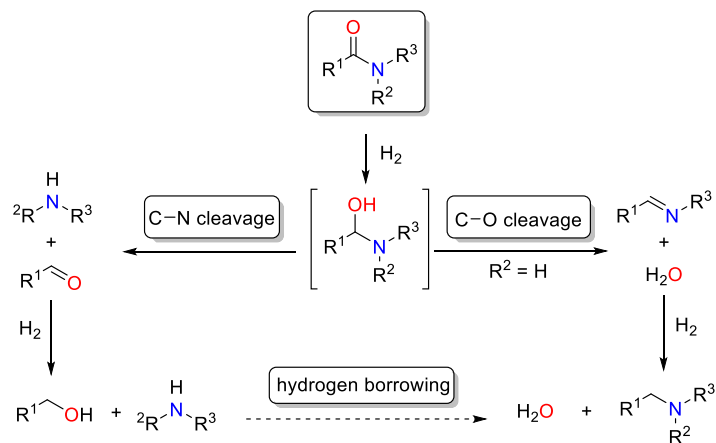


**Figure 4.** Selected examples of base metal pincer complexes, active in the hydrogenation of ketones.

Additionally, the group of Kirchner reported a structurally related iron PNP pincer complex, which was also shown to be active in the hydrogenation of ketones. However, the described system was less active (0.5 mol% **Fe-2**, 1.0 mol% KO<sup>t</sup>Bu, rt, EtOH) and showed a significantly smaller substrate scope.<sup>[64]</sup> In 2012, Hanson and co-workers described the first cobalt PNP catalyst **Co-1** (Figure 4), capable of reducing aliphatic and aromatic ketones to the respective alcohols. The described methodology operates under mild conditions (1 atm H<sub>2</sub>, 25–60 °C, 2 mol% **Co-1**, 24 h) and yields the desired products in nearly quantitative yield. However, the system required the addition of 2 mol% Brookhart's acid.<sup>[65]</sup> Later on, the group of Kempe reported a series of novel cobalt catalysts based on PN<sub>5</sub>P pincer ligands. Among the reported complexes **Co-2** (Figure 4) was found to be the most active example for the hydrogenation of carbonyl groups after activation with NaO<sup>t</sup>Bu. **Co-2** was shown to be a suitable catalyst for the reduction of aryl-alkyl-, diaryl- and aliphatic ketones under mild condition with a good functional group tolerance.<sup>[66]</sup> Additionally, also manganese pincer complexes have been demonstrated to be efficient catalysts for the homogeneous hydrogenation of ketones. In their report, Beller and co-workers described the application of Mn-PNP pincer complex **Mn-1** (Figure 4) as catalysts for the hydrogenation of a series of aliphatic and aromatic ketones. The system displays a good functional group tolerance as esters, amides, and C=C double bonds remain unaffected under the conditions developed.<sup>[67]</sup> Furthermore, Kempe prepared a series of PN<sub>5</sub>P Mn complexes which were active pre-catalysts for the reduction of ketones. Complex **Mn-2** (Figure 4) was shown to be the most active catalyst and subsequently was applied for the hydrogenation of structurally diverse aliphatic and aromatic ketones, with a high functional group tolerance.<sup>[68]</sup>

### 1.3.1.2 Hydrogenation of Amides Catalyzed by Base Metal Pincer Complexes

The transition metal mediated hydrogenation of carboxamides is a highly desirable transformation in homogeneous catalysis. It constitutes an attractive atom-economic and environmentally benign access to amines, which are of importance for the chemical and pharmaceutical industry.<sup>[69]</sup>

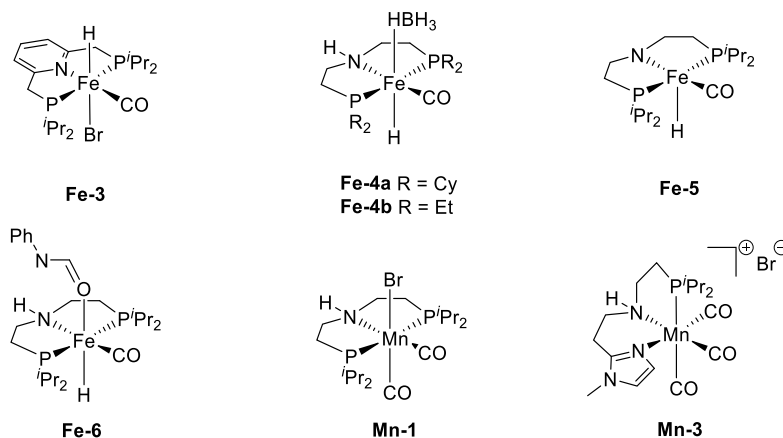


**Scheme 3.** Catalytic pathways for the hydrogenation of amides via C–O and C–N bond cleavage.

However, due to the low electrophilicity of the carbonyl group, amides represent particularly challenging substrates for any hydrogenation reaction. In general, amide hydrogenation can proceed either through C–N (hydrogenolysis) or C–O (hydrogenation) bond scission of an intermediate hemiaminal (Scheme 3). The C–O bond cleavage results in the formation of the alkylated/benzylated amine, producing H<sub>2</sub>O as the only by-product. On the contrary, breaking of the C–N bond yields the free amine and the respective alcohol.<sup>[69]</sup> Moreover, a novel amide hydrogenation pathway was disclosed recently, producing the alkylated/benzylated amine under specific acidic reaction conditions *via* a hydrogen borrowing/autotransfer mechanism.<sup>[70]</sup>

Initially, homogeneous ruthenium catalysts were explored regarding their potential as catalysts for the hydrogenation of amides. Following the seminal work of Cole-Hamilton and co-workers in 2012, several Ru-based systems for the highly selective cleavage of the C–N and the C–O bond, respectively, were described.<sup>[71]</sup> However, despite the remarkable advances regarding catalytic hydrogenations using base metal pincer complexes in recent years, reports on respective amide reductions are scarce. In 2016, the groups of Milstein, Langer and Sanford almost simultaneously published the first examples in this respect, based on iron PNP pincer complexes (**Fe-3** as well as **Fe-4a/b**, Scheme 4). The applied catalysts were shown to induce C–N bond scission in a number of different amides.<sup>[72]</sup> Milstein and co-workers demonstrated that **Fe-3** was a suitable catalyst for the hydrogenolysis of activated aliphatic and aromatic 2,2,2-trifluoroacetamides. However, activation with KHMDS was required and no reactivity was

observed with more common substrates including *N*-phenylacetamide and *N*-phenylbenzamide.<sup>[72a]</sup>



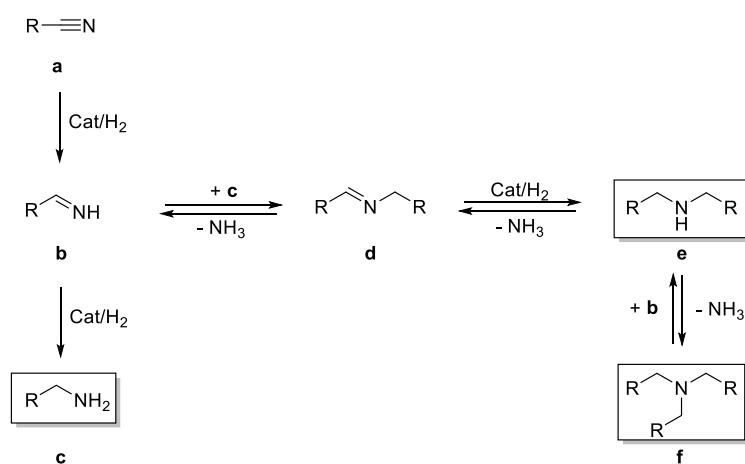
**Scheme 4.** Selected examples of non-noble metal pincer complexes for the catalytic hydrogenation of amides.

In contrast to this, catalysts **Fe-4a**<sup>[72b]</sup> and **Fe-4b**<sup>[72c]</sup> reported by Sanford and Langer, respectively, showed broader substrate scopes and could be utilized also for the hydrogenation of unactivated carboxamides. Bernskoetter and co-workers reported the pentavalent iron PNP-pincer complex **Fe-5** (Scheme 4) for the hydrogenolysis of a several secondary formamides and *N*-formylmorpholine. The system operates with an extremely low catalyst loading (0.018–0.07 mol%) and notably does not require an additional base. Interestingly, it was observed that the activity of **Fe-5** towards otherwise almost unreactive *N*-methylformamide could be significantly enhanced in the presence of 20 equivalents of formamide. Subsequent NMR experiments indicated that the catalyst forms a different resting state in the presence of the additive (**Fe-6**, Scheme 4). Consequently, **Fe-5** is less vulnerable towards deactivating side reactions.<sup>[73]</sup> The observed reactivity was rationalized by computational studies, suggesting that the added formamide assists in the C–N bond scission of the hemiaminal intermediate, which is the rate limiting step.<sup>[74]</sup> The very first example of a manganese catalyzed hydrogenolysis of amides was reported by Beller and co-workers. Upon activation with exogenous base, PNN pincer complex **Mn-3** (Scheme 4) was highly active for the reduction of various secondary and tertiary amides to the corresponding alcohols and amines under relatively mild conditions. Subsequently, also more challenging primary amides were amenable towards the developed methodology. However, more forcing conditions were shown to be necessary to obtain sufficient conversions and yields. Finally, the general applicability of the system was showcased by the successful hydrogenation of herbicide diflufenican.<sup>[75]</sup> In addition to this report, Prakash and co-workers described the hydrogenation

of several formamides to methanol and amines catalyzed by manganese PNP pincer complex **Mn-1** (Scheme 4).<sup>[76]</sup>

### 1.3.1.3 Hydrogenation of Nitriles Catalyzed by Base Metal Pincer Complexes

The reduction of nitriles generally represents an important synthetic strategy for the preparation of diverse amines.<sup>[77]</sup> More specifically, primary amines constitute important intermediates for various applications in organic synthesis as well as in the production of bulk and fine chemicals.<sup>[69]</sup> Consequently, numerous methods for their synthesis starting from nitriles have been described in the literature, among which catalytic homogenous hydrogenation using defined transition-metal complexes is particularly desirable. However, due to the underlying reaction mechanism, the selective catalytic hydrogenation of nitriles to primary amines is particularly challenging (Scheme 5).<sup>[78]</sup> Consequently, the development of novel (catalytic) methodologies for their synthesis continues to be on-going subject of significant relevance. Homogeneous catalysts based on precious metals prevailed for this purpose for many years in both, industrial and academic settings.<sup>[79]</sup> However, in the past two decades vast progress has been achieved regarding their substitution by more abundant and less toxic alternatives, in particular using pincer complexes of Fe, Co and Mn.<sup>[67,78b,80]</sup>



**Scheme 5.** Catalytic pathways for the hydrogenation of nitriles.

In 2014, Beller and co-workers published a report describing the highly selective hydrogenation of nitriles to primary amines catalyzed by iron PNP pincer complex **Fe-4c** (Figure 5). Overall, 41 substrates including aliphatic and (hetero)aromatic derivatives, were smoothly reduced and the desired products were obtained in excellent yields. **Fe-4c** operates under remarkably mild and even base-free conditions. Notably, also of several dinitriles, including industrially relevant adiponitrile, were successfully hydrogenated to the corresponding diamines.<sup>[80a]</sup> The first example of a related transformation, catalyzed by a manganese pincer complex, was disclosed by our group in 2016. Generally, complex **Mn-1** (Figure 5) showed a wide applicability and

aromatic, benzylic, and aliphatic nitriles were shown to be suitable substrates. However, harsher conditions compared to **Fe-4c** were shown to be necessary.<sup>[67]</sup>

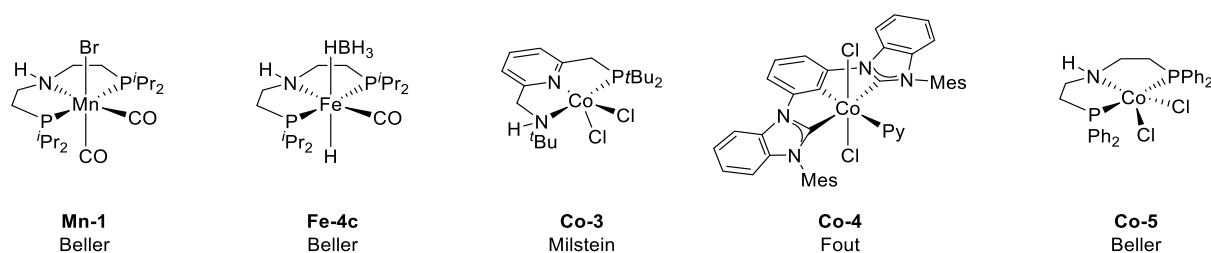


**Figure 5.** Selected examples of non-noble metal pincer complexes for the catalytic hydrogenation of nitriles to primary amines.

Milstein and co-workers demonstrated that **Co-3** (Figure 5) is a suitable catalyst for the selective hydrogenation of nitriles to the corresponding primary amines. Generally, 23 different aromatic and aliphatic nitriles were successfully hydrogenated, and the desired products were obtained in good to high yields. However, in the case of penta- and hexanitride, the formation of the corresponding secondary amines was observed.<sup>[80c]</sup> Fout and co-workers achieved an improved activity based on their air-stable Co(III) complex **Co-4** (Figure 5). Notably, **Co-4** represented the first example of a first-row transition metal complex capable of hydrogenating acetonitrile and *tert*-butylnitrile.<sup>[80g]</sup> Additionally, Beller and co-workers reported an efficient cobalt based PNP pincer complex for the selective hydrogenation of various aliphatic and aromatic nitriles to the respective primary amines. The applied Co catalyst **Co-5** (Figure 5) operates under milder conditions as compared to related cobalt-based systems and only requires the addition of NaBHET<sub>3</sub> to obtain catalytic activity.<sup>[80k]</sup>

## 1.4 Molybdenum (PNP) Pincer Complexes and their Application in Homogeneous Hydrogenations

In the past decade, non-noble metal complexes were investigated extensively for the application as catalysts in homogeneous hydrogenation reactions.<sup>[52b]</sup> Significant progress in this direction was achieved specifically using PNP pincer complexes of iron, cobalt, and manganese.<sup>[63–68,72–73,75–76,80]</sup> The “bifunctional” character of these metal-ligand systems enables a facile H-atom transfer onto polarized unsaturated substrates.<sup>[59c,81]</sup> Molybdenum would offer an attractive contribution to the field of base metal catalysis, given its comparably low cost and environmentally benign nature. However, reports on Mo PNP-pincer complexes were exceptionally scarce for a long time as compared to other metals.<sup>[82]</sup> The first examples of these coordination compounds were described by Haupt and Ellermann in 1987 and 1989, respectively (Figure 6).<sup>[83]</sup> Subsequently, the area remained relatively unexplored and only one additional complexes of this type was prepared as late as 2006.<sup>[84]</sup> Subsequently, efforts by



Kirchner and co-workers, but also the groups of Nishibayashi, Schneider, Jones, Bernskoetter, Berke and others gave access to diverse molybdenum PNP complexes.<sup>[85]</sup> Notably, the reported compounds largely featured pincer ligands with a central pyridine moiety (Figure 6).

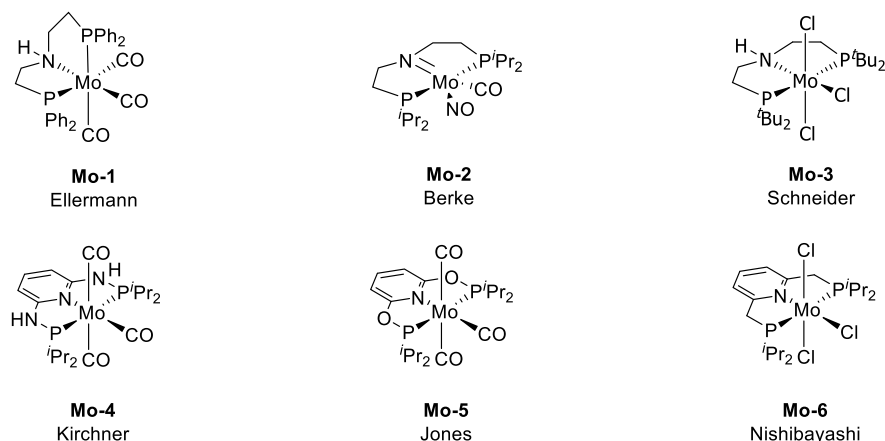
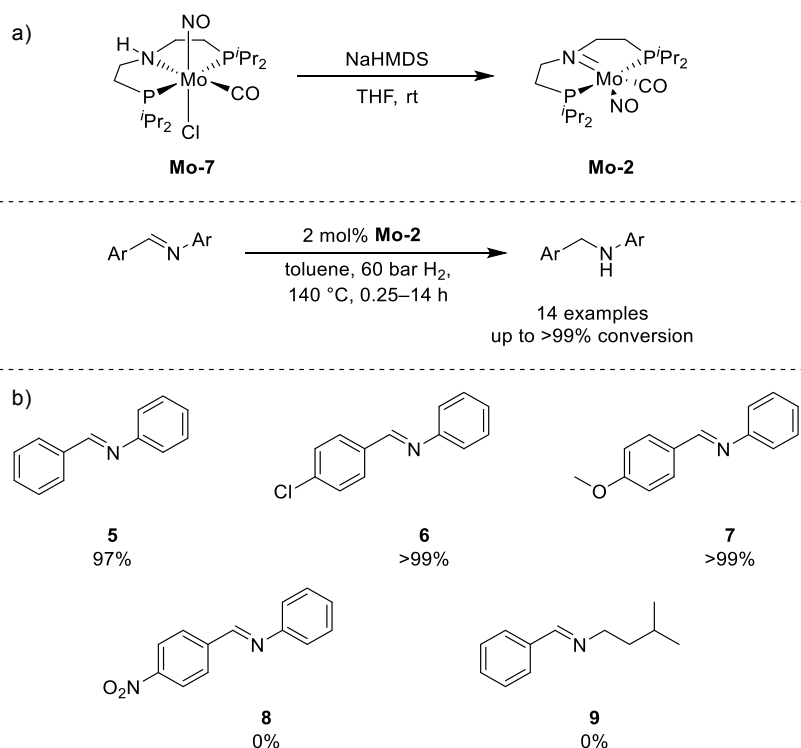


**Figure 6.** Selected examples of molybdenum PNP pincer complexes.

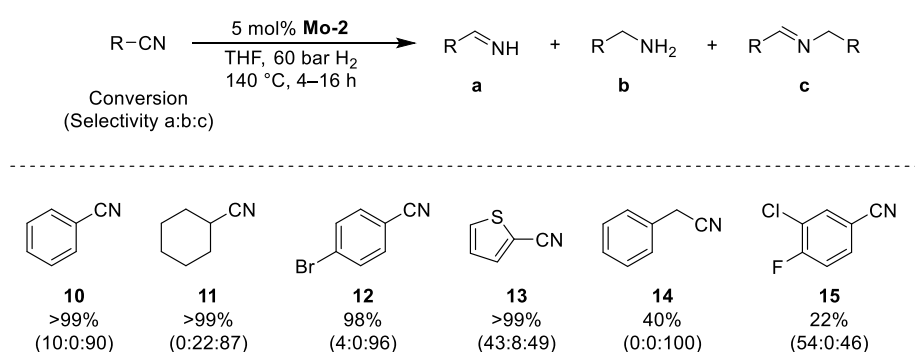
In stark contrast to their organometallic chemistry, reports on the catalytic activity of molybdenum PNP pincer complexes in homogenous hydrogenations continue to be surprisingly rare. In 2016, at the beginning of this thesis, only four reports on this topic were known.<sup>[82,85h,85j,86]</sup>



**Scheme 6.** a) Synthesis of **Mo-2**. b) Selected examples of the hydrogenation of secondary imines catalyzed by **Mo-2**.

In 2014, Berke and co-workers published their seminal work regarding the hydrogenation of secondary imines to the respective amines, catalyzed by the amido complex **Mo-2** (Scheme 6). This organometallic compound is accessible upon treatment of the parental Mo-chloride with NaHMDS (Scheme 6). Interestingly, treatment with KO<sup>t</sup>Bu resulted in the formation of the corresponding alkoxide complex *via* ligand exchange. Applying a catalyst loading of 2 mol% and toluene as solvent at 140 °C and 60 bar H<sub>2</sub>, a series of substrates bearing electron-rich and -poor substituents, were fully hydrogenated to the corresponding amines in less than one hour. However, a *p*-NO<sub>2</sub> substituted (**8**) as well as an aliphatic derivative (**9**) failed to display any catalytic activity (Scheme 6). Notably, the system does not require the addition of an exogenous base for catalyst activation. Moreover, Berke and co-workers also tested **Mo-2** for the hydrogenation of carbonyl compounds, selecting acetophenone and benzaldehyde as benchmark substrates. When acetophenone was applied, 1-phenylethanol was obtained in only 32% yield (3.5 h reaction time, 140 °C, 60 bar H<sub>2</sub> and 1 mol% **Mo-2**). Interestingly, under similar reaction conditions, no hydrogenation products of benzaldehyde were observed at all. [82]

Subsequently, the group of Berke demonstrated, that **Mo-2** was also an efficient catalyst for the hydrogenation of nitriles to secondary imines, including aliphatic cyclohexanecarbonitrile (Scheme 7). Selecting a catalyst loading of 5 mol% and THF as solvent, the system yielded the desired reaction products in modest to high yields and selectivities. Halides, including bromo-substituents (**12**) were well tolerated, and no dehalogenation was observed. However, application of 2-thiophenecarbonitrile (**13**), benzyl cyanide (**14**), and 3-chloro-4-fluorobenzonitrile (**15**) resulted in either poor conversions or selectivities. [86]



**Scheme 7.** Selected examples of the hydrogenation of nitriles catalyzed by **Mo-2**.

Moreover, Berke and Bernskoetter described the ability of molybdenum PNP pincer complexes for the hydrogenation of CO<sub>2</sub> in two independent reports. [85h,85j] Berke's group successfully applied **Mo-2** for the reduction of carbon dioxide to formate in the presence of NaHMDS. However, only stoichiometric reactions could be performed and efforts to conduct catalytic protocols resulted in maximum yields of up to 4%, even at 140 °C. [85h] Similarly, Bernskoetter and co-workers accomplished the reduction of CO<sub>2</sub> to formate, employing a structurally unique

molybdenum PNP complex. The utilized Mo-compound allows for catalytic hydrogenation in the presence of DBU and LiOTf as additives, yielding a maximum TON of 35.<sup>[85j]</sup>

In addition to this, only a handful of reports further demonstrated the potential of molybdenum PNP pincer complexes in catalytic applications. The group of Nishibayashi explored molybdenum based PNP pincer complexes based on pyridines and pyrroles for the reduction of N<sub>2</sub>.<sup>[85b,85d,85q]</sup> Further on, Jones and co-workers developed an acid-mediated isomerization of terminal olefins, catalyzed by PONOP-based hepta-coordinated hydrido-tricarbonyl Mo-PNP complexes.<sup>[85i]</sup>

## 2 Objectives of this work

The development of efficient non-noble metal catalysts featuring PNP pincer ligands for the homogenous hydrogenation of carboxylic acid derivatives has attracted significant attention recently. However, the group six metals Cr, Mo and W have been largely overlooked in this context. Molybdenum in particular would offer an interesting alternative, given its biocompatibility and low cost.<sup>[82]</sup> The organometallic chemistry of molybdenum PNP pincer complexes has been studied intensively for many years and numerous examples have been described to date.<sup>[83–85]</sup> Interestingly, the vast majority feature aromatic ligand structures, while exclusively aliphatic motifs are only scarcely investigated. More importantly, the potential of these organometallic compounds as catalysts for hydrogenations in general has almost been ignored.<sup>[82]</sup> Based on these observations, the present thesis has two focal points:

- (1) Synthesis and characterization of structurally new molybdenum pincer complexes featuring aliphatic (PNP) ligands.
- (2) Investigation of the performance of the prepared catalysts in the catalytic hydrogenation of organic substrates containing reducible C–C and C–X (X = O, N) multiple bonds.

Aside from this, an enantioselective hydrogenation of an industrially relevant intermediate was investigated in cooperation with an internationally known industrial company. The aim of the project was the development of an efficient Ir-based catalyst system, which provides an enantiopure route to the desired target molecule using an industrially feasible catalyst loading.<sup>[87]</sup>

Moreover, based on a recently published iron mediated example, the application of a cobalt based *in situ* catalyst system for the homogeneous hydrogenation of internal and terminal epoxides to *anti*-Markovnikov alcohols was explored here.<sup>[88]</sup>

## 3 Results and Discussion

### 3.1 Synthesis and Characterization of Molybdenum Pincer Complexes

At the beginning of our work we focused on the synthesis of new molybdenum pincer complexes featuring aliphatic PNP pincer ligands **L1–L4** (Figure 7).

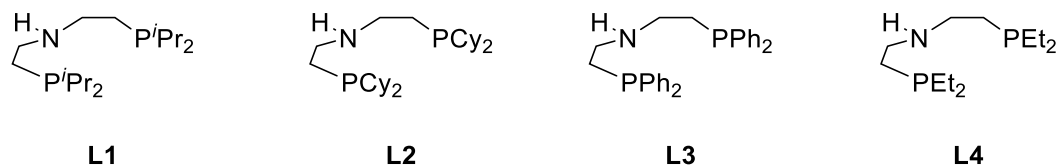
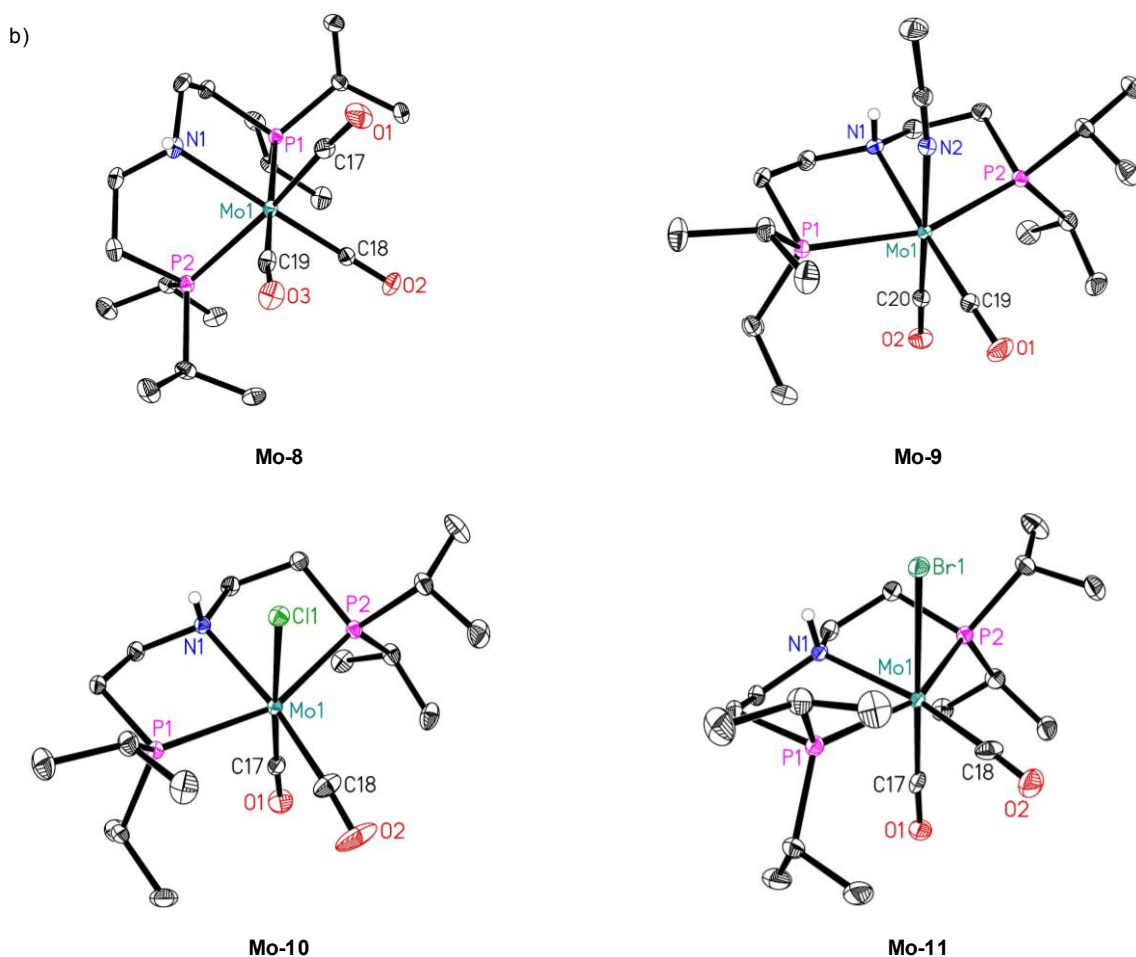
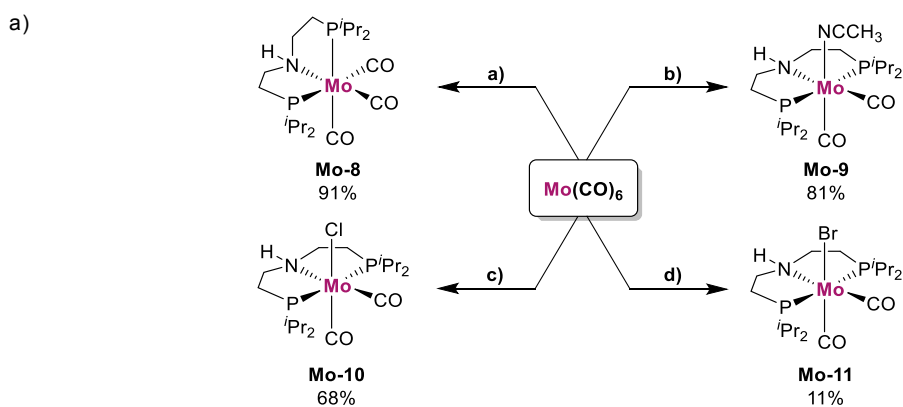


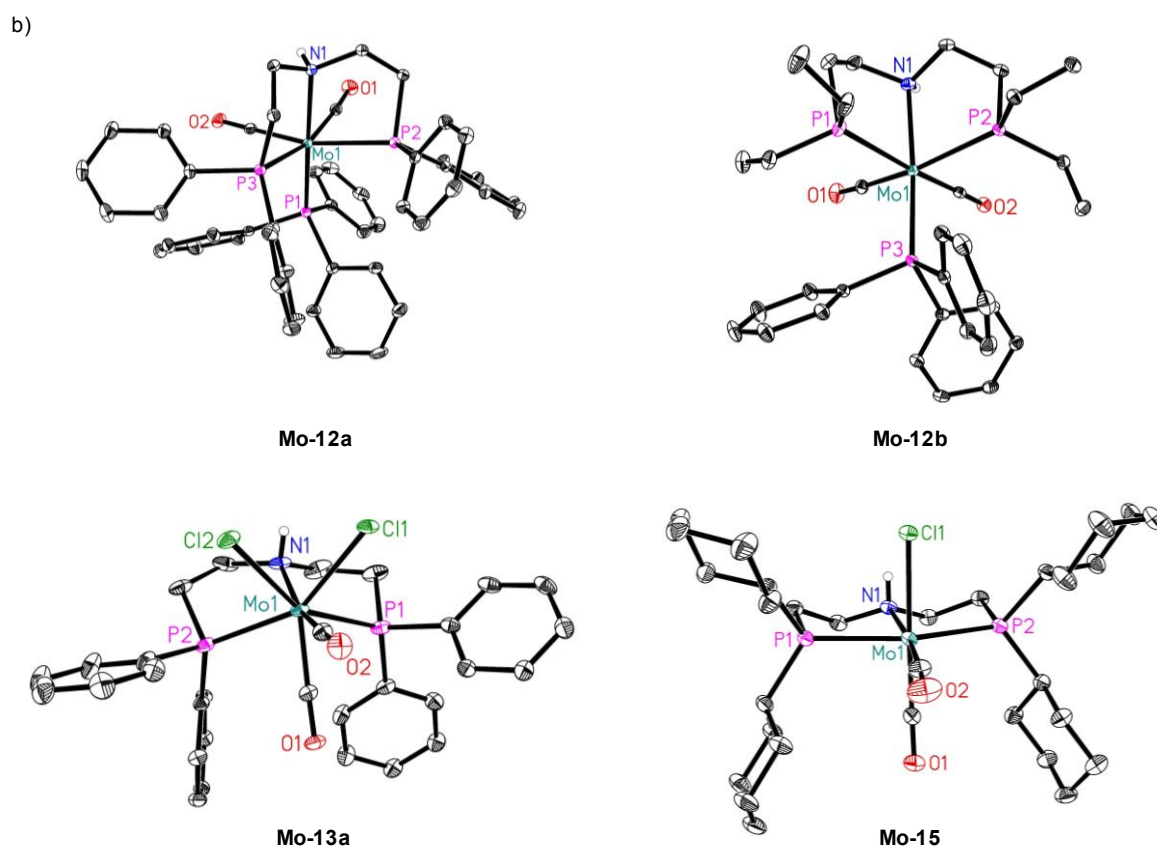
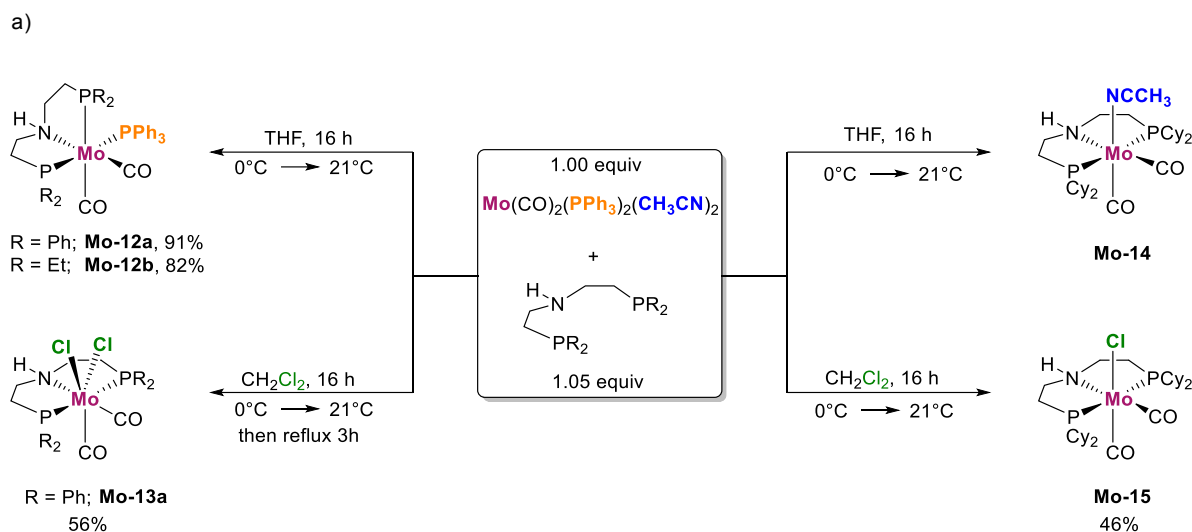
**Figure 7.** Aliphatic PNP pincer ligands **L1–L4** used for the synthesis of Mo-PNP complexes.

Initial efforts reacting commercially available  $\text{Mo}(\text{CO})_6$  and pincer ligand *bis*(2-diisopropylphosphinoethyl)amine **L1** in refluxing toluene resulted in the formation of **Mo-8** (Scheme 8) in 91% yield. Next, in order to prepare structurally and electronically more sophisticated compounds, we tested known molybdenum precursors  $\text{Mo}(\eta^3\text{-allyl})(\text{CO})_2(\text{CH}_3\text{CN})_2\text{Br}$  and  $\text{Mo}(\text{CO})_2(\text{PPh}_3)_2(\text{CH}_3\text{CN})_2$  for the reaction with **L1**. When  $\text{Mo}(\eta^3\text{-allyl})(\text{CO})_2(\text{CH}_3\text{CN})_2\text{Br}$  was treated with a slight excess of **L1** in toluene at room temperature, we were able to isolate the paramagnetic 17-electron complex **Mo-11** (Scheme 8) from the reaction mixture in 11% yield. Interestingly, the molybdenum central atom exists in a formal oxidation number of +I, rather than the anticipated +II state. Next, we investigated  $\text{Mo}(\text{PPh}_3)_2(\text{CO})_2(\text{CH}_3\text{CN})_2$  as the molybdenum precursor for the synthesis of corresponding pincer complexes. Applying THF as the reaction solvent under otherwise identical conditions as reported for the synthesis of **Mo-11**, we observed formation of **Mo-9** (Scheme 8) as a pale-yellow solid in 81% yield. **Mo-9** is an 18-electron complex, featuring a molybdenum(0) atom, which additionally to the pincer ligand, is coordinated by an acetonitrile molecule. During our efforts to prepare crystals of **Mo-9** suitable for X-ray analysis, we were surprised to obtain complex **Mo-10** (Scheme 8) when a mixture of  $\text{CH}_2\text{Cl}_2$ /toluene was used as solvent. Complex **Mo-10** is another example of a 17-electron molybdenum(I) complex, with the chlorine ligand presumably originating from a solvent molecule. Based on this observation, we subsequently aimed at the direct synthesis of **Mo-10**. Accordingly,  $\text{Mo}(\text{PPh}_3)_2(\text{CO})_2(\text{CH}_3\text{CN})_2$  was treated with **L1** in DCM as the reaction media, resulting in the formation of **Mo-10** in 68%, as a pale brownish solid. However, intensive efforts to prepare **Mo-11** analogously by using dibromomethane as solvent and brominating agent, including reaction at  $-78^\circ\text{C}$ , remained unsuccessful. In addition, an envisaged transformation of **Mo-10** into **Mo-11** via chloride/bromide exchange employing KBr and  $\text{NBu}_4\text{Br}$ , respectively, also failed.<sup>[89]</sup>



**Scheme 8.** a) Synthesis of molybdenum PNP complexes **Mo-8**, **Mo-9**, **Mo-10**, and **Mo-11**. a) 1.) Toluene, reflux, 16 h, 1.05 equiv. **L1**; b) 1.) CH<sub>3</sub>CN/benzene, 1.10 equiv. C<sub>3</sub>H<sub>5</sub>Br, reflux, 16 h; 2.) 3.00 equiv. PPh<sub>3</sub>, CH<sub>3</sub>CN, reflux, 1 h; 3.) 1.05 equiv. **L1**, toluene, 23 °C, 16 h; c) 1.) CH<sub>3</sub>CN/benzene, 1.10 equiv. C<sub>3</sub>H<sub>5</sub>Br, reflux, 16 h; 2.) 3.00 equiv. PPh<sub>3</sub>, CH<sub>3</sub>CN, reflux, 1 h; 3.) 1.05 equiv. **L1**, DCM, 23 °C, 16 h; d) 1.) CH<sub>3</sub>CN/benzene, 1.10 equiv. C<sub>3</sub>H<sub>5</sub>Br, reflux, 16 h; 2.) 1.05 equiv. **L1**, toluene, 23 °C, 24 h. b) Molecular structures of **Mo-8**, **Mo-9**, **Mo-10**, and **Mo-11** in the solid state. For **Mo-8**, only one molecule of the asymmetric unit is depicted. Thermal ellipsoids are drawn at 30% probability. Hydrogen atoms, except the *N*-bound, are omitted for clarity.

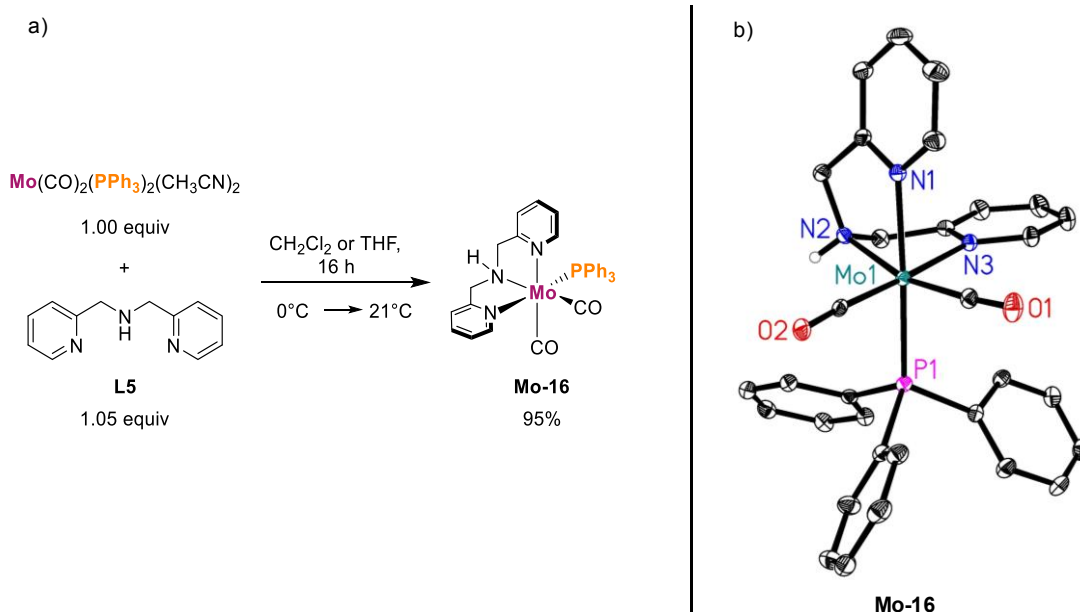
Next, we investigated the observed solvent-dependent reactivity of  $\text{Mo}(\text{PPh}_3)_2(\text{CO})_2(\text{CH}_3\text{CN})_2$  with respect to other aliphatic PNP ligands. For this purpose, *bis*(2-dicyclohexylphosphinoethyl)amine **L2**, *bis*(2-diphenylphosphinoethyl)amine **L3** as well as *bis*(2-diethylphosphinoethyl)amine **L4** were selected and subsequently tested for the reaction with  $\text{Mo}(\text{PPh}_3)_2(\text{CO})_2(\text{CH}_3\text{CN})_2$  in THF and  $\text{CH}_2\text{Cl}_2$ , respectively. Employing **L3** as ligand for the intended transformation in THF under ambient conditions, resulted in a clean reaction and we were able to isolate the Mo(0) complex **Mo-12a** (Scheme 9) in an excellent yield of 91%. Interestingly **Mo-12a**, in contrast to **Mo-9**, features a  $\text{PPh}_3$  moiety coordinated to the central atom instead the expected acetonitrile ligand. A similar reaction pattern was observed in the case of **L4**, yielding the corresponding molybdenum(0) complex **Mo-12b** (Scheme 9) in 81% yield. However, we were unable to synthesize the corresponding acetonitrile derivatives of **Mo-12a** and **Mo-12b**. On the contrary, when **L2** was applied, formation of the intended acetonitrile adduct **Mo-14** (Scheme 9) occurred. When the reaction media was switched to dichloromethane, **L2** again reacted similarly to **L1**, providing access to the corresponding Mo(I)-chloride complex **Mo-15** (Scheme 9) in a modest yield of 42%. Interestingly, treating  $\text{Mo}(\text{PPh}_3)_2(\text{CO})_2(\text{CH}_3\text{CN})_2$  with **L3** in  $\text{CH}_2\text{Cl}_2$  again resulted in the formation of **Mo-12a** according to  $^{31}\text{P}\{^1\text{H}\}$  NMR analysis of the reaction mixture. **Mo-12a** was stable towards chlorination under the applied conditions and remained nearly unaffected even after stirring for several days. Nevertheless, the slow formation of a new singlet resonance at +63 ppm was observed. Hence, the reaction mixture was heated to reflux for three hours. Subsequent analysis by  $^{31}\text{P}\{^1\text{H}\}$  NMR spectroscopy showed that **Mo-12a** was no longer present and revealed the unknown resonance at +63 ppm as the main species. Consequently, we were able to isolate the unknown product and determine its structure, by means of NMR spectroscopy as well as X-ray analysis, to be **Mo-13a** (Scheme 9). Surprisingly, **Mo-13a** represents a hepta-coordinated 18-electron Mo(II)-complex, featuring two chloride ligands attached to the central atom. Similar efforts applying **L4** as ligand remained inconclusive as the formation of complex product mixtures occurred in any case, even at low temperature.<sup>[90]</sup>



**Scheme 9.** a) Synthesis of Mo-PNP complexes **Mo-12a**, **Mo-12b**, **Mo-13a**, **Mo-14** and **Mo-15**. b) Molecular structures of **Mo-12a**, **Mo-12b**, **Mo-13a**, and **Mo-15** in the solid state. For **Mo-15** only one molecule of the asymmetric unit is depicted. Thermal ellipsoids are drawn at 30% probability. Hydrogen atoms, except the *N*-bound are omitted for clarity.

Additionally, also NNN pincer ligand *bis*-(2-pyridylmethyl)amine **L5** was reacted with  $\text{Mo}(\text{PPh}_3)_2(\text{CH}_3\text{CN})_2(\text{CO})_2$  in DCM as well as THF, respectively. Interestingly, no difference in reactivity was observed regarding the applied solvent and complex **Mo-16** (Scheme 10) was obtained in each case. Notably, **Mo-16** is stable towards chlorinated solvents such as DCM and DCE and no chlorinated products were observed even after refluxing for 24 h.<sup>[90]</sup>





**Scheme 10.** a) Synthesis of molybdenum NNN complex **Mo-16**. Molecular structure of **Mo-16** in the solid state. b) Thermal ellipsoids are drawn at 30% probability. Hydrogen atoms, except the *N*-bound are omitted for clarity.

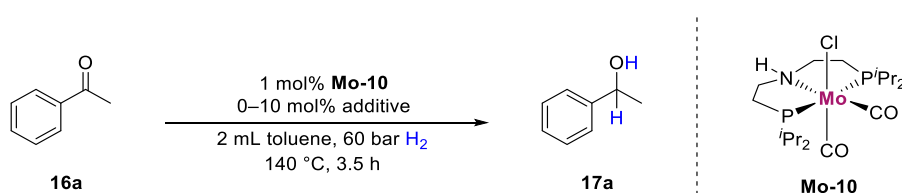
The solid-state structures of all herein reported coordination compounds were determined by X-ray analysis. In general, all described complexes, except for **Mo-13a**, display a distorted octahedral coordination geometry of the donor atoms around the molybdenum center. In complexes **Mo-8**, **Mo-12a** and **Mo-12b** as well as **Mo-16**, the pincer ligand adopts a *fac* geometry around the Mo(0) atom. The remaining coordination sites are occupied by three CO ligands (**Mo-8**) or two CO-ligands and a triphenylphosphine (**Mo-12a**, **Mo-12b** and **Mo-16**), respectively. In the case of **Mo-12a**, **Mo-12b** and **Mo-16**, the CO ligands are in a *cis* orientation to each other. The triphenylphosphine ligand adopts a *trans* orientation to the central nitrogen atom of the pincer backbone in **Mo-12a** and **Mo-12b**. However, in **Mo-16**, a *cis* geometry is observed. The PNP ligands in **Mo-9**, **Mo-10**, **Mo-11** and **Mo-15** all exhibit a *mer* coordination mode with the two carbonyl ligands again displaying a *cis* configuration. Moreover, the chloride- (**Mo-10**, **Mo-15**), bromide- (**Mo-11**) and acetonitrile ligands (**Mo-9**) are all in the corresponding *cis* orientation to the nitrogen atom of the pincer backbone. In hepta-coordinated molybdenum(II) complex **Mo-13a**, the coordination geometry around the molybdenum center can be best interpreted as distorted capped octahedral. The pincer ligand coordinates the metal center in a *meridional* fashion, while a *cis* geometry is observed once again for the CO ligands.

## 3.2 Catalytic Hydrogenations using Molybdenum Pincer Complexes

### 3.2.1 Catalytic Hydrogenations of Ketones and Styrenes

As described in the introduction, Berke and co-workers tested their molybdenum PNP pincer complex for the hydrogenation of acetophenone and benzaldehyde, respectively. However only poor conversions and product yields were reported, even under harsh conditions (1 mol% Mo-catalyst, 140 °C, 60 bar H<sub>2</sub>).<sup>[82]</sup> Due to its structural resemblance to Berke's complex, we first tested our molybdenum(I) catalyst **Mo-10** under similar conditions for the reduction of acetophenone **16**. However, no catalytic activity could be detected using NaHMDS as additive (Table 2, Entry 2). Subsequent attempts in the absence of any additional reagent as well as the presence of 10 mol% KO<sup>t</sup>Bu, respectively, also failed to give any conversion of the starting material (Table 2, Entries 1 and 3). Next, we studied the effect of NaBHET<sub>3</sub> (10 mol%), which is widely applied in pincer chemistry for catalyst activation, on the catalytic performance of **Mo-10**. Interestingly, complete consumption of the starting material was observed after 3.5 h at 140 °C, resulting in the formation of desired product 1-phenylethanol in 97% yield (Table 2, Entry 4). A similar experiment was then conducted using **Mo-9**, providing comparable results regarding conversion and product yield. However, based on practical reasons, we decided to select **Mo-10** for our further investigations.

**Table 2.** Catalytic hydrogenation of acetophenone in the presence and absence of **Mo-10** and selected additives.



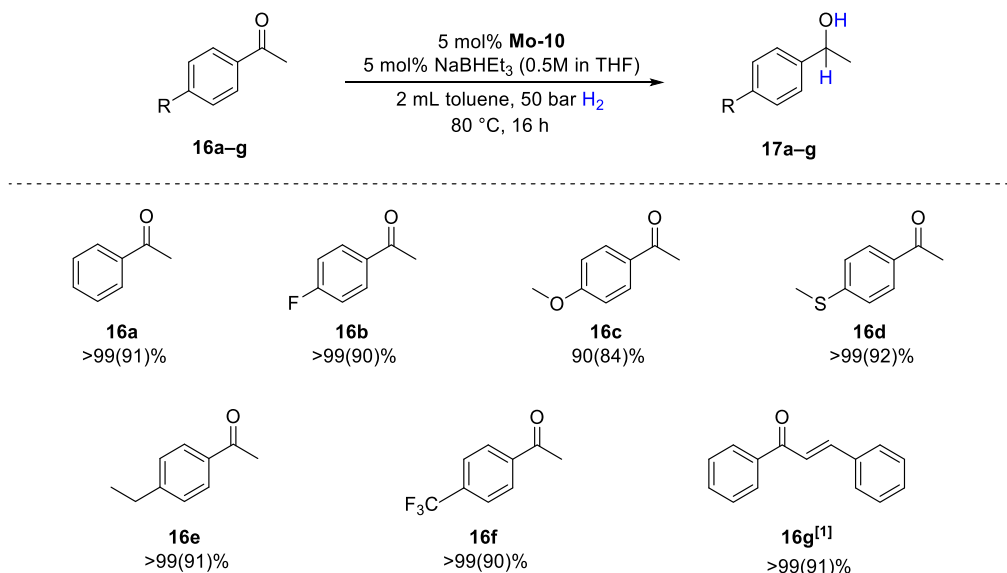
Entry	Additive	Amount [mol%]	Conversion [%] <sup>[1]</sup>	Yield [%] <sup>[1]</sup>
1	–	–	0	<1
2	NaHMDS	10	5	<1
3	KO <sup>t</sup> Bu	10	3	<1
4	NaBHET <sub>3</sub>	10	>99	97
5 <sup>[2]</sup>	NaBHET <sub>3</sub>	10	10	8

Reaction conditions: 0.5 mmol of substrate, 1 mol% **Mo-10**, 0–10 mol% additive, 2 mL toluene, 60 bar H<sub>2</sub>, 140 °C, 3.5 h. <sup>[1]</sup>Determined by GC analysis, using hexadecane as internal standard.

<sup>[2]</sup>Reaction in the absence of **Mo-10**.

A careful optimization of the reaction parameters revealed that full conversion for the benchmark substrate could still be achieved at 80 °C in toluene. However, the reaction had to

be carried out for 16 h with an increased catalyst loading of 5 mol%. Finally, the amount of additive needed for an efficient catalytic performance of **Mo-10** could be reduced to one equivalent with respect to the catalyst. With optimized conditions in hand, we subsequently applied a variety of electronically diverse *para*-substituted acetophenones to our developed methodology (Scheme 11).

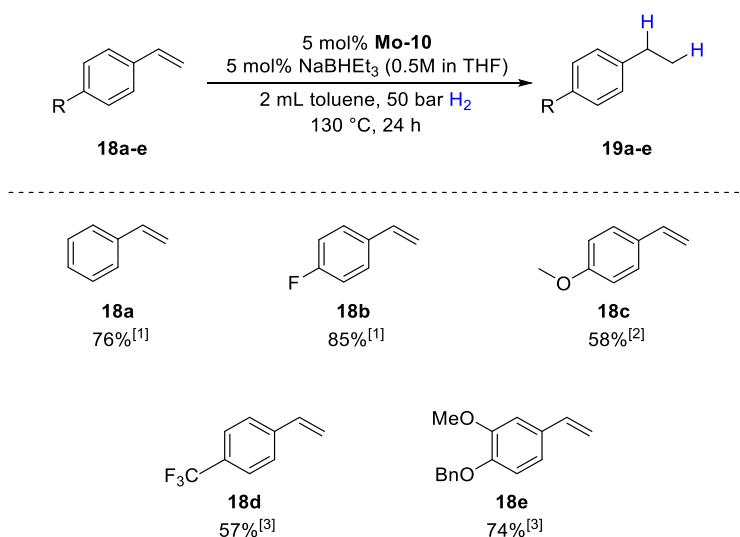


**Scheme 11.** Catalytic hydrogenation of acetophenones in the presence of **Mo-10**/NaBHET<sub>3</sub>. Reaction conditions: 0.5 mmol Substrate, 5 mol% **Mo-10**, 5 mol% NaBHET<sub>3</sub> (0.5M in THF), 2 mL toluene, 50 bar H<sub>2</sub>, 80 °C, 16 h. Conversions were determined by GC using hexadecane as internal standard. Isolated yields in parenthesis. <sup>[1]</sup>Reaction carried out for 24 h. 1,3-diphenyl-1-propanol was obtained as the reaction product.

It could be demonstrated that electron-rich as well as -deficient derivatives work equally well, giving access to the corresponding secondary alcohols in 84–91% isolated yield. No dehalogenation products were detected in case of 4-fluoroacetophenone **16b**. Notably, our catalyst system tolerated the presence of a thioether moiety (**16d**) and no catalyst poisoning effects were observed. Next, we studied the chemoselectivity of our catalyst system, selecting chalcone (**16g**) as a model substrate. However, under the applied conditions, full hydrogenation of both functional groups occurred, and 1,3-diphenyl-1-propanol was obtained in 91% yield.

Subsequently, we decided to probe the general suitability of **Mo-10** for the hydrogenation of unfunctionalized terminal and internal C=C double bonds, selecting 1-dodecene, styrene, and both *cis*- and *trans*-stilbene as benchmark substrates (Scheme 12). Only low catalyst activities were observed in the case of 1-dodecene, *cis*- and *trans*-stilbene, even at 130 °C. However, when more reactive styrene was used as a substrate at 130 °C, we were able to detect

ethylbenzene in a promising yield of 76%. Based on this result, we subjected electron-rich and -poor styrenes to the reaction with **Mo-10**. It could be demonstrated that the applied substrates were hydrogenated in medium to good yields (57–85 %) to the corresponding ethylbenzenes. In agreement with the *vide supra* reported reduction of **16d**, no defluorination products were detected during the hydrogenation of 4-fluorostyrene **18b**. Notably, no cleavage of the benzylether moiety took place when 4-benzyloxy-3-methoxy-styrene **18e** was tested.



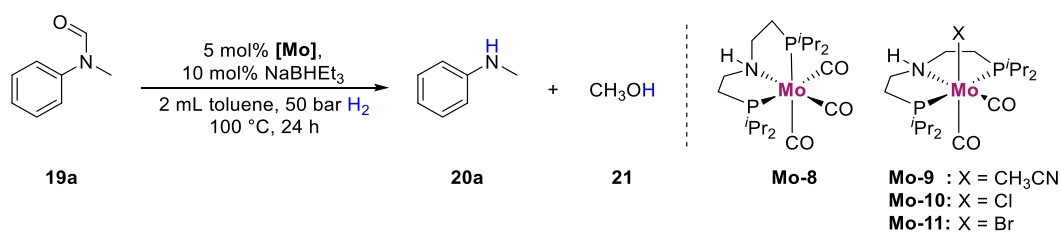
**Scheme 12.** Catalytic hydrogenation of styrenes in the presence of **Mo-10**/NaBHET<sub>3</sub>. Reaction conditions: 0.5 mmol substrate, 5 mol% **Mo-10**, 5 mol% NaBHET<sub>3</sub> (0.5M in THF), 2 mL toluene, 50 bar H<sub>2</sub>, 80 °C, 24 h. <sup>[1]</sup>Yield determined by GC using hexadecane as internal standard. <sup>[2]</sup>Yield determined by <sup>19</sup>F NMR of the reaction mixture using hexafluorobenzene as internal standard. <sup>[3]</sup>Yield determined by <sup>1</sup>H NMR of the reaction mixture using 1,3,5-trimethoxybenzene as internal standard.

More generally, **Mo-10** was tested for the selective hydrogenation of diphenylacetylene and benzonitrile, respectively, applying the conditions reported in Scheme 12. Diphenylacetylene showed a promising conversion of 75%, however formation of a mixture of 1,2-diphenylethane (41%), *cis*- (17%) and *trans*-stilbene (17%) was detected. In the case of benzonitrile a conversion of 42% was observed yielding the secondary imine *N*-benzylidene benzylamine and the benzylamine in 29% and 13%, respectively.

### 3.2.2 Catalytic Hydrogenations of Formanilides

As part of our on-going interest in base metal catalysis, we attempted the molybdenum catalyzed hydrogenation of amides to the corresponding amines and alcohols. Initially, the potential of our Mo-PNP pincer complexes **Mo-8**, **Mo-9**, **Mo-10**, and **Mo-11** for the hydrogenation of *N*-methylformanilide **19a** was evaluated (Table 3).

**Table 3.** Hydrogenation of *N*-methylformanilide **19a** to *N*-methylaniline **20a** and methanol **21** using different [Mo]-catalysts.



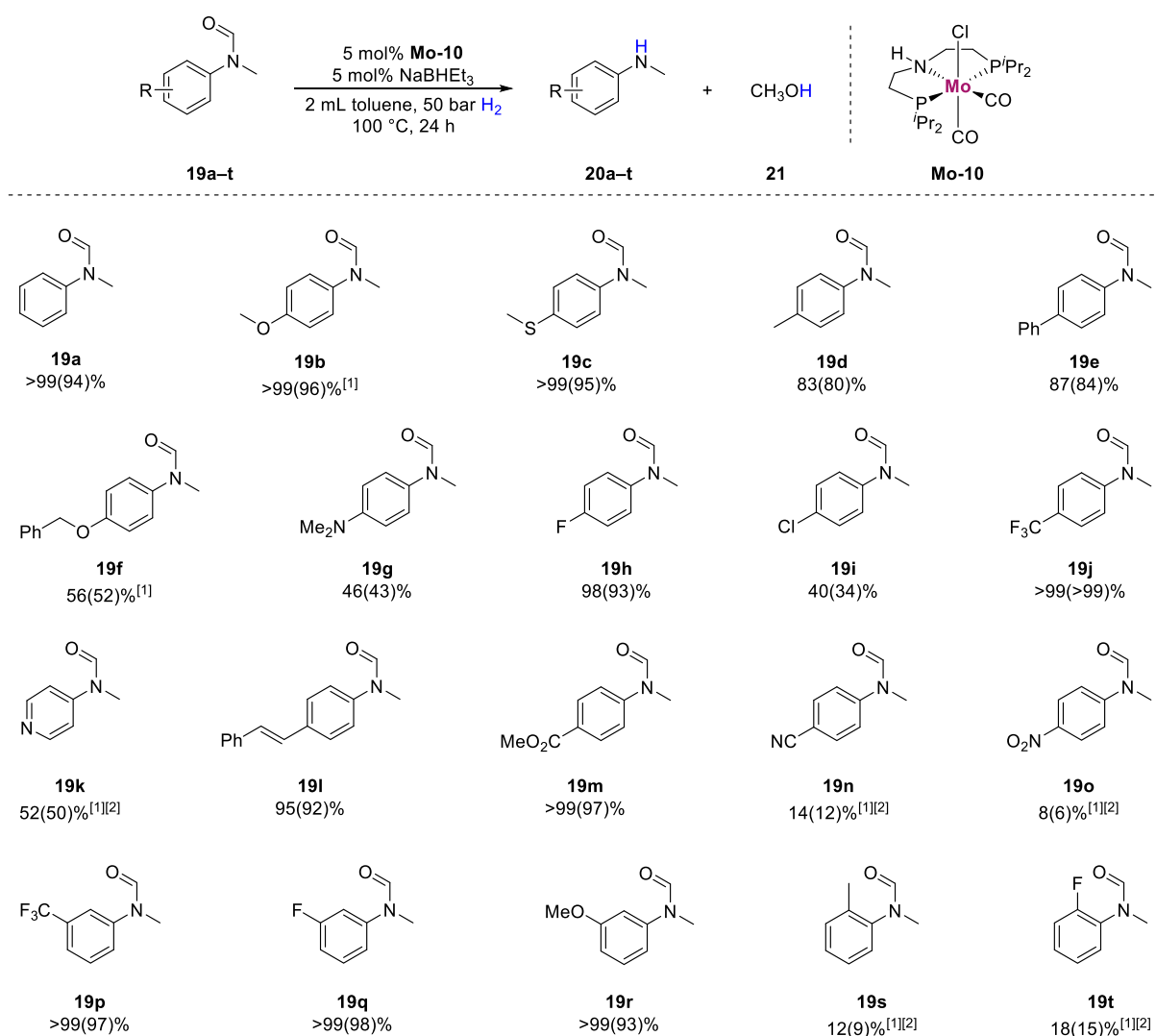
Entry	[Mo]	T [°C]	Conv. 19a [%] <sup>[1]</sup>	Yield 20a [%] <sup>[1]</sup>
1	<b>Mo-8</b>	130	10	9
2	<b>Mo-9</b>	130	>99	99
3	<b>Mo-10</b>	130	>99	99
4	<b>Mo-11</b>	130	>99	99
5 <sup>[2]</sup>	–	130	10	8
6	<b>Mo-10</b>	100	>99	98
7	<b>Mo-11</b>	100	>99	99
8	<b>Mo-9</b>	100	76	73
9	<b>Mo-10</b>	80	>99	99
10	<b>Mo-11</b>	80	>99	99
11 <sup>[3]</sup>	<b>Mo-10</b>	80	49	47
12 <sup>[3]</sup>	<b>Mo-11</b>	80	46	46

Reaction conditions: 0.5 mmol substrate, 5 mol% **Mo-10**, 10 mol% NaBHET<sub>3</sub> (0.5M in THF), 2 mL toluene, 50 bar H<sub>2</sub>, 80 °C, 24 h. Yield of **21** was not determined. <sup>[1]</sup>Determined by GC using hexadecane as internal standard. <sup>[2]</sup>Reaction in the absence of [Mo] catalyst. <sup>[3]</sup>Reaction was performed with 2.5 mol% of [Mo] catalyst.

While catalyst **Mo-8** failed to display any activity at all (Table 3, Entry 1), complexes **Mo-9**, **Mo-10** and **Mo-11** performed equally well under the selected reaction conditions (Table 3, Entries 2–4). A further comparison at reduced temperatures revealed **Mo-10** and **Mo-11** as the most active catalyst systems for the attempted transformation. Interestingly, application of either Mo-complex resulted in almost similar results, suggesting that both catalysts operate *via* the same active species. However, due to the low yielding synthesis of **Mo-11**, catalyst **Mo-10** was

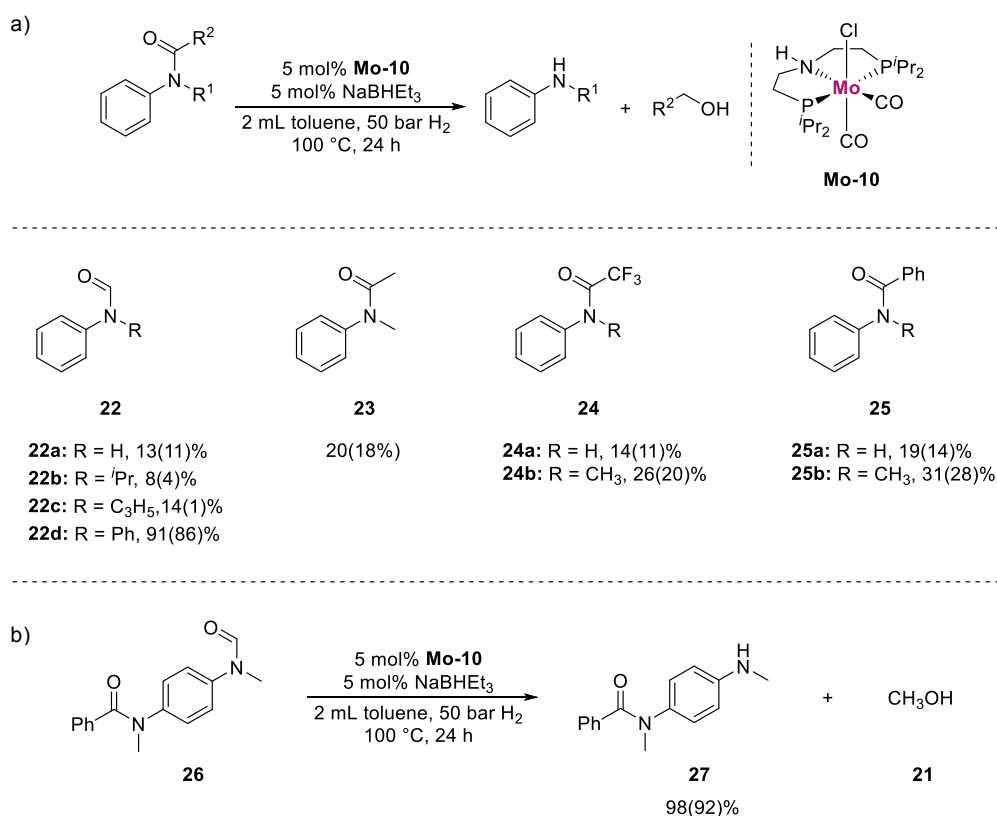
selected for the optimization reactions. Eventually, the desired target molecule *N*-methylaniline **20a** was obtained in 98% yield, applying a combination of 5 mol% of **Mo-10** and NaBHET<sub>3</sub>, respectively, at 100 °C in toluene in the presence of 50 bar H<sub>2</sub> (Table 3, Entry 6).

Next, we explored various *N*-methyl formanilides, bearing electron-donating and -withdrawing substituents (Scheme 13). Gratifyingly, most *meta*- and *para*-functionalized substrates were hydrogenated smoothly under the optimized conditions, yielding the desired *N*-methylanilines in good to excellent isolated yields. On the contrary, substituents in *ortho*-position resulted in significantly lower catalyst activities, even at 130 °C (**19s** and **19t**).



**Scheme 13.** Substrate scope of amide hydrogenation catalyzed by **Mo-10**. Reaction conditions: 0.5 mmol substrate, 5 mol% **Mo-10**, 5 mol% NaBHET<sub>3</sub> (0.5M in THF), 2 mL toluene, 50 bar H<sub>2</sub>, 80 °C, 24 h. Conversions of amides were determined by GC using hexadecane as internal standard. Isolated yields of anilines given in parenthesis. Yields of methanol were not determined. <sup>[1]</sup>Reaction at 130 °C. <sup>[2]</sup>Yield determined by GC using hexadecane as internal standard.

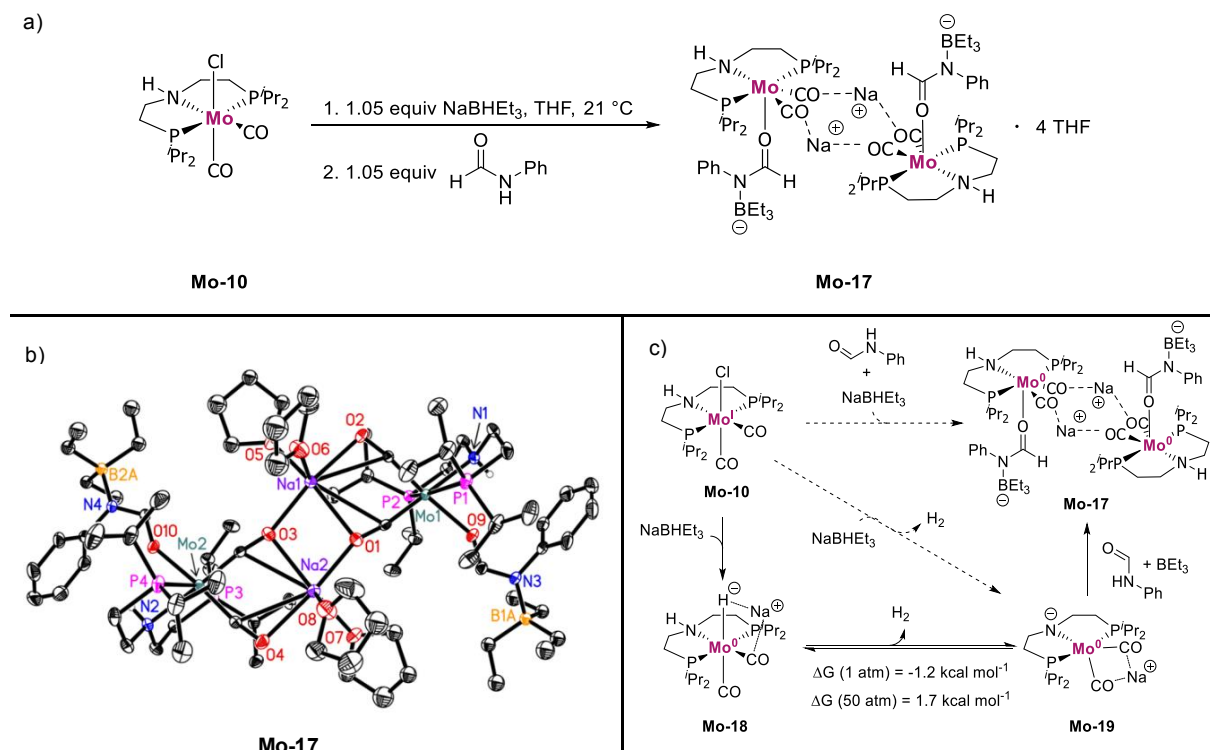
Electron-rich derivatives were shown to be less reactive under the developed methodology and higher temperatures were required in some cases (**19b**, **19f**, **19g**, **19i** and **19m**). The system could tolerate reducible functional groups including fluorides (**19h**), pyridines (**19k**), benzylic ethers (**19f**), C=C double bonds (**19l**) and esters (**19m**), and no competing side reactions were observed. Nevertheless, only low conversions and yields were obtained, when cyano- (**19n**) and nitro- (**19o**) moieties were applied, presumably due to their strongly coordinating nature. Additionally, partial dehalogenation was observed in the presence of chloride substituents (**19i**).



**Scheme 14.** a) Hydrogenation of different amides to the corresponding amines and alcohols catalyzed by **Mo-10**.<sup>[1][2]</sup> b) Selective hydrogenation of a formamide moiety in the presence of another amide catalyzed by **Mo-10**.<sup>[1][3]</sup> Reaction conditions: 0.5 mmol substrate, 5 mol% **Mo-10**, 5 mol% NaBH<sub>4</sub>Et<sub>3</sub> (0.5M in THF), 2 mL toluene, 50 bar H<sub>2</sub>, 80 °C, 24 h. <sup>[1]</sup>Conversions were determined by GC using hexadecane as internal standard. <sup>[2]</sup>Yields were determined by GC using hexadecane as internal standard and refer to anilines. Yields of alcohols were not determined. <sup>[3]</sup>Isolated yield of **27** given, yield of **21** was not determined.

Subsequently, we investigated the broader applicability of our catalyst system with respect to other aromatic amides (Scheme 14). However, with exception of *N,N*-diphenylformamide (**22d**), only modest conversions and yields were obtained, even in the case of activated trifluoroacetamides **24a** and **24b**. Interestingly, significantly lower reactivities were observed for secondary amides (**19a** vs **22a**, **24a** vs **24b**, **25a** vs **25b**), thus hinting at a detrimental effect

of an NH moiety on the catalyst performance. Eventually, based on the observed high preference of our molybdenum catalyst towards *N*-methylated formamides, we attempted a selective hydrogenation in the presence of another amide functionality. Hence, model substrate **26** was prepared and subsequently subjected to our benchmark conditions. Gratifyingly, the desired selective hydrogenolysis of the formamide moiety was observed, yielding target molecule **27** in 93% isolated yield. Notably, the benzamide moiety remained molecularly unaffected.



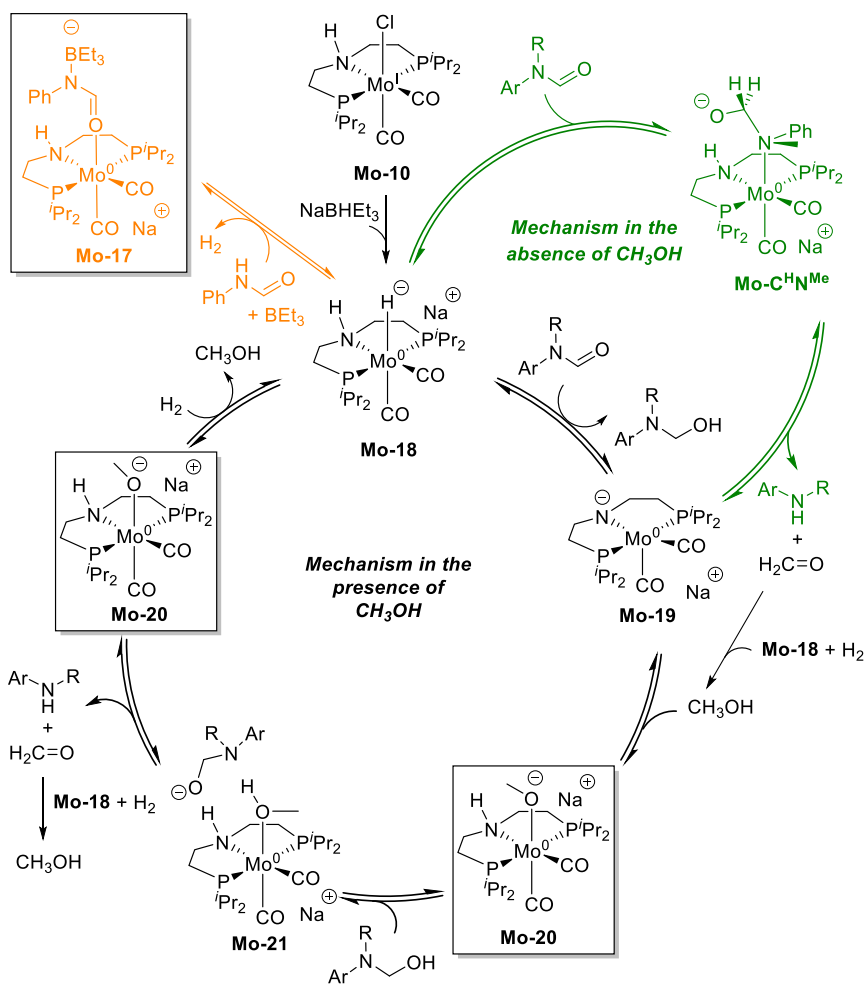
**Scheme 15.** a) Synthesis of catalytic intermediate **Mo-17** from **Mo-10**. Reaction conditions: 1.) 100  $\mu$ mol **Mo-10**, 105  $\mu$ mol NaBHET<sub>3</sub> (1M in THF), 10 mL THF, 21 °C, 1 h. 2.) 105  $\mu$ mol *N*-formylaniline, 21 °C, 1 h. b) Molecular structure of **Mo-17** in the crystal. Only one molecule of the asymmetric unit is depicted. Displacement ellipsoids correspond to 30% probability. Hydrogen atoms except the *N*-bound are omitted for clarity. c) Control experiments to get insight on the active catalyst species (dashed arrows) with the experimentally observed products (H<sub>2</sub> and the crystal structure of **Mo-17**) and the intermediates proposed (**Mo-18** and **Mo-19**). Gibbs energies calculated for the dehydrogenation of **Mo-19** at different pressure.

Next, we became interested in the nature of the active catalyst species and subsequently performed a series of control experiments for this purpose. In the course of our investigations, we noticed rapidly occurring gas evolution upon the treatment of **Mo-10** with NaBHET<sub>3</sub>. This gas could either be H<sub>2</sub> (formed e.g. by deprotonation of the pincer ligand with NaBHET<sub>3</sub>) or CO (via replacement of a carbonyl ligand with a hydride). Consequently, a scale up experiment (100  $\mu$ mol of **Mo-10**) was conducted and the obtained gas was analyzed by GC, revealing it to



be dihydrogen. Hence, we concluded, that **Mo-10** presumably forms a pincer amido species, which was additionally supported by analysis of the reaction mixture *via* HR-ESI mass spectrometry. Furthermore, we investigated the catalyst's poor reactivity regarding secondary amides in more detail. Carrying out a stoichiometric control experiment, using parental formanilide **22a** as substrate, we were able to isolate catalyst-substrate complex **Mo-17** from the reaction mixture (Scheme 15). Interestingly, **Mo-17** features two molybdenum centers in the formal oxidation states of (0), with the NH moieties of the pincer ligands being intact. The obtained structure suggests that a redox reaction has taken place at some point during the activation/reaction sequence. Therefore, **Mo-10** was analyzed by means of EPR spectroscopy after activation with NaBHET<sub>3</sub>. However, no signal of a paramagnetic species could be detected, indicating, that the observed reduction of the molybdenum central atom already occurs at this stage. A potential mechanism was proposed based on DFT calculations, using the M06 functional, including toluene solvation by the SMD model (Scheme 15). It could be shown that the hydrogenation of **Mo-19** to give **Mo-18**, is nearly isoenergetic, revealing a small preference for **Mo-19** at 1 bar and for **Mo-18** at 50 bar H<sub>2</sub>, respectively. These results are in agreement with the observed evolution of H<sub>2</sub> during the catalyst activation. Finally, the potential role of **Mo-17** in the catalytic cycle was reviewed by carrying out the benchmark reaction in the presence of 2.5 mol% of **Mo-17**. Gratifyingly, full conversion of **19a** was observed and we were able to isolate *N*-methylaniline **20a** in 92 % yield.

Moreover, the general reaction mechanism of the **Mo-10** catalyzed hydrogenolysis of amides was calculated by computational studies (Scheme 16). Generally, two different reaction pathways were considered. In absence of alcohol, the molybdenum catalyst induces the reduction of the amido carbonyl group to the corresponding hemiaminal and facilitates the subsequent cleavage of the C–N bond (green cycle). *N*-methylaniline is obtained as the reaction product alongside formaldehyde, which is further reduced to methanol by **Mo-18**. Catalyst **Mo-19** can then add another molecule of H<sub>2</sub> and induce another catalytic cycle. In the presence of alcohol, however, a Mo-alkoxide species (**Mo-20**) is formed, which represents the catalyst's resting state. **Mo-20** reacts with a hemiaminal to form **Mo-21**, which then assists in the following cleavage of the hemiaminal C–N bond and thus regenerates **Mo-20**. Eventually the active catalyst is regenerated by methanol displacement upon reaction of **Mo-20** with H<sub>2</sub>. Presumably, the catalyst adopts a different resting state when secondary amides are applied. Here, a reaction with **Mo-18** results in the formation of a relatively stable a catalyst-substrate complex (**Mo-17**) that inhibits the catalytic activity.

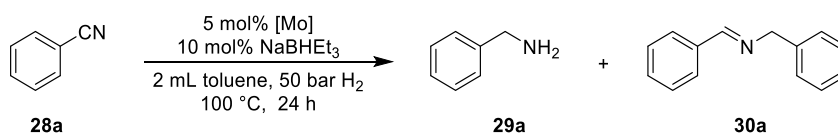


**Scheme 16.** General mechanism for the amide hydrogenation in the absence (green) and presence (black) of methanol. Squares indicate the catalyst resting state in the presence of MeOH and substrate (orange).

### 3.2.3 Catalytic Hydrogenations of Nitriles

During our investigations regarding the hydrogenation of ketones and styrenes, mediated by **Mo-9**, we also tested the catalyst's suitability for the selective reduction of benzonitrile **28a** to benzylamine **29a**. Applying 130 °C and 5 mol% catalyst loading in toluene, a modest conversion of 42% was observed. However, the system showed a poor product selectivity with respect to the intended primary amine (13%).<sup>[89]</sup> Assuming that catalyst decomposition might be a problem, we reinvestigated the desired transformation employing molybdenum complexes **Mo-8–Mo-16** under milder conditions (100 °C), alongside 10 mol% of NaBHET<sub>3</sub> (Table 4, Entries 1–13).

**Table 4.** Initial screening of [Mo]-catalysts and reaction parameters.



Entry	[Mo]	Conversion [%] <sup>[1]</sup>	Yield <b>29a</b> [%] <sup>[1]</sup>	Yield <b>30a</b> [%] <sup>[1]</sup>
1	<b>Mo-9</b>	>99	58	40
2	<b>Mo-10</b>	>99	52	42
3	<b>Mo-12a</b>	62	38	20
4	<b>Mo-12b</b>	70	41	24
5	<b>Mo-13a</b>	<1	<1	<1
6	<b>Mo-15</b>	78	41	35
7	<b>Mo-16</b>	<1	<1	<1
8 <sup>[2]</sup>	<b>Mo-9</b>	90	50	38
9 <sup>[2]</sup>	<b>Mo-10</b>	81	42	35
10 <sup>[3]</sup>	<b>Mo-9</b>	>99	55	41
11 <sup>[4]</sup>	<b>Mo-9</b>	>99	96	<1
12 <sup>[5]</sup>	<b>Mo-9</b>	4	<1	<1
13 <sup>[6]</sup>	–	7	<1	<1

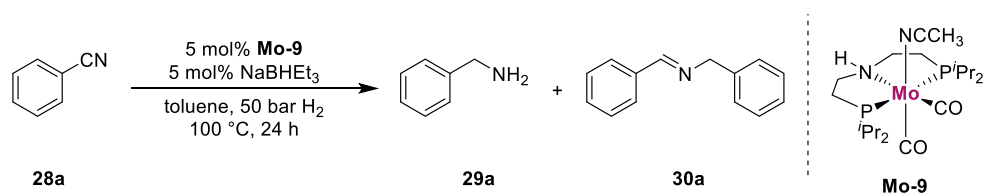
Reaction conditions: 0.5 mmol substrate, 5 mol% [Mo]-catalyst, 10 mol% NaBHET<sub>3</sub> (1M in THF), 2 mL toluene, 50 bar H<sub>2</sub>, 80 °C, 24 h. <sup>[1]</sup>Determined by GC using hexadecane as internal standard.

<sup>[2]</sup>80 °C. <sup>[3]</sup>5 mol% NaBHET<sub>3</sub> (0.5M in THF). <sup>[4]</sup>0.5 mmol substrate, 5 mL toluene. <sup>[5]</sup>No NaBHET<sub>3</sub> added. <sup>[6]</sup>No catalyst was used.

The most promising results were obtained using **Mo-9** and **Mo-10**, respectively, while all other catalysts either gave incomplete conversion of the starting material or displayed no catalytic activity at all. Nevertheless, despite showing promising activities, **Mo-9** and **Mo-10** were not selective under the reported conditions and **29a** and **30a** we observed as approximately 1:1

mixture in both cases (Table 4, Entries 1 and 2). Subsequent experiments eventually showed **Mo-9** to be the more active catalyst, as compared to **Mo-10**. In the due course of the optimization, a solvent screening revealed toluene to be the solvent of choice. Interestingly, no product formation was observed in *i*PrOH, which is among the most common solvents used in base metal catalyzed hydrogenations of nitriles.<sup>[67,80a,80d]</sup> Additionally, the amount of additive could be reduced to 5 mol% without any loss in catalyst activity. Finally, we probed the influence of the substrate concentration on the reaction outcome. Hence, in a series of experiments, the volume of the toluene was varied from 1–6 mL, corresponding to concentrations of **28a** from 0.08–0.5M (Table 5).

**Table 5.** Screening of different substrate concentrations.



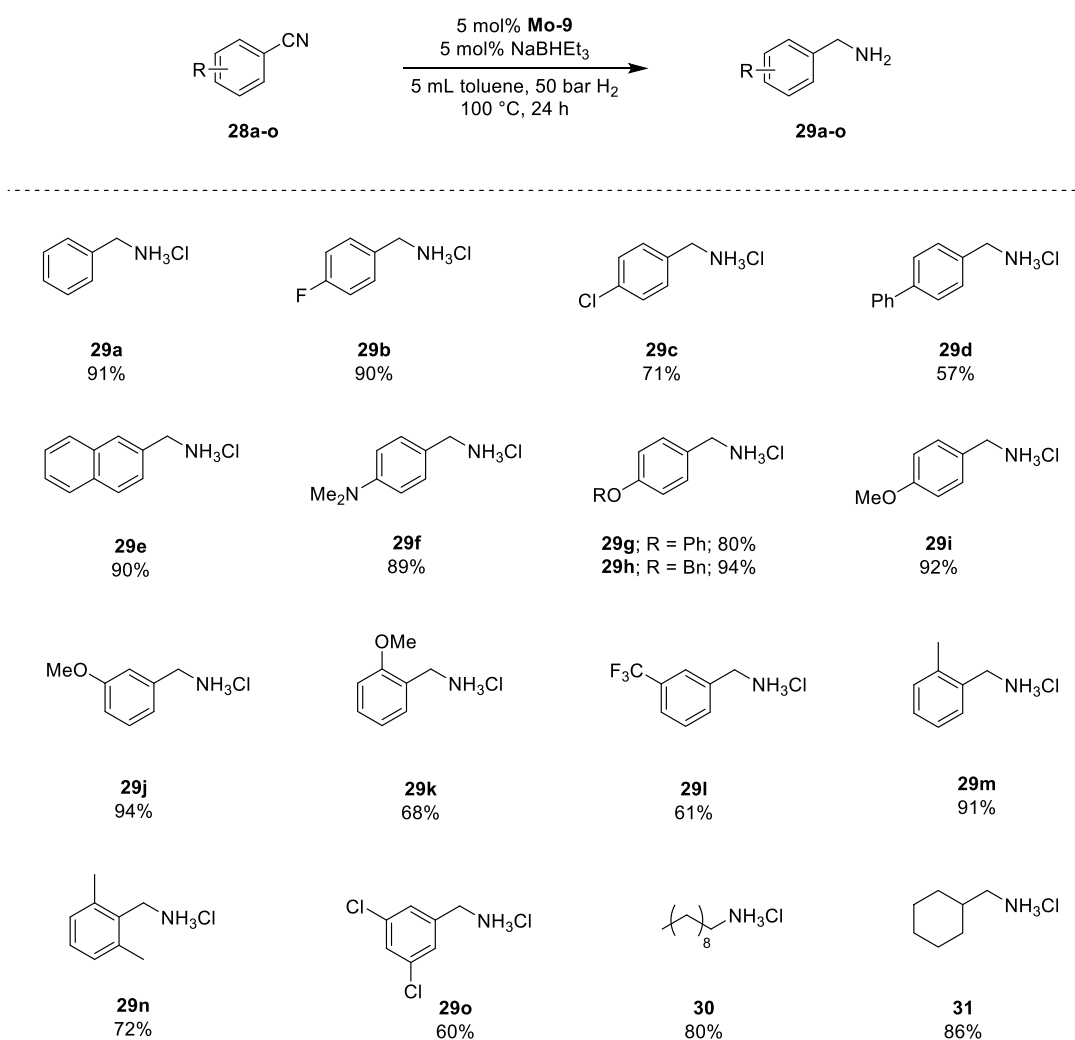
Entry	V [mL]	Conc. [M]	Conv. [%] <sup>[1]</sup>	Yield <b>29a</b> [%] <sup>[1]</sup>	Yield <b>30a</b> [%] <sup>[1]</sup>
1	1	0.50	>99	20	72
2	2	0.25	>99	58	40
3	3	0.17	>99	62	38
4	4	0.13	>99	79	13
5	5	0.10	>99	96	<1
6	6	0.08	90	87	<1

Reaction conditions: 0.5 mmol substrate, 5 mol% **Mo-9**, 5 mol% NaBHET<sub>3</sub> (0.5M in THF), 1–6 mL toluene, 50 bar H<sub>2</sub>, 80 °C, 24 h. <sup>[1]</sup>Determined by GC using hexadecane as internal standard.

As summarized in Table 5, deviations from the originally used solvent amount (2 mL, 0.25M) resulted in profound changes of the observed product selectivity. Increasing the dilution favored the formation of the desired primary amine **29a**, while decreasing it had a negative impact on the desired reactivity. Optimal results were obtained at a concentration of 0.1M. Here, full conversion of the starting material was still achieved, while the yield of benzylamine **29a** improved to 96%. When the amount of toluene was further increased, a drop of the catalyst activity occurred.

Next, we tested the general applicability of our developed methodology for the hydrogenation of electronically diverse benzonitriles (Scheme 17). Generally, it could be demonstrated that **Mo-9** is particularly well suited for the catalytic reduction of electron rich derivatives. Substitution in the *ortho*-, *meta*-, and *para*-positions were shown to have only minor influences on the catalytic performance of **Mo-9**. Notably, even a sterically more hindered substrate **28n** bearing

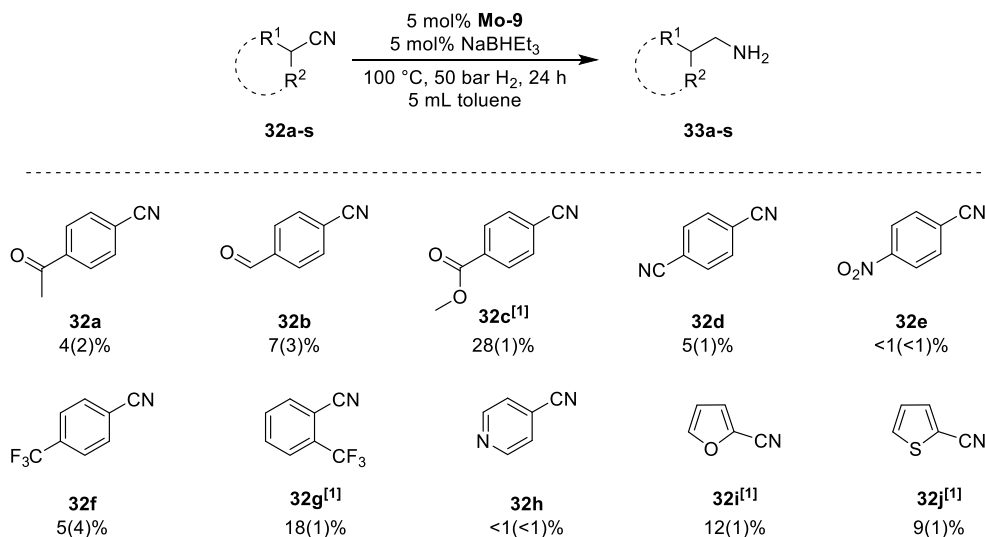
substituents in both ortho positions was hydrogenated smoothly without harsher conditions being required. Moreover, sensitive functional groups were tolerated well. No cleavage of benzylic ethers and dehalogenation of chlorides could be detected. In addition, we were able to demonstrate the applicability of our catalyst system for the hydrogenation of aliphatic nitriles. Decanitrile and cyclohexylcarbonitrile were successfully reduced in the presence of **Mo-9** to the corresponding primary amines **30** and **31** in 80% and 86% yield, respectively.



**Scheme 17.** Substrate scope for nitrile reduction catalyzed by **Mo-9**. Reaction conditions: 0.5 mmol substrate, 5 mol% **Mo-9**, 5 mol% NaBHET<sub>3</sub> (0.5M in THF), 5 mL toluene, 50 bar H<sub>2</sub>, 80 °C, 24 h. Isolated yields given.

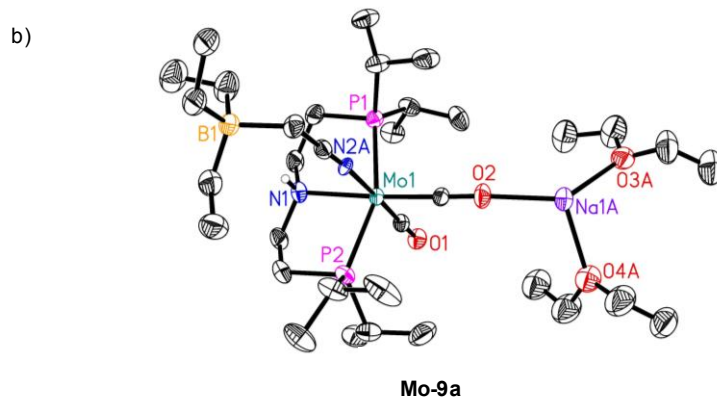
On the contrary, benzonitriles featuring electron-deficient groups, including carbonyl- (**32a** and **32b**), CO<sub>2</sub>Me- (**32c**), CN- (**32d**), NO<sub>2</sub>- (**32e**), and CF<sub>3</sub>- (**32f** and **32g**), and were significantly less reactive under our reaction conditions (Scheme 18). Here, only poor conversions and product yields were obtained. However, *meta*-CF<sub>3</sub>-substituted nitrile **28l** constituted an exception to this trend, as its corresponding primary amine could be isolated in 61% yield.

Moreover, we tested pyridine (**32h**), furan (**32i**), and thiophene (**32j**) based heteroaromatic derivatives. However, the desired primary amines could not be detected.



**Scheme 18.** Selected examples of unsuccessful nitriles. Reaction conditions: 0.5 mmol substrate, 5 mol% **Mo-9**, 5 mol%  $\text{NaBHET}_3$  (0.5M in THF), 5 mL toluene, 50 bar  $\text{H}_2$ , 80 °C, 24 h. Conversions and yields (in parenthesis) were determined by GC using hexadecane as internal standard. <sup>[1]</sup>Secondary imine was detected as the main product.

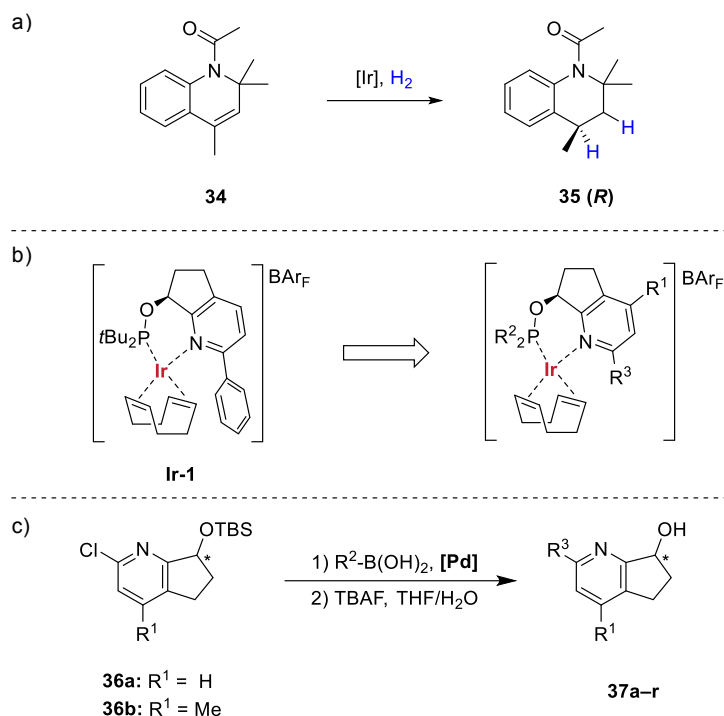
Finally, to understand the structural nature of the organometallic species formed upon the reaction of the pre-catalyst with the applied additive, a stoichiometric control experiment was conducted (Scheme 19). Therefore, 0.5 mmol of **Mo-9** were treated with two equivalents of  $\text{NaBHET}_3$  under ambient conditions using toluene as solvent. The formation of a clear, intensely red solution was observed within less than one minute, indicating a rapidly proceeding reaction.  $^{31}\text{P}\{^1\text{H}\}$  NMR spectroscopy after one hour revealed complete consumption of **Mo-9** and the formation of a new singlet resonance at +74 ppm. We were subsequently able to obtain crystals suitable for X-ray analysis from the reaction mixture, which then provided the solid-state structure of **Mo-9a**. Evidently,  $\text{NaBHET}_3$  reacts as a base and deprotonates the catalyst precursor **Mo-9**. However, the deprotonation occurs at the  $\text{CH}_3$ -group of the coordinated acetonitrile ligand, while the NH moiety of the pincer backbone remains surprisingly unaffected. Ultimately, to verify the role of **Mo-9a** in the catalytic cycle, the benchmark reaction was performed employing 5 mol% of **Mo-9a** in the absence of any additive. Remarkably, we observed full conversion of **28a** and formation of benzylamine **29a** as the sole reaction product in 92% yield.



**Scheme 19.** a) Synthesis of **Mo-9a**. b) Solid state structure of **Mo-9a**. Thermal ellipsoids are drawn at 30% probability level. Hydrogen atoms, except the *N*-bound are omitted for clarity. Disordered parts of the molecule are only shown in one orientation.

### 3.2.4 Ir-Catalyzed Enantioselective Hydrogenation of an Agrochemical Building Block

The enantioselective hydrogenation of unactivated, sterically hindered C=C bonds represents a challenging task in catalysis. Traditionally, the best results are obtained using chiral Crabtree/Pfaltz-type Iridium catalysts.<sup>[91]</sup> The development of an efficient Ir-based catalyst for the stereoselective synthesis of chiral tetrahydroquinoline **35**, needed for the synthesis of an agrochemical, *via* enantioselective hydrogenation of **34** was the aim of this project (Scheme 20, a).

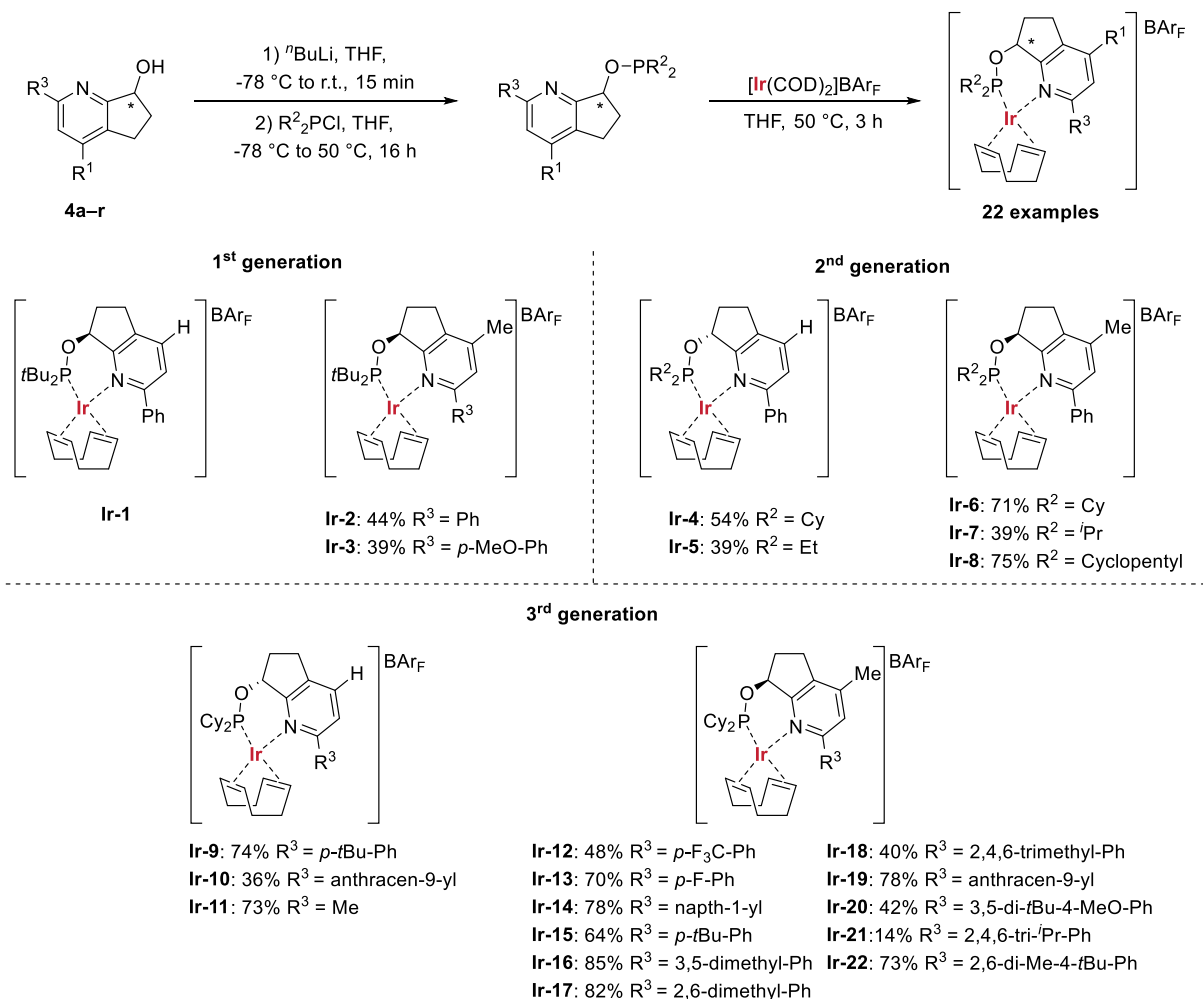


**Scheme 20.** a) Desired transformation. b) Lead structure **Ir-1** and potential parameters for structural optimization. c) General synthesis of pyridyl alcohols **37a-r**, used for the ligand synthesis.

At the outset of our studies, a catalyst screening revealed Ir-complex **Ir-1** as optimum system. Hence, **5a** was selected as starting point for a structural optimization, focusing on groups R<sup>1</sup>, R<sup>2</sup> and R<sup>3</sup> (Scheme 20, b). Chiral building blocks **36a** and **36b** were used as starting materials for the synthesis of ligand precursors **37a-r** *via* a Suzuki cross coupling/deprotection sequence and thus allowed for straightforward variations on both, R<sup>1</sup> and R<sup>3</sup> (Scheme 20, c). Eventually, iridium complexes **Ir-1–Ir-22** were obtained from the reaction of **37a-r** with different chlorodialkylphosphines and subsequent treatment of the *in situ* formed phosphonites with [Ir(COD)<sub>2</sub>]**BAr<sub>F</sub>** (Scheme 21). Next, the performance of the prepared pre-catalysts in the hydrogenation of **1** (60 bar H<sub>2</sub>, 85 °C, 6–40 h, HFIP, 0.1–0.01 mol% [Ir]) were probed. Interestingly, employing a methyl group in the 4-position of the pyridine moiety resulted in more reactive catalyst systems (**Ir-1** vs. **Ir-2**, **Ir-4** vs. **Ir-6** and **Ir-12** vs. **Ir-19**, Table 6, Entries 2 vs. 3,



5 vs. 7 and 12 vs. 17). Similarly, a catalyst bearing cyclohexyl substituents on the phosphorus atom was found to provide superior results in comparison to its *t*Bu analog (**Ir-2** vs. **Ir-6**, Table 6, Entries 4, 7). However, complexes featuring less bulky alkyl groups on the phosphorus atom showed reduced activities and enantioselectivities compared to **Ir-6** (**Ir-5**, **Ir-7** and **Ir-8**, Table 6, Entries 6, 8, 9).

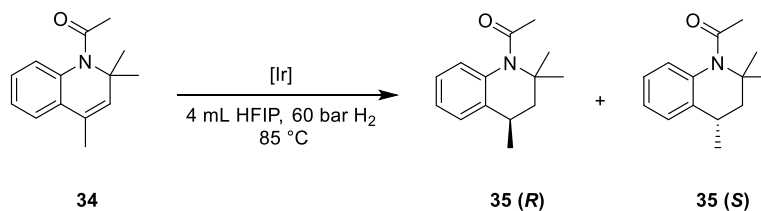


**Scheme 21.** Synthesis of [Ir]-catalysts.

Finally, the influence of  $R^2$  on the catalyst performance was investigated. Applying electron-deficient phenyl moieties had a profoundly negative impact on the reaction outcome (**Ir-10** and **Ir-11** vs. **Ir-6**, Table 6, Entries 7, 10, 11). On the contrary, *p-tert*-butyl-substituted derivative **Ir-15** provided an enhanced reactivity as compared to **Ir-6** (Table 6, Entry 13). Based on this observation, alkyl-substituted complexes **Ir-16–Ir-18** were prepared. While **Ir-16** and **Ir-17** were less active than **Ir-15** (Table 6, Entries 14, 15), application of **Ir-18** resulted in 98% conversion (Table 6, Entry 16). Employing sterically more demanding alkyl substituents did not result in catalytically more active systems (**Ir-20**, **Ir-21** and **Ir-22**; Table 6, Entries 18, 19 and 20). Notably, excellent conversion of the starting material and high enantioselectivity were maintained when the catalyst loading was reduced to 0.01 mol% (Table 6, Entry 21).

Additionally, the reaction was successfully scaled up to 25 mmol, revealing no loss in reactivity and selectivity (Table 6, Entry 22).

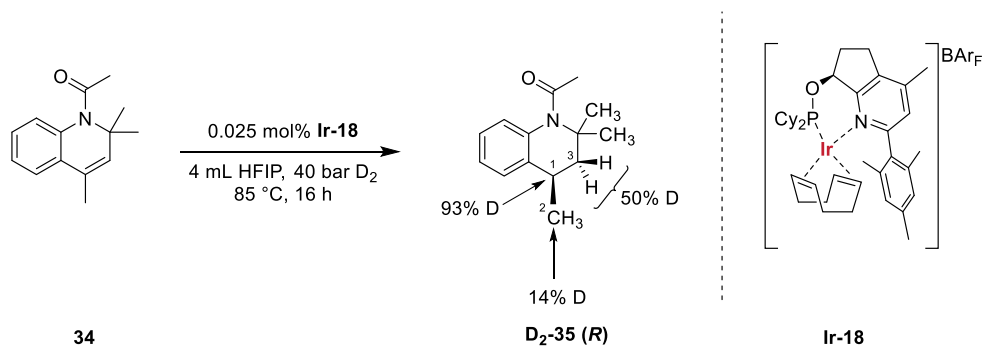
**Table 6.** Selected hydrogenation results of **34**.



Entry	[Ir]	Time [h]	Loading [mol%]	Conv. [%]	TON	ee [%]
1	<b>Ir-1</b>	16	0.1	99.2	992	98.0 ( <i>R</i> )
2	<b>Ir-1</b>	6	0.1	81.5	815	97.5 ( <i>R</i> )
3	<b>Ir-2</b>	6	0.1	94.5	945	97.5 ( <i>R</i> )
4	<b>Ir-2</b>	16.5	0.05	86.8	1736	97.6 ( <i>R</i> )
5	<b>Ir-4</b>	16.5	0.05	88.2	1764	97.6 ( <i>S</i> )
6	<b>Ir-5</b>	16	0.1	30	300	90.0 ( <i>S</i> )
7	<b>Ir-6</b>	16.5	0.05	94.4	1888	97.3 ( <i>R</i> )
8	<b>Ir-7</b>	6	0.1	76.0	760	96.0 ( <i>R</i> )
9	<b>Ir-8</b>	16.5	0.05	87.9	1758	95.8 ( <i>R</i> )
10	<b>Ir-10</b>	16.5	0.05	34.6	692	83.2 ( <i>R</i> )
11	<b>Ir-11</b>	16.5	0.05	64.7	1294	92.4 ( <i>R</i> )
12	<b>Ir-12</b>	16.5	0.05	98.9	1978	95.8 ( <i>S</i> )
13	<b>Ir-15</b>	16	0.025	91.6	3664	97.3 ( <i>R</i> )
14	<b>Ir-16</b>	16	0.025	42.2	1688	94.5 ( <i>R</i> )
15	<b>Ir-17</b>	16	0.025	81.7	3268	97.9 ( <i>R</i> )
16	<b>Ir-18</b>	16	0.025	98.0	3920	98.1 ( <i>R</i> )
17	<b>Ir-19</b>	16	0.025	94.1	3764	97.5 ( <i>R</i> )
18	<b>Ir-20</b>	16	0.025	60.0	2400	92.1 ( <i>R</i> )
19	<b>Ir-21</b>	16	0.025	74.0	2960	98.0 ( <i>R</i> )
20	<b>Ir-22</b>	16	0.025	97.5	3900	97.3 ( <i>R</i> )
21 <sup>[1]</sup>	<b>Ir-18</b>	40	0.01	93.9	9390	98.0 ( <i>R</i> )
22 <sup>[2]</sup>	<b>Ir-18</b>	40	0.01	93.4	9340	97.6 ( <i>R</i> )

Reaction conditions: 3 mmol substrate, 0.01–0.1 mol% [Ir]-catalyst, 4 mL HFIP, 60 bar H<sub>2</sub>, 85 °C, 6–40 h. <sup>[1]</sup>12 mmol scale, 16 mL HFIP. <sup>[2]</sup>25 mmol scale, 33 mL HFIP.

Ultimately, we investigated whether the reaction proceeds *via* a direct hydrogenation of the internal double bond, or if an initial isomerization to the terminal position at the C2 carbon takes place. Hence, a deuteration experiment was conducted, using 0.025 mol% of **Ir-18** and 40 bar D<sub>2</sub> (Scheme 22).



**Scheme 22.** Labeling experiments using  $\text{D}_2$ . Reaction conditions: 3 mmol Substrate, 0.025 mol% **Ir-18**, 4 mL HFIP, 40 bar  $\text{D}_2$ , 85 °C, 16h.

The obtained results suggest that **Ir-18** facilitates the direct hydrogenation of the internal C=C bond, as indicated by the observed deuteration at C1 and C3. Interestingly, some deuterium was also incorporated into the  $\text{CH}_3$  group attached to C1. This, however, would hint at the presence of a second and simultaneously occurring pathway, which involves an isomerization of the double bond from the C1–C3 to the C1–C2 position, prior to the deuteration event.

### 3.2.5 Catalytic Hydrogenations of Epoxides to *anti*-Markovnikov-Alcohols by a Cobalt/Tripos Catalyst

The development of efficient catalytic protocols for the synthesis of alcohols continues to attract significant attention from synthetic chemists.<sup>[14]</sup> Here, the selective hydrogenation of epoxides to *anti*-Markovnikov type alcohols *via* base metal catalysis represents a particularly interesting route.<sup>[92]</sup> The general feasibility of this methodology was recently demonstrated by our group applying a  $\text{Fe}(\text{BF}_4)_2 \cdot 6\text{H}_2\text{O}$ /tris(2-(diphenylphosphanyl)phenyl)phosphane (tetraphos) based catalyst system. Employing terminal epoxides as starting materials, the reported protocol yielded the corresponding primary alcohols in high yields and selectivities. However, internal epoxides did not undergo the desired transformation.<sup>[93]</sup> Hence, we became interested in the development of a more broadly applicable catalyst system.

**Table 7.** Optimization of cobalt-catalyzed hydrogenation of epoxide **36a**.

Reaction scheme: Epoxide **36a** (1-methyl-2-phenyloxirane) reacts under the following conditions: 3 mol% [Co], 6 mol% tripos, 3 mol% additive, THF, 40 bar  $\text{H}_2$ , 80–120 °C, 16 h. The reaction yields *anti*-Markovnikov alcohol **37a** (1-phenylethanol) and ketone **38a** (acetophenone). The tripos ligand structure is shown as a central carbon atom bonded to three diphenylphosphinoethyl groups.

Entry	[Co]	Additive <sup>1</sup>	T [°C]	Yield <b>37a</b> (%) <sup>[1]</sup>
<b>1</b> <sup>[2]</sup>	$\text{Co}(\text{BF}_4)_2 \cdot 6\text{H}_2\text{O}$	HNTf <sub>2</sub>	120	23
<b>2</b> <sup>[2]</sup>	$\text{Co}(\text{NTf}_2)_2$	–	120	43
<b>3</b>	$\text{Co}(\text{NTf}_2)_2$	–	100	<10
<b>4</b>	$\text{Co}(\text{NTf}_2)_2$	Zn(OTf) <sub>2</sub>	100	74
<b>5</b>	$\text{Co}(\text{NTf}_2)_2$	Zn(OTf) <sub>2</sub>	80	80
<b>6</b>	$\text{Co}(\text{NTf}_2)_2$	In(OTf) <sub>3</sub>	80	74
<b>7</b>	$\text{Co}(\text{NTf}_2)_2$	Al(OTf) <sub>3</sub>	80	<10
<b>8</b>	$\text{Co}(\text{NTf}_2)_2$	Fe(OTf) <sub>2</sub>	80	18
<b>9</b>	–	Zn(OTf) <sub>2</sub>	80	–
<b>10</b> <sup>[3]</sup>	$\text{Co}(\text{NTf}_2)_2$	Zn(OTf) <sub>2</sub>	80	–
<b>11</b> <sup>[4]</sup>	$\text{Co}(\text{NTf}_2)_2$	Zn(OTf) <sub>2</sub>	80	85
<b>12</b> <sup>[4]</sup>	$\text{Co}(\text{BF}_4)_2 \cdot 6\text{H}_2\text{O}$	Zn(OTf) <sub>2</sub>	80	80
<b>13</b> <sup>[4]</sup>	$\text{Co}(\text{ClO}_4)_2 \cdot 6\text{H}_2\text{O}$	Zn(OTf) <sub>2</sub>	80	73

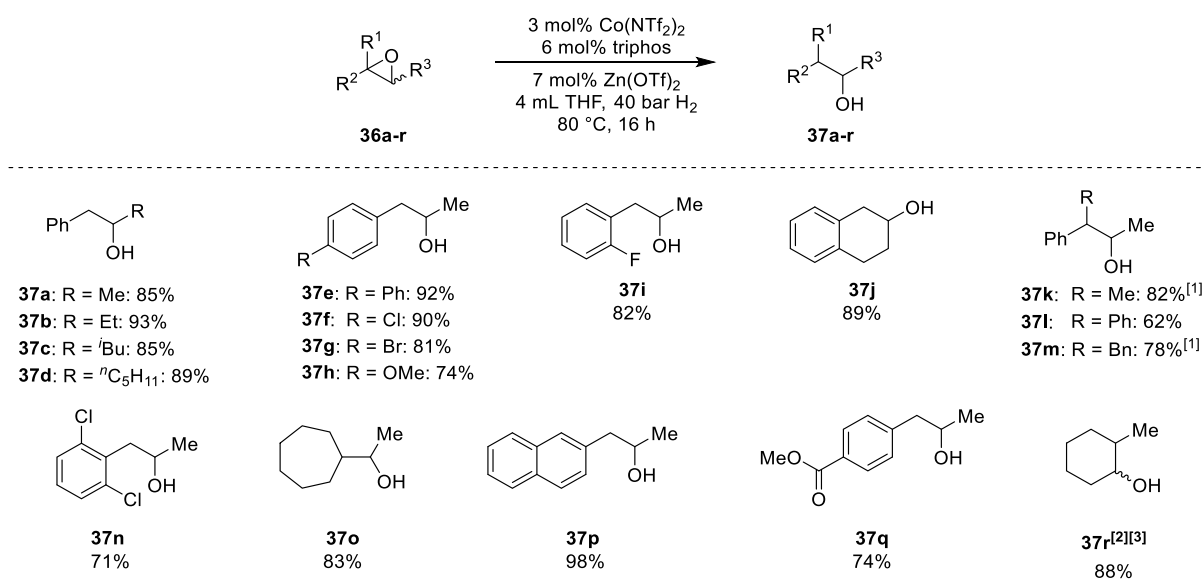
Reaction conditions: 0.5 mmol substrate, 3 mol% [Co]-catalyst, 6 mol% tripos, 3 mol% additive, 4 mL THF, 40 bar  $\text{H}_2$ , 80–120 °C, 16 h. <sup>[1]</sup>Determined by GC using hexadecane as internal standard.

<sup>[2]</sup>3 mol% tripos. <sup>[3]</sup>Without tripos. <sup>[4]</sup>7 mol% Zn(OTf)<sub>2</sub>.

Using 2-methyl-3-phenyloxirane **38a** as the benchmark substrate, an initial catalyst screening revealed the formation of the desired product **39a** in 23% yield, when a combination of

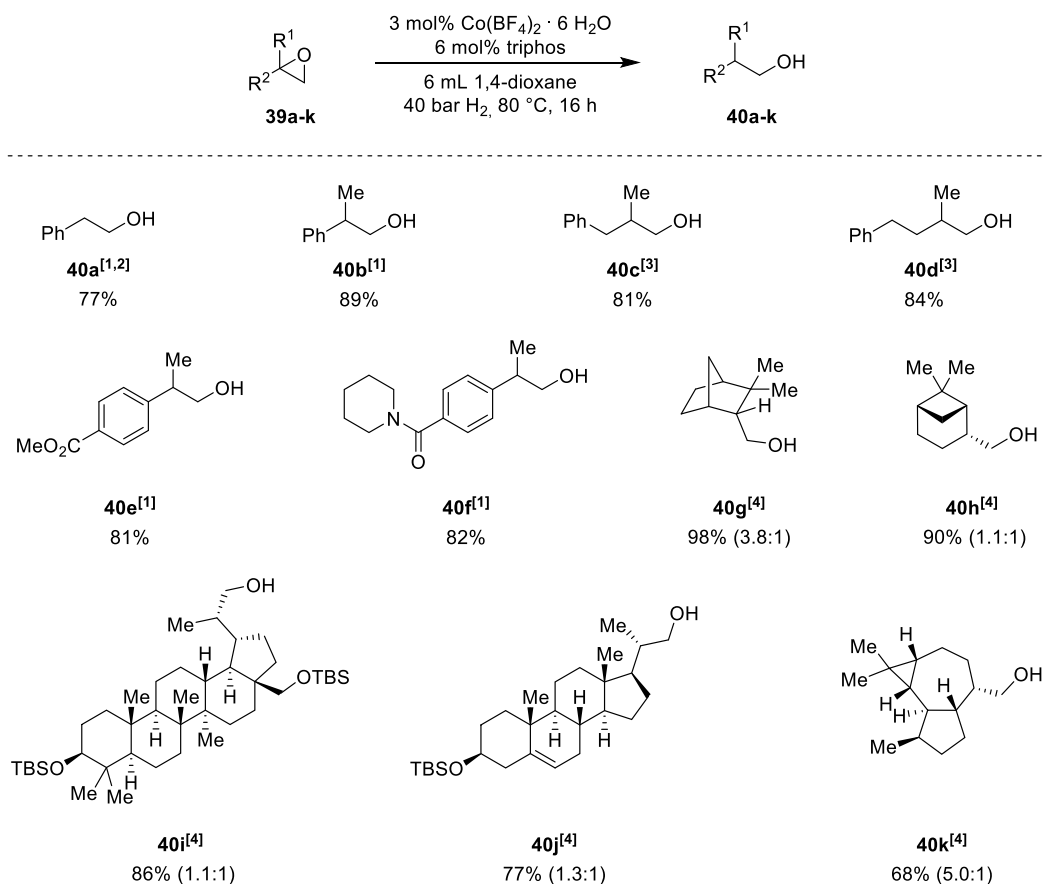
Co(BF<sub>4</sub>)<sub>2</sub>·6H<sub>2</sub>O/triphos/HNTf<sub>2</sub> was employed at 120 °C (Table 7, Entry 1). A more reactive catalyst system was obtained when Co(NTf<sub>2</sub>)<sub>2</sub> was applied as the cobalt precursor (Table 7, Entry 2). Notably, when 3 mol% of Zn(OTf)<sub>2</sub> were used as additive, the reaction temperature could be reduced to 80 °C and **39a** was observed in 80% yield (Table 7, Entry 5). Finally, optimal results were obtained, using a Co(NTf<sub>2</sub>)<sub>2</sub>/triphos based *in situ* catalyst in the presence of 7 mol% Zn(OTf)<sub>2</sub>, providing **39a** in 85% yield (Table 7, Entry 11).

Next, having optimized reaction conditions in hand, we explored the hydrogenation of various di- and trisubstituted internal epoxides (Scheme 23). Generally, both aromatic and aliphatic derivatives, were hydrogenated smoothly and the desired secondary alcohols were obtained in good yields with high regioselectivities. Moreover, the system showed a good functional group tolerance and no dehalogenation products were observed in the case of **37f**, **37g**, **37i** and **37n**. Notably, even an ester moiety (**37q**), typically hydrogenated by cobalt/triphos catalysts, was not reduced under our conditions.<sup>[94]</sup>



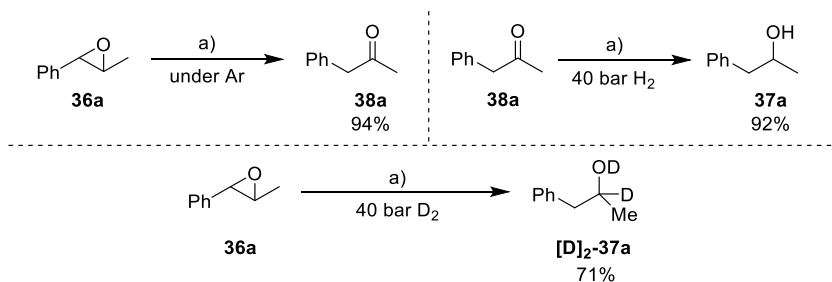
**Scheme 23.** Cobalt-catalyzed hydrogenation of internal epoxides. Reaction conditions: 0.5 mmol substrate, 3 mol% Co(NTf<sub>2</sub>)<sub>2</sub>, 6 mol% triphos, 7 mol% Zn(OTf)<sub>2</sub>, 4 mL THF, 40 bar H<sub>2</sub>, 80 °C, 16 h. <sup>[1]</sup>The diastereoisomeric ratio is 1:1.1. <sup>[2]</sup>3 mol% Co(BF<sub>4</sub>)<sub>2</sub>·6 H<sub>2</sub>O, 4 mL 1,4-dioxane, 60 °C, 20 h. <sup>[3]</sup>The diastereoisomeric ratio (2.8:1) and yield were determined by GC.

Additionally, also mono- and di-substituted terminal oxiranes were applicable to our methodology, yielding the corresponding linear alcohols in good yields and high regioselectivities (Scheme 24). Amide, silyloxy, alkene and ester substituents were well tolerated, and no hydrogenated by-products were observed. The versatility of our catalyst system was finally highlighted by the successful transformation of natural product-derived substrates **40g–40i**.



**Scheme 24.** Cobalt-catalyzed hydrogenation of terminal epoxides. Reaction conditions: 0.5 mmol substrate, 3 mol%  $\text{Co}(\text{BF}_4)_2 \cdot 6 \text{H}_2\text{O}$ , 6 mol% triphos, 6 mL 1,4-dioxane, 40 bar  $\text{H}_2$ , 80 °C, 16 h. <sup>[1]</sup>4 mL THF as solvent. <sup>[2]</sup>Yield was determined by GC using hexadecane as internal standard. <sup>[3]</sup>3 mol%  $\text{Co}(\text{NTf}_2)_2$ , 7 mol%  $\text{Zn}(\text{OTf})_2$ . <sup>[4]</sup>The major isomers are shown.

To understand the underlying reaction mechanism, a series of control experiments was carried out (Scheme 25). Initially, **36a** was reacted under benchmark conditions in the absence of dihydrogen, using an argon atmosphere. 1-Phenylpropan-2-one **38a** was isolated in 94% yield from the reaction mixture, indicating that a rearrangement to the carbonyl compound takes place in the first step of the reaction.



**Scheme 25.** Selected mechanistic studies. a) 0.5 mmol Substrate, 3 mol%  $\text{Co}(\text{NTf}_2)_2$ , 6 mol% triphos, 7 mol%  $\text{Zn}(\text{OTf})_2$ , 4 mL THF, 80 °C.

Consequently, in separate experiments, **38a** was exposed to our catalyst system in the presence of 40 bar H<sub>2</sub> and D<sub>2</sub> respectively, resulting in the formation of **37a** and [D]<sub>2</sub>-**37a** in 92% and 71% yield. Moreover, we investigated the influence of the applied cobalt and zinc salts on the observed Meinwald rearrangement of **36a** to **38a** (Table 8). Interestingly, the reaction already proceeded in the absence of the co-catalyst yielding **38a** in 53% (Table 8, Entry 2). Nevertheless, in the presence of Zn(OTf)<sub>2</sub>, an improved yield of **38a** was observed (Table 8, Entry 4).

**Table 8.** Control experiments regarding the role of Zn(OTf)<sub>2</sub>.

Entry	Co(NTf) <sub>2</sub> [mol%]	Triphos [mol%]	Zn(OTf) <sub>2</sub> [mol%]	Yield 36a [%] <sup>[1]</sup>	Yield 38a [%] <sup>[1]</sup>
1	–	–	–	98	–
2	3	6	–	41	53
3	–	–	7	<1	>99
4	3	6	7	30	64

Reaction conditions: 0.5 mmol substrate, 0–3 mol % Co(NTf)<sub>2</sub>, 0–6 mol% triphos, 0–7 mol% Zn(OTf)<sub>2</sub>, 4 mL THF, 40 bar N<sub>2</sub>, 80 °C, 16 h. <sup>[1]</sup>Determined by GC using hexadecane as internal standard.

Based on the obtained results, we concluded that the reaction generally proceeds *via* a Lewis acid induced rearrangement of the epoxide to the corresponding carbonyl compound followed by subsequent cobalt/triphos mediated hydrogenation to the respective *anti*-Markovnikov alcohol.

## 4 Summary and Outlook

The aim of the present work was the preparation and structural characterization of molybdenum complexes featuring aliphatic pincer ligands and, more importantly, the exploration of their potential as catalysts in homogeneous hydrogenation reactions. Reports on the synthesis of these coordination compounds and their utilization in catalytic reductions were exceptionally scarce until recently.

Initially, a synthetic methodology for the synthesis of the mentioned coordination compounds was developed, giving access to ten previously unknown Mo pincer complexes (Figure 8). Employing  $\text{Mo}(\text{PPh}_3)_2(\text{CO})_2(\text{CH}_3\text{CN})_2$  as molybdenum precursor, a strong influence, particularly of the employed solvent, but also of the applied ligand on the reaction outcome was observed. Interestingly, three 17-electron complexes featuring a molybdenum center in the unusual formal oxidation state of +I could be obtained (**Mo-10**, **Mo-11**, and **Mo-15**).

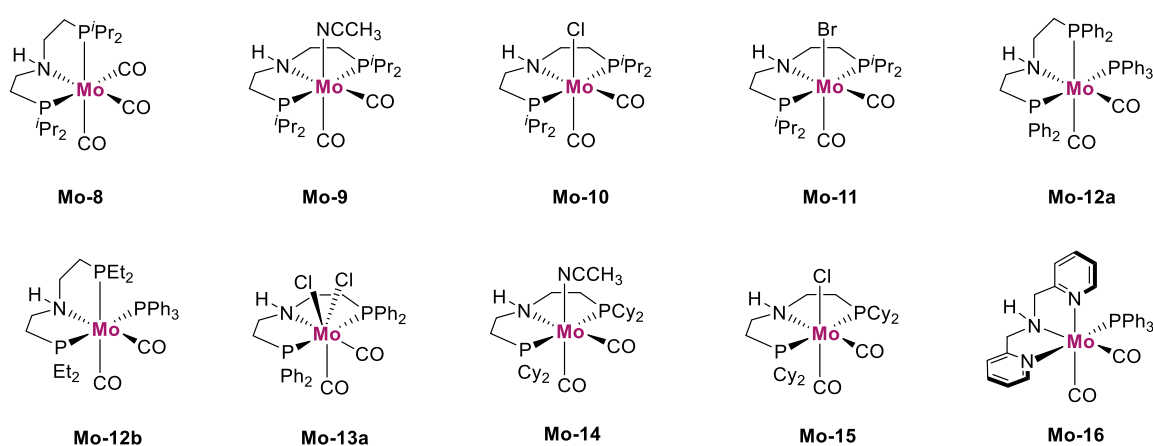


**Figure 8.** Overview of synthesized molybdenum complexes.

The synthesized molybdenum catalysts were subsequently investigated in more detail regarding their ability to hydrogenate different organic substrates. Extensive efforts demonstrate that **Mo-9** and **Mo-10** in particular are efficient catalysts for the (selective) hydrogenation of acetophenones, styrenes, *N*-methylated formamides, and both aromatic and aliphatic nitriles. The catalytic reduction of carboxamides by **Mo-10** was investigated more closely by means of DFT studies, which provided in-depth information regarding the potential active catalyst species, as well as the underlying reaction mechanism. Notably, we were able to isolate and structurally characterize catalytic intermediate **Mo-17**. The active role of this catalyst/substrate complex in the catalytic cycle was established in control experiments. Notably, this report constitutes the first example of a molybdenum pincer catalyzed hydrogenation of amides. In addition, we developed the first Mo-pincer based catalyst capable of selective hydrogenation of nitriles to primary amines in absence of ammonia. More



specifically, **Mo-9** was shown to hydrogenate electron-rich benzonitriles and aliphatic nitriles smoothly, even in the presence of other reducible functional groups. Benzonitriles bearing electron-withdrawing groups on the aromatic moiety worked less efficiently under the described conditions. Gratifyingly, we were able to isolate and characterize the molecular structure of **Mo-9** after activation with NaBHET<sub>3</sub>, revealing a new mode of catalyst activation in pincer chemistry (**Mo-9a**).

Asides from the described results, we developed a chiral Ir-catalyst for the enantioselective hydrogenation of an agrochemical intermediate in cooperation with an industrial partner. The catalyst system efficiently operates at a catalyst loading as low as 0.01 mol% and converts the applied starting material with an ee of 98% and a maximum TON of 9340.<sup>[87]</sup> Additionally, we reported a cobalt/triphos based catalyst for the hydrogenation of epoxides to *anti*-Markovnikov type alcohols. The *in situ* formed system hydrogenated terminal and internal oxiranes to the desired products with high yields and excellent regioselectivities.<sup>[88]</sup>

Over the course of the present thesis, we demonstrated the general ability of aliphatic molybdenum (PNP) pincer complexes to act as catalysts for hydrogenation reactions.<sup>[89,90,95]</sup> However, the reported systems generally required relative high catalyst loadings of 5 mol% and temperatures around 100 °C. For future studies it would be interesting to develop aromatic Mo-PNP derivatives and investigate their catalytic potential in the reported transformations. Here, the different modes of catalyst activation could increase the catalyst performance and/or lead to new reactivities. Moreover, also the application of pincer ligands exhibiting different donor motifs, e.g. SNS and PNN, might result in more active catalysts. In addition, the development of chiral molybdenum pincer complexes for the asymmetric reductions, e.g. of ketones, would be an interesting future research topic. Currently, such a transformation has not been reported with respect to molybdenum pincer-based catalysts.

## 5 References

- [1] J. Emsley, *Nature's Building Blocks*, Oxford University Press, Oxford, **2001**.
- [2] C. W. K. Scheele, *Svenska Vetensk. Academ. Handlingar*. **1779**, 40, 238–248.
- [3] P. J. Hjelm, *Svenska Vetensk. Academ. Handlingar*. **1788**, 49, 268–279.
- [4] A. A. Holder, *Molybdenum: Its Biological and Coordination Chemistry and Industrial Applications*, Nova Science, New Yorck, **2013**.
- [5] The corresponding data can be found at the “U.S. Geological Survey” website:  
“<https://prd-wret.s3-us-west-2.amazonaws.com/assets/palladium/production/atoms/files/mcs-2019-molyb.pdf>”.  
Visited on **10.07.2020**.
- [6] K. H. Lohmann, R. C. Young, *Inorg. Synth.* **1953**, 4, 97–101.
- [7] A. F. Holleman, E. Wiberg, N. Wiberg, *Lehrbuch der Anorganischen Chemie*, Walter de Gruiter Verlag, Berlin, **2007**.
- [8] F. A. Cotton, G. Wilkinson, C. A. Murillo, M. Bochmann, *Advanced Inorganic Chemistry*, John Wiley and Sons, New-Yorck, **1999**.
- [9] The corresponding data can be found at the “London Metal Exchange” website:  
“<https://web.archive.org/web/20120310004452/http://www.lme.com/minormetals/6782.asp>”.  
Visited on **10.07.2020**.
- [10] P. C. H. Mitchell, *Chem. Eng. News* **2003**, 81, 108.
- [11] S. Lal, R. S. Patil, *Environ. Monit. Asses.* **2001**, 68, 37–50.
- [12] W. O. Winer, *Wear* **1969**, 10, 422–452.
- [13] A. Gottschalk, *Annu. Rev. Med.* **1969**, 20, 131–140.
- [14] K. Weissermel, H. J. Arpe, *Industrielle Organische Chemie*, Wiley-VCH, Weinheim, **1998**.
- [15] L. Giebeler, P. Kempe, A. Wirth, A. H. Adams, J. Kunert, H. Fließ, H. Vogel, *J. Mol. Catal. A: Chem.* **2006**, 259, 309–318.
- [16] H. J. Arpe, *Industrielle Organische Chemie: Bedeutende Vor- und Zwischenprodukte*, Wiley-VCH, Weinheim, **2007**.
- [17] J. C. Mol, *J. Mol. Catal. A: Chem.* **2004**, 213, 39–45.
- [18] a) T. Kabe, A. Ishihara, W. Qian, *Hydrodesulfurization and Hydrodenitrogenation*, Wiley-VCH, Weinheim, **2000**. B) J. G. Speight, *Hydrodesulfurization of Heavy Oils and Residua*, CRC Press, Boca Raton, **1999**.
- [19] J. H. Seinfeld, S. N. Pandis, *Atmospheric Chemistry and Physics – From Air Pollution to Climate Change*, John Wiley and Sons, New Yorck, **1998**.
- [20] [20] Y. T. Shah, *Chemical Energy from Natural and Synthetic Gas*, CRC Press, Boca Raton, **2017**.
- [21] E. I. Stiefel, D. Coucouvanis, W. E. Newton, *Molybdenum Enzymes, Cofactors, and Model Systems*, American Chemical Society, Washington DC, **1993**.
- [22] R. Hille, J. Hille, P. Basu, *Chem. Rev.* **2014**, 114, 3963–4038.
- [23] J. H. Enemark, J. J. A. Cooney, J. J. Wang, R. H. Holm, *Chem. Rev.* **2004**, 104, 1175–1200.

- [24] M. Tejada-Jimenez, A. Chamizo-Ampudia, V. Calatrava, A. F. Galvan, L. A. Emilio, *Molecules* **2018**, *23*, 3287/1–3287/18.
- [25] C. Kisker, H. Schindelin, D. Baas, J. Rétey, R. U. Meckenstock, P. M. H. Kroneck, *FEMS Microbiol. Rev.* **1999**, *22*, 503–521.
- [26] The corresponding information can be found at the website of the “*International Molybdenum Association*”:  
 “[https://www.imoa.info/HSE/environmental\\_data/biology/reviews-of-molybdoenzymes/17-xanthine-dehydrogenase-and-xanthine-oxidase.php](https://www.imoa.info/HSE/environmental_data/biology/reviews-of-molybdoenzymes/17-xanthine-dehydrogenase-and-xanthine-oxidase.php)”.  
 Visited on **10.07.2020**.
- [27] R. R. Mendel, G. Schwarz, *Coord. Chem. Rev* **2011**, *255*, 1145–1158.
- [28] K. B. Swedo, J. H. Enemark, *J. Chem. Educ.* **1979**, *56*, 70–76.
- [29] J. Postgate, *Nitrogen Fixation*, Cambridge University Press, Cambridge, **1998**.
- [30] J. Aaseth, G. Crisponi, O. Anderson, *Chelation Therapy in the Treatment of Metal Intoxication*, Academic Press, San Diego, **2016**.
- [31] a) G. J. Brewer, P. Hedera, K. J. Kluin, M. Carlson, F. Askari, R. B. Dick, J. Sitterly, J. K. Fink, *Arch Neurol.* **2003**, *3*, 379–385. b) G. J. Brewer, F. Askari, M. T. Lorincz, M. Carlson, *Arch Neurol.* **2006**, *4*, 521–527. c) G. J. Brewer, F. Askari, R. B. Dick, J. Sitterly, J. K. Fink, M. Carlson, K. J. Kluin, M. T. Lorincz, *Transl. Res.* **2009**, *154*, 70–77.
- [32] a) C. Pettinari, F. Marchetti, D. Martini, *Comprehensive Coordination Chemistry II. From Biology to Nanotechnology*, Elsevier/Pergamon, Amsterdam, **2004**. b) J. G. d. Vries, C. J. Elsevier, *The Handbook of Homogeneous Hydrogenation*, Wiley-VCH, Weinheim, **2007**. c) P. A. Dub, T. Ikariya, *ACS Catal.* **2012**, *2*, 1718–1741.
- [33] P. Sabatier, J. B. Senderens, *C. r. d. l’Acad des sciences* **1897**, *124*, 1358–1361.
- [34] H. B. Kagan, *Angewan. Chem, Int. Ed.* **2012**, *51*, 7376–7382.
- [35] a) M. Calvin, M. Polanyi, *J. Chem. Soc. Faraday Trans.* **1938**, *34*, 1181–1191. b) M. Calvin, *J. Am. Chem. Soc.* **1939**, *61*, 2230–2234.
- [36] J. A. McCleverty, T. J. Meyer, *Comprehensive Coordination Chemistry II*, Pergamon Press, Oxford, **2003**.
- [37] a) F. H. Jardine, J. A. Osborn, G. Wilkinson, J. F. Young, *Chem. Ind.* **1965**, *13*, 560–561. b) J. F. Young, J. A. Osborn, F. H. Jardine, G. Wilkinson, *Chem. Commun.* **1965**, *7*, 131–132.
- [38] F. H. Jardine, *Prog. Inorg. Chem.* **1981**, *28*, 63–202.
- [39] a) R. R. Schrock, J. A. Osborn, *J. Am. Chem. Soc.*, **1971**, *93*, 2397–2407. b) R. R. Schrock, J. A. Osborn, *J. Am. Chem. Soc.* **1976**, *98*, 2134–2143. c) R. R. Schrock, J. A. Osborn, *J. Am. Chem. Soc.* **1976**, *98*, 2143–2147. d) R. R. Schrock, J. A. Osborn, *J. Am. Chem. Soc.* **1976**, *98*, 4450–4455. e) R. Noyori, H. Takaya, *Acc. Chem. Res.* **1990**, *23*, 345–350. f) J. K. Whitesell, *Chem. Rev.* **1989**, *89*, 1581–1590.
- [40] W. S. Knowles. *Acc. Chem. Res.* **1983**, *16*, 106–112.
- [41] a) R. Noyori, S. Hashiguchi, *Acc. Chem. Res.* **1997**, *30*, 97–102. b) R. Noyori, T. Ohkuma, *Angew. Chem. Int. Ed.* **2001**, *40*, 40–73. c) R. Noyori, M. Yamakawa, S. Hashiguchi, *J. Org. Chem.* **2001**, *66*, 7931–7944.
- [42] D. Adam, *Nature* **2001**, *413*, 661.

- [43] a) H. U. Blaser, B. Pugin, F. Spindler, M. Thommen, *Acc. Chem. Res.* **2007**, *40*, 1240–1250. b) P. N. Rylander, *Ullmann's Encyclopedia of Industrial Chemistry*, Wiley-VCH, Weinheim, **2012**. c) M. Stoffels, F. J. R. Klauck, T. Hamadi, F. Glorius, J. Leker, *Adv. Synth. Catal.* **2020**, *17*, 1258–1274.
- [44] a) P. N. Rylander, *Catalytic Hydrogenation in Organic Syntheses*, Elsevier, Oxford, **1979**. b) J. Seyden-Penne, *Reductions by the Alumino- and Borohydrides in Organic Synthesis*, Wiley-VCH, New York, **1997**.
- [45] L. H. Pignolet *Homogeneous Catalysis with Metal Phosphine Complexes*, Springer, New York, **1983**.
- [46] a) S. Werkmeister, J. Neumann, K. Junge, M. Beller, *Chem. Eur. J.* **2015**, *21*, 12226–12250. b) T. Zell, D. Milstein, *Acc. Chem. Res.* **2015**, *48*, 1979–1994.
- [47] a) K. Junge, V. Papa, M. Beller, *Chem. Eur. J.* **2019**, *25*, 122–143. b) W. Liu, B. Sahoo, K. Junge, M. Beller, *Acc. Chem. Res.* **2018**, *51*, 1858–1869.
- [48] a) M. Garbe, K. Junge, M. Beller, *Eur. J. Org. Chem.* **2017**, *30*, 4344–4362. b) B. Maji, M. K. Barman, *Synthesis* **2017**, *49*, 3377–3393. c) G. A. Filonenko, R. van Putten, E. J. M. Hensen, E. A. Pidko, *Chem. Soc. Rev.* **2018**, *47*, 1459–1483. d) A. Mukherjee, D. Milstein, *ACS Catal.* **2018**, *8*, 11435–11469. e) F. Kallmeier, R. Kempe, *Angew. Chem. Int. Ed.* **2018**, *57*, 46–60.
- [49] K. V. Vasudevan, B. L. Scott, S. K. Hanson, *Eur. J. Inorg. Chem.* **2012**, *30*, 4898–4906.
- [50] R. Watari, Y. Kayaki, S. Hirano, N. Matsumoto, T. Ikariya, *Adv. Synth. Catal.* **2015**, *357*, 1369–1373.
- [51] P. Jochmann, D. W. Stephan, *Angew. Chem. Int. Ed.* **2013**, *52*, 9831–9835.
- [52] a) M. E. van der Boom, D. Milstein, *Chem. Rev.* **2003**, *103*, 1759–1792. b) D. Benito-Garagorri, K. Kirchner, *Acc. Chem. Res.* **2008**, *41*, 201–213. c) G. van Koten, R. A. Gossage, *Topics in Organometallic Chemistry Vol. 54*, Springer, Heidelberg, **2016**.
- [53] a) C. J. Moulton, B. L. Shaw, *Dalton Trans.* **1976**, *11*, 1020–1024. b) H. D. Empsall, E. M. Hyde, R. Markham, W. S. McDonald, M. C. Norton, B. L. Shaw, B. Weeks, *J. Chem. Soc., Chem. Commun.* **1977**, *17*, 589–590. c) G. Van Koten, K. Timmer, J. G. Noltes, A. L. Spek, *J. Chem. Soc., Chem. Commun.* **1978**, *6*, 250–252. d) C. Crocker, R. J. Errington, R. Markham, C. J. Moulton, K. J. Odell, B. L. Shaw, *J. Am. Chem. Soc.* **1980**, *102*, 4373–4379. e) C. Crocker, R. J. Errington, R. Markham, C. J. Moulton, B. L. Shaw, *J. Chem. Soc., Dalton Trans.* **1982**, *2*, 387–395. f) J. R. Briggs, A. G. Constable, W. S. McDonald, B. L. Shaw, *J. Chem. Soc., Dalton Trans.* **1982**, *7*, 1225–1230. g) C. Crocker, H. D. Empsall, R. J. Errington, E. M. Hyde, W. S. McDonald, R. Markham, M. C. Norton, B. L. Shaw, B. Weeks, *J. Chem. Soc., Dalton Trans.* **1982**, *7*, 1217–1224. h) R. J. Errington, W. S. McDonald, B. L. Shaw, *J. Chem. Soc., Dalton Trans.* **1982**, *9*, 1829–1835.
- [54] G. Van Koten, *Pure Appl. Chem.* **1989**, *61*, 1681–1694.
- [55] a) K. J. Szabó, *Topics in Organometallic Chemistry Vol. 40*, Springer, Berlin, Heidelberg, **2013**. b) E. Peris, R. H. Crabtree, *Chem. Soc. Rev.* **2018**, *47*, 1959–1968. c) M. Albrecht, G. Van Koten, *Angew. Chem. Int. Ed.* **2001**, *40*, 3750–3781.
- [56] a) J. I. van der Vlugt, *Eur. J. Inorg. Chem.* **2012**, *3*, 363–375. b) T. Ikariya, M. Shibasaki, *Bifunctional Molecular catalysis*, Springer, Berlin, **2011**.

- [57] W. Jia, X. Chen, R. Guo, C. Sui-Seng, D. Amoroso, A. J. Lough, K. Abdur-Rashid, *Dalton Trans.* **2009**, 39, 8301–8307.
- [58] J. Zhang, G. Leitius, Y. Ben-David, D. Milstein, *Angew. Chem. Int. Ed.* **2006**, 45, 1113–1115.
- [59] a) H. Grützmacher, *Angew. Chem. Int. Ed.* **2008**, 47, 1814–1818. b) C. Gunanathan, D. Milstein, *Acc. Chem. Res.* **2011**, 44, 588–602. c) J. R. Khusnutdinova, D. Milstein, *Angew. Chem. Int. Ed.* **2015**, 54, 12236–12273. d) D. Milstein, *Philos. Trans. R. Soc. A* **2015**, 373, 1–10.
- [60] a) A. Choualeb, A. J. Lough, D. G. Gusev, *Organometallics* **2007**, 26, 5224–5229. b) S. Bi, Q. Xie, X. Zhao, Y. Zhao, X. Kong, *J. Organomet. Chem.* **2008**, 693, 633–638. c) S. Schneider, J. Meiners, B. Askevold, *Eur. J. Inorg. Chem.* **2012**, 412–429. d) B. Bichler, C. Holzhaacker, B. Stöger, M. Puchberger, L. F. Veiros, K. Kirchner, *Organometallics* **2013**, 32, 4114–4121.
- [61] B. Chen, U. Dingerdissen, J. G. E. Krauter, H. G. J. Lansink Rotgerink, K. Möbius, D. J. Ostgard, P. Panster, T. H. Riermeier, S. Seebald, T. Tacke, H. Trauthwein, *Appl. Catal. A*, **2005**, 280, 17–46.
- [62] a) H. A. Younus, N. Ahmad, W. Su, F. Verpoort, *Coord. Chem. Rev.* **2014**, 276, 112–152. b) C. Gunanathan, D. Milstein, *Chem. Rev.* **2014**, 114, 12024–12087. c) P. Meakin, J. P. Jesson, C. A. Tolman, *J. Am. Chem. Soc.* **1972**, 94, 3240–3242. d) J. Choi, A. H. R. MacArthur, M. Brookhart, A. S. Goldman, *Chem. Rev.* **2011**, 111, 1761–1779. e) N. Selander, K. J. Szabó, *Chem. Rev.* **2011**, 111, 2048–2076.
- [63] a) R. Langer, G. Leitius, Y. Ben-David, D. Milstein, *Angew. Chem. Int. Ed.* **2011**, 50, 2120–2124. b) G. Bauer, K. Kirchner, *Angew. Chem. Int. Ed.* **2011**, 50, 5798–5800.
- [64] N. Gorgas, B. Stöger, L. F. Veiros, E. Pittenauer, G. Allmaier, K. Kirchner, *Organometallics* **2014**, 33, 6905–6914.
- [65] a) G. Zhang, B. L. Scott, S. K. Hanson, *Angew. Chem. Int. Ed.* **2012**, 51, 12102–12106. *Angew. Chem.* **2012**, 124, 12268–12272. b) G. Zhang, K. Vasudevan, B. L. Scott, S.K. Hanson, *J. Am. Chem. Soc.* **2013**, 135, 8668–8681.
- [66] S. Rösler, J. Obenauf, R. Kempe, *J. Am. Chem. Soc.* **2015**, 137, 7998–8001.
- [67] S. Elangovan, C. Topf, S. Fischer, H. Jiao, A. Spannenberg, W. Baumann, R. Ludwig, K. Junge, M. Beller, *J. Am. Chem. Soc.* **2016**, 138, 8809–8814.
- [68] F. Kallmeier, T. Irrgang, Th. Dietel, R. Kempe, *Angew. Chem. Int. Ed.* **2016**, 128, 11984–11988.
- [69] A. M. Smith, R. Whyman, *Chem. Rev.* **2014**, 114, 5477–5510.
- [70] J. R. Cabrero-Antonino, E. Alberico, K. Junge, H. Junge, M. Beller, *Chem. Sci.* **2016**, 8, 3432–3442.
- [71] a) A. A. Nunez Magro, G. R. Eastham, D. J. Cole-Hamilton, *Chem. Commun.* **2007**, 30, 3154–3156. b) E. Balaraman, B. Gnanaprakasam, L. J. W. Shimon, D. Milstein, *J. Am. Chem. Soc.* **2010**, 132, 16756–16758. c) J. M. John, S. H. Bergens, *Angew. Chem. Int. Ed.* **2011**, 50, 10377–10380. d) J. Coetzee, D. L. Dodds, J. Klankermayer, S. Brosinksi, W. Leitner, A. M. Z. Slawin, D. J. Cole-Hamilton, *Chem. Eur. J.* **2013**, 19, 11039–11050. e) T. Miura, I. E. Held, S. Oishi, M. Naruto, S. Saito. *Tetrahedron Lett.* **2013**, 54, 2674–2678. f) T. vom Stein, M.

- Meureusch, D. Limper, M. Schmitz, M. Hölscher, J. Coetzee, D. J. Cole-Hamilton, J. Klankermayer, W. Leitner, *J. Am. Chem. Soc.* **2014**, *136*, 13217–13225. g) J. R. Cabrero-Antonino, E. Alberico, H. J. Drexler, W. Baumann, K. Junge, H. Junge, M. Beller, *ACS Catal.* **2016**, *6*, 47–54. h) L. Shi, X. Tan, J. Long, X. Xiong, S. Yang, P. Xue, H. Lv, X. Zhang, *Chem. Eur. J.* **2017**, *23*, 546–548.
- [72] a) J. A. Garg, S. Chakraborty, Y. Ben-David, D. Milstein, *Chem. Commun.* **2016**, *52*, 5285–5288. b) N. M. Rezayee, D. C. Samblanet, M. S. Sanford, *ACS Catal.* **2016**, *6*, 6377–6383. c) F. Schneck, M. Assmann, M. Balmer, K. Harms, R. Langer, *Organometallics* **2016**, *35*, 1931–1943.
- [73] U. Jayaranthe, Y. Zhang, N. Hazari, W. Bernskoetter, *Organometallics* **2017**, *36*, 409–416.
- [74] L. A. Suarez, Z. Culacova, D. Balcells, W. H. Bernskoetter, O. Eisenstein, K. I. Goldberg, N. Hazari, M. Tilset, A. Nova, *ACS Catal.* **2018**, *8*, 8751–8762.
- [75] V. Papa, J. R. Cabrero-Antonino, E. Alberico, A. Spannenberg, K. Junge, H. Junge, M. Beller, *Chem. Sci.* **2017**, *8*, 3576–3585.
- [76] S. Kar, A. Goeppert, J. Kothandaraman, J. K. S. Prakash, *ACS Catal.* **2017**, *7*, 6347–6351.
- [77] D. M. Bagal, B. M. Bhanage, *Adv. Synth. Catal.* **2015**, *357*, 883–900.
- [78] a) S. Werkmeister, K. Junge, M. Beller, *Org. Process. Res. Dev.* **2014**, *18*, 289–302. b) D. M. Sharma, B. Punji, *Chem. Asian. J.* **2020**, *15*, 690–708.
- [79] For selected examples on Rh, Ru, Ir and Re-catalyzed nitrile hydrogenations see: a) T. Yoshida, T. Okano, S. Otsuka, *J. Chem., Chem. Commun.* **1979**, 870–871. b) R. A. Grey, G. P. Pez, A. Wall, J. Corsi, *J. Chem. Soc., Chem. Commun.* **1980**, 783–784. c) R. A. Grey, G. P. Pez, A. Wallo, *J. Am. Chem. Soc.* **1981**, *103*, 7536–7542. d) C. Chin, B. Lee, *Catal. Lett.* **1992**, *14*, 135–140. e) T. Li, I. Bergner, F. N. Haque, M. Zimmer-De Iuliis, D. Song, R. Morris, *Organometallics* **2007**, *26*, 5940–5949. f) S. Enthaler, D. Addis, K. Junge, G. Erre, M. Beller, *Chem. Eur. J.* **2008**, *14*, 9491–9494. g) S. Enthaler, K. Junge, D. Addis, G. Erre, M. Beller, *ChemSusChem* **2008**, *1*, 1006–1010. h) D. Addis, S. Enthaler, K. Junge, B. Wendt, M. Beller, *Tetrahedron Lett.* **2009**, *50*, 3654–3656. i) R. Reguillo, M. Grellier, N. Vautravers, L. Vendier, S. Sabo-Etienne, *J. Am. Chem. Soc.* **2010**, *132*, 7854–7855. j) C. Gunanathan, M. Hölscher, W. Leitner, *Eur. J. Inorg. Chem.* **2011**, 3381–3386. k) K. Rajesh, B. Dudle, O. Blacque, H. Berke, *Adv. Synth. Catal.* **2011**, *353*, 1479–1484. l) S. Werkmeister, K. Junge, B. Wendt, A. Spannenberg, H. Jiao, C. Bornschein, M. Beller, *Chem. Eur. J.* **2014**, *20*, 427–431. m) J. Neumann, C. Bornschein, H. Jiao, K. Junge, M. Beller, *Eur. J. Org. Chem.* **2015**, 5944–5948. n) J.-H. Choi, M. H. G. Precht, *ChemCatChem* **2015**, *7*, 1023–1028. o) R. Adam, C. B. Bheeter, R. Jackstell, M. Beller, *ChemCatChem* **2015**, *8*, 1329–1334. p) R. Adam, E. Alberico, W. Baumann, H.-J. Drexler, R. Jackstell, H. Junge, M. Beller, *Chem. Eur. J.* **2016**, *22*, 4991–5002. q) Y. Sato, Y. Kayaki, T. Ikariya, *Organometallics* **2016**, *35*, 1257–1264.
- [80] For selected examples see: a) C. Bornschein, S. Werkmeister, B. Wendt, H. Jiao, E. Alberico, W. Baumann, H. Junge, K. Junge, M. Beller, *Nat. Commun.* **2014**, *5*, 4111. b) A. Mukherjee, D. Srimani, S. Chakraborty, Y. Ben-David, D. Milstein, *J. Am. Chem. Soc.* **2015**, *137*, 8888–8891. c) D. Srimani, A. Mukherjee, F. G. Goldberg, G. Leitius, Y. Diskin-Posner, L. J. W. Shimon, Y. Ben-David, D. Milstein, *Angew. Chem. Int. Ed.* **2015**, *54*, 12357–12360. *Angew.*

- Chem.* **2015**, 12534–12537. d) S. Lange, S. Elangovan, C. Cordes, A. Spannenberg, H. Jiao, S. Bachmann, M. Scalone, C. Topf, K. Junge, M. Beller, *Catal. Sci. Technol.* **2016**, *6*, 4768–4772. e) S. Chakraborty, D. Milstein, *Chem. Commun.* **2016**, *52*, 1812–1815. f) S. Chakraborty, D. Milstein, *ACS Catal.* **2017**, *7*, 3968–3972. g) K. Tokmic, B. J. Jackson, A. Salazar, T. J. Woods, A. R. Fout, *J. Am. Chem. Soc.* **2017**, *139*, 13554–13561. h) R. Adam, C. B. Bheeter, J. R. Cabrero-Antonino, K. Junge, R. Jackstell, M. Beller, *ChemSusChem* **2017**, *10*, 842–846. i) H. Li, A. Al-Dakhil, D. Lupp, S. S. Gholap, Z. Lai, L.-C. Liang, K. W. Huang, *Org. Lett.* **2018**, *20*, 6430–6435. j) H. Dai, H. Guan, *ACS Catal.* **2018**, *8*, 9125–9130. k) J. Schneekönig, J. Tannert, H. Hornke, M. Beller, K. Junge, *Catal. Sci. Technol.* **2019**, *9*, 1779–1783.
- [81] E. Ben-Ari, G. Leitus, L. J. W. Shimon, D. Milstein, *J. Am. Chem. Soc.* **2006**, *128*, 15390–15391.
- [82] S. Chakraborty, O. Blacque, T. Fox, H. Berke, *Chem. Asian J.* **2014**, *9*, 328–337.
- [83] a) J. Ellermann, M. Moll, N. Will, *J. Organomet. Chem.* **1989**, *378*, 73–79. b) W. Schirmer, U. Flörke, H. J. Haupt, *Z. Anorg. Allg. Chem.* **1989**, *574*, 239–255.
- [84] H. F. Lang, P. E. Fanwick, R. A. Walton, *Inorg. Chim. Acta* **2002**, *329*, 1–8.
- [85] a) B. Benito-Garagorri, E. Becker, J. Wiedermann, W. Lackner, M. Pollak, K. Meireiter, J. Kisala, K. Kirchner, *Organometallics* **2006**, *25*, 1900–1913. b) K. Arashiba, Y. Miyake, Y. Nishibayashi, *Nature Chem.* **2011**, *3*, 120–125. c) K. Arashiba, K. Sasaki, S. Kuriyama, Y. Miyake, Y. Nakanishi, Y. Nishibayashi, *Organometallics* **2012**, *31*, 2035–2041. d) E. Kinoshita, K. Arashiba, S. Kuriyama, Y. Miyake, Y. Shimazaki, H. Nakanishi, Y. Nishibayashi, *Organometallics* **2012**, *31*, 8437–8443. e) O. Öztopcu, C. Holzhacker, M. Puchberger, M. Weil, K. Meireiter, L. F. Veiros, K. Kirchner, *Organometallics* **2013**, *32*, 3042–3052. f) S. R. M. M. de Aguiar, B. Stöger, B. Pittenauer, M. Puchberger, G. Allmair, L. F. Veiros, K. Kirchner, *J. Organomet. Chem.* **2014**, *760*, 74–83. g) S. R. M. M. de Aguiar, O. Öztopcu, B. Stöger, K. Meireiter, L. F. Veiros, B. Pittenauer, G. Allmair, K. Kirchner, *Dalton Trans.* **2014**, *43*, 14669–14679. h) S. Chakraborty, O. Blacque, H. Berke, *Dalton Trans.* **2015**, *44*, 6560–6570. i) R. Castro-Rodrigo, S. Chakraborty, L. Munjanja, W. Brennessel, W. D. Jones, *Organometallics* **2016**, *35*, 3124–3131. j) Y. Zhang, P. G. Williard, W. H. Bernskoetter, *Organometallics* **2016**, *35*, 860–865. k) S. R. M. M. de Aguiar, B. Stöger, B. Pittenauer, G. Allmaier, L. F. Veiros, K. Kirchner, *Dalton Trans.* **2016**, *45*, 13834–13845. l) G. A. Silantyev, M. Förster, S. Schluschaß, J. Abbenetz, C. Würtele, C. Volkmann, M. C. Holthausen, S. Schneider, *Angew. Chem. Int. Ed.* **2017**, *56*, 5872–5876. m) S. R. M. M. de Aguiar, O. Öztopcu, A. Troiani, G. de Petris, M. Weil, B. Stöger, L. F. Veiros, B. Pittenauer, G. Allmair, K. Kirchner, *Eur. J. Inorg. Chem.* **2018**, *7*, 876–884. n) M. V. Joannou, M. J. Bezdek, P. J. Chirik, *ACS Catal.* **2018**, *8*, 5276–5285. o) M. J. Bezdek, P. J. Chirik, *Angew. Chem. Int. Ed.* **2018**, *8*, 2224–2228. p) M. J. Bezdek, P. J. Chirik, *Organometallics* **2019**, *38*, 1682–1687. q) Y. Ashida, S. Kondo, K. Arashiba, T. Kikuchi, K. Nakajima, S. Kakimoto, Y. Nishibayashi, *Synthesis* **2019**, *51*, 3792–3795. r) M. Alvarez, A. Galindo, P. J. Perez, E. Carmona, *Chem. Sci.* **2019**, *10*, 8541–8546. s) R. Tran, S. M. Kilyanek, *Dalton Trans.* **2019**, *43*, 16304–16311. t) M. Pfeil, T.

- A. Engesser, A. Koch, J. Junge, J. Krahmer, C. Näther, F. Tuczek, *Eur. J. Inorg. Chem.* **2019**, 1–13.
- [86] S. Chakraborty, H. Berke, *ACS Catal.* **2014**, *4*, 2191–2194.
- [87] J. Schneekönig, W. Liu, T. Leischner, K. Junge, C. Schotes, C. Baier, M. Beller, *Org. Process Res. Dev.* **2020**, *24*, 443–448.
- [88] W. Liu, T. Leischner, K. Junge, M. Beller, *Angew. Chem. Int. Ed.* **2020**, *132*, 1–5.
- [89] T. Leischner, A. Spannenberg, K. Junge, M. Beller, *Organometallics* **2018**, *37*, 4402–4408.
- [90] T. Leischner, L. A. Suarez, A. Spannenberg, K. Junge, A. Nova, M. Beller, *Chem. Sci.* **2019**, *10*, 10566–10576.
- [91] a) D. H. Woodmansee, A. Pfaltz, *Chem. Commun.* **2011**, *47*, 7912–7916. b) J. J. Verendel, O. Pàmies, M. Diéguez, P. G. Andersson, *Chem. Rev.* **2014**, *114*, 2130–2169. c) C. Margarita, P. G. Andersson, *J. Am. Chem. Soc.* **2017**, *139*, 1346–1356.
- [92] a) C.-Y. Huang, A. G. Doyle, *Chem. Rev.* **2014**, *114*, 8153–8198. b) C. Yao, T. Dahmen, A. Gansäuer, J. Norton, *Science* **2019**, *364*, 764–767.
- [93] W. Liu, W. Li, A. Spannenberg, K. Junge, M. Beller, *Nat. Catal.* **2019**, *2*, 523–528.
- [94] T. J. Korstanje, J. I. van der Vlugt, C. J. Elsevier, B. de Bruin, *Science* **2015**, *350*, 298–302.
- [95] T. Leischner, A. Spannenberg, K. Junge, M. Beller, *ChemCatChem*, Accepted Article, DOI:10.1002/cctc.202000736



## 6 Selected Publications

The following chapter contains the original publications wherein the previously presented research was reported. My contribution to each chapter is outlined in the subchapters:

### 6.1 Molecular Defined Molybdenum Pincer Complexes and Their Application in Catalytic Hydrogenations

Thomas Leischner, Anke Spannenberg, Kathrin Junge, Matthias Beller

*Organometallics* **2018**, 37, 4402–4408.

This manuscript regarding the synthesis of various molybdenum pincer complexes and their subsequent application in the catalytic hydrogenation of ketones and styrenes was prepared by me. I conducted all the experimental work described in the publication and mainly wrote the manuscript, including the supporting information. The determination of the reported solid-state structures alongside the corresponding measurements were carried out by Anke Spannenberg. My contribution to this publication is 80%.

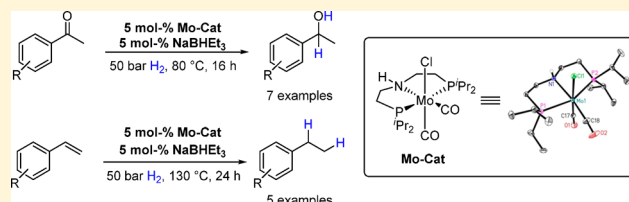
# Molecular Defined Molybdenum–Pincer Complexes and Their Application in Catalytic Hydrogenations

Thomas Leischner, Anke Spannenberg, Kathrin Junge, and Matthias Beller\*<sup>1</sup>

Leibniz Institut für Katalyse e.V. an der Universität Rostock, Albert-Einstein-Straße 29a, 18059 Rostock, Germany

## Supporting Information

**ABSTRACT:** A family of low-valent molybdenum complexes, supported by the pincer ligand  $(i\text{Pr}_2\text{PCH}_2\text{CH}_2)_2\text{NH}$ , was prepared and characterized. After activation by  $\text{NaBHET}_3$  coordination compounds **2** and **3-Cl** were found to be suitable catalysts for the hydrogenation of ketones and olefins.



## INTRODUCTION

Pincer ligands represent a well-known class of tridentate ligands, and their coordination chemistry has been intensively studied since the 1990s.<sup>1</sup> Especially in the past decade, numerous transition-metal complexes were reported, in part with interesting catalytic properties.<sup>2</sup> Notably, even the first industrial applications have been realized employing these compounds.<sup>3</sup>

Among the huge variety of different pincer ligands, complexes featuring PNP backbones have been shown to be particularly well suited for homogeneous hydrogenation reactions.<sup>4</sup> Here, the “bifunctional” character of the metal–ligand system allows for a facile H atom transfer onto unsaturated substrates.<sup>5,6</sup>

In comparison to other metals, the organometallic chemistry of group 6 PNP-pincer complexes, in particular of Mo, was poorly developed for a long time.<sup>5</sup> Although this type of complex was already described for the first time in the late 1980s by Haupt and Ellermann, only three different compounds of this type were known as late as 2006.<sup>7</sup> Later on, especially Kirchner and co-workers, but also the groups of Nishibayashi, Schneider, Jones, Bernskoetter, and Berke reported on the synthesis of molybdenum PNP complexes. The vast majority of the known compounds feature pincer ligands with a central pyridine moiety (Figure 1).<sup>5,8</sup>

In contrast to the well-studied metal organic chemistry of these Mo(PNP) complexes, reports on their catalytic activity remain scarce. As an example, Berke and co-workers showed that their Mo amido pincer complex (Figure 1), generated from the parent Mo chloride upon treatment with  $\text{NaHMDS}$ , was active in the catalytic hydrogenation of secondary imines, nitriles, and  $\text{CO}_2$ .<sup>5,9</sup> In addition, Bernskoetter described the reduction of carbon dioxide to formate by a molybdenum PNP complex in the presence of DBU, LiOTf, and dihydrogen.<sup>8i</sup> To the best of our knowledge, these are the only examples of Mo(PNP)-catalyzed reductions using molecular  $\text{H}_2$ .

Apart from that, only two other reports demonstrated the potential of this class of complexes in catalytic applications. In

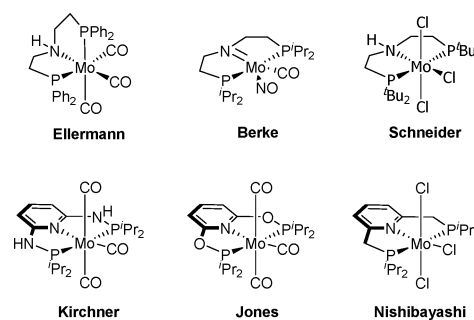


Figure 1. Selected examples of Mo(PNP) complexes.

addition to the works of Nishibayashi on the reduction of dinitrogen, Jones and co-workers established the acid-assisted isomerization of terminal olefins in the presence of PONOP-based heptacoordinated hydrido tricarbonyl Mo PNP catalysts.<sup>8h,10</sup>

As part of our ongoing interest in base-metal catalysis, we herein report the synthesis of a series of new Mo(PNP) pincer complexes containing the commercially available ligand  $(i\text{Pr}_2\text{PCH}_2\text{CH}_2)_2\text{NH}$  (Figure 2).

In addition, we report the hydrogenation of various ketones and styrenes using molecular dihydrogen with **3-Cl** as catalyst.

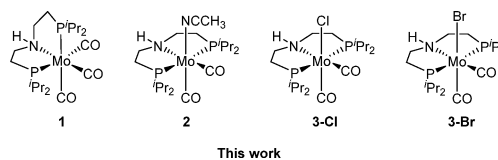


Figure 2. Selected examples of Mo(PNP) pincer complexes.

**Special Issue:** Organometallic Complexes of Electropositive Elements for Selective Synthesis

Received: June 13, 2018

Published: August 31, 2018

## RESULTS AND DISCUSSION

**Synthesis of Molybdenum(0) and Molybdenum(I) Complexes.** We started our studies by preparing the complex  $[\text{Mo}(\text{PNP-}i\text{Pr})(\text{CO})_3]$  (**1**). This compound can be easily synthesized in 91% yield by refluxing  $\text{Mo}(\text{CO})_6$  with a slight excess of the PNP ligand ( $(i\text{Pr}_2\text{PCH}_2\text{CH}_2)_2\text{NH}$ ) in toluene for 16 h (Figure 3). It has to be noted that, in 1989, Ellermann and co-workers already reported the synthesis of the related complex  $[\text{Mo}(\text{PNP-Ph})(\text{CO})_3]$  in 66% yield, using a related methodology.<sup>7b,11</sup>

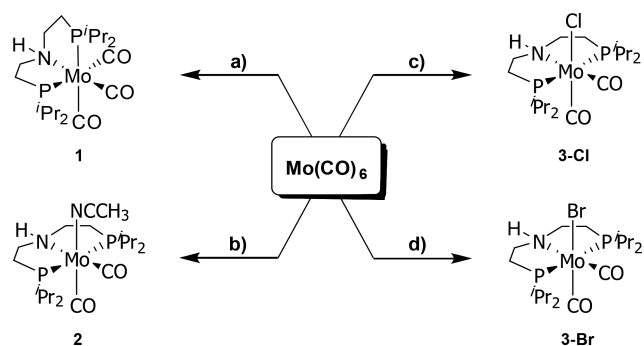


**Figure 3.** Synthesis of the reported Mo-PNP pincer complexes. Legend: (a) toluene, reflux, overnight, 1.05 equiv of  $(i\text{Pr}_2\text{PCH}_2\text{CH}_2)_2\text{NH}$ ; (b) (1) MeCN/benzene, 1.10 equiv of  $\text{C}_3\text{H}_5\text{Br}$ , reflux, overnight, (2) 3.00 equiv of  $\text{PPh}_3$ , MeCN, reflux, 1 h, (3) 1.05 equiv of  $(i\text{Pr}_2\text{PCH}_2\text{CH}_2)_2\text{NH}$ , toluene, room temperature, overnight; (c) (1) MeCN/benzene, 1.10 equiv of  $\text{C}_3\text{H}_5\text{Br}$ , reflux, overnight, (2) 3.00 equiv of  $\text{PPh}_3$ , MeCN, reflux, 1 h, (3) 1.05 equiv of  $(i\text{Pr}_2\text{PCH}_2\text{CH}_2)_2\text{NH}$ , DCM, room temperature, overnight; (d) (1) MeCN/benzene, 1.10 equiv of  $\text{C}_3\text{H}_5\text{Br}$ , reflux, overnight, (2) 1.05 equiv of  $(i\text{Pr}_2\text{PCH}_2\text{CH}_2)_2\text{NH}$ , toluene, room temperature, 24 h.

Next, we prepared the known molybdenum precursors  $\text{Mo}(\eta^3\text{-allyl})(\text{CO})_2(\text{CH}_3\text{CN})_2\text{Br}$  and  $\text{Mo}(\text{PPh}_3)_2(\text{CO})_2(\text{CH}_3\text{CN})_2$  according to literature procedures.<sup>12</sup> Subsequent treatment with the aforementioned PNP ligand in toluene at room temperature resulted in the formation of the new Mo complexes **2** and **3-Br**, respectively, in 82% and 11% yields. The paramagnetic 17-electron complex **3-Br**, which originates from the reaction between  $\text{Mo}(\eta^3\text{-allyl})(\text{CO})_2(\text{CH}_3\text{CN})_2\text{Br}$  and  $(i\text{Pr}_2\text{PCH}_2\text{CH}_2)_2\text{NH}$ , features a molybdenum center in the oxidation state +I, instead of the expected oxidation number +II.<sup>13</sup> When we used  $\text{Mo}(\text{PPh}_3)_2(\text{CO})_2(\text{CH}_3\text{CN})_2$  as the molybdenum source, we obtained complex **2** as a pale yellow and poorly soluble precipitate as the reaction product. Thereby, we were surprised to find that the central molybdenum atom in **2** still coordinates an acetonitrile molecule in place of an anticipated  $\text{PPh}_3$  ligand.

When we attempted to obtain X-ray-quality single crystals of complex **2** via crystallization from DCM/toluene, the desired complex was not obtained, however. Instead, the 17-electron  $\text{Mo}(\text{I})$  complex **3-Cl** was formed.<sup>13</sup> Presumably the chlorine atom originates from the solvent.

We subsequently tried to prepare **3-Cl** directly from  $\text{Mo}(\text{PPh}_3)_2(\text{CO})_2(\text{CH}_3\text{CN})_2$  and  $(i\text{Pr}_2\text{PCH}_2\text{CH}_2)_2\text{NH}$  by using DCM as the solvent. Indeed, we were able to isolate **3-Cl** in 68% yield as a pale brown powder. Attempts to synthesize compound **3-Br** via the same route using  $\text{CH}_2\text{Br}_2$  as the solvent resulted in the formation of an inseparable mixture of different species, even at low temperatures. Additional attempts to prepare **3-Br** starting from **3-Cl** via halide

exchange using  $\text{KBr}$  and  $\text{NBu}_4\text{Br}$ , respectively, were also unsuccessful.

The herein reported coordination compounds have all been characterized using IR spectroscopy and elemental analysis. Additionally, the solid-state structures of all reported complexes have been determined by X-ray crystallography. Structural views are depicted in Figures 4–7, respectively, with

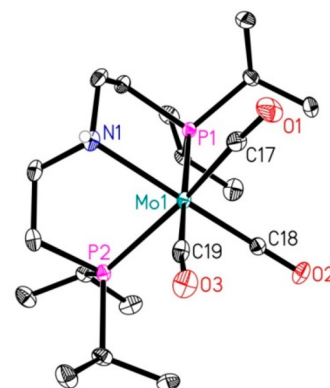


**Figure 4.** Molecular structure of **1** in the crystal. Only one molecule of the asymmetric unit is depicted. Displacement ellipsoids correspond to 30% probability. Hydrogen atoms except those bound to N are omitted for clarity. Selected bond lengths (Å) and bond angles (deg):  $\text{N1-Mo1} = 2.3505(16)$ ,  $\text{P1-Mo1} = 2.5387(5)$ ,  $\text{P2-Mo1} = 2.5304(5)$ ,  $\text{Mo1-C17} = 1.974(2)$ ,  $\text{Mo1-C18} = 1.9489(19)$ ,  $\text{Mo1-C19} = 1.948(2)$ ;  $\text{P1-Mo1-N1} = 76.92(4)$ ,  $\text{P2-Mo1-N1} = 77.59(4)$ ,  $\text{P1-Mo1-P2} = 100.778(16)$ ,  $\text{N1-Mo1-C17} = 94.21(7)$ ,  $\text{N1-Mo1-C18} = 171.83(7)$ ,  $\text{N1-Mo1-C19} = 100.13(7)$ .

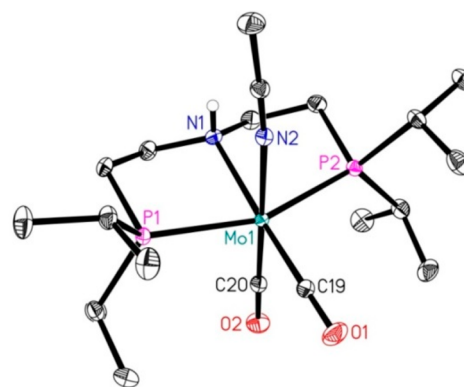


**Figure 5.** Molecular structure of **2** in the crystal. Displacement ellipsoids correspond to 30% probability. Hydrogen atoms except for those bound to N are omitted for clarity. Selected bond lengths (Å) and bond angles (deg):  $\text{N1-Mo1} = 2.3228(13)$ ,  $\text{P1-Mo1} = 2.4389(4)$ ,  $\text{P2-Mo1} = 2.4296(4)$ ,  $\text{Mo1-C19} = 1.9201(16)$ ,  $\text{Mo1-C20} = 1.9156(17)$ ,  $\text{Mo1-N2} = 2.2274(14)$ ;  $\text{N1-Mo1-P1} = 79.28(3)$ ,  $\text{N1-Mo1-P2} = 79.14(3)$ ,  $\text{N1-Mo1-C19} = 174.57(6)$ ,  $\text{N1-Mo1-C20} = 99.55(6)$ ,  $\text{N1-Mo1-N2} = 80.67(5)$ .

selected bond distances and angles given in the captions. However, we were only able to characterize complex **1** using standard NMR techniques. Due to the extremely low solubility of complex **2** in most organic solvents, including benzene, toluene, acetonitrile, THF, acetone, DMSO, and methanol, we were unable to obtain any NMR data of complex **2**. Moreover, complex **2** proved to be unstable in  $\text{CD}_2\text{Cl}_2$  and  $\text{CDCl}_3$ , presumably due to the acidic nature of these solvents or insertion into the C–Cl bond. Complexes **3-Cl** and **3-Br** are

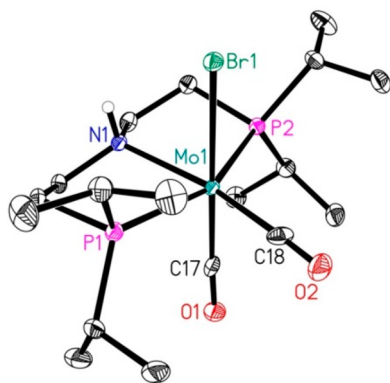


**Figure 6.** Molecular structure of **3-Br** in the crystal. Only one molecule of the asymmetric unit is depicted. Displacement ellipsoids correspond to 30% probability. Hydrogen atoms except for those bound to N are omitted for clarity. Selected bond lengths (Å) and bond angles (deg): N1–Mo1 = 2.298(2), P1–Mo1 = 2.5208(7), P2–Mo1 = 2.4834(7), Mo1–C17 = 1.923(3), Mo1–C18 = 1.970(3), Mo1–Br1 = 2.7435(3); N1–Mo1–P1 = 76.57(5), N1–Mo1–P2 = 78.96(5), N1–Mo1–C17 = 97.05(9), N1–Mo1–C18 = 164.55(10), N1–Mo1–Br1 = 82.10(5).

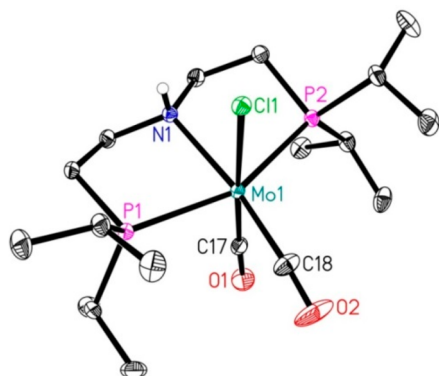


**Figure 7.** Molecular structure of **3-Cl** in the crystal. Displacement ellipsoids correspond to 30% probability. Hydrogen atoms except for those bound to N are omitted for clarity. Selected bond lengths (Å) and bond angles (deg): N1–Mo1 = 2.3029(15), P1–Mo1 = 2.5002(5), P2–Mo1 = 2.4877(5), Mo1–C17 = 1.9118(19), Mo1–C18 = 1.954(2), Mo1–Cl1 = 2.5817(4); N1–Mo1–P1 = 77.10(4), N1–Mo1–P2 = 78.80(4), N1–Mo1–C17 = 100.53(7), N1–Mo1–C18 = 171.20(9), N1–Mo1–Cl1 = 81.05(4).

NMR silent due to their paramagnetic nature and therefore could not be analyzed by this method.

In accordance with the initial report of Ellermann and co-workers on the related compound [Mo(PNP-Ph)(CO)<sub>3</sub>], complex **1** also adopts a *fac* coordination geometry in the solid state.<sup>7b</sup> The recorded IR spectrum likewise shows three absorption bands at 1924, 1805, and 1758 cm<sup>-1</sup>, respectively. The IR spectra for **2**, **3-Cl**, and **3-Br** all show medium to strong carbonyl absorption bands between 1889 and 1676 cm<sup>-1</sup>.

Complexes **2**, **3-Br**, and **3-Cl** all exhibit a distorted-octahedral arrangement of the donor atoms around the Mo center with the CO ligands being in a *cis* orientation. The N1–Mo, P1–Mo, and P2–Mo bond lengths as well as the N1–Mo–P1 and N1–Mo–P2 bond angles are in the same range for all of the mentioned compounds. Noteworthy are the deviations of the bond angles N1–Mo–C18 for **3-Br** and **3-Cl** and N1–Mo–C19 for **2** from ideal linearity. This deviation is

the most pronounced for **3-Br** (164.55(10)°) and steadily decreases from **3-Cl** (171.20(9)°) to **2** (174.57(6)°).

**Catalytic Hydrogenation of Acetophenones and Styrenes with 3-Cl.** In initial attempts we tested molybdenum PNP pincer complex **1** for the reduction of carbonyl moieties using acetophenone as the benchmark substrate. Unfortunately, with or without additives (*vide supra*) no conversion was obtained. Similarly, when **3-Cl** was used in the absence of additives or in the presence of 10 mol % of KO<sup>t</sup>Bu or NaHMDS, we did not observe any conversion of the starting material. However, addition of 10 mol % of NaBHET<sub>3</sub> resulted in full conversion of acetophenone under the given conditions (Table 1). Using the same methodology,

**Table 1.** Catalytic Hydrogenation of Acetophenone Using **3-Cl** and Different Additives<sup>a</sup>

additive	amount (mol %)	conversion (%) <sup>b</sup>	yield (%) <sup>c</sup>
none		0	0
KO <sup>t</sup> Bu	10	3	0
NaHMDS	10	5	0
NaBHET <sub>3</sub>	10	100	97
NaBHET <sub>3</sub> <sup>d</sup>	10	10	8

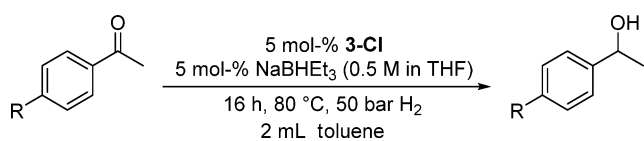
<sup>a</sup>0.5 mmol of substrate was used. <sup>b</sup>Conversions were determined by GC analysis using hexadecane (20 mg) as internal standard. <sup>c</sup>Yields were determined by GC analysis using hexadecane (20 mg) as internal standard. <sup>d</sup>No catalyst was used.

we demonstrated that complex **2** gave the same result. Nevertheless, due to practical reasons, we focused on **3-Cl** in the further course of our studies.

In order to rule out any heterogeneous side reactions during the hydrogenation catalysis, a mercury poisoning experiment was carried out. For this purpose, a drop of mercury was placed in the reaction vial and the catalysis was carried out as described above. To our delight, GC analysis of the resulting reaction mixture still showed full conversion of the benchmark substrate after 3.5 h, thus indicating that the developed system follows a homogeneous pathway. Deterred by the harsh conditions, we decided to investigate whether an increased catalyst loading would allow for a lower reaction temperature. Indeed, increasing the catalyst loading to 5 mol % led to full conversion of acetophenone in toluene at 80 °C, though an extended reaction time of 16 h was necessary. Additionally, we were able to reduce the amount of NaBHET<sub>3</sub> used to 5 mol %. Next, a variety of *para*-substituted acetophenones was subjected to the reaction conditions developed. For the given starting materials excellent conversions (90–100%) and isolated yields (84–91%) were obtained in all cases (Table 2).

When we used chalcone (Table 2, entry 7) as a substrate, in order to investigate whether our catalyst system displayed any selectivity toward either the C=C double bond or the carbonyl moiety, we found complete reduction of both functional groups and were able to isolate 1,3-diphenyl-1-propanol in 91% yield.

On the basis of this result, we decided to investigate the general reactivity of our catalyst system toward terminal and internal C=C double bonds in more detail. Here, 1-dodecene,

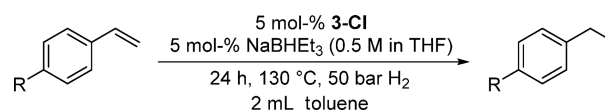
Table 2. Hydrogenation of Various Acetophenones with 3-Cl/NaBHET<sub>3</sub><sup>a</sup>

Entry	Substrate	Conversion [%] <sup>b</sup>	Yield [%] <sup>c</sup>
1		100	91
2		97	90
3		90	84
4		>99	92
5		100	91
6		>99	90
7 <sup>d</sup>		>99	91

<sup>a</sup>0.5 mmol of substrate was used. <sup>b</sup>Conversions determined by GC using hexadecane (20 mg) as internal standard. <sup>c</sup>Isolated yields given. <sup>d</sup>24 h reaction time.

styrene, and *cis*- and *trans*-stilbene were applied as model substrates. While 1-dodecene, as well as *cis*- and *trans*-stilbene, only showed low conversions of 4%, 25%, and 29%, respectively, styrene gave 76% conversion into ethylbenzene. Hence, we tested a number of different styrenes, bearing electron-donating and -withdrawing substituents on the aromatic ring (Table 3). In general, we obtained medium to good yields (57–85%), though harsher conditions were needed. Notably, no cleavage of the benzyl ether moiety was observed during the reduction of 3-benzoyloxy-3-methoxystyrene (Table 3, entry 5).

In order to evaluate the potential of complex 3-Cl in a broader sense, we finally tested diphenylacetylene and benzonitrile as substrates under the conditions shown in Table 3. When diphenylacetylene was applied, we obtained a conversion of 75%. However, the reaction turned out to be unselective, yielding a mixture of 41% 1,2-diphenylethane, 17% *cis*-stilbene, and 17% *trans*-stilbene. The hydrogenation of

Table 3. Hydrogenation of Various Styrenes with 3-Cl/NaBHET<sub>3</sub><sup>a</sup>

Entry	Substrate	Yield [%]
1		76 <sup>b</sup>
2		85 <sup>b</sup>
3		58 <sup>c</sup>
4		57 <sup>c</sup>
5		74 <sup>d</sup>

<sup>a</sup>0.5 mmol of substrate was used. <sup>b</sup>Yield determined by GC using hexadecane (20 mg) as internal standard. <sup>c</sup>NMR yield determined by <sup>19</sup>F NMR of the crude mixture using C<sub>6</sub>F<sub>6</sub> as internal standard. <sup>d</sup>NMR yield determined by <sup>1</sup>H NMR of the crude mixture using 1,3,5-trimethoxybenzene as internal standard.

benzonitrile proceeded with a modest conversion of 42% and gave *N*-benzylidenebenzylamine as the major reaction product with a yield of 29% along with 13% of benzylamine. All yields and conversions reported in this paragraph were determined by GC using hexadecane (20 mg) as internal standard.

## CONCLUSIONS

In conclusion, we have synthesized a series of four structurally new molybdenum complexes featuring the commercially available PNP-pincer ligand (*i*-Pr<sub>2</sub>PCH<sub>2</sub>CH<sub>2</sub>)<sub>2</sub>NH. These new coordination compounds can all be prepared in a straightforward manner by starting from known molybdenum precursors and were characterized by IR spectroscopy, elemental analysis, and X-ray crystallography. We demonstrated that the Mo(I) species 3-Cl is a suitable catalyst for the hydrogenation of various acetophenones and styrenes in the presence of NaBHET<sub>3</sub> as an additive. Moreover, we could show that 3-Cl is active in the hydrogenation of diphenylacetylene and benzonitrile, though low selectivities were observed.

## EXPERIMENTAL SECTION

**General Experimental Information.** Unless otherwise stated, all reactions were performed under an argon atmosphere with exclusion of moisture and air from reagents and glassware using standard Schlenk and glovebox techniques for manipulating air-sensitive compounds. Dry and oxygen-free solvents (acetonitrile, DCM, toluene, THF, and heptane) were collected from an Innovative Technology PS-MD-6 solvent purification system and stored over 3 Å molecular sieves. CD<sub>2</sub>Cl<sub>2</sub> was purchased from Eurisotop, degassed by freeze–pump–thaw techniques, and subsequently dried over 3 Å molecular sieves. All other chemicals were purchased and used



without further purification.  $\text{Mo}(\text{CO})_6$ ,  $\text{NaBHET}_3$  (1 M in THF), acetophenone, 4-F-acetophenone, 4-MeO-acetophenone, 4- $\text{CF}_3$ -acetophenone, 4-MeS-acetophenone, chalcone, 3-benzoyloxy-3-methoxystyrene, and *trans*-stilbene were purchased from Sigma-Aldrich.  $(\text{Pr}_2\text{PCH}_2\text{CH}_2)_2\text{NH}$  was obtained from Strem (10 wt % solution in THF). Styrene, 4-F-styrene, 4-MeO-styrene, and 4- $\text{CF}_3$ -styrene were purchased from TCI. 4-Ethylacetophenone and *cis*-stilbene were purchased from Alfa Aesar. 1-Dodecene was obtained from Fluka.  $\text{Mo}(\eta^3\text{-allyl})(\text{CO})_2(\text{CH}_3\text{CN})_2\text{Br}^{1,2}$  and  $\text{Mo}(\text{PPh}_3)_2(\text{CO})_2(\text{CH}_3\text{CN})_2^{12}$  were prepared according to literature procedures.  $^1\text{H}$ ,  $^{13}\text{C}$ , and  $^{19}\text{F}$  NMR spectra were recorded on Bruker AV 300 and Bruker AV 400 spectrometers. Chemical shift values in  $^1\text{H}$  and  $^{13}\text{C}$  NMR spectra were referenced internally to the residual solvent resonances, whereas  $^{19}\text{F}$  and  $^{31}\text{P}$  NMR spectra were referenced externally to  $\text{CCl}_3\text{F}$  and  $\text{H}_3\text{PO}_4$ , respectively. Abbreviations used in the reported NMR experiments are as follows: b, broad; s, singlet; d, doublet; t, triplet; m, multiplet. All measurements were carried out at room temperature. Infrared spectra were recorded in the solid state on a Bruker Alpha P FT-IR spectrometer. Elemental analyses were carried out using a Leco TruSpec Micro CHNS device. Gas chromatography was performed on a HP 6890 instrument with an HP5 column (Agilent) unless stated otherwise. All hydrogenation reactions were set up under Ar in a 300 mL autoclave (PARR Instrument Co.). In order to avoid unspecific reductions, all catalytic experiments were carried out in 4 mL glass vials, which were set up in an alloy plate and placed inside the autoclave.

**Synthesis of 1.** Under an argon atmosphere, a 50 mL Schlenk flask, equipped with a magnetic stirring bar and a reflux condenser, was charged with  $\text{Mo}(\text{CO})_6$  (105.6 mg, 400.0  $\mu\text{mol}$ , 1.00 equiv). A 10 mL portion of toluene was added, and the suspension was subsequently treated dropwise with  $(\text{Pr}_2\text{PCH}_2\text{CH}_2)_2\text{NH}$  (1.46 mL of a 10 wt % solution in THF, 420.0  $\mu\text{mol}$ , 1.05 equiv) at room temperature. The reaction mixture was heated to reflux overnight, and the resulting orange-red solution was cooled to room temperature again. The solvent was removed under reduced pressure until product precipitation occurred. The orange precipitate was filtered off, washed two times with 5 mL of toluene, and afterward redissolved in the minimum amount of DCM. Heptane was added until product precipitation occurred again. The resulting yellow solid was filtered off, washed two times with 5 mL of heptane/DCM 3/1 (v/v), and dried in vacuo to yield 176.7 mg (91%) of complex **1** as an intense yellow solid. Crystals suitable for X-ray analysis were obtained from a saturated solution of **1** in acetonitrile at 4 °C. Alternatively single crystals can be obtained by slowly allowing a layer of heptane to diffuse into a saturated solution of **1** in DCM or toluene at room temperature.  $^1\text{H}$  NMR (400 MHz,  $\text{CD}_2\text{Cl}_2$ ):  $\delta$  3.23–3.10 (m, 2H), 2.47–1.41 (m, 1H), 2.18–1.95 (m, 8H), 1.40–1.31 (m, 2H), 1.25–1.11 (m, 24H).  $^{13}\text{C}\{^1\text{H}\}$  NMR (101 MHz,  $\text{CD}_2\text{Cl}_2$ ):  $\delta$  232.1 (t,  $J$  = 6.1 Hz), 218.8 (t,  $J$  = 10.5 Hz), 216.2 (t,  $J$  = 9.0 Hz), 53, 57 (t,  $J$  = 8.1 Hz), 30.71 (t,  $J$  = 13.1 Hz), 29.06 (t,  $J$  = 9.1 Hz), 26.47 (t,  $J$  = 10.1 Hz), 19.93 (t,  $J$  = 3.0 Hz), 19.43 (t,  $J$  = 3.0 Hz), 18.99 (t,  $J$  = 3.0 Hz), 18.73 (s).  $^{31}\text{P}\{^1\text{H}\}$  NMR (162 MHz,  $\text{CD}_2\text{Cl}_2$ ):  $\delta$  75.6. Anal. Calcd for  $\text{C}_{19}\text{H}_{37}\text{MoNO}_3\text{P}_2$ : C, 47.01; H, 7.68; N, 2.89. Found: C, 47.35; H, 7.86; N, 2.84. IR (ATR,  $\text{cm}^{-1}$ ): 1924 ( $\nu_{\text{CO}}$ ), 1805 ( $\nu_{\text{CO}}$ ), 1758 ( $\nu_{\text{CO}}$ ).

**Synthesis of 2.** In a 25 mL Schlenk flask,  $\text{Mo}(\text{PPh}_3)_2(\text{CO})_2(\text{CH}_3\text{CN})_2$  (304.8 mg, 401.7  $\mu\text{mol}$ , 1.00 equiv) was suspended in 10 mL of THF and treated dropwise with  $(\text{Pr}_2\text{PCH}_2\text{CH}_2)_2\text{NH}$  (1.45 mL of a 10 wt % solution in THF, 421.8  $\mu\text{mol}$ , 1.05 equiv) at room temperature. The reaction mixture was stirred overnight, and the precipitated solid was filtered from the supernatant. Subsequent washing of the obtained pale yellow solid with three 5 mL portions of THF followed by removal of residual solvent under reduced pressure gave 126.3 mg (81% yield) of **2** as a pale yellow solid. Crystals suitable for X-ray analysis were obtained by slowly allowing a layer of toluene to diffuse into a saturated solution of **2** in THF at –30 °C. Anal. Calcd for  $\text{C}_{20}\text{H}_{40}\text{MoN}_2\text{O}_2\text{P}_2$ : C, 48.19; H, 8.09; N, 5.62. Found: C, 48.26; H, 8.30; N, 5.54. IR (ATR,  $\text{cm}^{-1}$ ): 2246 ( $\nu_{\text{CN}}$ ), 1762 ( $\nu_{\text{CO}}$ ), 1676 ( $\nu_{\text{CO}}$ ).

**Synthesis of 3-Br.** In a 10 mL Schlenk flask,  $\text{Mo}(\eta^3\text{-allyl})(\text{CO})_2(\text{CH}_3\text{CN})_2\text{Br}$  (150.4 mg, 423.6  $\mu\text{mol}$ , 1.00 equiv) was

suspended in 5 mL of toluene and cooled to 0 °C in an ice bath.  $(\text{Pr}_2\text{PCH}_2\text{CH}_2)_2\text{NH}$  (1.54 mL of a 10 wt % solution in THF, 444.8  $\mu\text{mol}$ , 1.05 equiv) was added dropwise, and the reaction mixture was warmed to room temperature overnight. The resulting opaque liquid was filtered, and the solid residue was extracted two times with 2 mL of toluene. The combined filtrates were dried under reduced pressure, and the resulting orange-brown solid was washed two times with 5 mL of heptane. The remaining residue was dissolved in the minimum amount of DCM and layered with heptane to afford 16.2 mg (11% yield) of **3-Br** as tiny brownish crystals. Crystals suitable for X-ray analysis were obtained by slowly allowing a layer of heptane to diffuse into a saturated solution of **3-Br** in DCM at room temperature. Anal. Calcd for  $\text{C}_{18}\text{H}_{37}\text{BrMoNO}_2\text{P}_2$ : C, 40.24; H, 6.94; N, 2.61. Found: C, 40.42; H, 7.01; N, 2.65. IR (ATR,  $\text{cm}^{-1}$ ): 1894 ( $\nu_{\text{CO}}$ ), 1780 ( $\nu_{\text{CO}}$ ), 1751 ( $\nu_{\text{CO}}$ ).

**Synthesis of 3-Cl.** In a 50 mL Schlenk flask,  $\text{Mo}(\text{PPh}_3)_2(\text{CO})_2(\text{CH}_3\text{CN})_2$  (540.2 mg, 712.0  $\mu\text{mol}$ , 1.00 equiv) was suspended in 15 mL of DCM and cooled to 0 °C in an ice bath.  $(\text{Pr}_2\text{PCH}_2\text{CH}_2)_2\text{NH}$  (2.6 mL of a 10 wt % solution in THF, 747.6  $\mu\text{mol}$ , 1.05 equiv) was added dropwise, and the reaction mixture was warmed to room temperature overnight. The resulting clear brown liquid was filtered, and the solvent was removed under reduced pressure until product precipitation occurred. The supernatant was filtered off, and the remaining other solid was washed three times with 5 mL of heptane/DCM 3/1 (v/v) and three times with 5 mL of THF. Removal of residual solvent under reduced pressure subsequently gave 238.6 mg (68% yield) of **3-Cl** as a pale brown powder. Crystals suitable for X-ray analysis were obtained from a saturated solution of **3-Cl** in acetonitrile at 4 °C. Alternatively single crystals can be obtained by slowly allowing a layer of heptane to diffuse into a saturated solution of **3-Cl** in DCM at room temperature. Anal. Calcd for  $\text{C}_{18}\text{H}_{37}\text{ClMoNO}_2\text{P}_2$ : C, 43.87; H, 7.57; N, 2.84. Found: C, 43.89; H, 7.30; N, 2.75. IR (ATR,  $\text{cm}^{-1}$ ): 1889 ( $\nu_{\text{CO}}$ ), 1782 ( $\nu_{\text{CO}}$ ), 1747 ( $\nu_{\text{CO}}$ ).

**General Procedure for Catalytic Experiments.** Under an argon atmosphere, a 4 mL glass vial containing a stirring bar was charged with complex **3-Cl** (12.5 mg; 5 mol %). Afterward, the reaction vial was capped with a septum and equipped with a syringe needle and toluene (2 mL) was added. The resulting brown suspension was treated with  $\text{NaBHET}_3$  (0.5 M in THF, 0.05 mL, 5 mol %) and stirred for 10 min, and the corresponding substrate was subsequently added to this mixture. The reaction vial was transferred into an autoclave. Once sealed, the autoclave was purged 10 times with 10 bar of dihydrogen, before the pressure was set to the desired value (50 bar). The reaction mixture was stirred for 16 h in a preheated aluminum block at 80 °C for ketones and 24 h at 130 °C for styrenes, respectively. Afterward, the autoclave was cooled in an ice bath and the remaining gas was released carefully. The solution was subsequently diluted with ethyl acetate and filtered through a small pad of Celite (1 cm in a Pasteur pipet). The Celite was washed with methanol (2 mL), and the combined filtrates were evaporated to dryness afterward. The remaining residue was purified by column chromatography ( $\text{SiO}_2$ , heptane/EtOAc, gradient 100/0  $\rightarrow$  0/100). For the characterization of the products of the catalysis, see the Supporting Information.

## ■ ASSOCIATED CONTENT

### Supporting Information

The Supporting Information is available free of charge on the ACS Publications website at DOI: 10.1021/acs.organomet.8b00410.

General procedure for hydrogenation reactions, characterization of the hydrogenated products, NMR spectra for complex **1**, IR spectra for complexes **1**, **2**, **3-Br**, and **3-Cl**, X-ray crystal structure analysis, and NMR spectra of the isolated products of the catalysis (PDF)

## Accession Codes

CCDC 1847003–1847006 contain the supplementary crystallographic data for this paper. These data can be obtained free of charge via [www.ccdc.cam.ac.uk/data\\_request/cif](http://www.ccdc.cam.ac.uk/data_request/cif), or by emailing [data\\_request@ccdc.cam.ac.uk](mailto:data_request@ccdc.cam.ac.uk), or by contacting The Cambridge Crystallographic Data Centre, 12 Union Road, Cambridge CB2 1EZ, UK; fax: +44 1223 336033.

## AUTHOR INFORMATION

## Corresponding Author

\*E-mail for M.B.: [Matthias.Beller@catalysis.de](mailto:Matthias.Beller@catalysis.de).

## ORCID

Matthias Beller: 0000-0001-5709-0965

## Notes

The authors declare no competing financial interest.

## ACKNOWLEDGMENTS

We gratefully acknowledge the support from the Federal Ministry of Education and Research of Germany, the State of Mecklenburg-West Pomerania, and the European Union (ERC-Advanced Grant 670986-NoNaCat). We thank the analytical department (S. Schareina, S. Buchholz, A. Lehmann) of the Leibniz-Institute for Catalysis, Rostock.

## REFERENCES

(1) Benito-Garagorri, B.; Kirchner, K. Modularly Designed Transition Metal PNP and PCP Pincer Complexes based on Aminophosphines: Synthesis and Catalytic Applications. *Acc. Chem. Res.* **2008**, *41*, 201–213.

(2) (a) Kawatsura, M.; Hartwig, J. F. Transition Metal-Catalyzed Addition of Amines to Acrylic Acid Derivatives. A High-Throughput Method for Evaluating Hydroamination of Primary and Secondary Alkylamines. *Organometallics* **2001**, *20*, 1960–1964. (b) Stambuli, J. P.; Stauffer, S. R.; Shaughnessy, K. H.; Hartwig, J. F. Screening of Homogeneous Catalysts by Fluorescence Resonance Energy Transfer. Identification of Catalysts for Room-Temperature Heck Reactions. *J. Am. Chem. Soc.* **2001**, *123*, 2677–2678. (c) Kloek, S. M.; Heinekey, D. M.; Goldberg, K. I. Stereoselective Decarbonylation of Methanol to Form a Stable Iridium(III) trans-Dihydride Complex. *Organometallics* **2006**, *25*, 3007–3011. (d) Pelczar, E. M.; Emge, T. J.; Krogh-Jespersen, K.; Goldman, A. S. Unusual Structural and Spectroscopic Features of Some PNP-Pincer Complexes of Iron. *Organometallics* **2008**, *27*, 5759–5767. (e) van der Vlugt, J. I.; Pidko, E. A.; Vogt, D.; Lutz, M.; Spek, A. L.; Meetsma, A. T-Shaped Cationic Cu(I) Complexes with Hemilabile PNP-Type Ligands. *Inorg. Chem.* **2008**, *47*, 4442–4444. (f) Tanaka, R.; Yamashita, M.; Nozaki, K. Catalytic Hydrogenation of Carbon Dioxide Using Ir(III)-Pincer Complexes. *J. Am. Chem. Soc.* **2009**, *131*, 14168–14169. (g) van der Vlugt, J. I.; Siegler, M. A.; Janssen, M. L.; Vogt, D.; Spek, A. L. A Cationic Ag(I)(PNP<sup>t</sup>Bu) Species Acting as PNP Transfer Agent: Facile Synthesis of Pd(PNP<sup>t</sup>Bu)(alkyl) Complexes and Their Reactivity Compared to PCP<sup>t</sup>Bu Analogues. *Organometallics* **2009**, *28*, 7025–7032. (h) Cucciolito, M. E.; D'Amora, A.; Vitagliano, A. Catalytic hydroalkylation of olefins by stabilized carbon nucleophiles promoted by dicationic platinum(II) and palladium(II) complexes. *Organometallics* **2010**, *29*, 5878–5884. (i) Gnanaprakasam, B.; Zhang, J.; Milstein, D. Direct synthesis of imines from alcohols and amines with liberation of H<sub>2</sub>. *Angew. Chem., Int. Ed.* **2010**, *49*, 1468–1471. (j) Hahn, C. Structural Investigations of Platinum(II) Styrene and Styryl Complexes and Mechanistic Study of Vinylic Deprotonation. *Organometallics* **2010**, *29*, 1331–1338. (k) Khaskin, E.; Iron, M. A.; Shimon, L. J. W.; Zhang, J.; Milstein, D. N-H Activation of Amines and Ammonia by Ru via Metal-Ligand Cooperation. *J. Am. Chem. Soc.* **2010**, *132*, 8542–8543. (l) Schwartsburd, L.; Iron, M. A.; Konstantinovskii, L.; Diskin-Posner, Y.; Leitun, G.; Shimon, L. J. W.; Milstein, D. Synthesis and reactivity of an iridium(I) acetylonyl PNP

complex. Experimental and computational study of metal-ligand cooperation in H-H and C-H bond activation via reversible ligand dearomatization. *Organometallics* **2010**, *29*, 3817–3827. (m) Nakajima, Y.; Shiraiishi, Y.; Tsuchimoto, T.; Ozawa, F. Synthesis and coordination behavior of Cu(I) bis(phosphaethenyl)pyridine complexes. *Chem. Commun.* **2011**, *47*, 6332–6334.

(3) Kuriyama, W.; Matsumoto, T.; Ogata, O.; Ino, Y.; Aoki, K.; Tanaka, S.; Ishida, K.; Kobayashi, T.; Sayo, N. Catalytic hydrogenation of esters. development of an efficient catalyst and processes for synthesising (R)-1,2-propanediol and 2-(l-menthoxy). *Org. Process Res. Dev.* **2012**, *16*, 166–171.

(4) *The Chemistry of Pincer Compounds*; Morales-Morales, D., Jensen, C. M., Eds.; Elsevier Science: Amsterdam, 2007.

(5) Chakraborty, S.; Blacque, O.; Fox, T.; Berke, H. Highly Active, Low-Valence Molybdenum- and Tungsten-Amide Catalysts for Bifunctional Imine-Hydrogenation Reactions. *Chem. - Asian J.* **2014**, *9*, 328–337.

(6) (a) Ben-Ari, E.; Leitun, G.; Shimon, L. J. W.; Milstein, D. Metal-Ligand Cooperation in C-H and H<sub>2</sub> Activation by an Electron-Rich PNP Ir(I) System: Facile Ligand Dearomatization-Aromatization as Key Steps. *J. Am. Chem. Soc.* **2006**, *128*, 15390–15391. (b) Khusnutdinova, J. R.; Milstein, D. Metal-Ligand Cooperation. *Angew. Chem., Int. Ed.* **2015**, *54*, 12236–12273.

(7) (a) Schirmer, W.; Flörke, U.; Haupt, H. J. Preparation, properties, and molecular structures of a rigid tridentate chelate ligand N,N'-bis(diphenylphosphino)-2,6-diaminopyridine with M(II) and M(0) transition metals [M(II) = nickel, palladium, platinum; M(0) = chromium, molybdenum, tungsten]. *Z. Anorg. Allg. Chem.* **1987**, *545*, 83–97. (b) Ellermann, J.; Moll, M.; Will, N. Chemistry of polyfunctional molecules. CV. Chromium, molybdenum and tungsten tricarbonyl complexes of bis[2-(diphenylphosphino)ethyl]amine. *J. Organomet. Chem.* **1989**, *378*, 73–79. (c) Lang, H. F.; Fanwick, P. E.; Walton, R. A. Reactions of quadruply bonded dimolybdenum(II) and dirhenium(III) complexes with 2,6-bis(dicyclohexylphosphinomethyl)pyridine and the related behavior of the mixed P,S,P ligand bis(diphenylphosphinomethyl)sulfide. *Inorg. Chim. Acta* **2002**, *329*, 1–8.

(8) (a) Benito-Garagorri, B.; Becker, E.; Wiedermann, J.; Lackner, W.; Pollak, M.; Mereiter, K.; Kisala, J.; Kirchner, K. Achiral and Chiral Transition Metal Complexes with Modularly Designed Tridentate PNP Pincer-Type Ligands Based on N-Heterocyclic Diamines. *Organometallics* **2006**, *25*, 1900–1913. (b) Arashiba, K.; Sasaki, K.; Kuriyama, S.; Miyake, Y.; Nakanishi, H.; Nishibayashi, Y. Synthesis and Protonation of Molybdenum- and Tungsten-Dinitrogen Complexes Bearing PNP-Type Pincer Ligands. *Organometallics* **2012**, *31*, 2035–2041. (c) Kinoshita, E.; Arashiba, K.; Kuriyama, S.; Miyake, Y.; Shimazaki, R.; Nakanishi, H.; Nishibayashi, Y. Synthesis and Catalytic Activity of Molybdenum-Dinitrogen Complexes Bearing Unsymmetric PNP-Type Pincer Ligands. *Organometallics* **2012**, *31*, 8437–8443. (d) Öztöpcü, O.; Holzhaecker, C.; Puchberger, M.; Weil, M.; Mereiter, K.; Veiros, L. F.; Kirchner, K. Synthesis and Characterization of Hydrido Carbonyl Molybdenum and Tungsten PNP Pincer Complexes. *Organometallics* **2013**, *32*, 3042–3052. (e) de Aguiar, S. R. M. M.; Stöger, B.; Pittenauer, B.; Puchberger, M.; Allmaier, G.; Veiros, L. F.; Kirchner, K. A complete series of halocarbonyl molybdenum PNP pincer complexes - Unexpected differences between NH and NMe spacers. *J. Organomet. Chem.* **2014**, *760*, 74–83. (f) de Aguiar, S. R. M. M.; Öztöpcü, O.; Stöger, B.; Mereiter, K.; Veiros, L. F.; Pittenauer, B.; Allmaier, G.; Kirchner, K. Synthesis and reactivity of coordinatively unsaturated halocarbonyl molybdenum PNP pincer complexes. *Dalton Trans* **2014**, *43*, 14669–14679. (g) Chakraborty, S.; Blacque, O.; Berke, H. Ligand assisted carbon dioxide activation and hydrogenation using molybdenum and tungsten amides. *Dalton Trans* **2015**, *44*, 6560–6570. (h) Castro-Rodrigo, R.; Chakraborty, S.; Munjanja, L.; Brennessel, W. W.; Jones, W. D. Synthesis, Characterization, and Reactivities of Molybdenum and Tungsten PONOP Pincer Complexes. *Organometallics* **2016**, *35*, 3124–3131. (i) Zhang, Y.; Williard, P. G.; Bernskoetter, W. H. Synthesis and characterization of pincer-molybdenum precatalysts for

CO<sub>2</sub> hydrogenation. *Organometallics* **2016**, *35*, 860–865. (j) de Aguiar, S. R. M. M.; Stöger, B.; Pittenauer, B.; Allmaier, G.; Veiros, L. F.; Kirchner, K. Structural diversity of halocarbonyl molybdenum and tungsten PNP pincer complexes through ligand modifications. *Dalton Trans* **2016**, *45*, 13834–13845. (k) Silantyev, G. A.; Förster, M.; Schluschaß, S.; Abbenseth, J.; Würtele, C.; Volkmann, C.; Holthausen, M. C.; Schneider, S. Dinitrogen Splitting Coupled to Protonation. *Angew. Chem., Int. Ed.* **2017**, *56*, 5872–5876.

(9) (a) Chakraborty, S.; Berke, H. Homogeneous Hydrogenation of Nitriles Catalyzed by Molybdenum and Tungsten Amides. *ACS Catal.* **2014**, *4*, 2191–2194. (b) Chakraborty, S.; Blacque, O.; Berke, H. Ligand assisted carbon dioxide activation and hydrogenation using molybdenum and tungsten amides. *Dalton Trans* **2015**, *44*, 6560–6570.

(10) Arashiba, K.; Miyake, Y.; Nishibayashi, Y. A molybdenum complex bearing PNP-type pincer ligands leads to the catalytic reduction of dinitrogen into ammonia. *Nat. Chem.* **2011**, *3*, 120–125.

(11) A series of related Mn and Re complexes featuring the PNP ligand (<sup>i</sup>Pr<sub>2</sub>PCH<sub>2</sub>CH<sub>2</sub>)<sub>2</sub>NH have been reported: (a) Fu, S.; Shao, Z.; Wang, Y.; Liu, Q. Manganese-Catalyzed Upgrading of Ethanol into 1-Butanol. *J. Am. Chem. Soc.* **2017**, *139*, 11941–11948. (b) Piehl, P.; Pena-Lopez, M.; Frey, A.; Neumann, H.; Beller, M. Hydrogen auto-transfer and related dehydrogenative coupling reactions using a rhenium(I) pincer catalyst. *Chem. Commun.* **2017**, *53*, 3265–3268. (c) Wei, D.; Roisnel, T.; Darcel, C.; Clot, E.; Sortais, J.-B. Hydrogenation of Carbonyl Derivatives with a Well-Defined Rhenium Precatalyst. *ChemCatChem* **2017**, *9*, 80–83.

(12) Anderson, S.; Cook, D. J.; Hill, A. F. Metallathiirenes. Thiocarbonyl and Alkoxythiocarbonyl Complexes of Molybdenum(II) and Tungsten(II). *Organometallics* **2001**, *20*, 2468–2476.

(13) A series of related Mn, Fe, and Ru complexes featuring the PNP ligand (<sup>i</sup>Pr<sub>2</sub>PCH<sub>2</sub>CH<sub>2</sub>)<sub>2</sub>NH have been reported: (a) Tondreau, A. M.; Boncella, J. M. The synthesis of PNP-supported low-spin nitro manganese(I) carbonyl complexes. *Polyhedron* **2016**, *116*, 96–104. (b) Elangovan, S.; Topf, C.; Fischer, S.; Jiao, H.; Spannenberg, A.; Baumann, W.; Ludwig, R.; Junge, K.; Beller, M. Selective Catalytic Hydrogenations of Nitriles, Ketones, and Aldehydes by Well-Defined Manganese Pincer Complexes. *J. Am. Chem. Soc.* **2016**, *138*, 8809–8814. (c) Koehne, I.; Schmeier, T. J.; Bielinski, E. A.; Pan, C. J.; Lagaditis, P. O.; Bernskoetter, W. H.; Takase, M. K.; Würtele, C.; Hazari, N.; Schneider, S. Synthesis and Structure of Six-Coordinate Iron Borohydride Complexes Supported by PNP Ligands. *Inorg. Chem.* **2014**, *53*, 2133–2143. (d) Rozenel, S. S.; Arnold, J. Bimetallic Ruthenium PNP Pincer Complex As a Platform to Model Proposed Intermediates in Dinitrogen Reduction to Ammonia. *Inorg. Chem.* **2012**, *51*, 9730–9739.



## 6.2 Highly Selective Hydrogenation of Amides Catalyzed by a Molybdenum Pincer Complex: Scope and Mechanism.

T. Leischner, L. A. Suarez, A. Spannenberg, K. Junge, A. Nova, M. Beller

*Chem. Sci.* **2019**, *10*, 10566–10576.

The publication dealing with the reduction of substituted formamides catalyzed by a molybdenum pincer complex was mostly done by myself. I synthesized all pincer complexes reported in this publication, conducted the optimization of the reaction conditions, performed the substrate scope and prepared all commercially not available substrates. Moreover, I mainly wrote the manuscript as well as the supporting information. The computational studies as well as the corresponding part in the manuscript/supporting information were done by L. A. Suarez and A. Nova. The determination of the reported solid-state structures, alongside the corresponding measurements were carried out by Anke Spannenberg. My contribution to this work is approximately 60%.

Cite this: *Chem. Sci.*, 2019, 10, 10566

All publication charges for this article have been paid for by the Royal Society of Chemistry

# Highly selective hydrogenation of amides catalysed by a molybdenum pincer complex: scope and mechanism†

Thomas Leischner,<sup>a</sup> Lluís Artús Suárez,<sup>b</sup> Anke Spannenberg,<sup>a</sup> Kathrin Junge,<sup>a</sup> Ainara Nova<sup>b\*</sup> and Matthias Beller<sup>b\*</sup>

A series of molybdenum pincer complexes has been shown for the first time to be active in the catalytic hydrogenation of amides. Among the tested catalysts, **Mo-1a** proved to be particularly well suited for the selective C–N hydrogenolysis of *N*-methylated formamides. Notably, high chemoselectivity was observed in the presence of certain reducible groups including even other amides. The general catalytic performance as well as selectivity issues could be rationalized taking an anionic Mo(0) as the active species. The interplay between the amide C=O reduction and the catalyst poisoning by primary amides accounts for the selective hydrogenation of *N*-methylated formamides. The catalyst resting state was found to be a Mo–alkoxo complex formed by reaction with the alcohol product. This species plays two opposed roles – it facilitates the protolytic cleavage of the C–N bond but it encumbers the activation of hydrogen.

Received 12th July 2019  
Accepted 21st September 2019

DOI: 10.1039/c9sc03453f

rsc.li/chemical-science

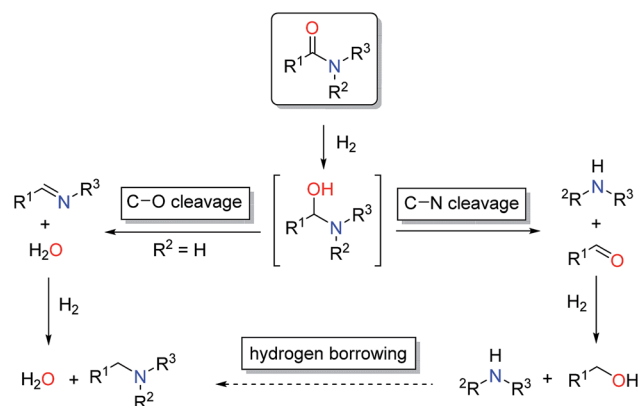
## Introduction

The reduction of carboxylic acid derivatives *via* catalytic homogeneous hydrogenation represents an attractive atom-economic and environmentally benign methodology.<sup>1,2</sup> To date, the vast majority of homogeneous catalysts for these transformations rely on noble metals.<sup>3</sup> The limited availability of these elements along with their toxicity and pollutive nature initiated efforts for their replacement. Significant progress in this direction has been achieved in the past decade, in particular with respect to iron,<sup>4</sup> manganese<sup>5</sup> and cobalt<sup>6</sup> based systems. Thus, several examples of base metal catalysed hydrogenations of aldehydes, ketones, carboxylic acids, esters and nitriles have been reported in recent years, some of them with remarkable activities and selectivities.<sup>2a,7</sup> On the contrary, hydrogenation of amides is known to a much less extent.<sup>8</sup> The latter can be attributed to the extremely low electrophilicity of the carbonyl group, which renders their hydrogenation particularly challenging.

In general, catalytic hydrogenation of amides can proceed *via* either C–N (hydrogenolysis) or C–O (hydrogenation) bond cleavage of the intermediate hemiaminal (Scheme 1). While the

C–O bond scission results in the formation of the alkylated/benzylated amine with H<sub>2</sub>O as the only by-product, the C–N bond cleavage leads to the free amine and the corresponding alcohol. Recently, an additional amide hydrogenation pathway was demonstrated, where the alkylated/benzylated amine is produced by a hydrogen borrowing/autotransfer mechanism from the initially formed alcohol and amine under specific acidic reaction conditions.<sup>9</sup> Until today, the development of catalytic systems that enable these chemoselective transformations continues to be challenging and therefore are subject of ongoing research.

Initial efforts in this direction mainly focused on homogeneous ruthenium catalysts.<sup>10</sup> Since the inspiring report by Cole-



Scheme 1 Pathways for amide reduction.

<sup>a</sup>Leibniz Institut für Katalyse e. V., Albert-Einstein-Straße 29a, Rostock, 18059, Germany. E-mail: Matthias.Beller@catalysis.de<sup>b</sup>Hylleraas Centre for Quantum Molecular Sciences, Department of Chemistry, University of Oslo, P.O. Box 1033, Blindern, N-0315, Oslo, Norway. E-mail: Ainara.nova@kjemi.uio.no

† Electronic supplementary information (ESI) available. See DOI: 10.1039/c9sc03453f



Hamilton and co-workers in 2012, various Ru-based systems for the highly selective scission of either the C–N or the C–O bond have been described.<sup>10</sup>

In sharp contrast, reports on homogeneous base metal catalysts for this important reaction are particularly scarce. Pioneering work in this area was published by the groups of Milstein, Langer and Sanford only as late as 2016.<sup>11–13</sup> For the first time, they could demonstrate the ability of certain iron PNP pincer complexes (**Fe-1** as well as **Fe-2a/b**, Scheme 2) to promote the C–N bond cleavage in a number of different amides.

More specifically, Milstein and co-workers reported, that **Fe-1**, after activation with KHMDS, induced the hydrogenolysis of activated aliphatic and aromatic 2,2,2-trifluoroacetamides. However, no reaction was observed, with more common substrates such as *N*-phenylacetamide and *N*-phenylbenzamide.<sup>11</sup> The protocols described by Sanford (**Fe-2a**) and Langer (**Fe-2b**) showed more general substrate scopes and obtained notable conversions and yields also for unactivated amides.<sup>12,13</sup>

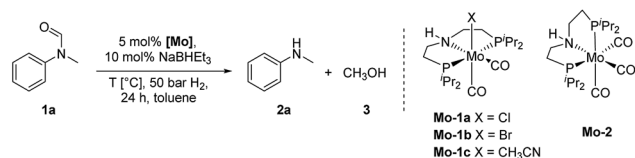
Additionally, Bernskoetter and co-workers showed that the pentavalent iron PNP-pincer complex **Fe-3** is particularly active for the hydrogenolysis of a number of secondary formamides and *N*-formylmorpholine (Scheme 2). The system stands out due to its extremely low catalyst loading (0.018–0.07 mol%) and notably operates under base-free conditions. Interestingly, the group of Bernskoetter demonstrated that an addition of 20 equivalents of formanilide resulted in a significantly improved activity of the system towards otherwise almost unreactive *N*-methylformanilide. Based on NMR experiments, the authors concluded that the catalyst adopts a different resting state in the presence of the additive (**Fe-4**, Scheme 2) and thus is less prone towards deactivating side reactions.<sup>14</sup> The computational study of this reaction also suggested that the formanilide additive is involved in the C–N bond cleavage of the hemiaminal intermediate, which is the rate limiting step.<sup>15</sup>

Recently, our group reported the very first example of a manganese catalysed deaminative hydrogenation of amides

under relatively mild conditions.<sup>16</sup> After activation with exogenous base, the PNN pincer complex **Mn-1** (Scheme 2) exhibits remarkable activity for the hydrogenation of a broad scope of secondary and tertiary amides to the corresponding alcohols and amines. Notably, also more challenging primary amides were successfully cleaved in modest yields, though more forcing conditions were shown to be necessary. The generality of the system was finally highlighted by the cleavage of the amide bond in the herbicide diflufenican. To date, **Mn-1** represents one of the most active and broadly applicable non-noble metal catalysts for amide hydrogenation. In a related study, Prakash and co-workers demonstrated that the manganese PNP pincer complex **Mn-2** is a suitable catalyst for the hydrogenation of formamides. The reaction proceeds *via* cleavage of the C–N bond to produce methanol and the corresponding amine.<sup>17</sup>

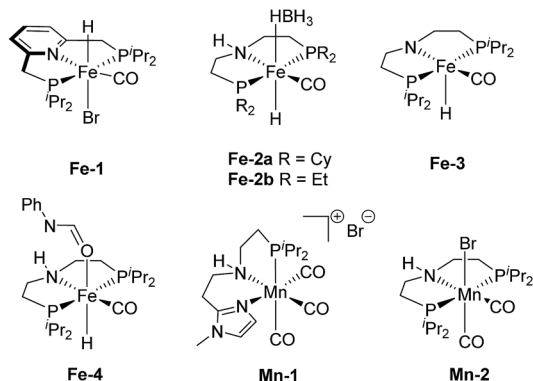
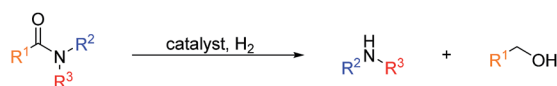
In 2018, we published the synthesis of a number of structurally related molybdenum PNP pincer complexes. Among the described complexes, **Mo-1a** (Table 1) was shown to be active in the catalytic hydrogenation of different acetophenones and styrenes.<sup>18</sup> Similar Mo-systems have also been used for the hydrogenation of CO<sub>2</sub>, imines and nitriles.<sup>19</sup> Based on these reports and our previous work, we became interested in the behaviour of such base-metal catalysts for the reductive cleavage of amides. Herein, we demonstrate its suitability for the hydrogenolysis of *N*-methylated formamides under relatively mild conditions. To the best of our knowledge, PNP pincer supported molybdenum complexes have not been described for such transformations. Interestingly, the optimal catalyst

Table 1 Hydrogenation of *N*-methylformanilide **1a** to *N*-methylaniline **2a** and methanol **3** using Mo catalysts **Mo-1a–c** and **Mo-2**



Entry <sup>a,b</sup>	[Mo]	T [°C]	Conv. <sup>c</sup> [%]	<b>2a</b> <sup>c</sup> [%]
1	<b>Mo-1a</b>	130	>99	99
2	<b>Mo-1b</b>	130	>99	99
3	<b>Mo-1c</b>	130	>99	99
4	<b>Mo-2</b>	130	10	9
5 <sup>d</sup>	—	130	10	8
6	<b>Mo-1a</b>	100	>99	98
7	<b>Mo-1b</b>	100	>99	99
8	<b>Mo-1c</b>	100	76	73
9	<b>Mo-1a</b>	80	89%	86%
10	<b>Mo-1b</b>	80	87%	84%
11 <sup>e</sup>	<b>Mo-1a</b>	80	49	47
12 <sup>e</sup>	<b>Mo-1b</b>	80	46	46

<sup>a</sup> Standard reaction conditions: *N*-methylformanilide **1a** (67.6 mg, 0.5 mmol), NaBHET<sub>3</sub> (50 μL, 0.05 mmol, 10 mol%), 2 mL toluene, 50 bar H<sub>2</sub>, 24 h. <sup>b</sup> Yield of **3** was not determined. <sup>c</sup> Conversion of **1a** and yield of **2a** were determined by GC using hexadecane as internal standard. <sup>d</sup> No catalyst was used. <sup>e</sup> Reaction was performed with 2.5 mol% of Mo catalyst.



Scheme 2 Base metal catalysts reported for the hydrogenolysis (C–N bond cleavage) of amides.



exhibits a high selectivity for formamides. This preference has been rationalized by means of DFT calculations, which suggest that the produced MeOH reacts with the catalyst and changes the mechanism and rate limiting step of the reaction. This result, which is not observed in related Fe-catalysts, indicates that the catalyst design strategy should be adapted to the nature of the metal centre.

## Results and discussion

### Catalytic hydrogenation of amides using molybdenum pincer complexes

At the outset of our study, we explored molybdenum-based PNP pincer complexes **Mo-1a-c** and **Mo-2** (Table 1), recently synthesised by our group, as potential catalysts for the hydrogenation of amides. Using *N*-methylformanilide **1a** as benchmark substrate, preliminary experiments were conducted using 5 mol% of Mo catalyst in toluene at 50 bar H<sub>2</sub> and 130 °C, in the presence of 10 mol% of NaBHET<sub>3</sub>. The reaction proceeded smoothly for complexes **Mo-1a-c** to afford *N*-methylaniline **2a** in quantitative yield along with methanol as the only by-product (Table 1, entries 1–3). However, complex **Mo-2** failed to display any catalytic activity (Table 1, entry 4). Next, the activity of the complexes was tested at reduced temperatures (Table 1, entries 6–10). It was found, that complexes **Mo-1a** as well as **Mo-1b** were equally efficient, when the reaction was conducted at 100 °C. Catalyst **Mo-1c**, however, gave a somewhat lower conversion and yield. Further reduction of the reaction temperature to 80 °C resulted once again in similar conversions and yields for **Mo-1a** and **Mo-1b**, respectively. Based on these observations, the catalyst loading was reduced to 2.5 mol% under otherwise identical reaction conditions (Table 1, entries 11 and 12). It turned out, that changing this parameter also led to almost identical outcomes for both catalytic systems. Therefore we concluded that, under reaction conditions, **Mo-1a** and **Mo-1b** very likely form the same active species. On the basis of the obtained results and due to the more challenging synthesis of **Mo-1b**, we decided to focus on catalyst **Mo-1a** in the due course of the study.

Selecting 80 °C reaction temperature and 5 mol% of **Mo-1a** (Table 1, entry 8) as the optimal setting for further optimization, we tested several different solvents. In contrast to previous work on manganese catalysed hydrogenolysis of amides, toluene was found to give the best results. Cyclohexane yielded slightly lower activities, while *n*-heptane as well as polar solvents, were shown to be significantly less suitable for the attempted transformation (Fig. 1).

Subsequently, we studied the influence of dihydrogen pressure, catalyst loading as well as the amount of additive used on the reaction outcome (Table 1, see ESI†). Lowering the pressure to 30 bar H<sub>2</sub> resulted in a sharp drop in activity. However, no loss of reactivity was observed when the amount of NaBHET<sub>3</sub> was decreased to 5 mol%. A rise of the reaction temperature to 100 °C resulted in full conversion of the benchmark substrate to *N*-methylaniline in the presence of 5 mol% NaBHET<sub>3</sub> and **Mo-1a**, respectively. Further mitigation of the catalyst loading as well as

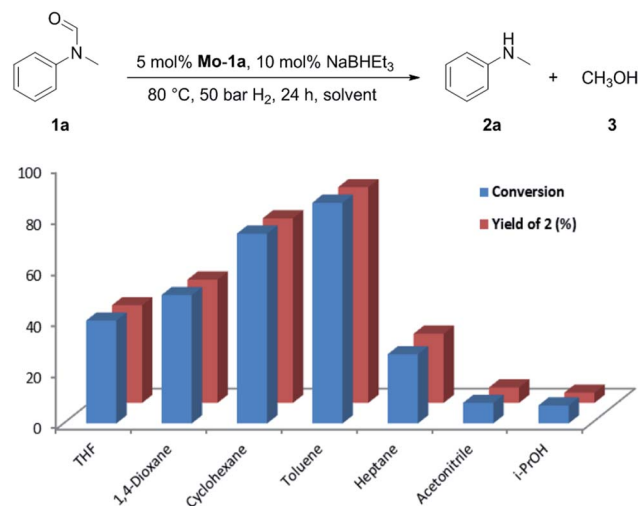


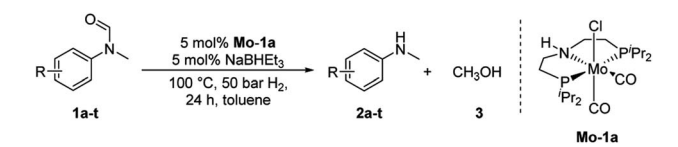
Fig. 1 Study of the solvent effect in the hydrogenation of *N*-methylformanilide **1a** to *N*-methylaniline **2a** and methanol **3** catalysed by **Mo-1a**.

the amount of NaBHET<sub>3</sub>, however, had negative effects on the catalytic performance of the system.

Having optimised conditions in hand, we proceeded to the application of **Mo-1a** in the hydrogenation of a variety of different *N*-methylformanilides to the corresponding anilines and methanol (Table 2).

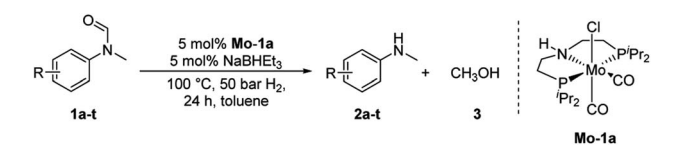
Most substrates were hydrogenated in good to excellent yields under optimised conditions at 100 °C and 50 bar H<sub>2</sub> over 24 h, using toluene as solvent. In general, *meta*- and *para*-substitution were well tolerated, while substituents in *ortho*-position (Table 2, entries 19 and 20) appeared to be troublesome, probably due to steric hindrance. Amides containing electron donating groups were less reactive under standard conditions as compared to the benchmark substrate. In some cases higher reaction temperatures were required, in order to achieve good conversions (Table 2, entries 2, 6, 7). Notably, the thiomethyl substituted derivative (Table 2, entry 3) was fully hydrogenated and no catalyst poisoning effect was observed. Moreover, the system tolerated fluoro-substituents (Table 2, entries 8, 17, 20) and no dehalogenation products were detected. Interestingly, the system showed a good functional group tolerance towards substrates containing other reducible moieties such as benzyl ethers, C=C double bonds and esters (Table 2, entries 6, 12, 13). Noteworthy, no double bond isomerisation occurred during the reduction of a stilbene derivative (Table 2, entry 12). Additionally, pyridines, nitriles and nitro arenes remained unaffected under our reaction conditions; however, only poor to modest conversions were observed when the reaction was carried out at 130 °C (Table 2, entries 11, 14, 15). Presumably, this effect originates from substrate coordination to the metal centre and subsequent catalyst deactivation. The system turned out to be sensitive towards halides other than fluorine. Hence, during one of the hydrogenations, small amounts of the dehalogenation product were detected (Table 2, entry 9).



Table 2 Substrate scope in the hydrogenation of *N*-methylformanilides to *N*-methylanilines **2** and methanol **3** catalysed by **Mo-1a**

Entry <sup>a,b</sup>	Formamide	Conv. <sup>c</sup> (%)	Yield <sup>d</sup> of <b>2</b> (%)
1		>99	94
2 <sup>e</sup>		>99	96
3		>99	95
4		83	80
5		87	84
6 <sup>e</sup>		56	52
7 <sup>eg</sup>		46	43
8		98	93
9		40	34 <sup>f</sup>

Table 2 (Contd.)



Entry <sup>a,b</sup>	Formamide	Conv. <sup>c</sup> (%)	Yield <sup>d</sup> of <b>2</b> (%)
10		>99	>99
11 <sup>e</sup>		52	50
12		95	92
13		>99	97
14 <sup>e</sup>		14	12 <sup>f</sup>
15 <sup>e</sup>		8	6 <sup>f</sup>
16		>99	97
17		>99	98

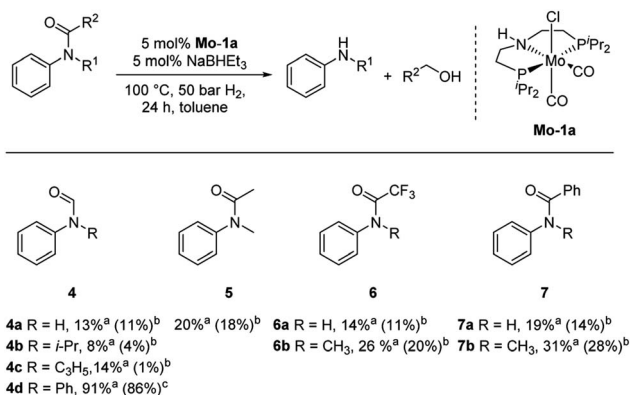


Table 2 (Contd.)

Entry <sup>a,b</sup>	Formamide	Conv. <sup>c</sup> (%)	Yield <sup>d</sup> of 2 (%)
18		>99	93
19 <sup>e</sup>		12	9 <sup>f</sup>
20 <sup>e</sup>		18	15 <sup>f</sup>

<sup>a</sup> Standard reaction conditions: *N*-methylformanilide (0.5 mmol), **Mo-1a** (12.5 mg, 5 mol%), NaBHET<sub>3</sub> (50 μL, stock solution 0.5 M in THF, 5 mol%), 2 mL toluene, 50 bar H<sub>2</sub>, 24 h. <sup>b</sup> Yield of **3** was not determined. <sup>c</sup> Conversions of *N*-methylformanilides were determined by GC using hexadecane as internal standard. <sup>d</sup> Isolated yields. <sup>e</sup> Reaction was carried out at 130 °C. <sup>f</sup> Yields were determined by GC using hexadecane as internal standard. <sup>g</sup> Yield was determined based on the hydrochloride salt.

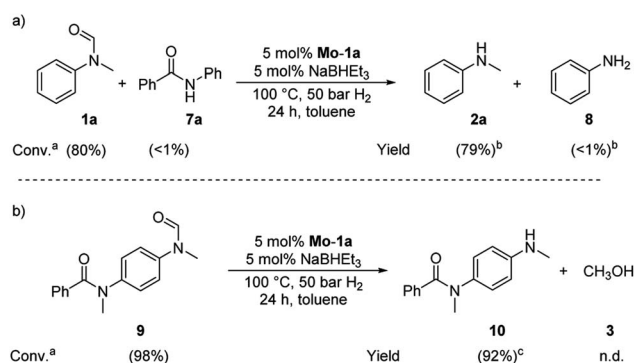
Subsequently, we investigated the more general applicability of our PNP pincer complex **Mo-1a** in the hydrogenation of other amides. Initial experiments focussed on the role of the nitrogen



**Scheme 3** Hydrogenation of different amides (**4–7**) to the corresponding amines and alcohols catalysed by **Mo-1a**. <sup>a</sup>Conversions of amides were determined by GC using hexadecane as internal standard. <sup>b</sup>Yields were determined by GC using hexadecane as internal standard and refer to anilines, yields of alcohols were not determined. <sup>c</sup>Isolated yields of anilines.

substitution on the reaction outcome. For this purpose, a series of different secondary and tertiary formanilides were subjected to our protocol (**Scheme 3**). The presence of an NH moiety turned out to be detrimental, as was observed for the parental formanilide (**4a**). This is in sharp contrast with the results obtained with Fe pincer complexes, in which formanilide derivatives give the highest conversion.<sup>14</sup> In order to further validate this, 2,2,2-trifluoroacetanilide (**6a**) and simple benzanilide (**7a**) were employed and results comparable to formanilide (**4a**) were obtained. Likewise, only low conversions and yields were obtained in the case of *N*-*i*-Pr- (**4b**) and *N*-allylformanilide (**4c**), respectively. Surprisingly, when *N*-allylformanilide was tested as substrate, the formation of *N*-allylaniline was only observed in traces. The main product was identified to be aniline, thus hinting at a deallylation pathway that additionally takes place to the envisaged hydrogenolysis. In contrast, *N,N*-diphenylformanilide (**4d**) was reduced smoothly and *N,N*-diphenylamine was isolated in excellent yield. Next, the hydrogenation of *N*-methylacetanilide (**5**) and the more activated 2,2,2-*N*-methyltrifluoroacetanilide (**6b**), respectively, were attempted. In either case, only poor conversions were determined demonstrating the high preference of this complex for specific formanilides. This was further supported by the low reactivity of *N*-methylbenzanilide (**7b**) and some aliphatic formamides (see **Table 2**, ESI†).

Based on these observations, we were curious to demonstrate selective formamide reduction in the presence of other amide moieties. In a proof of concept experiment, the hydrogenation of the benchmark amide in the presence of benzamide **7a** was conducted (**Scheme 4**, eqn (a)). It could be shown that **Mo-1a** was capable to cleave *N*-methylformanilide (**1a**) with extremely high preference. Notably, the reaction still proceeded with 80% conversion with respect to *N*-methylformanilide (**1a**). To further highlight the scope of our system, we designed model substrate **9** combining two amide functionalities in one structure. After 24 h reaction, the intended hydrogenolysis of



**Scheme 4** Selective hydrogenations of (a) *N*-methylformanilide **1a** in the presence of benzamide **7a** and (b) *N*-methyl-*N*-(4-(*N*-methylformamide)phenyl)benzamide **9**. Standard conditions: substrate(s) 0.5 mmol (each), **Mo-1a** (12.5 mg, 0.025 mmol, 5 mol%), NaBHET<sub>3</sub> (50 μL, 0.5 M stock solution in THF, 0.025 mmol, 5 mol%), toluene (2 mL), 50 bar H<sub>2</sub>, 100 °C, 24 h. <sup>a</sup>Conversions determined by GC using hexadecane as internal standard. <sup>b</sup>Yields determined by GC using hexadecane as internal standard. <sup>c</sup>Isolated yield.





the formamide moiety in **9** had occurred smoothly and the target molecule **10** was isolated in a very high yield (92%). Notably, no cleavage of the benzamide was observed.

We believe these results could pave the way towards new and selective deprotection strategies in organic synthesis mediated by this base metal PNP pincer complex.

### Reaction mechanism

In order to understand the general reactivity of **Mo-1a** and its performance with different amides, DFT calculations and supporting experiments were conducted. Scheme 5 shows the experiments performed to determine the active catalytic species. Treatment of **Mo-1a** with NaBHET<sub>3</sub> resulted in rapid hydrogen evolution. The nature of the gas was determined in a scale up experiment (100 μmol of **Mo-1a**) using GC-analysis. This observation prompted us to assume that the obtained reaction product was likely to be a pincer amido species such as **Mo-3**, in which Mo(I) has been reduced to Mo(0). This conclusion was further supported by HR-ESI mass spectrometry of the corresponding reaction mixture. When the distinct reactivity of the catalyst towards formanilide was studied, we isolated **Mo-4** in form of colorless needles from the reaction mixture (Fig. 2; for detailed experimental procedure see ESI†).

Notably, the crystal structure of **Mo-4** (Fig. 2 and Scheme 5) features two anionic Mo(0) complexes neutralized by two Na<sup>+</sup> cations interacting with the CO ligands. In order to investigate, whether **Mo-4** is involved in the catalytic cycle, the reduction of *N*-methylformanilide was carried out using 2.5 mol% of **Mo-4** under conditions optimized for **Mo-1a**. In fact, we observed full conversion of the substrate and isolated *N*-methylaniline in 92% yield. Thus, we conclude, that the catalytically active species contains a Mo(0) center. This is also consistent with the EPR-silent nature of the product formed in the activation of **Mo-1a** by NaBHET<sub>3</sub>.

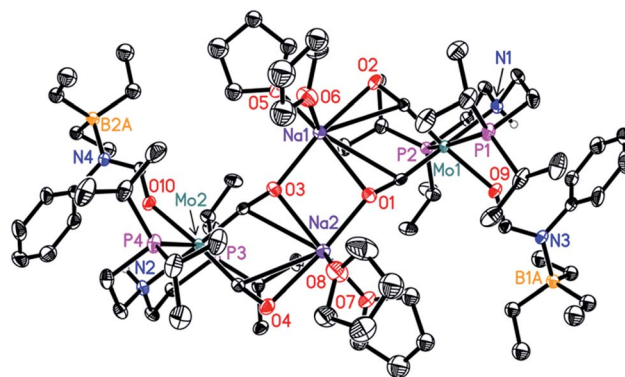


Fig. 2 Molecular structure of **Mo-4** in the crystal (see Scheme 5 for a graphical representation). Displacement ellipsoids correspond to 30% probability. Hydrogen atoms except the N-bound are omitted for clarity.

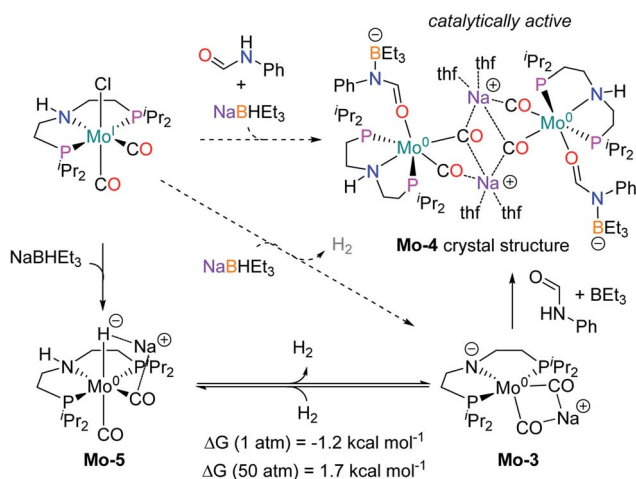
The observed activity of **Mo-4** suggests that the Mo(0)-complexes **Mo-3** and **Mo-5**, shown in Scheme 5, are presumably the main catalytic intermediates. Similar species have been proposed for the isoelectronic Fe(II)-complexes **Fe-2**, **Fe-3** and the Mn(I)-complex **Mn-2** (Scheme 2).<sup>20</sup>

Based on these results, DFT calculations, with the M06 functional, including toluene solvation with the SMD model, were used to get further insights into the reaction mechanism (see computational details and ESI for details†). The hydrogenation of **Mo-3** to yield **Mo-5**, was found to be almost isoenergetic, with a small preference for **Mo-3** at 1 bar and **Mo-5** at 50 bar (Scheme 5). These energies agree with the bubbling of H<sub>2</sub> observed experimentally during the catalyst activation reaction.

As represented in Scheme 1, amide hydrogenolysis is proposed to consist in three steps: amide C=O reduction, C–N bond protonolysis of the formed hemiaminal, and aldehyde C=O reduction. These steps were computed for *N*-methylformanilide and the energy profiles for the preferred pathways are given in Fig. 3 and 5, and the ESI.†

The mechanism for the amide C=O hydrogenation by **Mo-5** consists of the hydride transfer from Mo to the amide carbonyl group (**Mo-ts-6-7**), followed by proton transfer from the ligand nitrogen to the amide oxygen (**Mo-ts-7-8**). This pathway was computed for formanilide (**Mo-ts-6-7<sup>NH</sup>** in Fig. 3) and *N*-methylformanilide. With both substrates, the hydride transfer has the highest energy barrier (10.6 kcal mol<sup>-1</sup> with formanilide and 13.1 kcal mol<sup>-1</sup> with *N*-methylformanilide). Interestingly, these energies are lower than those reported by us for the analogous Fe catalyst with formanilide (15.8 kcal mol<sup>-1</sup>, **Fe-ts-6-7** in Fig. 3).<sup>15</sup>

The mechanism for the C–N bond cleavage from the formed hemiaminal (Scheme 1) was also investigated. In the case of **Fe-3**, this step was reported to proceed *via* the transition state **Fe-ts-C<sup>H</sup>-N<sup>H</sup>** (Fig. 4).<sup>15</sup> With Mo and *N*-methylformanilide, the same pathway involves a Gibbs energy barrier of 22.9 kcal mol<sup>-1</sup> (**Mo-ts-C<sup>H</sup>-N<sup>Me</sup>**). An increase of less than 1 kcal mol<sup>-1</sup> is observed by changing the substrate to *N*-methylacetanilide (**Mo-ts-C<sup>Me</sup>-N<sup>Me</sup>**).



Scheme 5 Reactions performed to get insight on the active catalytic species (in dashed arrows) with the experimental observed products (H<sub>2</sub> and the crystal structure of **Mo-4**, in color) and the intermediates proposed (**Mo-3** and **Mo-5**). Gibbs energies calculated for the dehydrogenation of **Mo-5** at different pressure.



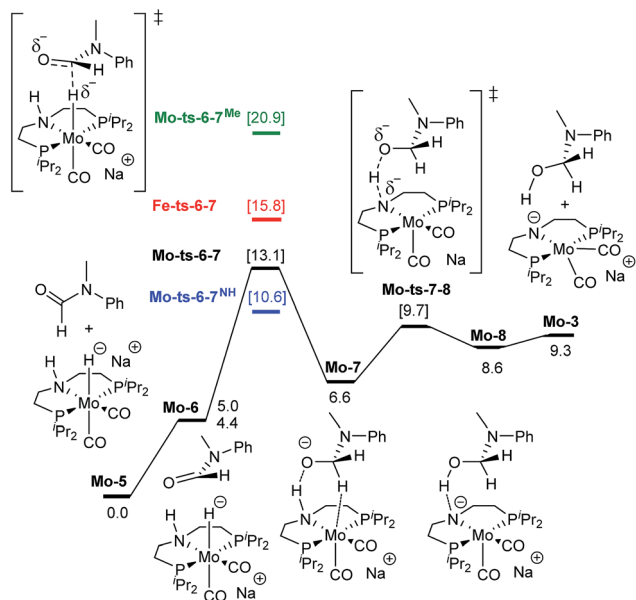


Fig. 3 Reaction pathway for the hemiaminal formation from the *N*-methyl formanilide with **Mo-5**. Gibbs energies in toluene (SMD) at 50 atm and 373 K are given in kcal mol<sup>-1</sup>. In blue and green, energies for the hydride transfer using formanilide and *N*-methylacetanilide, respectively. In red, energy for the hydride transfer using the reported **Fe-3** complex at 30 atm (Scheme 2).<sup>15</sup>

The similar energy barriers obtained with these substrates did not account for the large differences in yield observed experimentally (99% Conv. in *N*-methylformanilide vs. 20% Conv. in *N*-methylacetanilide). In addition, the lower energy barriers obtained with Mo compared to Fe are inconsistent with the higher H<sub>2</sub> pressure and time required to accomplish amide hydrogenation with **Mo-1a** compared to **Fe-3**.<sup>14</sup>

These discrepancies were explained by considering the reaction of **Mo-3** with methanol leading to the Mo-methoxy intermediate **Mo-9a** (Fig. 5). This reaction, which involves the deprotonation of MeOH by the amido ligand (**Mo-ts-3-9a**), has a low energy barrier ( $\Delta G^\ddagger = 2.8$  kcal mol<sup>-1</sup>) and is highly exergonic ( $\Delta G = -11.4$  kcal mol<sup>-1</sup>). The formation of related M-methoxy species have been observed for similar Fe, Ru, Os and Mn PNP-pincer complexes.<sup>20c,21,22</sup> This species can promote the protonolysis of the C–N bond by assisting the OH-deprotonation and *N*-protonation of the hemiaminal

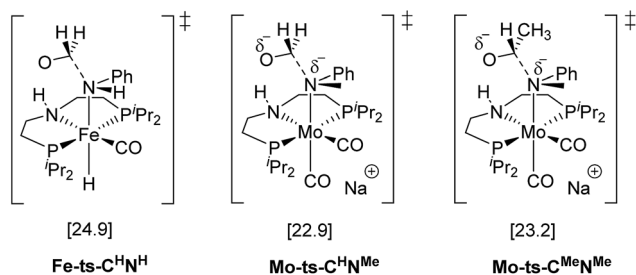


Fig. 4 TSs for the C–N bond cleavage step via the mechanism previously reported for **Fe-3**.<sup>15</sup>

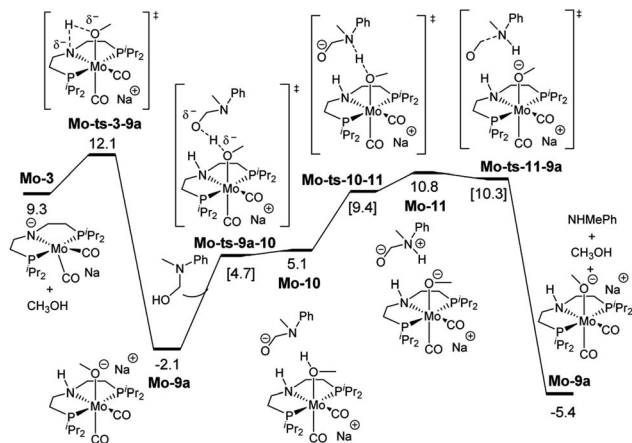
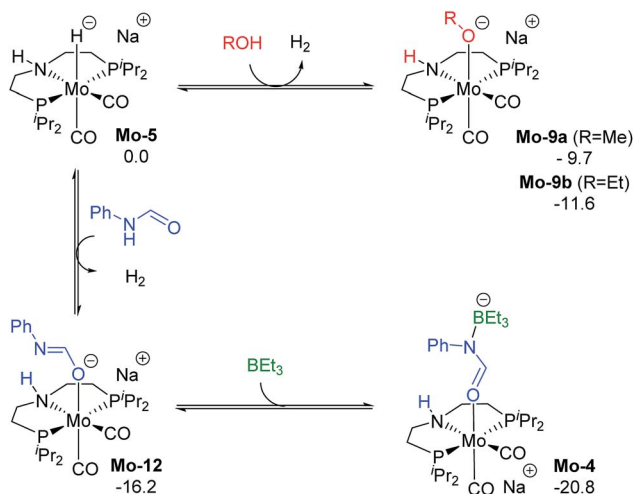


Fig. 5 Reaction pathway of the MeOH assisted hemiaminal proton transfer and posterior C–N bond cleavage. Gibbs energies in toluene (SMD) at 50 atm and 373 K are given in kcal mol<sup>-1</sup>.

intermediate (**Mo-ts-11-9a**). The highest energy of this process is 10.8 kcal mol<sup>-1</sup>, which corresponds to the zwitterion hemiaminal intermediate interacting with the methoxide–Mo complex (**Mo-11**). This energy is lower than the energy barrier for the hydride transfer (13.1 kcal mol<sup>-1</sup>), indicating that the C–N bond cleavage is not the rate limiting step once MeOH is formed (note: for a comparison of this mechanism with Mo and Fe-systems see ESI<sup>†</sup>).

The reaction of **Mo-5** with MeOH yields hydrogen and is exergonic ( $\Delta G = -9.7$  kcal mol<sup>-1</sup>, Scheme 6). The methoxy intermediate **Mo-9a** is thus the resting state of the catalyst.

Formanilide, and other secondary amides, can also displace H<sub>2</sub> from the catalyst (**Mo-12** in Scheme 6). This reaction is even more exergonic ( $\Delta G = -16.2$  kcal mol<sup>-1</sup>) than with MeOH increasing the global energy barrier for the hydride transfer from 10.6 to 26.8 kcal mol<sup>-1</sup> with formanilide. This energy may increase to 31.4 kcal mol<sup>-1</sup> by reaction with BEt<sub>3</sub> (**Mo-4**). In



Scheme 6 Calculated Gibbs energies (kcal mol<sup>-1</sup>) for the substitution of H<sub>2</sub> in **Mo-5** by methanol, ethanol, formanilide and BEt<sub>3</sub> yielding **Mo-9a**, **b**, **Mo-10** and **Mo-4**, respectively.





contrast, with *N*-methylformanilide, the only penalty to pay is the addition of MeOH. Therefore, the energy barrier for the hydride transfer increases from 13.1 to 22.9 kcal mol<sup>-1</sup>, which is lower than the barrier for formanilide, consistent with the larger conversion obtained with *N*-methylformanilide. In the case of *N*-methylacetanilide, the addition of ethanol instead of methanol is expected. The higher stability of the ethoxide complex **Mo-9b** compared to **Mo-9a** by *ca.* 2 kcal mol<sup>-1</sup> (Scheme 6), together with the higher energy barrier for the hydride transfer with this substrate ( $\Delta G = 20.9$  kcal mol<sup>-1</sup>, Fig. 3), is consistent with the low yields obtained experimentally with *N*-methylacetanilide.

The mechanism of catalyst recovery by addition of H<sub>2</sub> to the methoxide complex **Mo-9a** is shown in Fig. S3.† In this pathway, methanol assists the activation of the Mo-H<sub>2</sub> complex (**Mo-14**) by acting as a proton-shuttle with a global energy barrier of 23.0 kcal mol<sup>-1</sup>. Similar mechanisms have been proposed with Ru-N and Fe-N complexes (see ESI†).<sup>21b,23</sup>

The results from the computational study can be summarized in the catalytic cycle represented in Fig. 6. In the absence of alcohol, the Mo-catalyst is involved in the hemiaminal C-N bond cleavage after the amide C=O reduction (blue cycle). This reaction yields amine and formaldehyde, which is reduced to alcohol by the catalyst **Mo-5** in a subsequent reaction (in red). In the presence of alcohol, a Mo-alkoxo intermediate is formed, **Mo-9a**. This species, which becomes the catalyst resting state, is involved in the hemiaminal C-N bond cleavage. Finally, the

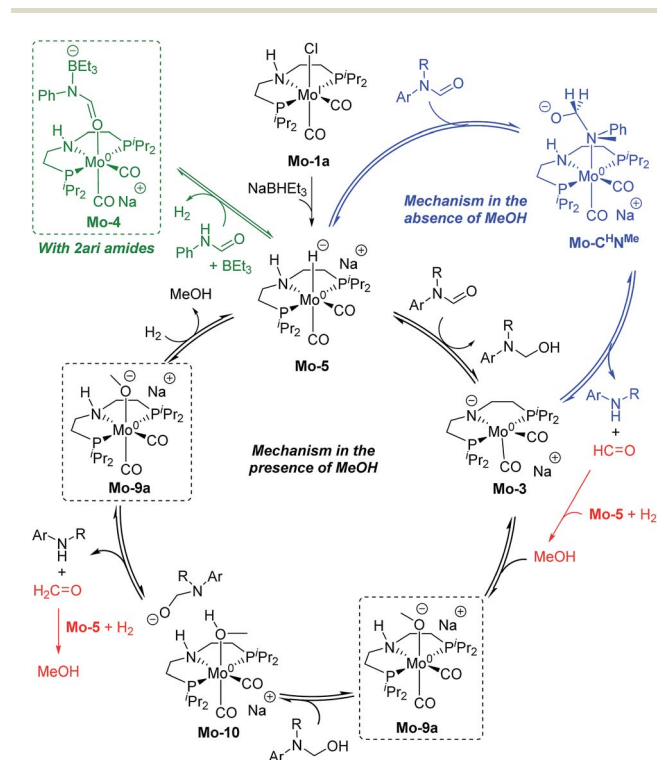


Fig. 6 General mechanism for the amide hydrogenation in the absence (in blue) and presence (in black) of methanol with the formaldehyde hydrogenation in red. Dashed squares indicate the catalyst resting state in the presence of MeOH and 2ari amides (in green).

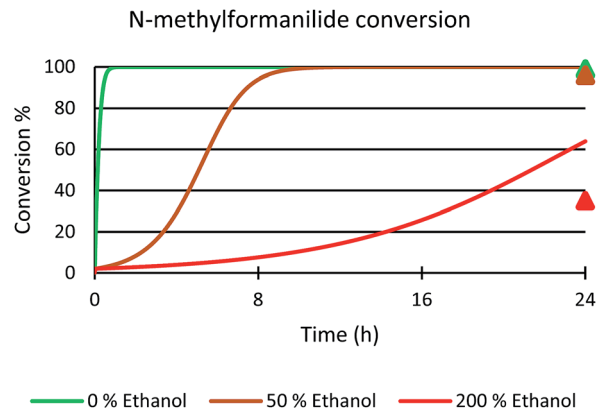


Fig. 7 Microkinetic simulation of *N*-methylformanilide **1a** conversion with 0% (green), 50% (brown) and 200% (red) ethanol in solution. The initial concentration of reactants were the same as those used in the experiments; *i.e.* 0.25 M *N*-methylformanilide **1a**, 0.207 M of dihydrogen and 12.5 mM of **Mo-5**. Experimental values at 24 hours represented with triangles.

catalyst recovery takes place by the displacement of alcohol by H<sub>2</sub>. The nature of the catalyst resting state may change with secondary amides, which reacts with the catalyst forming an adduct (**Mo-4**, in green) that hampers the reaction.

In order to validate this mechanism and the nature of Mo(0) active species, the role of the counter-cation in this reaction was explored computationally and experimentally by using LiHBET<sub>3</sub>, NaHBET<sub>3</sub>, and KHBET<sub>3</sub>. Carrying out the benchmark reaction at 80 °C, 5 mol% of the alkali metal hydrides were added to activate **Mo-1a**. It could be shown, that for NaHBET<sub>3</sub> and KHBET<sub>3</sub> similar conversions of *N*-methylformanilide (**1a**) (76% and 77%, respectively) and yields of **2a** (75% and 73%, respectively) were obtained. However, when LiHBET<sub>3</sub> was used, only 10% conversion of **1a** and 9% yield of *N*-methylaniline **2a** was obtained. These results were in agreement with the trends on the energy barriers obtained for the amide C=O reduction step, which are 22.9, 23.0 and 28.8 kcal mol<sup>-1</sup> with Na<sup>+</sup>, K<sup>+</sup> and Li<sup>+</sup>, respectively, taking **Mo-9a** as energy reference. The stronger electrostatic interaction of Li<sup>+</sup> with the methoxide intermediate (**Mo-9a<sup>Li</sup>**), accounts for the highest energy barrier predicted for this system (see ESI†).

Next, the role of the alcohol was explored by adding different amounts of ethanol to the benchmark system. In the presence of 50 mol% of EtOH, 96% conversion of *N*-methylformanilide (**1a**) and 93% product yield were obtained. However, the addition of 200 mol% resulted in a sharp decrease in conversion and yield (35% conversion, 32% yield). Thus, it was concluded that ethanol has a detrimental effect on the performance of the catalytic system. Notably, these trends were reproduced with a microkinetic model based on the general mechanism represented in Fig. 6 (in Fig. 7). This model predicted 100% conversion after 24 h of reaction for both 0% and 50% concentrations of ethanol. In contrast, and in line with the experiments, the same model predicted a significant decrease of conversion to 64% with an ethanol concentration of 200% (see ESI for further details†).



## Conclusions

Well-defined molybdenum–PNP pincer complexes have been used for the first time in the hydrogenation of a range of amides to the corresponding alcohols and amines. *N*-Alkylated and *N*-arylated formamides can be hydrogenated to the corresponding products in good to high yields. Applying complex **Mo-1a** high selectivity for the hydrogenation of formamides was observed in the presence of other reducible groups. These results pave the way for potential applications of this type of complexes in synthetic methodologies.

The DFT study shows that the active Mo(0) species (**Mo-5**) reduces the C=O group of the amide through low-energy barriers, compared to Fe-based systems. However, the alcohol product and secondary amides react with the catalyst forming stable adducts encumbering catalyst recovery and increasing the overall barrier for the reduction of the C=O group. These results suggest that further catalyst design should focus on preventing the formation of these adducts, while keeping the high hydricity of the complex.

## Experimental details

### General experimental information

All hydrogenation reactions were set up under Ar in a 300 mL autoclave (PARR Instrument Company). In order to avoid unspecific reductions, all catalytic experiments were carried out in 4 mL glass vials, which were set up in an alloy plate and placed inside the autoclave.

In a glove box, a 4 mL glass vial containing a stirring bar was charged with complex **Mo-1a** (12.5 mg; 5 mol%). Toluene (2 mL) was added and the corresponding brown suspension was treated with NaBH<sub>4</sub>Et<sub>3</sub> (0.5 M in THF; 50 μL; 10 mol%). The reaction mixture was stirred for 10 minutes and the corresponding substrate was subsequently added. Afterwards, the vial was capped and transferred into an autoclave. Once sealed, the autoclave was purged three times with 10 bar of hydrogen, then pressurized to the desired hydrogen pressure (50 bar), and placed into an aluminum block that was preheated to the desired temperature (100 °C). After 24 h, the autoclave was cooled in an ice bath and the remaining gas was released carefully. The solution was subsequently diluted with ethyl acetate and filtered through a small pad of Celite (1 cm in a Pasteur pipette). The Celite was washed with methanol (2 mL) and the combined filtrates were subsequently evaporated to dryness. The remaining residue was purified by column chromatography (SiO<sub>2</sub>, heptane/EtOAc, gradient 100 : 0 → 0 : 100). In the case of substrate 7, the purified product was dissolved in 5 mL of Et<sub>2</sub>O and subsequently treated with 1 mL of HCl (2 M in Et<sub>2</sub>O). The reddish precipitate was filtered off, washed three times with 5 mL of Et<sub>2</sub>O and finally dried *in vacuo*. For the characterization of the products of the catalysis, see ESI.†

### Computational details

DFT calculations were carried out with Gaussian 09<sup>24</sup> with the M06<sup>25</sup> functional and the double-z LANL2DZ (on Mo, including

relativistic effects)<sup>26</sup> and 6-31+G\*\* (on all other elements)<sup>27</sup> basis sets. Calculations were done using the full system. The location of the Na<sup>+</sup> cation was evaluated in some of the intermediates, and the preferred position is represented in figures and schemes of the manuscript (see ESI†). The geometry optimization and energies of the possible spin states of **Mo-1a** and **Mo-4** were consistent with a doublet and singlet ground state, respectively (see ESI†). Vibrational frequencies were computed at the same level of theory to obtain the thermochemistry corrections (zero-point, thermal and entropy energies) at the experimental *p* = 50 atm and *T* = 373.15 K. The energy of the optimized geometries was refined by single point calculations with triple-z quality basis sets, including the LANL2TZ<sup>26</sup> on Mo and the 6-311+G\*\* on all other elements.<sup>28</sup> The energies reported in the text were obtained by adding the thermochemistry corrections to the refined potential energies. The solvation effects of toluene were included in both the geometry optimizations and energy refinements using the continuum SMD model.<sup>29</sup> The ultrafine (99 590) grid was used in all calculations for higher numerical accuracy. A repository containing all input and output files is available on-line from ioChem BD at <https://iochem-bd.bsc.es/browse/handle/100/193698>.<sup>30</sup> Microkinetic models were simulated with the COPASI software<sup>31</sup> using the LSODA algorithm. See ESI for further details.†

## Conflicts of interest

There are no conflicts to declare.

## Acknowledgements

T. Leischner, K. Junge and M. Beller thank the analytical department (S. Schareina, S. Buchholz, A. Lehmann) of the Leibniz-Institute for Catalysis, Rostock. Ll. A. and A. N. thank the support from the Research Council of Norway (FINATEK Grant No. 250044 and Center of Excellence Grant No 262695), the Norwegian Metacenter for Computational Science (NOTUR, nn4654k) and the 'Nordic Consortium for CO<sub>2</sub> Conversion' (NordForsk project no 85378, <http://site.uit.no/nordco2>).

## Notes and references

- (a) P. Roose, K. Eller, E. Henkes, R. Rossbacher and H. Hönke, *Ullmann's Encyclopedia of Industrial Chemistry*, Germany, 2000; (b) P. G. Jessop, *The Handbook of Homogeneous Hydrogenation*, Germany, 2006.
- For selected examples of carboxylic acid derivatives hydrogenation, see: (a) S. Werkmeister, K. Junge, B. Wendt, E. Alberico, H. J. Jiao, W. Baumann, H. Junge, F. Gallou and M. Beller, *Angew. Chem., Int. Ed.*, 2014, **53**, 8722–8726; (b) T. vom Stein, M. Meureusch, D. Limper, M. Schmitz, M. Holscher, J. Coetzee, D. J. Cole-Hamilton, J. Klankermayer and W. Leitner, *J. Am. Chem. Soc.*, 2014, **136**, 13217–13225; (c) D. Srimani, A. Mukherjee, A. F. G. Goldberg, G. Leitner, Y. Diskin-Posner, L. J. W. Shimon, Y. Ben David and D. Milstein, *Angew. Chem., Int. Ed.*, 2015, **54**, 12357–12360; (d) X. J. Cui,



- Y. H. Li, C. Topf, K. Junge and M. Beller, *Angew. Chem., Int. Ed.*, 2015, **54**, 10596–10599; (e) T. J. Korstanje, J. I. van der Vlugt, C. J. Elsevier and B. de Bruin, *Science*, 2015, **350**, 298–301; (f) M. Naruto and S. Saito, *Nat. Commun.*, 2015, **6**, 8140; (g) J. R. Cabrero-Antonino, I. Sorribes, K. Junge and M. Beller, *Angew. Chem., Int. Ed.*, 2016, **55**, 387–391.
- 3 (a) B. Cornils and W. A. Herrmann, *Applied Homogenous Catalysis with Organometallic Compounds: A Comprehensive Handbook in Two Volumes*, Germany, 1996; (b) D. L. Dodds and D. L. Cole-Hamilton, *Sustainable Catalysis*, United States of America, 2013.
- 4 D. Wie, C. Netkaew and C. Darcel, *Eur. J. Inorg. Chem.*, 2019, 2471–2487.
- 5 M. Garbe, K. Junge and M. Beller, *Eur. J. Org. Chem.*, 2017, **30**, 4344–4362.
- 6 G. A. Filonenko, R. van Putten, E. J. M. Jensen and E. A. Pidko, *Chem. Soc. Rev.*, 2018, **47**, 1459–1483.
- 7 For selected examples see: (a) R. Langer, G. Leitus, Y. Ben-David and D. Milstein, *Angew. Chem., Int. Ed.*, 2011, **50**, 2120–2124; (b) N. Gorgas, B. Stöger, L. F. Veiros, E. Pittenauer, G. Allmaier and K. Kirchner, *Organometallics*, 2014, **33**, 6905–6914; (c) T. Zell, Y. Ben-David and D. Milstein, *Catal. Sci. Technol.*, 2015, **5**, 822–826; (d) N. Gorgas, B. Stöger, L. F. Veiros and K. Kirchner, *ACS Catal.*, 2016, **6**, 2664–2672; (e) S. Elangovan, B. Wendt, C. Topf, S. Bachmann, M. Scalone, A. Spannenberg, H. Jiao, W. Baumann, K. Junge and M. Beller, *Adv. Synth. Catal.*, 2016, **358**, 820–825; (f) S. Lange, S. Elangovan, C. Cordes, A. Spannenberg, H. Jioa, H. Junge, S. Bachmann, M. Scalone, C. Topf, K. Junge and M. Beller, *Catal. Sci. Technol.*, 2016, **6**, 4768–4772; (g) S. Elangovan, C. Topf, S. Fischer, H. Jiao, A. Spannenberg, W. Baumann, R. Ludwig, K. Junge and M. Beller, *J. Am. Chem. Soc.*, 2016, **138**, 8809–8814.
- 8 (a) P. M. Rylander, *Hydrogenation Methods*, Academic Press, London, 1985; (b) J. Hartwig, *Organotransition Metal Chemistry*, University Science Books, 2010.
- 9 (a) D. Cantillo, *Eur. J. Inorg. Chem.*, 2011, **19**, 3008–3013; (b) P. A. Dub and T. Ikariya, *ACS Catal.*, 2012, **2**, 1718–1741; (c) A. M. Smith and R. Whyman, *Chem. Rev.*, 2014, **114**, 5477–5510.
- 10 (a) A. A. Nunez Magro, G. R. Eastham and D. J. Cole-Hamilton, *Chem. Commun.*, 2007, **30**, 3154–3156; (b) E. Balaraman, B. Gnanaprakasam, L. J. W. Shimon and D. Milstein, *J. Am. Chem. Soc.*, 2010, **132**, 16756–16758; (c) J. M. John and S. H. Bergens, *Angew. Chem., Int. Ed.*, 2011, **50**, 10377–10380; (d) J. Coetzee, D. L. Dodds, J. Klankermayer, S. Brosinski, W. Leitner, A. M. Z. Slawin and D. J. Cole-Hamilton, *Chem.–Eur. J.*, 2013, **19**, 11039–11050; (e) T. Miura, I. E. Held, S. Oishi, M. Naruto and S. Saito, *Tetrahedron Lett.*, 2013, **54**, 2674–2678; (f) T. vom Stein, M. Meureusch, D. Limper, M. Schmitz, M. Hölscher, J. Coetzee, D. J. Cole-Hamilton, J. Klankermayer and W. Leitner, *J. Am. Chem. Soc.*, 2014, **136**, 13217–13225; (g) J. R. Cabrero-Antonino, E. Alberico, H. J. Drexler, W. Baumann, K. Junge, H. Junge and M. Beller, *ACS Catal.*, 2016, **6**, 47–54; (h) L. Shi, X. Tan, J. Long, X. Xiong, S. Yang, P. Xue, H. Lv and X. Zhang, *Chem.–Eur. J.*, 2017, **23**, 546–548.
- 11 J. A. Garg, S. Chakraborty, Y. Ben-David and D. Milstein, *Chem. Commun.*, 2016, **52**, 5285–5288.
- 12 N. M. Rezayee, D. C. Samblanet and M. S. Sanford, *ACS Catal.*, 2016, **6**, 6377–6383.
- 13 F. Schneck, M. Assmann, M. Balmer, K. Harms and R. Langer, *Organometallics*, 2016, **35**, 1931–1943.
- 14 U. Jayaranthe, Y. Zhang, N. Hazari and W. Bernskoetter, *Organometallics*, 2017, **36**, 409–416.
- 15 L. A. Suarez, Z. Culacova, D. Balcells, W. H. Bernskoetter, O. Eisenstein, K. I. Goldberg, N. Hazari, M. Tilset and A. Nova, *ACS Catal.*, 2018, **8**, 8751–8762.
- 16 V. Papa, J. R. Cabrero-Antonino, E. Alberico, A. Spannenberg, K. Junge, H. Junge and M. Beller, *Chem. Sci.*, 2017, **8**, 3576–3585.
- 17 S. Kar, A. Goeppert, J. Kothandaraman and J. K. S. Prakash, *ACS Catal.*, 2017, **7**, 6347–6351.
- 18 T. Leischner, A. Spannenberg, K. Junge and M. Beller, *Organometallics*, 2018, **37**, 4402–4408.
- 19 (a) S. Chakraborty, O. Blacque, T. Fox and H. Berke, *Chem.–Asian J.*, 2014, **9**, 328–337; (b) S. Chakraborty, O. Blacque and H. Berke, *Dalton Trans.*, 2015, **44**, 6560–6570; (c) S. Chakraborty and H. Berke, *ACS Catal.*, 2014, **4**, 2191–2194; (d) Y. Zhang, P. G. Williard and W. H. Bernskoetter, *Organometallics*, 2016, **35**, 860–865.
- 20 (a) S. Chakraborty, P. Lagaditis, M. Förster, E. A. Bielinski, N. Hazari, M. C. Holthausen, W. D. Jones and S. Schneider, *ACS Catal.*, 2014, **4**, 3994–4003; (b) E. A. Bielinski, P. Lagaditis, Y. Zhang, B. Q. Mercado, C. Würtele, W. H. Bernskoetter, N. Hazari, S. Schneider and P. O. Lagaditis, *J. Am. Chem. Soc.*, 2014, **136**, 10234–10237; (c) D. Nguyen, X. Trivelli, F. Capet, J. F. Paul, F. Dumeignil and R. M. Gauvin, *ACS Catal.*, 2017, **7**, 2022–2032.
- 21 (a) Z. Shao, Y. Wang, Y. Liu, Q. Wang, X. Fu and Q. Liu, *Org. Chem. Front.*, 2018, **5**, 1248–1256; (b) X. Chen, Y. Jing and X. Yang, *Chem.–Eur. J.*, 2016, **22**, 1950–1957; (c) E. Bielinski, M. Förster, Y. Zhang, W. H. Bernskoetter, N. Hazari and M. Holthausen, *ACS Catal.*, 2015, **5**, 2404–2415.
- 22 D. Gusev, *ACS Catal.*, 2017, **7**, 6656–6662.
- 23 (a) G. Zhang and S. Hanson, *Chem. Commun.*, 2013, **49**, 10151–10153; (b) Z. Wie, A. De Aguirre, K. Junge, M. Beller and H. Jiao, *Catal. Sci. Technol.*, 2018, **8**, 3649–3665.
- 24 M. J. Frisch, G. W. Trucks, H. B. Schlegel, G. E. Scuseria, M. A. Robb, J. R. Cheeseman, G. Scalmani, V. Barone, B. Mennucci, G. A. Petersson, H. Nakatsuji, M. Caricato, X. Li, H. P. Hratchian, A. F. Izmaylov, J. Bloino, G. Zheng, J. L. Sonnenberg, M. Hada, M. Ehara, K. Toyota, R. Fukuda, J. Hasegawa, M. Ishida, T. Nakajima, Y. Honda, O. Kitao, H. Nakai, T. Vreve, J. A. Montgomery, J. E. Peralta, F. Ogliare, M. Bearpark, J. J. Heyd, E. Brothers, K. N. Kudin, V. N. Staroverov, T. Keith, R. Kobayashi, J. Normand, K. Raghvachari, A. Rendell, J. C. Burant, S. S. Iyengar, J. Tomasi, M. Cossi, N. Rega, J. M. Millam, M. Klene, J. E. Knox, J. B. Cross, V. Bakken,



- C. Adamo, J. Jaramillo, R. Gomperts, R. E. Stratmann, O. Yazyev, A. J. Austin, R. Cammi, C. Pomelli, J. W. Ochterski, R. L. Martin, K. Morokuma, V. G. Zakrzewski, G. A. Voth, P. Salvador, J. J. Dannenberg, S. Dapprich, A. D. Daniels, O. Farkas, J. B. Foresman, J. V. Ortiz, J. Cioslowski and D. J. Fox, *Gaussian 09, Revision D.01*, Gaussian, Inc., Wallingford CT, 2013.
- 25 Y. Zhao and D. Truhlar, *Theor. Chem. Acc.*, 2008, **120**, 215–241.
- 26 (a) P. Hay and W. Wadt, *J. Chem. Phys.*, 1985, **82**, 270–283; (b) W. Wadt and P. Hay, *J. Chem. Phys.*, 1985, **82**, 284–298.
- 27 (a) W. J. Hehre, R. Ditchfield and J. A. Pople, *J. Chem. Phys.*, 1972, **56**, 2257–2261; (b) W. Kohn, A. D. Becke and R. G. Parr, *J. Phys. Chem.*, 1996, **1**, 12974–12980.
- 28 A. McLean and G. Chandler, *J. Chem. Phys.*, 1980, **72**, 5639–5648.
- 29 A. Marenich, C. Cramer and D. Truhlar, *J. Phys. Chem. B*, 2009, **113**, 6378–6396.
- 30 M. Álvarez-Moreno, C. De Graaf, N. López, F. Maseras, J. M. Poblet and C. Bo, *J. Chem. Inf. Model.*, 2015, **55**, 95–103.
- 31 S. Hoops, R. Gauges, C. Lee, J. Pahle, N. Simus, M. Singhal, L. Xu, P. Mendes and U. Kummer, *Bioinformatics*, 2006, **22**, 3067–3074.



### **6.3 Synthesis of Molybdenum Pincer Complexes and Their Application in the Catalytic Hydrogenation of Nitriles**

T. Leischner, A. Spannenberg, K. Junge, M. Beller

The publication describing the preparation of several molybdenum pincer complexes and their subsequent application in the catalytic hydrogenation aromatic and aliphatic nitriles was prepared by me. I performed all the experimental work described in the publication and mainly wrote the manuscript, including the supporting information. The determination of the reported solid-state structures, alongside the corresponding measurements were carried out by Anke Spannenberg. My contribution to this publication is 80%.

*ChemCatChem* **2020**, *12*, 4543–4549.





# Synthesis of Molybdenum Pincer Complexes and Their Application in the Catalytic Hydrogenation of Nitriles

Thomas Leischner,<sup>[a]</sup> Anke Spannenberg,<sup>[a]</sup> Kathrin Junge,<sup>[a]</sup> and Matthias Beller\*<sup>[a]</sup>

Dedicated to Prof. Dr. Uwe Rosenthal on the occasion of his 70<sup>th</sup> birthday

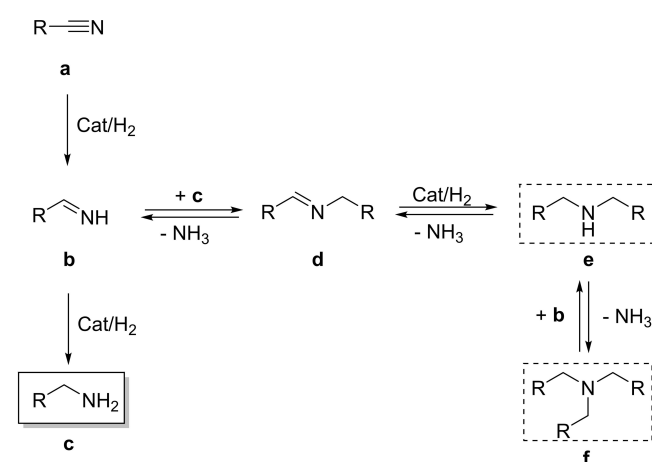
A series of molybdenum(0), (I) and (II) complexes ligated by different PNP and NNN pincer ligands were synthesized and structurally characterized. Along with previously described Mo–PNP complexes **Mo-1** and **Mo-2**, all prepared compounds were tested in the catalytic hydrogenation of aromatic nitriles to primary amines. Among the applied catalysts, **Mo-1** is

particularly well suited for the hydrogenation of electron-rich benzonitriles. Additionally, two aliphatic nitriles were transformed into the desired products in 80 and 86%, respectively. Moreover, catalytic intermediate **Mo-1a** was isolated and its role in the catalytic cycle was subsequently demonstrated.

## Introduction

Reduction of nitriles continues to attract significant attention of synthetic chemists for the preparation of diverse amines.<sup>[1]</sup> Traditionally, these reactions are carried out on laboratory scale using an excess of stoichiometric reducing agents, resulting in at least equimolar amounts of waste products.<sup>[2,3]</sup> On the contrary, catalytic homogenous hydrogenation using defined organometallic complexes provides an environmentally benign alternative, as it is more atom-economic with less waste generation.<sup>[3b,4]</sup> Nevertheless, the selective catalytic hydrogenation of nitriles to primary amines remains to be challenging for certain substrates, due to the underlying reaction mechanism (see Scheme 1).<sup>[5]</sup>

In general, primary amines are important intermediates for various applications in organic synthesis as well as in the production of bulk and fine chemicals.<sup>[6]</sup> Therefore, the development of novel (catalytic) protocols for their synthesis remains of particular interest. Until recently, noble metal-based catalyst systems prevailed for this purpose in both, industrial processes and academic research.<sup>[7]</sup> However, their comparably high price, limited availability and toxicity issues, set incentives for their replacement. Yet, in the past two decades significant progress in this direction has been achieved using for example Fe, Co and Mn complexes supported by pincer ligands.<sup>[8]</sup>



Scheme 1. General scheme for the hydrogenation of nitriles.

In this respect, also molybdenum constitutes an attractive substitute for precious metals, due to its low costs and environmentally benign nature.<sup>[9]</sup> Although the organometallic chemistry of molybdenum, particularly of its pincer complexes, has been studied in-depth in recent years,<sup>[10]</sup> reports on its application in catalytic homogeneous nitrile hydrogenation are exceptionally scarce. In fact to date, only three examples have been reported for related reductions (Scheme 2). In 2012, Nikonov and co-workers described the application of imido-hydrido Mo(IV) complex **I** for the catalytic hydroboration of nitriles in the presence of HBCat (Cat = catechol). However, only aceto- and benzonitrile were tested as substrates.<sup>[11]</sup>

The group of Berke developed a molybdenum-catalyzed homogeneous nitrile hydrogenation, based on molybdenum(I)-amido pincer catalyst **II**. However, the developed protocol operated under relatively harsh conditions (5 mol% catalyst, 140 °C) to yield secondary imines in high selectivity.<sup>[5]</sup>

In 2020, Wang and co-workers published an efficient transfer hydrogenation of nitriles using molybdenum-thiolate complex **III** in combination with NH<sub>3</sub>BH<sub>3</sub> as hydrogen donor.

[a] T. Leischner, Dr. A. Spannenberg, Dr. K. Junge, Prof. Dr. M. Beller  
Leibniz Institute for Catalysis  
Albert-Einstein-Straße 29a, 18059 Rostock (Germany)  
E-mail: Matthias.Beller@catalysis.de

Supporting information for this article is available on the WWW under  
<https://doi.org/10.1002/cctc.202000736>

This publication is part of a joint Special Collection with EurJIC on "Pincer Chemistry & Catalysis". Please follow the link for more articles in the collection.

© 2020 The Authors. Published by Wiley-VCH Verlag GmbH & Co. KGaA. This is an open access article under the terms of the Creative Commons Attribution Non-Commercial License, which permits use, distribution and reproduction in any medium, provided the original work is properly cited and is not used for commercial purposes.



derivative remained unsuccessful. Surprisingly, when the reaction was carried out in DCM under otherwise identical conditions, selective formation of **Mo-3a** was observed again. Even after stirring for several days at room temperature,  $^{31}\text{P}\{^1\text{H}\}$  NMR analysis revealed **Mo-3a** as the main species. However, slow formation of a new resonance at 63 ppm occurred. Assuming, that **Mo-3a** is relatively stable towards chlorination, the reaction mixture was heated to 40 °C for three hours.  $^{31}\text{P}\{^1\text{H}\}$  NMR analysis showed complete conversion of **Mo-3a** into the new species at 63 ppm. Subsequent isolation and characterization provided diamagnetic Mo(II) pincer complex **Mo-4a** in 56% yield.

When exploring the reactivity of  $(\text{Et}_2\text{PCH}_2\text{CH}_2)_2\text{NH}$ , we observed a similar reaction behavior as compared to  $(\text{Ph}_2\text{PCH}_2\text{CH}_2)_2\text{NH}$ . Performing the reaction in THF, we were able to isolate the corresponding Mo(0) **Mo-3b** in 82% yield. Nevertheless, carrying out the reaction in DCM resulted in the formation of complex product mixtures, even at  $-20^\circ\text{C}$ .

Finally, the NNN pincer ligand *bis*-(2-pyridylmethyl)amine was applied. The ligand reacted readily with Mo

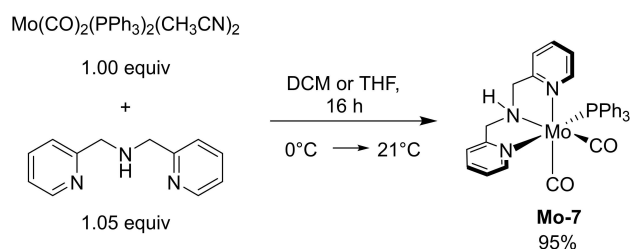
$(\text{PPh}_3)_2(\text{CH}_3\text{CN})_2(\text{CO})_2$  in DCM and THF, respectively, resulting in the formation of **Mo-7** in both cases (Scheme 4).

Complex **Mo-7** proved to be remarkably stable towards chlorination and remained molecularly unchanged even after refluxing for 24 h in DCM and DCE, respectively. All prepared coordination compounds have been characterized by standard techniques including  $^1\text{H}$ ,  $^{13}\text{C}$  and  $^{31}\text{P}\{^1\text{H}\}$  NMR (except **Mo-6** and **Mo-7**, see *vide infra*) and IR spectroscopy as well as elemental analysis (for NMR and IR spectra, see supporting information). Additionally, we were able to determine solid-state structures of complexes **Mo-3a**, **Mo-3b**, **Mo-4a**, **Mo-6** as well as **Mo-7** by X-ray analysis of suitable single crystals. Their structural views are depicted in Figure 2. However, due to the insolubility of **Mo-7** in all common NMR solvents, including benzene, toluene, THF, acetonitrile, DMSO and methanol, as well as the paramagnetic nature of **Mo-6**, we were unable to obtain meaningful NMR data of these complexes.

Complexes **Mo-3a**, **Mo-3b** and **Mo-7** adopt a distorted octahedral coordination geometry at the molybdenum center, with the CO ligands being in a *cis*-orientation. The coordinated pincer ligands all exhibit a *fac*-arrangement around the central metal atom. However, in complex **Mo-6** the *mer*-coordination mode of the pincer ligand is observed with the CO ligands being in a *cis*-arrangement. The described characteristics for **Mo-6** are in agreement with our previously published solid state structure of **Mo-2**.<sup>[13]</sup> The coordination geometry at the Mo atom of the heptacoordinated Mo(II)-complex **Mo-4a** can be best described as distorted capped octahedral.

The recorded IR spectra of the reported complexes all show medium to strong carbonyl absorption bands between  $1921\text{ cm}^{-1}$  and  $1679\text{ cm}^{-1}$ .

Next, we tested the catalytic activity of the newly described molybdenum pincer complexes **Mo-3a**, **Mo-3b**, **Mo-4a**, **Mo-6**



**Scheme 4.** Synthesis of previously unknown molybdenum NNN pincer complex **Mo-7**.

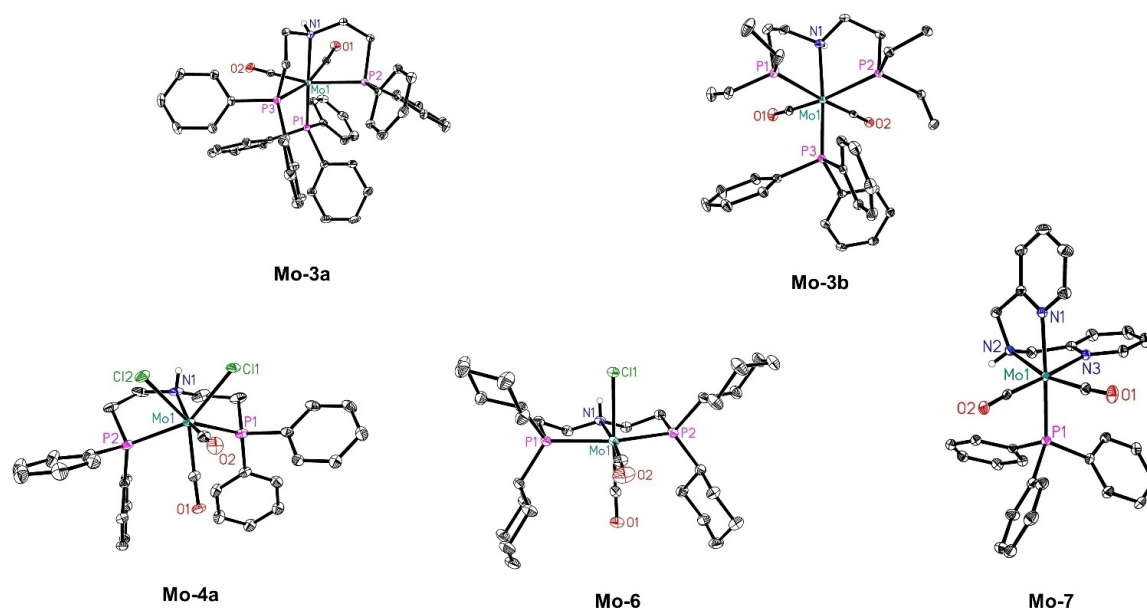


**Figure 2.** Molecular structures of **Mo-3a**, **Mo-3b**, **Mo-4a**, **Mo-6** and **Mo-7** in the solid state. Thermal ellipsoids are drawn at 30% probability level. Hydrogen atoms, except the *N*-bound are omitted for clarity. For **Mo-6**, only one molecule of the asymmetric unit is shown.



and **Mo-7**, as well as of the previously reported compounds **Mo-1** and **Mo-2**, in the catalytic hydrogenation of benzonitrile **1a**. It has to be noted, that in our initial work some activity was reported in this transformation, using **Mo-2** as the catalyst, without further optimization. However, under the reported conditions, only modest conversion (42%) and poor product selectivity (13%) for the desired primary amine were observed.<sup>[13]</sup> In order to minimize potential decomposition of the homogeneous molybdenum catalysts, the initial catalyst screening was carried out at 100 °C in the presence of 10 mol% NaBHET<sub>3</sub>. Under these conditions full conversion was observed for **Mo-1** and **Mo-2**, yielding approximately 1:1 mixtures of **2a** and **3a** (Table 1, entries 1–2). All other Mo-complexes, however, provided inferior results (Table 1, entries 3–7). Interestingly, **Mo-4a** as well as **Mo-7** failed to give any conversion at all.

The activity of **Mo-1** and **Mo-2** was subsequently compared at a reduced temperature of 80 °C (Table 1, entries 8 and 9). Here, **Mo-1** provided a superior conversion of 90%. Based on this result and its more convenient synthesis, we focused on **Mo-1** in the due course of the optimization process. Selecting

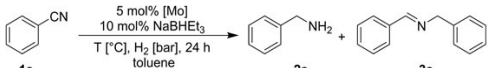
80 °C reaction temperature and 5 mol% of **Mo-1** (Table 1, entry 8) as the optimal setting, we explored several different solvents. In contrast to previous reports on base metal catalyzed hydrogenation of nitriles, **Mo-1** was found to be completely inactive in *i*-PrOH, while toluene as solvent provided the best results. Applying THF, 1,4-dioxane and Bu<sub>2</sub>O resulted in significantly lower activities and predominantly yielded **3a** as the reaction product. Other aliphatic solvents such as *n*-heptane and cyclohexane, were not suitable for the attempted transformation (Figure 3).

Subsequently, we investigated the influence of dihydrogen pressure, catalyst loading, the amount of additive used (Table S1, see supporting information), as well as the substrate concentration (Table S2, see supporting information) on the reaction outcome. Reducing the catalyst loading to 2.5 mol% resulted in a significantly less active system. However, lowering the amount of additive to 5 mol% led to no loss in reactivity.

Increasing the H<sub>2</sub> pressure to 80 bar showed no observable effect. Albeit, carrying out the reaction at 30 bar of dihydrogen caused a sharp drop in catalyst activity. A rise of the reaction temperature to 100 °C eventually resulted in full conversion of **1a** in the presence of 5 mol% NaBHET<sub>3</sub> and **Mo-1**, respectively (Table 1, entry 10). Next, we evaluated several substrate concentrations based on 0.5 mmol of **1a**, ranging from 0.08 to 0.5 M. Notably, using 5 mL of toluene proved to be the optimal concentration, providing the desired product benzylamine **2a** in 96% yield (Table 1, entry 11). Finally, a series of control experiments were carried out. In the absence of **Mo-1**, no catalytic reaction took place (Table 1, entry 12). Similarly, no product formation could be detected, when the reaction was performed in the absence of NaBHET<sub>3</sub> (Table 1, entry 13). In order to confirm, that no heterogeneous catalysis takes place, a mercury poisoning experiment was conducted, revealing no loss of activity (Table S2, see supporting information).

Having optimized conditions in hand, we proceeded to the application of **Mo-1** in the hydrogenation of a variety of different benzonitriles to the corresponding benzylamines. As shown in Scheme 5 our developed methodology appeared to be particularly well suited for electron-rich benzonitriles and the intended primary amines were consistently obtained in high yields. Substituents in *para*-, *meta*- and *ortho*-position of the phenyl ring were well tolerated and even sterically hindered nitriles **1k** and **1m** were successfully converted, furnishing **2k** and **2m** in isolated yields of 68% and 91%, respectively. Notably, when the steric bulk was further increased, using 2,6-dimethylbenzonitrile **1n**, we were still able to isolate the desired primary amine **2n** in a good yield of 72%. The system proved to be insensitive towards halides such as fluoride and chloride (**2b** and **2c**) and no dehalogenation products were observed during the catalysis. This was additionally the case when 3,5-dichlorobenzonitrile **1o** was employed, providing 3,5-dichlorobenzylamine **2o** in 60% isolated yield. Moreover, also a benzylether moiety, often cleaved under hydrogenation conditions, remained unaffected and no deprotection could be detected in product **2h**. However, some (hetero)benzonitriles with substituents in either *ortho*- or *para*-position, such as H<sub>2</sub>N-, CF<sub>3</sub>-, CO<sub>2</sub>Me-, carbonyl-, cyano- and nitro groups, either gave only

**Table 1.** Initial screening of Mo-catalysts and reaction parameters.<sup>[a]</sup>



Entry	Catalyst	Conv. [%] <sup>[b]</sup>	Yield 2 [%] <sup>[b]</sup>	Yield 3 [%] <sup>[b]</sup>
1	<b>Mo-1</b>	>99	58	40
2	<b>Mo-2</b>	>99	52	42
3	<b>Mo-3a</b>	62	38	20
4	<b>Mo-3b</b>	70	41	24
5	<b>Mo-4a</b>	<1	<1	<1
6	<b>Mo-6</b>	78	41	35
7	<b>Mo-7</b>	<1	<1	<1
8 <sup>[c]</sup>	<b>Mo-1</b>	90	50	38
9 <sup>[c]</sup>	<b>Mo-2</b>	81	42	35
10 <sup>[d]</sup>	<b>Mo-1</b>	>99	55	41
11 <sup>[e]</sup>	<b>Mo-1</b>	>99	96	<1
12 <sup>[f]</sup>	–	4	<1	<1
13 <sup>[g]</sup>	<b>Mo-1</b>	7	<1	<1

[a] Reaction conditions: 0.5 mmol substrate, 2 mL toluene, 5 mol% catalyst, 10 mol% NaBHET<sub>3</sub> (1 M in THF), 50 bar H<sub>2</sub>, 100 °C, 24 h. [b] Determined by GC using hexadecane as internal standard. [c] 80 °C. [d] 5 mol% NaBHET<sub>3</sub> (0.5 M in THF). [e] 5 mL toluene, 0.5 mmol substrate. [f] No catalyst was used. [g] No NaBHET<sub>3</sub> added.

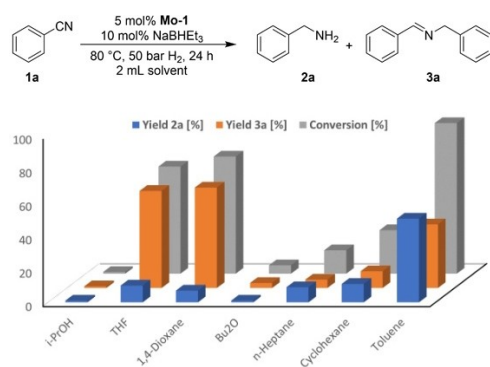
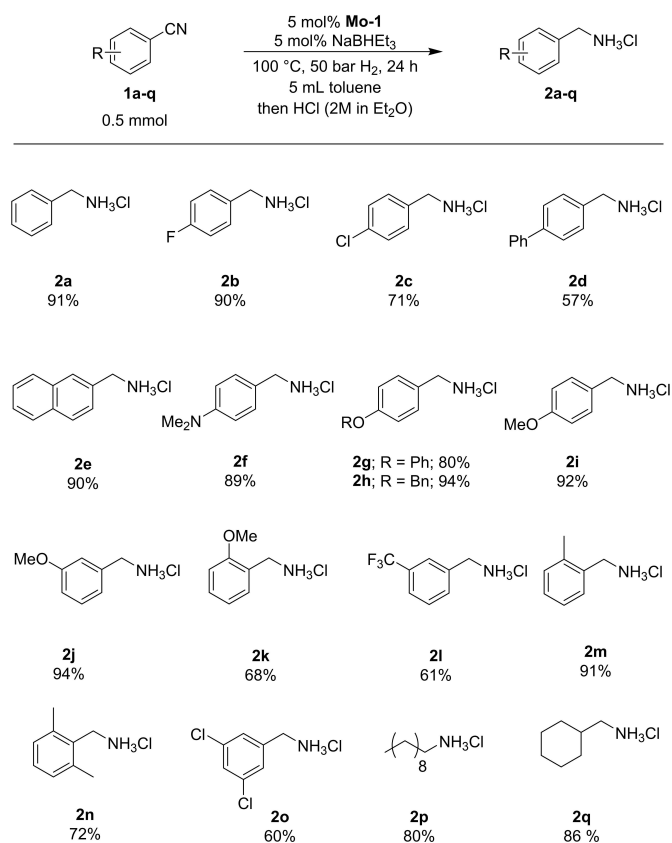


**Figure 3.** Study of the solvent effect in the hydrogenation of benzonitrile **1a** to benzylamine **2a** and *N*-benzylidenebenzylamine **3a** catalyzed by **Mo-1**.



**Scheme 5.** Substrate scope for nitrile reduction with molybdenum pincer complex **Mo-1**.

poor conversions or did not yield the desired primary amines in sufficient quantities (see Table S3, supporting information). Clearly, in these cases the observed reactivity of the catalyst is not an easy function of the electron-donating or electron-withdrawing character of the respective substituents. Apparently, there are several factors influencing the observed reactivity. In Table S3 some of the observed side products are mentioned.

Interestingly, for 2- and 4-trifluoromethyl-substituted benzonitriles low conversions and negligible product yields were observed, while in the case of *meta*- $\text{CF}_3$ -substituted nitrile **1l** the corresponding primary amine **2l** could be isolated in 61% yield. Furthermore, we successfully applied two aliphatic nitriles **1p** and **1q** to our reported protocol. In both cases, **Mo-1** proved to be a suitable catalyst and we were able to isolate the intended reaction products **2p** and **2q** in 80% and 86% yield, respectively.

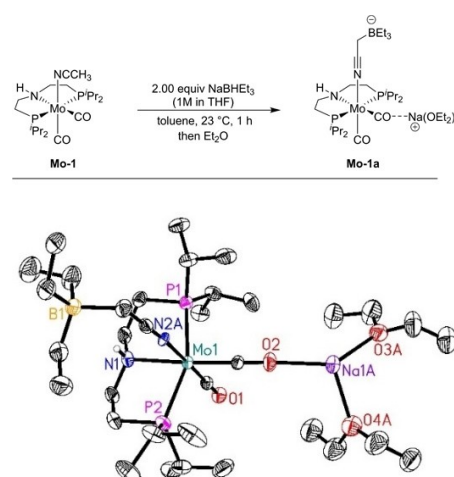
Finally, with respect to the mechanism we became interested in the molecular structure of the organometallic species formed from the reaction of **Mo-1** and  $\text{NaBHET}_3$ . Hence, we conducted a control experiment, treating 0.5 mmol of **Mo-1** with an excess of  $\text{NaBHET}_3$  in toluene at room temperature (for experimental details, see Supporting Information). The reaction proceeded rapidly, resulting in the formation of a clear red solution within less than one minute. The  $^{31}\text{P}\{^1\text{H}\}$  NMR analysis of the crude reaction mixture revealed the formation of a strong

singlet resonance at 74 ppm as the main product alongside some free ligand. Attempts to characterize the corresponding species by X-ray analysis of suitable crystals were successful and provided the solid-state structure of **Mo-1a** (Scheme 6). As expected, the applied additive acts as base and abstracts a proton from **Mo-1**. Interestingly, the deprotonation does not involve the NH moiety of the pincer ligand but takes place at the  $\text{CH}_3$ -group of the coordinated acetonitrile ligand, resulting in the formation of a covalent C–B bond. This observed reactivity is in sharp contrast to classical reaction patterns observed for pincer supported (base) metal catalysts, where basic additives typically activate the catalyst by deprotonation of the ligand backbone.<sup>[14]</sup>

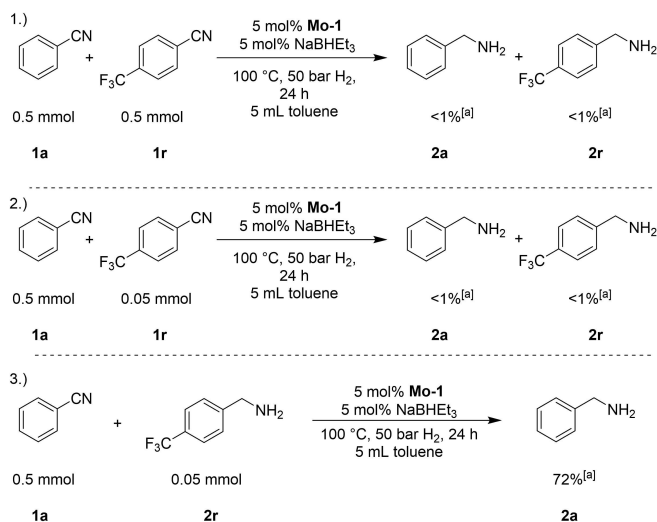
In order to confirm that **Mo-1a** indeed plays an active role in the catalysis, the benchmark reaction was carried out using 5 mol% **Mo-1a** in the absence of  $\text{NaBHET}_3$  under otherwise identical conditions. Benzylamine **2a** was observed in 92% yield, proving the involvement of **Mo-1a** in the catalytic hydrogenation of benzonitrile **1a**. Next, we were interested in the reactivity of **Mo-1a** towards dihydrogen. Therefore, **Mo-1** was activated with two equivalents of  $\text{NaBHET}_3$  in  $d_8$ -toluene and subsequently stirred for 3 h at 100 °C in the presence of 50 bar  $\text{H}_2$  (for experimental details see Supporting Information). Analysis of the reaction mixture by  $^{31}\text{P}$  NMR spectroscopy revealed two new main resonances at 89.1 and 75.9 ppm, thus proving that **Mo-1a** had undergone a reaction with  $\text{H}_2$ . However, no hydride signals could be detected according to the obtained  $^1\text{H}$  NMR spectrum. The resonance at 75.9 ppm corresponds to the Mo(0) complex *fac*- $[(\text{Pr}_2\text{PCH}_2\text{CH}_2)_2\text{NH}]\text{Mo}(\text{CO})_3$ ,<sup>[13a]</sup> revealing a potential catalyst deactivation pathway.

Furthermore, to understand the poor catalytic performance of **Mo-1** when electron deficient nitriles are applied, a series of control experiments were conducted, too (Scheme 7).

Adding 0.5 mmol of 4-(trifluoromethyl)benzonitrile **1r** to the benchmark reaction resulted in a complete shut-down of catalyst activity and no benzylamine **2a** could be detected.



**Scheme 6.** Synthesis of **Mo-1a** (top). Molecular structure of **Mo-1a** in the solid state (bottom). Thermal ellipsoids are drawn at 30% probability level. Hydrogen atoms, except the N-bound are omitted for clarity. Disordered parts of the molecule are only shown in one orientation.



**Scheme 7.** Control experiments carried out. [a] Yields determined by GC using hexadecane as internal standard. 1.) Poisoning experiment using 1 equiv. of **1r**. 2.) Poisoning experiment using 10 mol% of **1r**. 3.) Poisoning experiment using 10 mol% of **2r**.

Interestingly, also in the presence of only 10 mol% of **1r**, no formation of **2a** occurred. We therefore conclude, that **1r** acts as a strong catalyst poison and thus inhibits the catalysis (for experimental details on the described reactions, see Supporting Information). Subsequently, we investigated whether the corresponding primary amine, 4-(trifluoromethyl)benzylamine **2r**, could act as catalyst poison too. Interestingly, adding 10 mol% of **2r** resulted in full conversion of **1a** and benzylamine was observed in 72% yield.

## Conclusions

In summary, we reported the synthesis and structural characterization of a series of previously unknown molybdenum pincer complexes. Depending on the used pincer ligand and the reaction solvent, different complex structures are obtained. Furthermore, the first molybdenum-catalyzed reduction of nitrile to primary amines using molecular hydrogen is described. In fact, Mo-pincer complex, **Mo-1**, can be used as efficient catalyst for the selective catalytic hydrogenation of selected aromatic and aliphatic nitriles to give the corresponding primary amines. Additionally, we isolated and identified catalytic intermediate **Mo-1a** and subsequently proved its role in the catalytic process.

## Experimental Section

**General Procedure for Catalysis Experiments:** All hydrogenation reactions were set up under Ar in a 300 mL autoclave (PARR Instrument Company). In order to avoid unspecific reductions, all catalytic experiments were carried out in separate 8 mL glass vials, which were set up in an alloy plate and placed inside the autoclave.

In a glove box, an 8 mL glass vial containing a stirring bar was charged with complex **Mo-1** (12.5 mg; 5 mol%). Toluene (5 mL) was added and the corresponding greenish suspension was treated with NaBHET<sub>3</sub> (0.5 M in THF; 50  $\mu$ L; 5 mol%). The reaction mixture was stirred for 20 minutes and the corresponding substrate was subsequently added. Afterwards, the vial was capped and transferred into an autoclave. Once sealed, the autoclave was purged three times with 10 bar of hydrogen, then pressurized to the desired hydrogen pressure (50 bar) and placed into an aluminum block that was preheated to the desired temperature (100 °C). After 24 h, the autoclave was cooled in an ice bath and the remaining gas was released carefully. The solution was subsequently diluted with 50 mL Et<sub>2</sub>O and filtered through a small pad of silica. The silica was washed with DCM (10 mL) and the combined filtrates were treated with 2 mL of HCl (2 M in Et<sub>2</sub>O). The obtained precipitate was filtered off, washed two times with 20 mL ethyl acetate and two times with 20 mL Et<sub>2</sub>O and subsequently dried *in vacuo*. For the characterization of the products of the catalysis, see Supporting Information.

## Acknowledgements

This work was supported by the BMBF, the state Mecklenburg-Western Pomerania and the European Union as part of the NoNoMeCat (675020) project. We thank the analytic department of LIKAT for their support and assistance. Open access funding enabled and organized by Projekt DEAL.

## Conflict of Interest

The authors declare no conflict of interest.

**Keywords:** molybdenum · pincer complexes · hydrogenation · nitrile · primary amine

- [1] a) D. M. Bagal, B. M. Bhanage, *Adv. Synth. Catal.* **2015**, *357*, 883–900.  
 [2] For a general book about organic reductions, see: a) J. Seyden-Penne, *Reductions by the Alumino- and Borohydrides in Organic Synthesis*, 2<sup>nd</sup> edition, Wiley-VCH, New York, United States of America **1997**; for selected examples see: b) S. Zhou, K. Junge, D. Addis, S. Das, M. Beller, *Angew. Chem. Int. Ed.* **2009**, *48*, 9507–9510; *Angew. Chem.* **2009**, *121*, 9671–9674; c) S. Das, D. Addis, S. L. Zhou, K. Junge, M. Beller, *J. Am. Chem. Soc.* **2010**, *132*, 1770–1771; d) G. Pelletier, W. S. Bechara, A. B. Charette, *J. Am. Chem. Soc.* **2010**, *132*, 12817–12819; e) S. Das, D. Addis, K. Junge, M. Beller, *Chem. Eur. J.* **2011**, *17*, 12186–12192; f) C. Cheng, M. Brookhart, *J. Am. Chem. Soc.* **2012**, *134*, 11304–11307; g) S. Das, B. Wendt, K. Moller, K. Junge, M. Beller, *Angew. Chem. Int. Ed.* **2012**, *51*, 1662–1666; *Angew. Chem.* **2012**, *124*, 1694–1698; h) S. Park, M. Brookhart, *J. Am. Chem. Soc.* **2012**, *134*, 640–653; i) T. Dombay, C. Helleu, C. Darcel, J. B. Sortais, *Adv. Synth. Catal.* **2013**, *355*, 3358–3362; j) J. T. Reeves, Z. L. Tan, M. A. Marsini, Z. X. S. Han, Y. B. Xu, D. C. Reeves, H. Lee, B. Z. Lu, C. H. Senanayakea, *Adv. Synth. Catal.* **2013**, *355*, 47–52; k) E. Blondiaux, T. Cantat, *Chem. Commun.* **2014**, *50*, 9349–9352; l) N. L. Lampland, M. Hovey, D. Mukherjee, A. D. Sadow, *ACS Catal.* **2015**, *5*, 4219–4226; m) D. Mukherjee, S. Shirase, K. Mashima, J. Okuda, *Angew. Chem. Int. Ed.* **2016**, *55*, 13326–13329; *Angew. Chem.* **2016**, *128*, 13520–13523.  
 [3] a) H. C. Brown, S. Narasimhan, Y. M. Choi, *Synthesis* **1981**, 441–442; b) S. Werkmeister, K. Junge, M. Beller, *Org. Process Res. Dev.* **2014**, *18*, 289–302.

- [4] a) P. A. Dub, T. Ikariya, *ACS Catal.* **2012**, *2*, 1718–1741; b) A. M. Smith, R. Whyman, *Chem. Rev.* **2014**, *114*, 5477–5510; c) A. M. Smith, R. Whyman, *Chem. Rev.* **2014**, *114*, 5477–5510.
- [5] a) S. Chakraborty, H. Berke, *ACS Catal.* **2014**, *4*, 2191–2194.
- [6] K. Levay, L. Hegedüs, *Curr. Org. Chem.* **2019**, *23*, 1881–1900.
- [7] For selected examples see on Rh, Ru, Ir and Re-catalyzed nitrile hydrogenations see: a) T. Yoshida, T. Okano, S. Otsuka, *J. Chem. Soc. Chem. Commun.* **1979**, 870–871; b) R. A. Grey, G. P. Pez, A. Wall, J. Corsi, *J. Chem. Soc. Chem. Commun.* **1980**, 783–784; c) R. A. Grey, G. P. Pez, A. Wallo, *J. Am. Chem. Soc.* **1981**, *103*, 7536–7542; d) C. Chin, B. Lee, *Catal. Lett.* **1992**, *14*, 135–140; e) T. Li, I. Bergner, F. N. Haque, M. Zimmer-De luliis, D. Song, R. Morris, *Organometallics* **2007**, *26*, 5940–5949; f) S. Enthaler, D. Addis, K. Junge, G. Erre, M. Beller, *Chem. Eur. J.* **2008**, *14*, 9491–9494; g) S. Enthaler, K. Junge, D. Addis, G. Erre, M. Beller, *ChemSusChem* **2008**, *1*, 1006–1010; h) D. Addis, S. Enthaler, K. Junge, B. Wendt, M. Beller, *Tetrahedron Lett.* **2009**, *50*, 3654–3656; i) R. Reguillo, M. Grellier, N. Vautravers, L. Vendier, S. Sabo-Etienne, *J. Am. Chem. Soc.* **2010**, *132*, 7854–7855; j) C. Gunanathan, M. Hölscher, W. Leitner, *Eur. J. Inorg. Chem.* **2011**, 3381–3386; k) K. Rajesh, B. Dudle, O. Blacque, H. Berke, *Adv. Synth. Catal.* **2011**, *353*, 1479–1484; l) S. Werkmeister, K. Junge, B. Wendt, A. Spannenberg, H. Jiao, C. Bornschein, M. Beller, *Chem. Eur. J.* **2014**, *20*, 427–431; m) J. Neumann, C. Bornschein, H. Jiao, K. Junge, M. Beller, *Eur. J. Org. Chem.* **2015**, 5944–5948; n) J.-H. Choi, M. H. G. Precht, *ChemCatChem* **2015**, *7*, 1023–1028; o) R. Adam, C. B. Bheeter, R. Jackstell, M. Beller, *ChemCatChem* **2015**, *8*, 1329–1334; p) R. Adam, E. Alberico, W. Baumann, H.-J. Drexler, R. Jackstell, H. Junge, M. Beller, *Chem. Eur. J.* **2016**, *22*, 4991–5002; q) Y. Sato, Y. Kayaki, T. Ikariya, *Organometallics* **2016**, *35*, 1257–1264.
- [8] For a general review regarding Co, Fe and Mn catalyzed homogeneous nitrile hydrogenations see: a) D. M. Sharma, B. Punji, *Chem. Asian J.* **2020**, *15*, 690–708; For selected examples see: b) C. Bornschein, S. Werkmeister, B. Wendt, H. Jiao, E. Alberico, W. Baumann, H. Junge, K. Junge, M. Beller, *Nat. Commun.* **2014**, *5*, 4111; c) A. Mukherjee, D. Srimani, S. Chakraborty, Y. Ben-David, D. Milstein, *J. Am. Chem. Soc.* **2015**, *137*, 8888–8891; d) S. Lange, S. Elangovan, C. Cordes, A. Spannenberg, H. Jiao, S. Bachmann, M. Scalone, C. Topf, K. Junge, M. Beller, *Catal. Sci. Technol.* **2016**, *6*, 4768–4772; e) S. Chakraborty, D. Milstein, *Chem. Commun.* **2016**, 52, 1812–1815; f) S. Elangovan, C. Topf, S. Fischer, H. Jiao, A. Spannenberg, W. Baumann, R. Ludwig, K. Junge, M. Beller, *J. Am. Chem. Soc.* **2016**, *138*, 8809–8814; g) S. Chakraborty, D. Milstein, *ACS Catal.* **2017**, *7*, 3968–3972; h) K. Tokmic, B. J. Jackson, A. Salazar, T. J. Woods, A. R. Fout, *J. Am. Chem. Soc.* **2017**, *139*, 13554–13561; i) R. Adam, C. B. Bheeter, J. R. Cabrero-Antonino, K. Junge, R. Jackstell, M. Beller, *ChemSusChem* **2017**, *10*, 842–846; j) H. Li, A. Al-Dakhil, D. Lupp, S. S. Gholap, Z. Lai, L.-C. Liang, K. W. Huang, *Org. Lett.* **2018**, *20*, 6430–6435; k) H. Dai, H. Guan, *ACS Catal.*, **2018**, *8*, 9125–9130; l) J. Schneekönig, J. Tannert, H. Hornke, M. Beller, K. Junge, *Catal. Sci. Technol.* **2019**, *9*, 1779–1783.
- [9] S. Chakraborty, O. Blacque, T. Fox, H. Berke, *Chem. Asian J.* **2014**, *9*, 328–337.
- [10] a) W. Schirmer, U. Flörke, H. Haupt, *Z. Anorg. Allg. Chem.* **1987**, *545*, 83–97; b) J. Ellermann, M. Moll, N. Will, *J. Organomet. Chem.* **1989**, *378*, 73–79; c) H. F. Lang, P. E. Fanwick, R. A. Dalton, *Inorg. Chim. Acta* **2002**, *329*, 1–8; d) B. Benito-Garagorri, E. Becker, J. Wiedermann, W. Lackner, M. Pollak, K. Meireiter, J. Kisala, K. Kirchner, *Organometallics* **2006**, *25*, 1900–1913; e) K. Arashiba, Y. Miyake, Y. Nishibayashi, *Nat. Chem.* **2011**, *3*, 120–125; f) K. Arashiba, K. Sasaki, S. Kuriyama, Y. Miyake, Y. Nakanishi, Y. Nishibayashi, *Organometallics* **2012**, *31*, 2035–2041; g) E. Kinoshita, K. Arashiba, S. Kuriyama, Y. Miyake, Y. Shimazaki, H. Nakanishi, Y. Nishibayashi, *Organometallics*, **2012**, *31*, 8437.8443; h) O. Öztöpcü, C. Holzhaacker, M. Puchberger, M. Weil, K. Meireiter, L. F. Veiros, K. Kirchner, *Organometallics*, **2013**, *32*, 3042–3052; i) S. R. M. M. de Aguiar, B. Stöger, B. Pittenauer, M. Puchberger, G. Allmair, L. F. Veiros, K. Kirchner, *J. Organomet. Chem.* **2014**, *760*, 74–83; j) S. R. M. M. de Aguiar, O. Öztöpcü, B. Stöger, K. Meireiter, L. F. Veiros, B. Pittenauer, G. Allmair, K. Kirchner, *Dalton Trans.* **2014**, *43*, 14669–14679; k) S. Chakraborty, O. Blacque, H. Berke, *Dalton Trans.* **2015**, *44*, 6560–6570; l) R. Castro-Rodrigo, S. Chakraborty, L. Munjanja, W. Brennessel, W. D. Jones, *Organometallics* **2016**, *35*, 3124–3131; m) Y. Zhang, P. G. Williard, W. H. Bernskoetter, *Organometallics* **2016**, *35*, 860–865; n) S. R. M. M. de Aguiar, B. Stöger, B. Pittenauer, G. Allmair, L. F. Veiros, K. Kirchner, *Dalton Trans.* **2016**, *45*, 13834–13845; o) G. A. Silant'ev, M. Förster, S. Schluschaß, J. Abbenetz, C. Würtele, C. Volkmann, M. C. Holthausen, S. Schneider, *Angew. Chem. Int. Ed.* **2017**, *56*, 5872–5876; *Angew. Chem.* **2017**, *129*, 5966–5970; p) S. M. M. de Aguiar, O. Öztöpcü, A. Troiani, G. de Petris, M. Weil, B. Stöger, L. F. Veiros, B. Pittenauer, G. Allmair, K. Kirchner, *Eur. J. Inorg. Chem.* **2018**, *7*, 876–884; q) M. V. Joannou, M. J. Bezdek, P. J. Chirik, *ACS Catal.* **2018**, *8*, 5276–5285; r) M. J. Bezdek, P. J. Chirik, *Angew. Chem. Int. Ed.* **2018**, *8*, 2224–2228; s) M. J. Bezdek, P. J. Chirik, *Organometallics* **2019**, *38*, 1682–1687; t) Y. Ashida, S. Kondo, K. Arashiba, T. Kikuchi, K. Nakajima, S. Kakimoto, Y. Nishibayashi, *Synthesis* **2019**, *51*, 3792–3795; u) M. Alvarez, A. Galindo, P. J. Perez, E. Carmona, *Chem. Sci.* **2019**, *10*, 8541–8546; v) R. Tran, S. M. Kilyanek, *Dalton Trans.* **2019**, *48*, 16304–16311; w) M. Pfeil, T. A. Engesser, A. Koch, J. Junge, J. Krahmer, C. Näther, F. Tuczek, *Eur. J. Inorg. Chem.* **2020**, 1437–1448.
- [11] A. Y. Khalimon, P. Farha, L. G. Kuzmina, G. I. Nikonov, *Chem. Commun.* **2012**, *48*, 455–457.
- [12] S. F. Hou, J. Y. Chen, M. Xue, M. Jia, X. Zhai, R.-Z. Liao, C.-H. Tung, W. Wang, *ACS Catal.* **2020**, *10*, 380–390.
- [13] a) T. Leischner, A. Spannenberg, K. Junge, M. Beller, *Organometallics* **2018**, *37*, 4402–4408; b) T. Leischner, L. A. Suarez, A. Spannenberg, K. Junge, A. Nova, M. Beller, *Chem. Sci.* **2019**, *10*, 10566–10576.
- [14] a) E. Ben-Ari, G. Leitus, L. J. W. Shimon, D. Milstein, *J. Am. Chem. Soc.* **2006**, *128*, 15390–15391; b) J. R. Khusnutdinova, D. Milstein, *Angew. Chem. Int. Ed.* **2015**, *54*, 12236–12273; *Angew. Chem.* **2015**, *127*, 12406–12445.

Manuscript received: April 30, 2020  
Revised manuscript received: May 28, 2020  
Accepted manuscript online: June 5, 2020  
Version of record online: July 9, 2020

## **6.4 Application of Crabtree/Pfaltz-Type Iridium Complexes for the Catalyzed Asymmetric Hydrogenation of an Agrochemical Building Block**

J. Schneekönig, W. Liu, T. Leischner, K. Junge, C. Schotes, C. Baier, M. Beller

*Org. Process Res. Dev.* **2020**, *24*, 443–447.

Herein I was mainly involved in the optimization of the catalytic reaction. I conducted the hydrogenation reactions, testing the described complexes. The organometallic compounds and corresponding ligands were synthesized and characterized by Dr. J. Schneekönig and Dr. W. Liu. The manuscript was mainly written by Dr. J. Schneekönig. Additionally, I performed control experiments under deuterium atmosphere, carried out scale-up reactions, and took part in the writing of the manuscript and the supporting information. My own contribution amounts to approximately 30%.

# Application of Crabtree/Pfaltz-Type Iridium Complexes for the Catalyzed Asymmetric Hydrogenation of an Agrochemical Building Block

Jacob Schneekönig,<sup>||</sup> Weiping Liu,<sup>||</sup> Thomas Leischner,<sup>||</sup> Kathrin Junge, Christoph Schotes, Christian Beier, and Matthias Beller\*<sup>||</sup>

**Cite This:** *Org. Process Res. Dev.* 2020, 24, 443–447

**Read Online**

ACCESS |

Metrics & More

Article Recommendations

Supporting Information

**ABSTRACT:** Herein we report improved chemo- and enantioselective hydrogenations of 1-(2,2,4-trimethylquinolin-1(2*H*)-yl)ethan-1-one (**1**) toward (*R*)-1-(2,2,4-trimethyl-3,4-dihydroquinolin-1(2*H*)-yl)ethan-1-one (**2**) using well-defined novel Crabtree-type iridium complexes.

**KEYWORDS:** asymmetric hydrogenation, alkene reduction, catalyst design, iridium catalysis, unactivated olefins, *N*-heterocycles

Aminoindanes are important building blocks for the synthesis of aminoindane amides (Scheme 1), which

## Scheme 1. Selected Example of the Synthesis of an Aminoindane Amide Fungicide<sup>4</sup>

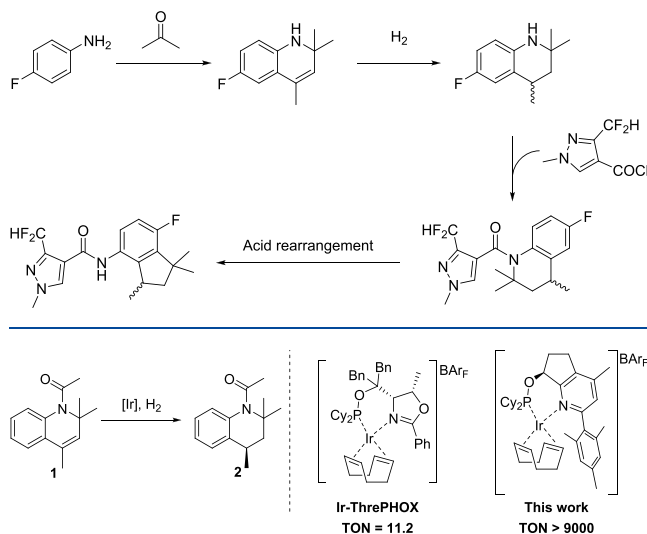


**Figure 1.** Crabtree/Pfaltz-type iridium complexes for the desired transformation.

were disclosed to be active compounds for the control of phytopathogenic fungi.<sup>1</sup> The first protocols for the preparation of this class of compounds were reported in 1985 by the Sumitomo Chemical Company.<sup>2</sup> Since then, the majority of commercially available fungicides of this type have been used as racemic mixtures. Since the individual enantiomers usually exhibit different performances, an enantioselective synthesis is highly desirable for efficiency and sustainability. Thus, the first attempts to isolate enantiomerically pure building blocks used crystallization of diastereomeric salts with *D*-tartaric acid.<sup>3</sup>

However, the asymmetric hydrogenation of 1-(2,2,4-trimethylquinolin-1(2*H*)-yl)ethan-1-one would represent a much more elegant solution, as it offers advantageous features such as excellent atom economy and quantitative yields as well as high levels of stereoselectivity. Following this approach, a selective hydrogenation of the nonfunctionalized trisubstituted alkene moiety has to be achieved. The selective hydrogenation of such types of double bonds is still challenging, and the best results are typically obtained using chiral Crabtree/Pfaltz-type iridium complexes.<sup>5</sup> Previously, it was discovered that replacing the established hexafluorophosphate anion with the weakly coordinating  $\text{BAR}_F^-$  anion not only enabled the use of catalyst loadings lower than 1 mol % but also provided a catalytic system that is less sensitive to moisture.<sup>6</sup> Impressive examples of asymmetric hydrogenation using these complexes were the hydrogenation of  $\gamma$ -tocotrienyl acetate<sup>7</sup> and the total synthesis of demethyl methoxycalamenene.<sup>8</sup> Unfortunately, utilizing a 1.25 mol % loading of the commercially available complex  $[\text{Ir}(\text{COD})\text{ThrePHOX}]\text{BAR}_F$  for the asymmetric hydrogenation of **1** to **2** resulted only in 14% conversion and low enantioselectivity (31% *ee*) (Figure 1).<sup>9</sup> Clearly, from an industrial point of view neither the activity nor the selectivity is suitable for any application. In order to justify the use of an expensive iridium precursor, a lower catalyst loading and a higher selectivity have to be achieved.

Here we report a state-of-the-art process for this transformation that allows for the first time a practical and industrially feasible synthesis of **2** and related building blocks via asymmetric hydrogenation.

**Received:** October 28, 2019

**Published:** February 20, 2020





## RESULTS AND DISCUSSION

A preliminary catalyst screening using commercially available and tailor-made iridium complexes revealed complex **5a** as a

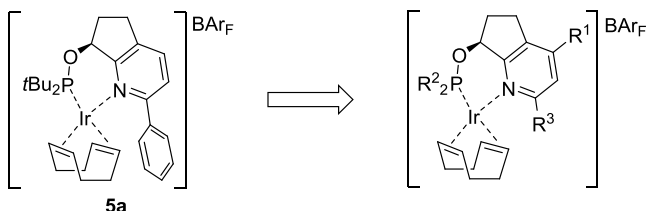


Figure 2. Benchmark catalyst for the hydrogenation of **1**.

benchmark catalyst (Figure 2).<sup>10</sup> Notably, this type of complex was originally introduced by Pfaltz and co-workers for asymmetric hydrogenation of olefins and furan derivatives.<sup>11</sup>

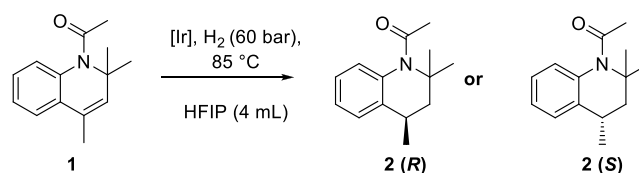
Initially, we investigated the influence of different substituents of **5a** (indicated by the R groups in Figure 2). Following the protocol reported by Pfaltz and co-workers, we started synthesizing chiral pyridyl alcohols using the building blocks (*R*)-7-((*tert*-butyldimethylsilyloxy)-2-chloro-6,7-dihydro-5*H*-cyclopenta[*b*]pyridine) (**3a**) and (*S*)-7-((*tert*-butyldimethylsilyloxy)-2-chloro-4-methyl-6,7-dihydro-5*H*-cyclopenta[*b*]pyridine) (**3b**) (Scheme 2).<sup>12</sup> Eighteen different pyridyl alcohols (**4a–r**) were obtained overall in moderate to good yields from the Suzuki reaction of **3a** or **3b** with the corresponding boronic acids followed by deprotection of the silyl ether.

For the majority of the boronic acids, [1,3-bis(2,6-diisopropylphenyl)-4,5-dihydroimidazol-2-ylidene](chloro)(3-phenylallyl)palladium(II) (CX 32) was found to be a suitable precatalyst for the coupling step. However, for highly bulky boronic acids, higher temperatures and longer reaction times (for **4m**, **4n**, and **4r**) or even other palladium precursors ((*dppf*)PdCl<sub>2</sub>·DCM for **4o** or Pd(PPh<sub>3</sub>)<sub>4</sub> for **4q**) were necessary in order to obtain decent product yields. Next, these pyridyl alcohols were used to synthesize 22 different bench-stable iridium precatalysts via the corresponding phosphonites (Scheme 3).

We then investigated the effect of the different precatalysts in the benchmark hydrogenation of **1** (60 bar H<sub>2</sub>, 85 °C, 6–40 h, HFIP, 0.1–0.01 mol % Ir). In order to get a fast insight into the catalytic behavior of the precatalysts and to avoid single hydrogenation reactions, all of the experiments were performed in a 6-fold parallel manner (see the Supporting Information). To our delight, in this “1st generation” screening a positive influence on the reaction outcome was obtained by replacing the proton at the 4-position of the pyridine moiety (R<sup>1</sup>) with a methyl group (**5a** vs **5b**; Table 1, entries 2 and 3). This observation was also confirmed by later examples (**5d** vs **5f** and **5l** vs **5s**; Table 1, entries 6, 8, 15, and 22). Next, a set of complexes were synthesized in order to elucidate the influence of the R<sup>2</sup> groups on the phosphorus atom (Scheme 3, “2nd generation”). Since aryl-substituted phosphonites showed poor activity, we focused on alkyl phosphonites. Gratifyingly, when the *tert*-butyl groups on the phosphorus atom were replaced with cyclohexyl groups, increased activity and high enantioselectivity were observed (**5b** vs **5f**; Table 1, entries 4 and 8) at a low catalyst loading (0.05 mol %). This result is in contrast to previous work by Pfaltz and co-workers using similar types of ligands for the hydrogenation of (*E*)-2-(4-methoxyphenyl)-2-butene. In their work, usually the *tert*-butyl-substituted complexes gave significantly higher

enantioselectivities than the cyclohexyl-substituted ones.<sup>11a</sup> Inspired by the work of Woodmansee et al.,<sup>11b</sup> we synthesized other complexes with less sterically demanding alkyl groups on the phosphorus atom.<sup>13</sup> However, the resulting complexes were less active and also less selective than **5f** (**5e**, **5g**, and **5h**; Table 1, entries 7, 9, and 10).

Table 1. Results for Hydrogenation of **1**<sup>a,b</sup>

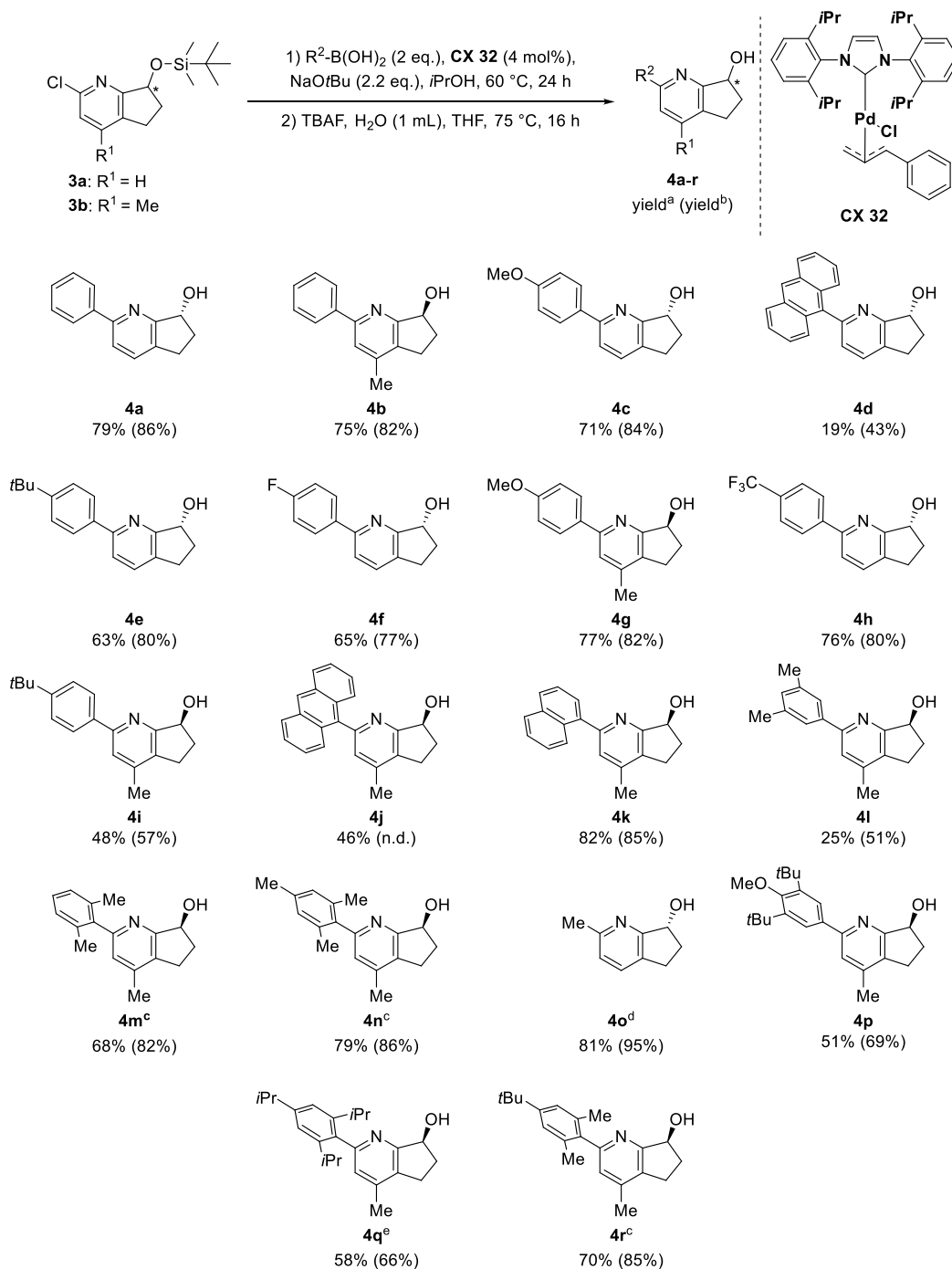


entry	complex	time [h]	loading [mol %]	conv. [%]	TON	ee [%]
1	<b>5a</b>	16	0.1	99.2	992	98.0 (R)
2	<b>5a</b>	6	0.1	81.5	815	97.5 (R)
3	<b>5b</b>	6	0.1	94.5	945	97.5 (R)
4	<b>5b</b>	16.5	0.05	86.8	1736	97.6 (R)
5	<b>5c</b>	6	0.1	91.2	912	97.0 (R)
6	<b>5d</b>	16.5	0.05	88.2	1764	97.6 (S)
7	<b>5e</b>	16	0.1	30	300	90.0 (S)
8	<b>5f</b>	16.5	0.05	94.4	1888	97.3 (R)
9	<b>5g</b>	6	0.1	76.0	760	96.0 (R)
10	<b>5h</b>	16.5	0.05	87.9	1758	95.8 (R)
11	<b>5i</b>	16.5	0.05	98.4	1968	96.8 (S)
12	<b>5i</b>	16	0.025	67.2	2688	97.3 (S)
13	<b>5j</b>	16.5	0.05	34.6	692	83.2 (S)
14	<b>5k</b>	16.5	0.05	64.7	1294	92.4 (S)
15	<b>5l</b>	16.5	0.05	98.9	1978	95.8 (S)
16	<b>5l</b>	16	0.025	79.5	3180	97.5 (S)
17	<b>5n</b>	16.5	0.05	92.4	1848	96.9 (R)
18	<b>5o</b>	16	0.025	91.6	3664	97.3 (R)
19	<b>5p</b>	16	0.025	42.2	1688	94.5 (R)
20	<b>5q</b>	16	0.025	81.7	3268	97.9 (R)
21	<b>5r</b>	16	0.025	98.0	3920	98.1 (R)
22	<b>5s</b>	16	0.025	94.1	3764	97.5 (R)
23	<b>5m</b>	16	0.025	7.2	288	70.8 (S)
24	<b>5t</b>	16	0.025	60.0	2400	92.1 (R)
25	<b>5u</b>	16	0.025	74.0	2960	98.0 (R)
26	<b>5v</b>	16	0.025	97.5	390	97.3 (R)
27 <sup>c</sup>	<b>5r</b>	40	0.01	93.9	9390	98.0 (R)
28 <sup>d</sup>	<b>5r</b>	40	0.01	93.4	9340	97.6 (R)

<sup>a</sup>In general, only the lowest tested catalyst loading for each complex is presented. <sup>b</sup>Standard reaction conditions: **1** (3 mmol), [Ir], HFIP (4 mL), H<sub>2</sub> (60 bar), 85 °C. <sup>c</sup>12 mmol scale, 16 mL of HFIP. <sup>d</sup>25 mmol scale, 33 mL of HFIP.

From the evaluation of complexes **5i–v** in the benchmark reaction (Scheme 3, “3rd generation”), some interesting trends were found. An electron-withdrawing group, such as fluoro or trifluoromethyl, at the para position of the phenyl moiety lowered the activity as well as the selectivity dramatically (**5j** and **5k** vs **5d**; Table 1, entries 6, 13, and 14). Interestingly, previous work by Zhou’s group did not show a similar trend in activity.<sup>14</sup> Replacing the phenyl group at the 2-position of **5d** with an anthracenyl group led to a more active catalyst (**5l**), which gave nearly full conversion at a 0.05 mol % catalyst loading and still good conversion of 79.5% when a 0.025 mol % loading was used. The naphthyl-substituted analogue **5n**, however, was slightly less active than its phenyl-substituted counterpart **5f** (Table 1, entries 8 and 17). As expected, **5s** was more active than **5l**, giving

Scheme 2. Synthesis of Chiral Pyridyl Alcohols



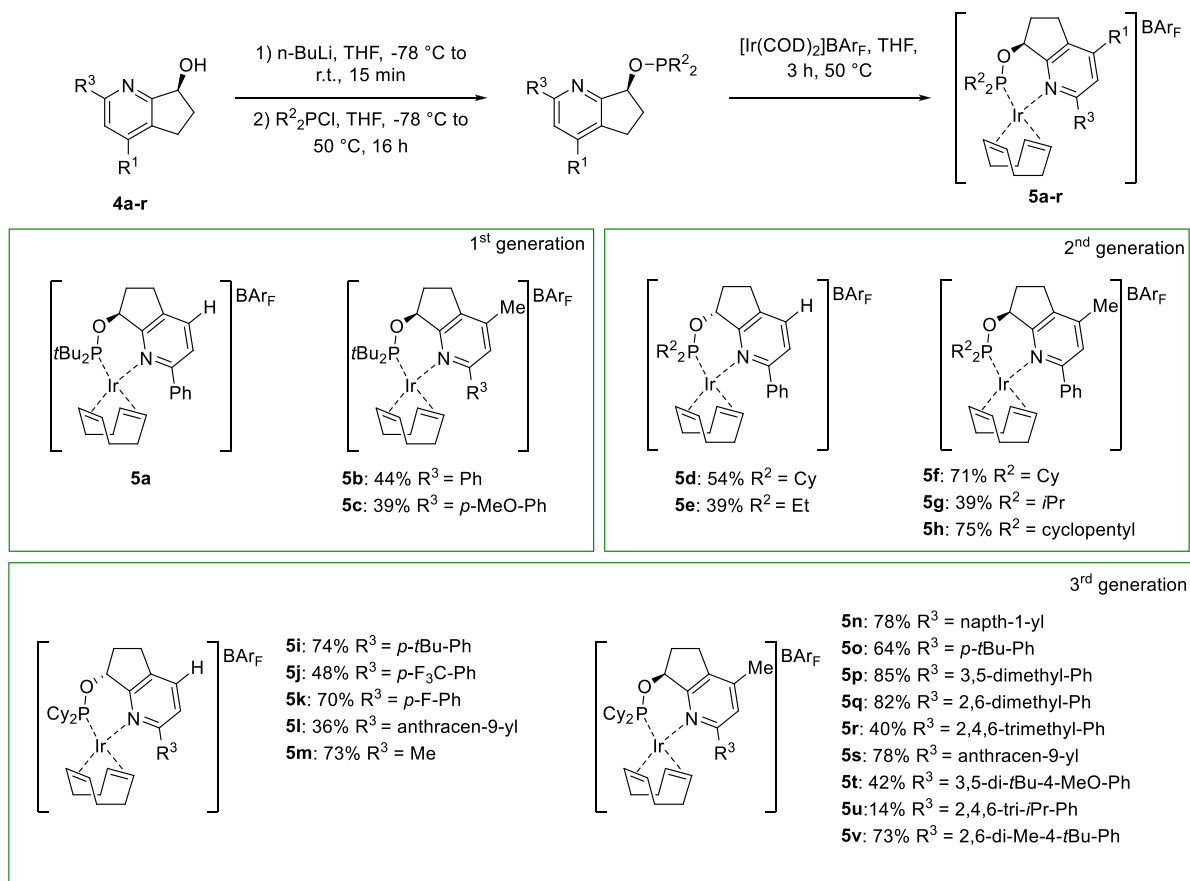
<sup>a</sup>Isolated yield over two steps. <sup>b</sup>Isolated yield of the Suzuki reaction. <sup>c</sup>**3b** (2 mmol), boronic acid (2.3 mmol), **CX 32** (2 mol %), NaOH, *i*PrOH, H<sub>2</sub>O, 115 °C, 48 h. <sup>d</sup>**3a** (2 mmol), trimethylboroxine (1.5 equiv), (dppf)PdCl<sub>2</sub>·DCM (5 mol %), K<sub>2</sub>CO<sub>3</sub> (3 equiv), 1,4-dioxane, 120 °C, 20 h. <sup>e</sup>**3b** (1 mmol), (2,4,6-triisopropylphenyl)boronic acid (1.2 equiv), Pd(PPh<sub>3</sub>)<sub>4</sub> (15 mol %), K<sub>3</sub>PO<sub>4</sub> (5.0 equiv), H<sub>2</sub>O (1.0 mL), DME (5.0 mL), 110 °C, 24 h.

a very good conversion of 94.1% at a 0.025 mol % catalyst loading (Table 1, entry 22). While the methoxy-substituted complex **5c** was less active than **5b** (Table 1, entries 3 and 5), the *p*-*tert*-butyl-substituted derivative **5o** was more active than **5f**, providing the product in 91.4% yield (Table 1, entry 18). Encouraged by the results achieved with **5o**, we synthesized the complexes **5p–r** using the corresponding commercially available boronic acids. While **5p** and **5q** exhibited lower performance than **5o** (Table 1, entries 19 and 20), **5r** gave 98%

conversion at a 0.025 mol % catalyst loading (Table 1, entry 21). Further increasing the steric demand of the ligand led to either a less active catalytic system (**5u**; Table 1, entry 25) or an equally active catalytic system (**5v**; Table 1, entry 26). The motif in complex **5t**, which was used before by Pfaltz' group,<sup>11b</sup> gave only poor results for the desired reaction. As **5r** gave a higher yield and selectivity compared with **5v**, we continued working with this complex. Notably, using only a 0.01 mol % loading of **5r** was sufficient to give a 93.9% yield of the product with an *ee* of 98%



Scheme 3. Synthesis of Iridium Precatalysts



(R). Furthermore, this reaction was successfully scaled up to 25 mmol, yielding **2** in 93.4% yield with an excellent enantioselectivity of 97.6% *ee*.

## CONCLUSION

We synthesized and tested 22 different chiral iridium complexes for the hydrogenation of **1** to **2**, which is of general interest for the preparation of novel agrochemicals. In the presence of the optimal iridium catalyst **5r**, this transformation proceeds with high efficiency (turnover number (TON) > 9300) and excellent enantioselectivity (up to 98% *ee*), allowing industrially viable catalyst loadings to be achieved.

## EXPERIMENTAL PROCEDURES

**General Experimental Procedure.** The Ir complex (catalyst loading given) and the substrate (3 mmol) were placed in an 8 mL autoclave vial containing a PTFE-coated stirring bar. The autoclave vial was closed using a screw cap with a septum, placed in a fitted metal plate, connected to a Schlenk line, and subsequently flushed with argon (10 min). HFIP (4 mL) was added to the vial via the septum. The vial was placed in an argon-containing autoclave, and the autoclave was flushed with argon (10 min). The autoclave was pressurized with hydrogen gas (10 bar) and subsequently depressurized to atmospheric pressure three times. After this, the autoclave was pressurized to a hydrogen pressure of 60 bar and placed in a suitable alumina block. After heating to  $85\text{ }^\circ\text{C}$  ( $\sim 4\text{ }^\circ\text{C}/\text{min}$ ; 15 min), the reaction mixture was kept at this temperature for the given time. The autoclave was placed in an ice bath to allow fast cooling to room temperature. After depressurization, the vial

was taken out of the autoclave, and the reaction outcome was determined by GC-FID analysis (diluted with EtOH) and the enantiomeric excess by HPLC analysis.

**General Procedure for the 12 mmol Scale-Up Experiment.** Complex **5r** (0.01 mol %) and the substrate (12 mmol) were placed in a 25 mL autoclave containing a PTFE-coated stirring bar and dissolved in HFIP (16 mL). The autoclave was closed, flushed with Ar for 10 min, and subsequently pressurized with hydrogen gas (10 bar) and depressurized to atmospheric pressure three times. After this, the autoclave was pressurized to a hydrogen pressure of 60 bar and placed in a suitable alumina block. After heating to  $85\text{ }^\circ\text{C}$  ( $\sim 4\text{ }^\circ\text{C}/\text{min}$ ; 15 min), the reaction mixture was kept at this temperature for the given time. The autoclave was placed in an ice bath to allow fast cooling to room temperature. After depressurization, the reaction outcome was determined by GC-FID analysis (diluted with EtOH) and the enantiomeric excess by HPLC analysis.

**General Procedure for Scale-Up Experiment (25 mmol).** Complex **5r** (0.01 mol %) and the substrate (25 mmol) were placed in a 50 mL autoclave containing a PTFE-coated stirring bar and dissolved in HFIP (33 mL). The autoclave was closed, flushed with Ar for 10 min, and subsequently pressurized with hydrogen gas (10 bar) and depressurized to atmospheric pressure three times. After this, the autoclave was pressurized to a hydrogen pressure of 60 bar and placed in a suitable alumina block. After heating to  $85\text{ }^\circ\text{C}$  ( $\sim 4\text{ }^\circ\text{C}/\text{min}$ ; 15 min), the reaction mixture was kept at this temperature for the given time. The autoclave was placed in an ice bath to allow fast cooling to room temperature. After depressurization, the reaction outcome was determined by GC-

FID analysis (diluted with EtOH) and the enantiomeric excess by HPLC analysis.

## ■ ASSOCIATED CONTENT

### SI Supporting Information

The Supporting Information is available free of charge at <https://pubs.acs.org/doi/10.1021/acs.oprd.9b00466>.

Synthetic procedures; NMR data for TBS-protected pyridyl alcohols, deprotected pyridyl alcohols, and synthesized Ir complexes; HRMS data for the synthesized Ir complexes; results of deuterium experiments; experimental procedures for catalytic tests (PDF)

## ■ AUTHOR INFORMATION

### Corresponding Author

Matthias Beller – Leibniz-Institut für Katalyse e. V, 18059 Rostock, Germany; [orcid.org/0000-0001-5709-0965](https://orcid.org/0000-0001-5709-0965);  
Email: [matthias.beller@catalysis.de](mailto:matthias.beller@catalysis.de)

### Authors

Jacob Schneekönig – Leibniz-Institut für Katalyse e. V, 18059 Rostock, Germany

Weiping Liu – Leibniz-Institut für Katalyse e. V, 18059 Rostock, Germany; College of Chemistry, Chemical Engineering and Biotechnology, Donghua University, Shanghai 201620, China; [orcid.org/0000-0002-1064-7276](https://orcid.org/0000-0002-1064-7276)

Thomas Leischner – Leibniz-Institut für Katalyse e. V, 18059 Rostock, Germany

Kathrin Junge – Leibniz-Institut für Katalyse e. V, 18059 Rostock, Germany; [orcid.org/0000-0001-7044-8888](https://orcid.org/0000-0001-7044-8888)

Christoph Schotes – Product Supply—Active Ingredient Manufacturing Innovation, CropScience Division, Bayer AG, 41539 Dormagen, Germany

Christian Beier – Product Supply—Active Ingredient Manufacturing Innovation, CropScience Division, Bayer AG, 41539 Dormagen, Germany

Complete contact information is available at: <https://pubs.acs.org/doi/10.1021/acs.oprd.9b00466>

### Author Contributions

<sup>†</sup>J.S., W.L., and T.L. contributed equally.

### Funding

This work was supported by Bayer AG, the State of Mecklenburg-Vorpommern, and the BMBF, Germany.

### Notes

The authors declare no competing financial interest.

## ■ ACKNOWLEDGMENTS

We thank the analytical team of LIKAT for their kind support. We especially thank Dr. Wolfgang Baumann for NMR measurements and detailed interpretation of analytical data.

## ■ ABBREVIATIONS

HFIP = 1,1,1,3,3,3-hexafluoropropan-2-ol; BAr<sub>F</sub> = tetrakis[3,5-bis(trifluoromethyl)phenyl]borate

## ■ REFERENCES

(1) (a) Venturini, I.; Vazzola, M. S.; Pellacini, F.; Filippini, L. Aminoindanes Amides Having a High Fungicidal Activity and Their Phytosanitary Compositions. WO 2012/084812 A1, 2012. (b) Swart, G. M.; Oostendorp, M. Fungicidal Compositions. WO 2015/049168 A1, 2015. (c) Kiguchi, S. Synergistic Fungicidal Composition for

Controlling Plant Diseases. WO 2017/155088 A1. (d) Montagne, C.; Hildebrand, S.; Es-Sayed, M.; Görtz, A.; Wachendorf-Neumann, U. Active Compound Combinations. WO 2018/108977 A1, 2018.

(2) Nishida, S.; Ohsumi, T.; Tsushima, K.; Matsuo, N.; Maeda, K.; Inoue, S.; Bourgognon, J.-M. Pyrazolecarboxamide Derivatives, Process for Their Preparation, and Bactericides Containing Them as Effective Ingredients. WO 1986/002641 A1, 1986.

(3) Matsunaga, T.; Hiraguri, N.; Takahashi, T.; Inui, T.; Tanimoto, M.; Nakayama, T. Method for Producing (R)-1,1,3-Trimethyl-4-aminoindane. WO 2015/118793 A1, 2015.

(4) This reaction scheme is analogous to the one presented by Bellandi et al.: Bellandi, P.; Zanardi, G.; Datar, R. V.; Devarajan, C.; Murali, S.; Swamy, N. Process for the Preparation of 4-Aminoindane Derivates and Related Aminoindane Amides. WO 2017/178868 A1, 2017.

(5) For excellent reviews about the development of Crabtree-type iridium complexes for the hydrogenation of alkenes, see: (a) Woodmansee, D. H.; Pfaltz, A. Asymmetric hydrogenation of alkenes lacking coordinating groups. *Chem. Commun.* **2011**, 47, 7912–7916. (b) Verendel, J. J.; Pàmies, O.; Diéguez, M.; Andersson, P. G. Asymmetric Hydrogenation of Olefins Using Chiral Crabtree-type Catalysts: Scope and Limitations. *Chem. Rev.* **2014**, 114, 2130–2169. (c) Margarita, C.; Andersson, P. G. Evolution and Prospects of the Asymmetric Hydrogenation of Unfunctionalized Olefins. *J. Am. Chem. Soc.* **2017**, 139, 1346–1356.

(6) (a) Lightfoot, A.; Schnider, P.; Pfaltz, A. Enantioselective Hydrogenation of Olefins with Iridium – Phosphanodihydrooxazole Catalysts. *Angew. Chem., Int. Ed.* **1998**, 37, 2897–2899. (b) Smidt, S. P.; Zimmermann, N.; Studer, M.; Pfaltz, A. Enantioselective Hydrogenation of Alkenes with Iridium-PHOX Catalysts: A Kinetic Study of Anion Effects. *Chem. - Eur. J.* **2004**, 10, 4685–4693.

(7) Bell, S.; Wüstenberg, B.; Kaiser, S.; Menges, F.; Netscher, T.; Pfaltz, A. Asymmetric Hydrogenation of Unfunctionalized, Purely Alkyl-Substituted Olefins. *Science* **2006**, 311, 642–644.

(8) Schrems, M. G.; Pfaltz, A. NeoPHOX—an easily accessible P,N-ligand for iridium-catalyzed asymmetric hydrogenation: preparation, scope and application in the synthesis of demethyl methoxycalamene. *Chem. Commun.* **2009**, 6210–6212.

(9) Takashi, T.; Ujita, S.; Method for Manufacturing Optically Active Compound. WO 2015/141564 A1, 2015.

(10) This screening was performed as part of cooperation between Solvias AG and Bayer AG.

(11) (a) Kaiser, S.; Smidt, S. P.; Pfaltz, A. Iridium Catalysts with Bicyclic Pyridine–Phosphinite Ligands: Asymmetric Hydrogenation of Olefins and Furan Derivatives. *Angew. Chem., Int. Ed.* **2006**, 45, 5194–5197. (b) Woodmansee, D. H.; Müller, M.-A.; Neuburger, M.; Pfaltz, A. Chiral pyridyl phosphinites with large aryl substituents as efficient ligands for the asymmetric iridium-catalyzed hydrogenation of difficult substrates. *Chem. Sci.* **2010**, 1, 72–78.

(12) **3a** and **3b** were provided by Bayer AG.

(13) Tolman, C. A. Steric Effects of Phosphorus Ligands in Organometallic Chemistry and Homogeneous Catalysis. *Chem. Rev.* **1977**, 77, 313–348.

(14) Liu, Q.-B.; Yu, C.-B.; Zhou, Y.-G. Synthesis of tunable phosphinite–pyridine ligands and their applications in asymmetric hydrogenation. *Tetrahedron Lett.* **2006**, 47, 4733–4736.

## 6.5 A General Regioselective Synthesis of Alcohols by Cobalt Catalyzed Hydrogenation of Epoxides

W. Liu, T. Leischner, W. Li, K. Junge, M. Beller

*Angew. Chem. Int. Ed.* **2020**, *132*, 11417–11420.

In this publication, I mainly participated in the realization of the substrate scope. I synthesized a number of substrates, carried out all the control experiments and was involved in the writing of the manuscript as well as the supporting information. My own contribution amounts to approximately 40%.

## Homogeneous Catalysis

## A General Regioselective Synthesis of Alcohols by Cobalt-Catalyzed Hydrogenation of Epoxides

Weiping Liu<sup>+</sup>, Thomas Leischner<sup>+</sup>, Wu Li, Kathrin Junge, and Matthias Beller<sup>\*</sup>

**Abstract:** A straightforward methodology for the synthesis of anti-Markovnikov-type alcohols is presented. By using a specific cobalt triphos complex in the presence of Zn(OTf)<sub>2</sub> as an additive, the hydrogenation of epoxides proceeds with high yields and selectivities. The described protocol shows a broad substrate scope, including multi-substituted internal and terminal epoxides, as well as a good functional-group tolerance. Various natural-product derivatives, including steroids, terpenoids, and sesquiterpenoids, gave access to the corresponding alcohols in moderate-to-excellent yields.

Alcohols are a class of important organic compounds that are ubiquitous in bulk and fine chemicals, as well as in natural products.<sup>[1]</sup> Among the numerous established procedures for the synthesis of alcohols, the classic hydroboration/oxidation protocol still prevails on a laboratory scale (Figure 1 A). Advantageously, this methodology allows for a formal anti-Markovnikov functionalization of linear alcohols from olefins, however, stoichiometric amounts of borane agents have to be employed.<sup>[2]</sup> To overcome this problem, various catalytic approaches to provide similar products have been developed. For example, a formal anti-Markovnikov hydration of mono-substituted styrenes by triple-relay catalysis was demonstrated by Grubbs and co-workers.<sup>[3]</sup> More recently, Lei and co-workers established a visible-light-mediated anti-Markovnikov hydration of water to olefins, by using a photoredox catalyst in combination with a redox-active hydrogen-atom donor.<sup>[4]</sup> Additionally, the Arnold group realized a regioselective redox hydration of styrenes catalyzed by a metal-oxo enzyme.<sup>[5]</sup>

Conceptually, the selective hydrogenation of epoxides, which are readily available from alkenes by a one-step oxidation using peroxyacids or hydrogen peroxide,<sup>[6]</sup> offers an

attractive alternative (Figure 1 B).<sup>[7]</sup> Heterogeneous catalysts such as Pd/C generally facilitate this transformation, but are limited to aryl epoxides, whereas Markovnikov-type alcohols are formed as the major products in the case of alkyl epoxides.<sup>[8]</sup> On the contrary, homogeneous catalysts have been scarcely investigated for this task. Until very recently, the only known examples featured rhodium- and ruthenium-based systems and suffered from poor product selectivities.<sup>[9]</sup>

In 2019, Gansäuer, Norton, and co-workers disclosed an elegant strategy that used cooperative catalysis to give linear alcohols by combining titanocene-mediated<sup>[10]</sup> epoxide opening with chromium-catalyzed hydrogen activation and radical reduction (Figure 1 C).<sup>[11]</sup> Independently, our group developed the first non-noble-metal-catalyzed hydrogenation of terminal epoxides to give primary alcohols. Using a combination of Fe(BF<sub>4</sub>)<sub>2</sub>·6H<sub>2</sub>O and *tris*(2-(diphenylphosphanyl)phenyl)phosphane (tetraphos) the desired products are obtained in high yields and selectivities.<sup>[12]</sup> However, a drawback of this procedure was that only terminal epoxides were suitable

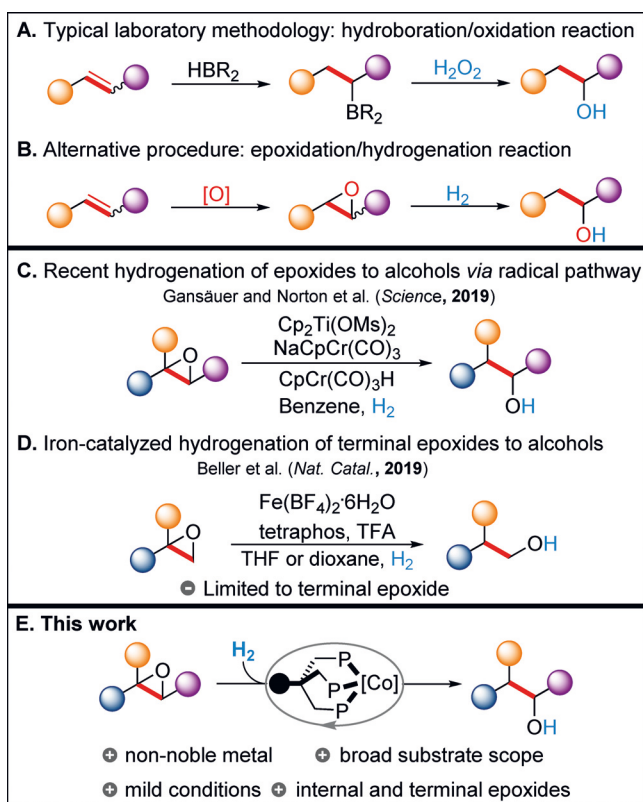


**Figure 1.** Synthesis of alcohols from olefins and hydrogenation of epoxides to alcohols.

[\*] Dr. W. Liu<sup>[†]</sup>

College of Chemistry, Chemical Engineering and Biotechnology  
Donghua University  
201620, Shanghai (P. R. China)

Dr. W. Liu,<sup>[†]</sup> T. Leischner,<sup>[†]</sup> Dr. W. Li, Dr. K. Junge, Prof. Dr. M. Beller  
Leibniz-Institut für Katalyse e.V.  
Albert-Einstein-Straße 29a, 18059 Rostock (Germany)  
E-mail: matthias.beller@catalysis.de

[†] These authors contributed equally to this work.

Supporting information and the ORCID identification number(s) for the author(s) of this article can be found under:  
<https://doi.org/10.1002/anie.202002844>.

© 2020 The Authors. Published by Wiley-VCH Verlag GmbH & Co. KGaA. This is an open access article under the terms of the Creative Commons Attribution Non-Commercial License, which permits use, distribution and reproduction in any medium, provided the original work is properly cited, and is not used for commercial purposes.

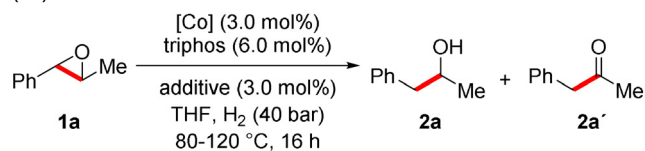


substrates and internal epoxides did not undergo hydrogenation to provide secondary alcohols (Figure 1D).

Herein, we describe a general and efficient non-noble-metal catalyst system<sup>[13]</sup> to enable selective hydrogenation<sup>[14]</sup> of both internal and terminal epoxides to the corresponding alcohols under mild conditions (Figure 1E).

Based on our former studies, we explored the hydrogenation of 2-methyl-3-phenyloxirane (**1a**) as a benchmark substrate. As expected, the previous Fe(BF<sub>4</sub>)<sub>2</sub>/tetraphos system gave no significant amount of alcohols. Similarly, in the presence of related multidentate phosphines, for example, 1,1,1-tris(diphenyl-phosphinomethyl)ethane (triphos), no desired product formation occurred. Moreover, well-known molecularly defined noble-metal complexes [Ru(acac)<sub>3</sub>/triphos]<sup>[15]</sup> and [Rh(PPh<sub>3</sub>)<sub>3</sub>Cl] also failed to furnish the desired product under otherwise identical reaction conditions (for experimental details, see the Supporting Information). Interestingly, applying the combination of Co(BF<sub>4</sub>)<sub>2</sub>·6H<sub>2</sub>O and tetraphos in the presence of HNTf<sub>2</sub> resulted in formation of the desired anti-Markovnikov-type product 1-phenylpropan-2-ol (**2a**), albeit in a low yield (17%), with 1-phenylpropan-2-one (**2a'**) produced as a side product (for experimental details, see the Supporting Information). When triphos was tested as the ligand, a slight increase in activity was observed (Table 1, entry 1). Changing the catalyst precursor to Co(NTf<sub>2</sub>)<sub>2</sub> further improved the observed yield (Table 1, entry 2); however, when the reaction temperature was decreased (to 100 °C), the hydrogenation process almost completely stopped and only minor amounts of **2a** could be detected (Table 1, entry 3). Notably, the addition of catalytic amounts of Zn(OTf)<sub>2</sub> (3.0 mol%) significantly improved catalyst activity, even at a lower temperature (80 °C) (Table 1, entries 4 and 5).

**Table 1:** Optimization of Cobalt-catalyzed hydrogenation of epoxide (**1a**).<sup>[a]</sup>



Entry	Catalyst	Additive	T [°C]	<b>2a</b> [%] <sup>[b]</sup>
1 <sup>[c]</sup>	Co(BF <sub>4</sub> ) <sub>2</sub> ·6H <sub>2</sub> O	HNTf <sub>2</sub>	120	23
2 <sup>[c]</sup>	Co(NTf <sub>2</sub> ) <sub>2</sub>	–	120	43
3	Co(NTf <sub>2</sub> ) <sub>2</sub>	–	100	< 10
4	Co(NTf <sub>2</sub> ) <sub>2</sub>	Zn(OTf) <sub>2</sub>	100	74
5	Co(NTf <sub>2</sub> ) <sub>2</sub>	Zn(OTf) <sub>2</sub>	80	80
6	Co(NTf <sub>2</sub> ) <sub>2</sub>	In(OTf) <sub>3</sub>	80	74
7	Co(NTf <sub>2</sub> ) <sub>2</sub>	Al(OTf) <sub>3</sub>	80	< 10
8	Co(NTf <sub>2</sub> ) <sub>2</sub>	Fe(OTf) <sub>2</sub>	80	18
9	–	Zn(OTf) <sub>2</sub>	80	–
10 <sup>[d]</sup>	Co(NTf <sub>2</sub> ) <sub>2</sub>	Zn(OTf) <sub>2</sub>	80	–
11 <sup>[e]</sup>	Co(NTf <sub>2</sub> ) <sub>2</sub>	Zn(OTf) <sub>2</sub>	80	85
12 <sup>[e]</sup>	Co(BF <sub>4</sub> ) <sub>2</sub> ·6H <sub>2</sub> O	Zn(OTf) <sub>2</sub>	80	80
13 <sup>[e]</sup>	Co(ClO <sub>4</sub> ) <sub>2</sub> ·6H <sub>2</sub> O	Zn(OTf) <sub>2</sub>	80	73

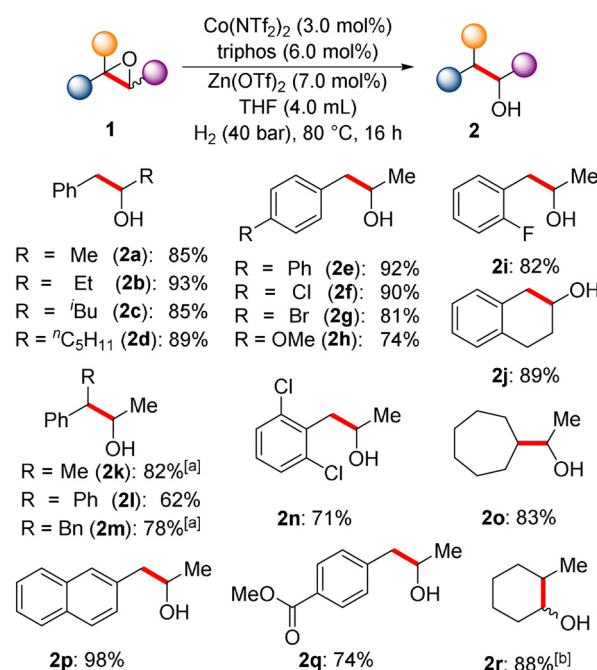
[a] Reaction conditions: **1a** (0.5 mmol), [Co] (3.0 mol%), triphos (6.0 mol%), additive (3.0 mol%), THF (4 mL), 16 h, yields were determined by GC analysis with *n*-hexadecane as an internal standard.

[b] 1-Phenylpropan-2-one **2a'** is the main side product. [c] triphos (3.0 mol%). [d] Without triphos. [e] Zn(OTf)<sub>2</sub> (7.0 mol%).

Other Lewis acids, such as In(OTf)<sub>3</sub>, Al(OTf)<sub>3</sub>, and Fe(OTf)<sub>2</sub>, provided inferior results (Table 1, entries 6–8). Control experiments indicated that the synergistic combination of triphos and cobalt precursor is crucial for the epoxide hydrogenation process (Table 1, entries 9 and 10). Increasing the amount of additive further improved the obtained yield of **2a** to 85% (Table 1, entry 11). In general, other cobalt precursors could be applied in this benchmark process, but resulted in slightly lower catalyst activities (Table 1, entries 12 and 13). It should be noted that standard heterogeneous catalysts, such as PtO<sub>2</sub>, Pd/C, and Raney-Ni, exhibited significantly lower or even no activity, even in the presence of Zn(OTf)<sub>2</sub> (for experimental details, see the Supporting Information).

With the optimized reaction conditions in hand, we tested the suitability of our methodology towards various internal epoxides. As shown in Scheme 1, various di- and tri-substituted internal epoxides were successfully applied and yielded the desired secondary alcohols in good yields and high regioselectivities. All the reactions occurred under relatively mild conditions and importantly, tolerate a variety of valuable substituents and functional groups irrespective of their location at the *ortho*-, *meta*-, or *para*-position. Notably, ester **2q**, which is typically reduced by cobalt/triphos catalysts, remained unaffected under the applied conditions and led to the corresponding alcohol in 74% yield (Scheme 1).<sup>[13a]</sup> In addition, asymmetric dialkyl-substituted internal epoxides **2k**, **2m**, and **2r** were successfully transformed to diastereomeric secondary alcohols.

However, when the tetra-substituted epoxide 2,2,3,3-tetramethyloxirane **1s** (see the Supporting Information) was

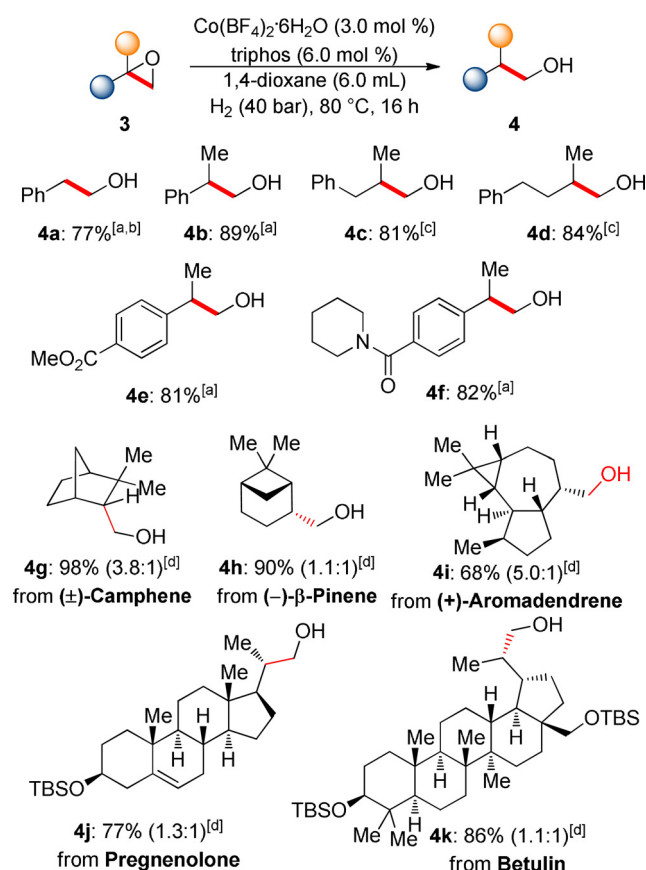


**Scheme 1.** Cobalt-catalyzed hydrogenation of internal epoxides. Reaction condition: **1** (0.5 mmol), Co(NTf<sub>2</sub>)<sub>2</sub> (3.0 mol%), triphos (6.0 mol%), Zn(OTf)<sub>2</sub> (7.0 mol%), THF, 80 °C, 16 h. [a] The diastereoisomer ratio is 1:1.1. [b] Co(BF<sub>4</sub>)<sub>2</sub>·6H<sub>2</sub>O (3.0 mol%), 1,4-dioxane, 60 °C, 20 h, the diastereoisomer ratio (2.8:1) and yield were determined by GC analysis.

applied to our reaction conditions, only the formation of a complex product mixture was observed.

The applied cobalt-based catalyst system is not restricted to the hydrogenation of internal oxiranes. In fact, numerous terminal epoxides, including several natural-product derivatives (steroids, terpenoids, and sesquiterpenoids), were effectively hydrogenated to the linear alcohols with high regioselectivities. Compared to our previously disclosed iron/tetraphos catalyst system, the cobalt/triphos catalyst demonstrated a wider applicability for such substrates (Scheme 2).<sup>[12]</sup> More specifically, both mono- and di-substituted terminal epoxides were suitable substrates and provided the desired anti-Markovnikov-type alcohols in good yields, tolerating amide, silyloxy, alkene, and ester substituents. Using renewable terpenes, such as ( $\pm$ )-camphene (**3g**), ( $-$ )- $\beta$ -pinene (**3h**), and (+)-aromadendrene (**3i**), which are the main constituents of essential oil, the respective primary alcohols were isolated in high yields and selectivities.

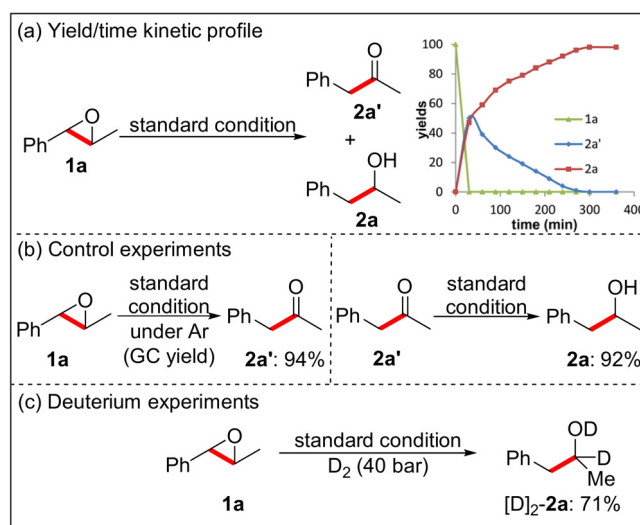
Additionally, the bioactive pentacyclic triterpenoid betulin (**3k**), which is abundant in the bark of birch trees and, moreover, plays an active role in antiviral, analgesic, and antineoplastic agents, also furnished the hydrogenated products in good yields. Similarly, pregnenolone (**3j**), an important steroid, underwent the hydrogenation process smoothly, providing the isolated diastereomeric alcohols in 77% yield.



**Scheme 2.** Cobalt-catalyzed hydrogenation of terminal epoxides. Reaction condition: **3** (0.5 mmol),  $\text{Co}(\text{BF}_4)_2 \cdot 6\text{H}_2\text{O}$  (3.0 mol %), triphos (6.0 mol %), 1,4-dioxane (6 mL), 80 °C, 16 h. [a] THF (4 mL) as solvent. [b] Yields were determined by GC analysis with *n*-hexadecane as an internal standard. [c]  $\text{Co}(\text{NTf}_2)_2$  (3.0 mol %),  $\text{Zn}(\text{OTf})_2$  (7.0 mol %). [d] The major isomers are shown. TBS = *tert*-Butyldimethylsilyl.

To better understand the strong performance of our cobalt/triphos catalyst, a set of mechanistic experiments was performed. Firstly, kinetic studies using the model substrate 2-methyl-3-phenyloxirane (**1a**) were performed. As shown in Scheme 3a, **1a** is quickly isomerized<sup>[16]</sup> to 1-phenylpropan-2-one (**2a'**), followed by subsequent hydrogenation to the desired alcohol **2a**.<sup>[17]</sup> To further prove that **2a'** is indeed a reaction intermediate, a control experiment employing **1a** as the starting material under an argon atmosphere without hydrogen present was conducted. Accordingly, 1-phenylpropan-2-one (**2a'**) was isolated in almost quantitative yield. Next, **2a'** was used as the substrate under the standard reaction conditions, yielding the corresponding hydrogenation product **2a** in 92% yield (Scheme 3b). In agreement with these observations,  $[\text{D}]_2$ -**2a** was obtained as the final product in a deuterium-labelling experiment that applied  $\text{D}_2$  instead of  $\text{H}_2$  (Scheme 3c). Finally, to understand whether the cobalt or zinc salts catalyze the isomerization of epoxides to the corresponding ketones, several control experiments were conducted (Supporting Information). Interestingly, the Meinwald rearrangement of **1a** to **2a'** also proceeded without a co-catalyst; however, addition of  $\text{Zn}(\text{OTf})_2$  improved this reaction step. Based on the obtained results, we propose that the reaction takes place via Meinwald rearrangement of the epoxide to the corresponding carbonyl compound, followed by subsequent cobalt/triphos-catalyzed hydrogenation to the desired anti-Markovnikov alcohols.

In summary, the first cobalt-catalyzed hydrogenation of epoxides for the synthesis of anti-Markovnikov alcohols is reported. The presented methodology is suitable for internal, as well as terminal, epoxides and works smoothly even with multi-substituted derivatives under mild conditions. This novel cascade transformation is well-suited for the reduction of natural-product-derived epoxides, including steroids, terpenoids, and sesquiterpenoids. Mechanistic studies indicate that initially a Meinwald rearrangement of the epoxides to the corresponding ketones/aldehydes takes place followed by cobalt/triphos-catalyzed hydrogenation. In general, this transformation offers an attractive alternative compared to the traditional hydroboration/oxidation protocol of olefins.



**Scheme 3.** Selected mechanistic studies.

## Acknowledgements

We thank the analytic department (LIKAT) for their support, the State of Mecklenburg-Western Pomerania, the Federal State of Germany (BMBF), and the EU (Grant 670986) for financial support.

## Conflict of interest

The authors declare no conflict of interest.

**Keywords:** anti-Markovnikov · cobalt · epoxides · homogeneous catalysis · hydrogenation

- [1] K. Weissermel, H.-J. Arpe, *Industrial organic chemistry*, Wiley, Hoboken, **2008**.
- [2] a) H. C. Brown, G. Zweifel, *J. Am. Chem. Soc.* **1959**, *81*, 247–247; b) K. Burgess, M. J. Ohlmeyer, *Chem. Rev.* **1991**, *91*, 1179–1191; c) J. V. Obligacion, P. J. Chirik, *Nat. Rev. Chem.* **2018**, *2*, 15–34; d) H. Wen, G. Liu, Z. Huang, *Coord. Chem. Rev.* **2019**, *386*, 138–153.
- [3] G. Dong, P. Teo, Z. K. Wickens, R. H. Grubbs, *Science* **2011**, *333*, 1609–1612.
- [4] X. Hu, G. Zhang, F. Bu, A. Lei, *ACS Catal.* **2017**, *7*, 1432–1437.
- [5] S. C. Hammer, G. Kubik, E. Watkins, S. Huang, H. Minges, F. H. Arnold, *Science* **2017**, *358*, 215.
- [6] a) T. Katsuki, K. B. Sharpless, *J. Am. Chem. Soc.* **1980**, *102*, 5974–5976; b) W. Zhang, J. L. Loebach, S. R. Wilson, E. N. Jacobsen, *J. Am. Chem. Soc.* **1990**, *112*, 2801–2803; c) C. A. Denard, M. J. Bartlett, Y. Wang, L. Lu, J. F. Hartwig, H. Zhao, *ACS Catal.* **2015**, *5*, 3817–3822.
- [7] C.-Y. Huang, A. G. Doyle, *Chem. Rev.* **2014**, *114*, 8153–8198.
- [8] a) H. Sajiki, K. Hattori, K. Hirota, *Chem. Commun.* **1999**, 1041–1042; b) S. V. Ley, C. Mitchell, D. Pears, C. Ramarao, J.-Q. Yu, W. Zhou, *Org. Lett.* **2003**, *5*, 4665–4668; c) M. S. Kwon, I. S. Park, J. S. Jang, J. S. Lee, J. Park, *Org. Lett.* **2007**, *9*, 3417–3419; d) E. Thiery, J. Le Bras, J. Muzart, *Eur. J. Org. Chem.* **2009**, 961–985.
- [9] a) I. Mochida, S.-i. Shirahama, H. Fujitsu, K. Takeshita, *Chem. Lett.* **1977**, *6*, 421–422; b) H. Fujitsu, S. Shirahama, E. Matsumura, K. Takeshita, I. Mochida, *J. Org. Chem.* **1981**, *46*, 2287–2290; c) H. Fujitsu, E. Matsumura, S. Shirahama, K. Takeshita, I. Mochida, *J. Chem. Soc. Perkin Trans. 1* **1982**, 855–859; d) M. Ito, M. Hirakawa, A. Osaku, T. Ikariya, *Organometallics* **2003**, *22*, 4190–4192; e) W. W. N. O, A. J. Lough, R. H. Morris, *Chem. Commun.* **2010**, *46*, 8240–8242; f) S. Murru, K. M. Nicholas, R. S. Srivastava, *J. Mol. Catal. A* **2012**, *363–364*, 460–464; g) S. Thiyagarajan, C. Gunanathan, *Org. Lett.* **2019**, *21*, 9774–9778.
- [10] a) A. Gansäuer, C.-A. Fan, F. Piester, *J. Am. Chem. Soc.* **2008**, *130*, 6916–6917; b) A. Gansäuer, M. Klatt, G. M. Brändle, J. Friedrich, *Angew. Chem. Int. Ed.* **2012**, *51*, 8891–8894; *Angew. Chem.* **2012**, *124*, 9021–9024; c) K.-Y. Ye, T. McCallum, S. Lin, *J. Am. Chem. Soc.* **2019**, *141*, 9548–9554.
- [11] C. Yao, T. Dahmen, A. Gansäuer, J. Norton, *Science* **2019**, *364*, 764–767.
- [12] W. Liu, W. Li, A. Spannenberg, K. Junge, M. Beller, *Nat. Catal.* **2019**, *2*, 523–528.
- [13] a) T. J. Korstanje, J. I. van der Vlugt, C. J. Elsevier, B. de Bruin, *Science* **2015**, *350*, 298–302; b) R. Adam, C. B. Bheeter, J. R. Cabrero-Antonino, K. Junge, R. Jackstell, M. Beller, *ChemSusChem* **2017**, *10*, 842–846; c) R. Adam, J. R. Cabrero-Antonino, A. Spannenberg, K. Junge, R. Jackstell, M. Beller, *Angew. Chem. Int. Ed.* **2017**, *56*, 3216–3220; *Angew. Chem.* **2017**, *129*, 3264–3268; d) J. R. Cabrero-Antonino, R. Adam, K. Junge, M. Beller, *Chem. Sci.* **2017**, *8*, 6439–6450; e) J. R. Cabrero-Antonino, R. Adam, V. Papa, M. Holsten, K. Junge, M. Beller, *Chem. Sci.* **2017**, *8*, 5536–5546; f) B. G. Schieweck, J. Klankermayer, *Angew. Chem. Int. Ed.* **2017**, *56*, 10854–10857; *Angew. Chem.* **2017**, *129*, 10994–10997; g) J. Schneidewind, R. Adam, W. Baumann, R. Jackstell, M. Beller, *Angew. Chem. Int. Ed.* **2017**, *56*, 1890–1893; *Angew. Chem.* **2017**, *129*, 1916–1919; h) W. Liu, B. Sahoo, A. Spannenberg, K. Junge, M. Beller, *Angew. Chem. Int. Ed.* **2018**, *57*, 11673–11677; *Angew. Chem.* **2018**, *130*, 11847–11851; i) B. Emayavaramban, P. Chakraborty, B. Sundararaju, *ChemSusChem* **2019**, *12*, 3089–3093.
- [14] a) R. M. Bullock, *Science* **2013**, *342*, 1054–1055; b) P. J. Chirik, *Acc. Chem. Res.* **2015**, *48*, 1687–1695; c) S. Murugesan, K. Kirchner, *Dalton Trans.* **2016**, *45*, 416–439; d) X. Du, Z. Huang, *ACS Catal.* **2017**, *7*, 1227–1243; e) F. Kallmeier, R. Kempe, *Angew. Chem. Int. Ed.* **2018**, *57*, 46–60; *Angew. Chem.* **2018**, *130*, 48–63; f) G. A. Filonenko, R. van Putten, E. J. M. Hensen, E. A. Pidko, *Chem. Soc. Rev.* **2018**, *47*, 1459–1483; g) W. Liu, B. Sahoo, K. Junge, M. Beller, *Acc. Chem. Res.* **2018**, *51*, 1858–1869; h) A. Mukherjee, D. Milstein, *ACS Catal.* **2018**, *8*, 11435–11469; i) L. Alig, M. Fritz, S. Schneider, *Chem. Rev.* **2019**, *119*, 2681–2751; j) W. Ai, R. Zhong, X. Liu, Q. Liu, *Chem. Rev.* **2019**, *119*, 2876–2953; k) K. Junge, V. Papa, M. Beller, *Chem. Eur. J.* **2019**, *25*, 122–143.
- [15] a) A. A. Núñez Magro, G. R. Eastham, D. J. Cole-Hamilton, *Chem. Commun.* **2007**, 3154–3156; b) F. M. A. Geilen, B. Engendahl, M. Hölscher, J. Klankermayer, W. Leitner, *J. Am. Chem. Soc.* **2011**, *133*, 14349–14358; c) T. vom Stein, M. Meuresch, D. Limper, M. Schmitz, M. Hölscher, J. Coetzee, D. J. Cole-Hamilton, J. Klankermayer, W. Leitner, *J. Am. Chem. Soc.* **2014**, *136*, 13217–13225; d) S. Savourey, G. Lefèvre, J.-C. Berthet, P. Thuéry, C. Genre, T. Cantat, *Angew. Chem. Int. Ed.* **2014**, *53*, 10466–10470; *Angew. Chem.* **2014**, *126*, 10634–10638; e) X. Cui, Y. Li, C. Topf, K. Junge, M. Beller, *Angew. Chem. Int. Ed.* **2015**, *54*, 10596–10599; *Angew. Chem.* **2015**, *127*, 10742–10745; f) Y. Li, C. Topf, X. Cui, K. Junge, M. Beller, *Angew. Chem. Int. Ed.* **2015**, *54*, 5196–5200; *Angew. Chem.* **2015**, *127*, 5285–5289; g) L. Zhang, Z. Han, L. Zhang, M. Li, K. Ding, *Chin. J. Org. Chem.* **2016**, *36*, 1824–1838; h) R. Adam, J. Cabrero-Antonino, K. Junge, R. Jackstell, M. Beller, *Angew. Chem. Int. Ed.* **2016**, *55*, 11049–11053; *Angew. Chem.* **2016**, *128*, 11215–11219.
- [16] a) G. Jiang, J. Chen, H.-Y. Thu, J.-S. Huang, N. Zhu, C.-M. Che, *Angew. Chem. Int. Ed.* **2008**, *47*, 6638–6642; *Angew. Chem.* **2008**, *120*, 6740–6744; b) R. Hrdina, C. E. Müller, R. C. Wende, K. M. Lippert, M. Benassi, B. Spengler, P. R. Schreiner, *J. Am. Chem. Soc.* **2011**, *133*, 7624–7627; c) D. J. Vyas, E. Larionov, C. Besnard, L. Guénee, C. Mazet, *J. Am. Chem. Soc.* **2013**, *135*, 6177–6183; d) J. R. Lamb, M. Mulzer, A. M. LaPointe, G. W. Coates, *J. Am. Chem. Soc.* **2015**, *137*, 15049–15054; e) Y. Tian, E. Jürgens, D. Kunz, *Chem. Commun.* **2018**, *54*, 11340–11343.
- [17] a) G. Zhang, B. L. Scott, S. K. Hanson, *Angew. Chem. Int. Ed.* **2012**, *51*, 12102–12106; *Angew. Chem.* **2012**, *124*, 12268–12272; b) G. Zhang, K. V. Vasudevan, B. L. Scott, S. K. Hanson, *J. Am. Chem. Soc.* **2013**, *135*, 8668–8681; c) D. Gärtner, A. Welther, B. R. Rad, R. Wolf, A. Jacobi von Wangelin, *Angew. Chem. Int. Ed.* **2014**, *53*, 3722–3726; *Angew. Chem.* **2014**, *126*, 3796–3800; d) S. Rösler, J. Obenauf, R. Kempe, *J. Am. Chem. Soc.* **2015**, *137*, 7998–8001; e) R. Zhong, Z. Wei, W. Zhang, S. Liu, Q. Liu, *Chem* **2019**, *5*, 1552–1566.

Manuscript received: February 24, 2020

Accepted manuscript online: March 20, 2020

Version of record online: May 11, 2020

## 7. Appendix

### 7.1 Curriculum Vitae

#### General

**Name:** Thomas Leischner  
**Date of birth:** 16.10.1989  
**Place of birth:** Kassel  
**Nationality:** German  
**Address:** Auf der Huder 1b, 18055 Rostock  
**Phone:** +49(0)1722814034  
**Email:** Tommy.leischner@freenet.de

#### Education

Oct. 2016 – today	PhD Student  „Molybdenum Pincer Complexes and Their Application in Homogeneous Hydrogenation Reactions”  Advisor: Prof. Dr. M. Beller  <i>University of Rostock, Germany</i>
Feb. 2015 – Aug. 2015	Master Thesis  „Synthesis of Polydentate <i>P,S</i> -Ligands Bearing <i>P</i> -Chiral 1-Phosphanorbomanes“  Advisor: Prof. Dr. E. M. Hey-Hawkins  <i>University of Leipzig, Germany</i>
Oct. 2012 – Aug. 2015	Master of Science (M. Sc.) – Chemistry  <i>University of Leipzig, Germany</i>



Feb. 2012 – Aug. 2012

Bachelor Thesis

“Synthesis of Zirconiumphosphinidene-Complexes”

Advisor: Prof. Dr. E. M. Hey-Hawkins

*University of Leipzig, Germany*

Oct. 2009 – Aug. 2012

Bachelor of Science (M. Sc.) – Chemistry

*University of Leipzig, Germany*

Jun. 2009

High School Graduation

Georg-Christoph-Lichtenberg-Gymnasium

*Kassel, Germany*

### **Research and Professional Skills**

Sep. 2015 – Dec. 2015

Research Internship

*Bayer Healthcare, Wuppertal, Germany*

Advisors: Prof. Dr. J. Mittendorf / Dr. H. Beck

Jan. 2013 – Aug. 2013

ERASMUS Internship

*University of Helsinki, Finland*

### **7.2 List of Publications**

- 1.) T. Leischner, A. Spannenberg, K. Junge, M. Beller *Organometallics* **2018**, 37, 4402–4408.
- 2.) T. Leischner, L. A. Suarez, A. Spannenberg, K. Junge, A. Nova, M. Beller *Chem. Sci.* **2019**, 10, 10566–10576.
- 3.) T. Leischner, A. Spannenberg, K. Junge, M. Beller, *ChemCatChem* **2020**, 12, 4543–4549.
- 4.) J. Schneekönig, W. Liu, T. Leischner, K. Junge, C. Schotes, C. Baier, M. Beller, *Org. Process. Res. Dev.* **2020**, 24, 443–447.
- 5.) W. Liu, T. Leischner, W. Li, K. Junge, M. Beller *Angew. Chem. Int. Ed.* **2020**, 132, 11417–11420.

6.) P. Ryabchuk, T. Leischner, K. Kreyenschulte, K. Junge, M. Beller *Angew. Chem. Int. Ed.* **2020**, *132*, 18838–18844.

### 7.3 Conference Participations

1) Poster: “Molecular Defined Molybdenum PNP Pincer Complexes for the Application in Homogeneous Catalysis”, T. Leischner, K. Junge, M. Beller, *51<sup>st</sup> German Catalysis Meeting*, Weimar, March **2018**.

2) Oral Presentation: “Molybdenum Pincer and Their Application in Homogeneous Catalysis”, T. Leischner, K. Junge, M. Beller, *17<sup>th</sup> Ferrocene-Colloquium*, Rostock, February **2019**.

3) Poster: “Molecular Defined Molybdenum PNP Pincer Complexes for the Application in Homogeneous Catalysis”, T. Leischner, K. Junge, M. Beller, *21<sup>st</sup> JCF-Frühjahrssymposium*, Bremen, March **2019**.